Alma Mater Studiorum – Università di Bologna

DOTTORATO DI RICERCA IN

Biotecnologie Mediche

Ciclo XXV

Settore Concorsuale di afferenza: 06/F1

Settore Scientifico disciplinare: MED/28

Biomaterials for Clinical Application in Endodontics

Presentata da: Dr. Francesco Siboni

Coordinatore Dottorato **Relatore**

Prof.ssa Marialuisa Zerbini **Prof. Carlo Prati**

Esame finale anno 2013

Part I

Chapter 1- Introduction

1.1 Calcium-silicate MTA based cements

Endodontic therapy consists in the management of several tissues such as pulp tissue, periodontal tissue, periapical bone and dentine. These tissues are often contaminated by blood, periapical exudates and biological fluids which may compromise the setting reaction and stability of many materials employed for endodontics. An ideal orthograde or retrograde filling material should be non toxic, noncarcinogenic, nongenotoxic, biocompatible with the host tissues, insoluble in tissue fluids, and dimensionally stable (Torabinejad 1996, Ribeiro 2008).

The existing materials used in endodontics did not posses these ideal characteristics, especially in clinical application the moist highly affects the sealing ability and stability of endodontic cements. For these reason mineral trioxide aggregate (MTA) was developed and recommended initially as a root-end filling material and subsequently has been used for pulp capping, pulpotomy, apexogenesis, apical barrier formation in teeth with open apexes, repair of root perforations, and as a root canal filling material.

Calcium-silicate MTA cements are biocompatible bioactive hydrophilic materials (Gandolfi 2009-2011) and are able to release calcium and hydroxide ions. The calcium releasing and the alkalinization of surrounding environment have been demonstrated as the main factor of calcium-silicate MTA cement chemical and biological properties.

1.2 Chemical Properties

MTA based cements contains a fine hydrophilic powder of Portland cement with radiopacifyng agent such as bismuth oxyde (camilleri 2005). The main constituents of the hydrophilic powder are tricalcium silicate (3CaOSiO2), tricalcium aluminate (3CaO•Al2O3), dicalcium silicate (2CaOSiO2)and only for GrayMTA (GMTA) tetracalcium alluminoferrite (tetracalcium aluminoferrite 4CaOAl2O3Fe2O3) (Islam 2006).

The MTA cements setting reaction is trigged by the mixing of the hydrophilic powder with water. The hydration of calcium silicate and aluminate causes the formation of a porous solid gel (Camilleri 2007) with calcium and hydroxide ions (CH) release. The precipitated CH produce an high alkalinization of surrounding environments during the hydration steps.

The ideal powder-to-liquid ratio was set in 3:1 (Torabinejad 1993), in order to obtain a proper setting reaction. It has been demonstrated that physical and chemical properties of MTA cement might be negatively affected by changing in powder/liquid ratio, method of mixing, pH of the environment and temperature (Watts 2007, Islam 2006, Gandolfi 2009).

Unfortunately MTA cement setting is over 170 minutes (Gandolfi 2009) much longer than clinical requirement, so the long setting time is one of the major drawbacks (Gandolfi 2010, Parirokh 2010).

1.3 Biocativity

As reported by Kokubo & Takadama (2006) a bioactive material can bind to living bone by the formation of a bone-like apatite layer on its surface in the body environment.

The hydroxyapatite (HA) is the main inorganic component of human hard tissues such as bone, dentine and enamel with a Ca/P molar ratio of 1.67 and a structure very similar to that of natural apatite.

The bioactivity of calcium-silicate cement was first suggested by Sarkar (2005), and later confirmed by Coleman (2007), Tay and Pashley (2007), and Gandolfi (2010). In these studies MTA cements were immersed in phosphate buffered solutions (PBS) in order to simulate the body fluids (SBF) interaction such as blood, saliva and cervical fluids.

During the hydration steps of calcium-silicates the Ca ions released combine with the P ions of the SBF forming calcium-phosphates precipitation on the cement surface. The OH^- ions released from the CSH phase contribute to the alkalinization of the surrounding environment and induce the amorphous Ca-P precipitates to mature into a B-type HCA phase (Gandolfi 2010).

Hydroxyapatite is biocompatible and osteoconductive, so the bioactivity (i.e. apatite formation ability) of MTA based cements might give a significant clinical advantage over the other commercial cements in rootend or root-perforation reparation.

1.4 References

- Camilleri J, Montesin FE, Brady K, Sweeney R, Curtis RV, Ford TR. The constitution of mineral trioxide aggregate. Dent Mater 2005;21:297–303.

- Camilleri J. Hydration mechanisms of mineral trioxide aggregate. Int Endod J 2007;40:462–70.

- Coleman NJ, Nicholson JW, Awosanya K. A preliminary investigation of the in vitro bioactivity of white portland cement. Cem Concr Res 2007;37:1518–23.

- Gandolfi MG, Ciapetti G, Perut F, Taddei P, Modena E, Rossi PL, Prati C. Biomimetic calcium-silicate cements aged in simulated body solutions. Osteoblasts response and analyses of apatite coating. J Appl Biomater Biomech 2009; 7: 160-170.

- Gandolfi MG, Iacono F, Agee K, Siboni F, Tay F, Pashley DH, Prati C. Setting time and expansion in different soaking media of experimental accelerated calcium-silicate cements and ProRoot MTA. Oral Surg Oral Med Oral Pathol Oral Radiol Endod 2009;108:39-45. Gandolfi MG, Taddei P, Tinti A, Prati C. Apatite-forming ability (bioactivity) of ProRoot MTA. Int Endod J 2010; 43: 917-929.

- Gandolfi MG, Van Landuyt K, Taddei P, Modena E, Van Meerbeek B, Prati C. ESEM–EDX and Raman techniques to study ProRoot MTA and calcium-silicate cements in wet conditions and in real-time. J Endod 2010;36:851–7.

- Gandolfi MG, Ciapetti G, Taddei P, Perut F, Tinti A, Cardoso MV, Van Meerbeek B, Prati C. Apatite formation on bioactive calcium-silicate cements for dentistry affects surface topography and human marrow stromal cells proliferation. Dent Mater 2010; 26: 974-992.

- Gandolfi MG, Taddei P, Siboni F, Modena E, Ginebra MP, Prati C. Fluoride-containing nanoporous calcium-silicate MTA cements for endodontics and oral surgery: early fluorapatite formation in a phosphate-containing solution. Int Endod J 2011; 44: 938-949.

- Kokubo T, Takadama H. How useful is SBF in predicting in vivo bone bioactivity? Biomaterials 2006; 27: 2907–15.

- Islam I, Chng HK, Yap AU. X-ray diffraction analysis of mineral trioxide aggregate and Portland cement. Int Endod J 2006;39:220–5.

- Islam I, Chng HK, Yap AU. Comparison of the physical and mechanical properties of MTA and Portland cement. J Endod 2006;32:193–7.

- Parirokh M, Torabinejad M. Mineral trioxide aggregate: a comprehensive literature review--Part I: chemical, physical, and antibacterial properties. J Endod. 2010;36:16-27.

- Ribeiro DA. Do endodontic compounds induce genetic damage? a comprehensive review. Oral Surg Oral Med Oral Pathol Oral Radiol Endod 2008;105:251–6.

- Sarkar NK, Caicedo R, Ritwik P, Moiseyeva R, Kawashima I. Physicochemical basis of the biologic properties of mineral trioxide aggregate. J Endod 2005;31:97–100.

- Tay FR, Pashley DH, Rueggeberg FA, Loushine RJ, Weller RN. Calcium phosphate phase transformation produced by the interaction of the portland cement component of white mineral trioxide aggregate with a phosphate-containing solution. J Endod 2007;33:1347.

- Torabinejad M, Pitt Ford TR. Root end filling materials: a review. Endod Dent Traumatol 1996;12:161–78.

- Torabinejad M, Watson TF, Pitt Ford TR. Sealing ability of a mineral trioxide aggregate when used as a root end filling material. J Endod 1993;19:591–5.

- Watts JD, Holt DM, Beeson TJ, Kirkpatrick TC, Rutledge RE. Effects of pH and mixing agents on the temporal setting of tooth-colored and gray mineral trioxide aggregate. J Endod 2007;33:970–3.

Part II

Setting time and expansion in different soaking media of experimental accelerated calcium-silicate cements and ProRoot MTA

Maria Giovanna Gandolfi, Bio, DSc, PhD,[a,b] Francesco Iacono, DDS,[a] Kelli Agee, BS,[c] Francesco Siboni, BS,[a] Franklin Tay, BDS, PhD,[c] David Herbert Pashley, DMD, PhD,[c] and Carlo Prati, MD, DDS, PhD,[a] Bologna, Italy, and Augusta, GA
UNIVERSITY OF BOLOGNA AND MEDICAL COLLEGE OF GEORGIA

Objectives. The setting time and the expansion in deionized water, phosphate-buffered saline (PBS), 20% fetal bovine serum (FBS)/80% PBS or hexadecane oil of experimental accelerated calcium-silicate cements and ProRoot MTA were evaluated.

Study design. Different compounds such as sodium fluoride, strontium chloride, hydroxyapatite, and tricalcium phosphate were separately added to a basic experimental calcium-silicate cement to test their effect on setting and expansion.

The initial and final setting times were determined using appropriate Gilmore needles. A linear variable differential transformer (LVDT) device was used to test the restricted hygroscopic linear expansion over 180 minutes of cements immersed in different solutions. Results were statistically compared using a 2-way ANOVA test (cement type versus solution type).

Results. All experimental cements showed initial setting times between 28 and 45 minutes and final setting times between 52 and 80 minutes. MTA showed a final setting time of 170 minutes. Final setting time of all experimental cements was faster than MTA.

All cements showed slight (0.04%-0.77%) expansion in water, PBS, or FBS/PBS. Only fluoride-containing cement showed a significant expansion in water (6.68%) and in PBS (6.72%). The PBS/FBS contamination significantly reduced the expansion of fluoride-containing cement (2.98%) and MTA (0.07%). In contrast, cements showed a slight shrinkage when immersed in hexadecane, especially fluoride-containing cement.

Conclusions. The study demonstrated that: (1) the setting time of calcium-silicate cements may be effectively reduced; (2) the expansion is a water dependent mechanism owing to water uptake, because no expansion occurred in cements immersed in oil; (3) a correlation between setting time and expansion in water and PBS exists; (4) fluorine-containing cement showed a significant expansion in water and in PBS; (5) the immersion in FBS/PBS strongly reduced the expansion of MTA and fluoride-doped cement suggesting that fluid contamination (ie, blood) during surgical procedures may greatly affect the expansion of some calcium-silicate cements. (Oral Surg Oral Med Oral Pathol Oral Radiol Endod 2009;108:e39-e45)

Calcium-silicate cements (like ProRoot MTA [mineral trioxide aggregate] and other Portland-based cements) are mainly composed of hydrophilic particles of dicalcium silicate and tricalcium silicate. They are hydraulic cements able to set in presence of blood or other fluids. They have been proposed in dentistry as root-end and root perforation repair materials and later as pulp-capping agents and root canal sealers.[1,2] However, these materials present some disadvantages, such as prolonged setting time and poor handling when used as root-end fillings.[3] A root-end filling material should set as soon as it is placed in contact with oral hard tissues to allow dimensional stability of the restoration and to confer adequate strength to avoid displacement during restorative procedures. Recent studies attempted to improve the physical and chemical properties of calcium-silicate cements in regard to their relatively slow setting time.[4-14] To reduce setting time and extend their clinical use, new calcium-silicate materials may be designed by adding different compounds. Experimental cements demonstrated adequate in vitro marginal adaptation and sealing ability[8,15,16] and good biocompatibility[9,10] and bioactivity by formation of an apatite coating layer when immersed in phosphate-containing solutions.[17]

[a]Department of Dental Sciences, Endodontic Clinical Section, University of Bologna, Bologna, Italy.
[b]Department of Earth Science, University of Bologna, Bologna, Italy.
[c]Department of Oral Biology, School of Dentistry, Medical College of Georgia, Augusta, GA, USA.
Received for publication Jun 22, 2009; accepted for publication Jul 20, 2009.
1079-2104/$ - see front matter

doi:10.1016/j.tripleo.2009.07.039

Table I. Composition of experimental cements

Designations	Composition
WPC (control)	White Portland cement (thermally and mechanically treated), calcium sulphate, calcium chloride
TC1	WPC and montmorillonite 1 wt%
TC2	WPC and montmorillonite 2 wt%
TC5	WPC and montmorillonite 5 wt%
TC-TCP	WPC, montmorillonite 1 wt% and tricalcium phosphate 5 wt%
TC-HA	WPC, montmorillonite1 wt%, and hydroxyapatite 5 wt%
TC-Sr	WPC, montmorillonite 1 wt% and strontium chloride 5 wt%
TC-CaP	WPC, montmorillonite 1 wt%, calcium hydrogen phosphate 4 wt% and calcium carbonate 2 wt%
TC-F	WPC, montmorillonite 1 wt% and sodium fluoride 1 wt%

ProRoot MTA is often placed in moist environments where it can take up more water than might be ideal. The presence of different moisture during surgical application (such as blood, plasma, and other fluids) can modify the physical properties of these materials.[3,18]

The purpose of this study was to investigate the setting times and the linear expansion between the initial and final setting times of experimental accelerated calcium-silicate cements and ProRoot MTA after immersion in various soaking solutions such as phosphate-buffered saline (PBS), fetal bovine serum (FBS), hexadecane oil, and deionized water.

MATERIALS AND METHODS

A white Portland cement (CEM I Aalborg, Aalborg, Denmark) was used as base material for the experimental calcium-silicate cements because it contains the same active components of white ProRoot MTA (Dentsply, Tulsa, OK) that was used as control. The compositions of the experimental cements are shown in Table I.

Setting time

The setting time of calcium-silicate cements and MTA was determined using Gilmore needles (ASTM International, West Conshohocken, PA) in accordance with ASTM standard C266-07[19] with the following exceptions. Ten grams of cement were mixed instead of 650 g (because of the high cost of materials). The experimental cements and MTA were mixed with deionized water (powder:liquid ratio of 3:1) on a glass slab with a stainless steel spatula. The mixtures were placed into a mold measuring 14 mm in diameter and 2.5 mm in thickness instead of the 13-mm thickness required by the ASTM standard. Room temperature, dry powders, mixing glass, and mixing water were maintained at 23 3°C. The mold was completely filled and the excess material was removed to obtain a flat surface. The samples were then stored in the gas phase of a sealed chamber containing a saturated solution of magnesium nitrate hexahydrate to hold the relative humidity (RH) at 50% as required by ASTM standard[19] and maintained at 37°C. The temperature of 37°C was used instead of 23°C[19] because the cements inserted in root canals are set at physiological temperature. The use of an electronic hygrometer (Hanna Instruments, Model HI9065/C, Woonsocket, RI) confirmed that the gas phase above this solution had a relative humidity of 50% 1%.

The initial setting time represents the time required by the test cement to set and rigidify enough to support the lighter Gilmore needle; the final setting time is the time necessary for the test specimen to bear the heavier Gilmore needle without appreciable indentation.

The initial setting time was measured using a Gilmore needle weighing 113.4 g with a tip diameter of 2.12 mm. After the initial setting time was measured, the specimens were tested every 10 minutes with a Gilmore needle weighing 453.6 g with a tip diameter of 1.06 mm. As the final setting time approached, specimens were tested every minute to determine the exact final setting time. The test was repeated 3 times for each material and the means were statistically compared using a 1-way analysis of variance (ANOVA) test seeking significant differences. When significant differences were found, they were identified and compared using Tukey multiple comparison tests at 0.05.

Expansion

A linear variable differential transformer (LVDT) device was used to test the expansion of each material during 180 minutes. Before starting the expansion measurements the samples were stored (immediately after mixing) for 30 minutes at 37°C and 50% RH, to avoid the deterioration of cement surface by the LVDT probe.

Aluminium stock was milled to create cylindrical wells measuring 11 mm in diameter and 5 mm in depth (volume of 475 mm^3). The mold was only open at the top to constrain the material displacement in the vertical direction in a manner similar to its use in reverse root-end fillings. The materials were mixed and placed into the mold as described previously. Samples were stored for 30 minutes in an incubator at 37°C and 50% RH to set the cements.

A thin coating of a viscous cyanoacrylate was placed on the bottom side of the aluminium wells to fix it beneath the contact probe (Fig. 1) of an LVDT device (Model TMS-2, Perkin Elmer, Boston, MA). A weight pan on top of the LVDT was loaded with 0.01 N of

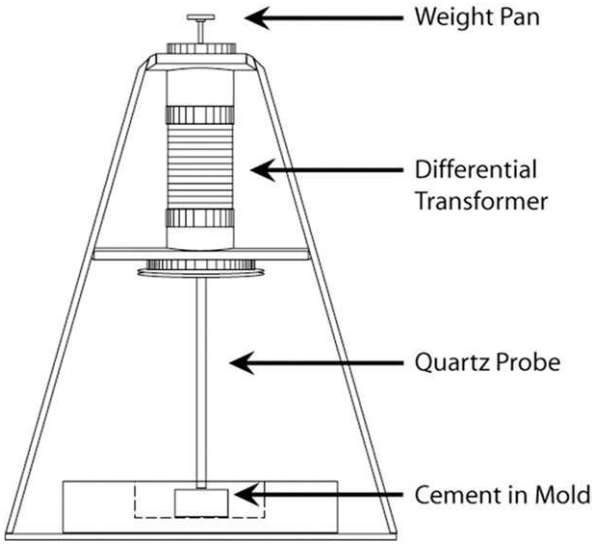

Fig. 1. Schematic figure of LVDT used to test the linear constrained expansion of cements immersed in different solutions.

force. This was necessary to balance the buoyancy of a hydraulic damper system to keep the probe in contact with the cement during dimensional changes. The LVDT has a sensitivity of 0.5 m over a range of 4 mm.

The expansion of the cements was evaluated 6 times in 4 different solutions: (A) deionized water, (B) PBS (Mediatech Inc, Herndon, VA), (C) 20% FBS (Mediatech Inc) mixed with 80% PBS, and (D) hexadecane oil (Fisher Chemicals, Fair Lawn, NJ).

The samples were removed from the incubator and then covered by these solutions approximately 1 minute after the probe contacted the surface of the cement. The materials remained covered by 1 of the 4 test solutions until the experiment was finished. A computer logged the probe position every 3 seconds for 180 minutes and the expansion of the samples was monitored as a function of time. The results were statistically compared by using a 2-way ANOVA test (type of cement as one factor versus type of solution).

RESULTS

Setting time

The initial and the final setting times of the cements are shown in Table II. The final setting times of all calcium-silicate cements were faster than MTA. All the materials tested demonstrated initial setting times between 28 and 45 minutes. TC-Sr had the shortest initial setting time (28 1 minute). Cement containing hydroxyapatite (TC-HA) showed an initial setting time of 30 1 minute, similar to TC2 (31 2 minutes) and WPC (31 2 minutes). Longer initial setting times were obtained with TC-TCP (39 1 minute), TC-CaP (39 2 minutes), and MTA (41 1 minute), whereas TC-F was 45 1 minute. The final setting times of all the experimental materials were between 52 and 80 minutes, whereas MTA required 170 2 minutes (P .05).

Table II. Initial and final setting times of cements

Cement	Initial setting time		Final setting time	
WPC	31	$2^{a,d}$	55	3^{h}
TC1	36	$1^{b,c}$	70	$1^{i,k}$
TC2	31	$2^{a,d}$	52	1^{h}
TC5	33	$3^{a,b}$	64	$1^{j,k}$
TC-TCP	39	$1^{c,f}$	71	2^{i}
TC-HA	30	$1^{a,e}$	66	2^{k}
TC-Sr	28	$1^{d,e}$	65	2^{k}
TC-CaP	39	$2^{c,f}$	80	3^{l}
TC-F	45	1^{g}	77	3^{l}
MTA	41	1^{f}	170	2^{m}

Initial and final setting times of cements stored at 37°C and 50% relative humidity.
Different superscript letters indicate significant differences (P .005). N 3.
MTA, mineral trioxide aggregate; other acronyms per Table I.

Expansion

Pilot experiments using LVDT on the materials beginning 10 minutes after initial mixing revealed that the surface texture of the cements deteriorated within 30 to 60 minutes when any of aqueous solution was placed on the cements. For this reason, a humid environment (50% RH) was used to set the cements (for 30 minutes at 37°C) before sample immersion. None of the experimental cements or MTA showed any shrinkage in aqueous solutions. All materials exhibited variable amounts of linear expansion in water, varying from 0.06% 0.00% for TC5 to 6.68 0.83 for TC-F cements (Table III). When the cements were covered with 20% FBS/80% PBS, TC-TCP and TC-CaP expanded significantly more than in PBS, whereas TC-F and MTA were more dimensionally stable (Table III). When initial setting times were plotted against cement expansion in water or PBS (water P .005, PBS P .05) significant correlations were found (water R^2 0.67, PBS R^2 0.46) (Fig. 2).

DISCUSSION

The study investigated the linear expansion between the initial and the final setting times of MTA and experimental cements in different soaking solutions. MTA and the experimental cements contain the same active hydrophilic compounds, mainly dicalcium sili-

Table III. Expansion (positive values) and shrinkage (negative values) of cements

Cement	Water		PBS		80% PBS/20% FBS		Hexadecane	
WPC	0.10	0.03[a]	0.22	0.08[b]	0.12	0.04[a]	0.06	0.02[c]
TC1	0.23	0.00[a]	0.22	0.09[a]	0.25	0.06[a]	0.07	0.02[b]
TC2	0.07	0.04[a]	0.14	0.05[a]	0.15	0.05[a]	0.12	0.01[b]
TC5	0.06	0.00[a,b]	0.14	0.07[a]	0.13	0.04[a]	0.04	0.01[b]
TC-TCP	0.27	0.10[a]	0.04	0.01[b]	0.29	0.03[a]	0.22	0.03[c]
TC-HA	0.24	0.09[a]	0.28	0.12[a]	0.33	0.05[a]	0.10	0.01[b]
TC-Sr	0.17	0.03[a]	0.08	0.01[b]	0.16	0.03[a]	0.11	0.02[c]
TC-CaP	0.31	0.10[a]	0.50	0.16[a]	0.83	0.22[b]	0.14	0.03[c]
TC-F	6.68	0.83[a]	6.72	0.88[a]	2.98	0.13[b]	0.48	0.06[c]
MTA	0.77	0.27[a,b]	1.04	0.25[b]	0.07	0.05[a,b]	0.15	0.03[a]

Expansion (positive values) and shrinkage (negative values) during 150 minutes of cements immersed in water, PBS, FBS/PBS and hexadecane. Values are % linear expansion. Groups identified by different superscript lowercase letters in horizontal rows are significantly different at P .05. N 10.

PBS, phosphate-buffered saline; FBS, fetal bovine serum; MTA, mineral trioxide aggregate; other acronyms per Table I.

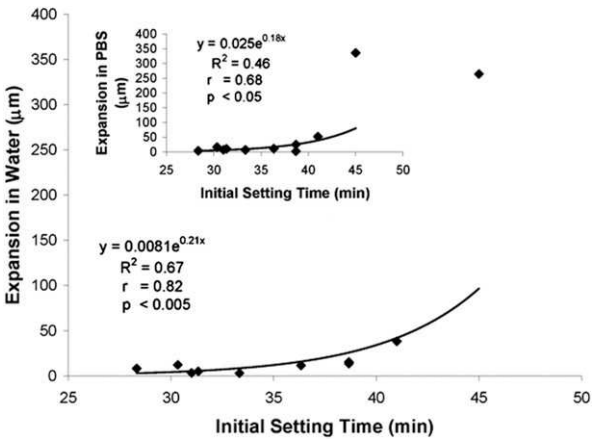

Fig. 2. Initial setting times plotted against cement expansion in water or PBS. Significant correlations were found. In water P .005 and R^2 0.67; in PBS P .05 and R^2 0.46.

cate and tricalcium silicate, that allow the materials to set in presence of water or other fluids.

To investigate the setting time, all specimens were stored in a chamber at 37°C with 50% RH, to avoid both water uptake and dehydration of the samples, as required by the ASTM specifications.[19]

The setting time of specimens stored at 37°C and 25% RH was previously assessed in the pilot study. In these conditions, the setting time occurred too rapidly because of water loss from the specimens. The comparison of the results obtained from the 2 different humidity conditions (ie, 25% versus 50%) revealed the direct proportionality between RH and setting time. That is, at 25% RH, the time the cements needed to reach the initial and final setting time was exactly half of the time required to reach the setting time at 50% RH.

Under the conditions of this study (50% RH and 37°C), the experimental cements showed an initial setting time of 28 to 45 minutes, whereas MTA showed an initial setting time of 41 1 minute, which was faster than TC-F (45 1 minute). MTA was used as a comparison material to establish the consistency of our results with previous investigations. The results of this study are in agreement with the prolonged final setting time of MTA previously reported.[4,20-23] Ber et al.[4] showed a final setting time of 202 minutes, which was greater than the time reported by Torabinejad et al.[1] (175 minutes), but they used a Vicat needle. Islam et al.[21] using a Gilmore needle, found a setting time of 140 minutes and 175 minutes for white MTA and grey MTA, respectively. The results of the present study indicated a final setting time of MTA of 170 2 minutes. The use of different needles with differing weights (300 g Vicat versus 453.6 g Gilmore needle), humidity conditions, and temperatures may be responsible for the differences in setting times.[24]

The experimental material exhibited final setting times between 52 and 80 minutes, which were all faster setting than MTA. The inclusion of $CaCl_2$ in the composition of all experimental cements reduced the setting time, according to earlier studies.[4,11,25]

The montmorillonite seemed to delay the final setting time in TC1. According to previous studies on glass-ionomer and calcium-phosphate cements[26,27] and in cements used as building materials,[28] montmorillonite was added to improve the dimensional stability of cements. Montmorillonite is a phyllosilicate mineral (derived from deposits of weathered volcanic ash) characterized by high and irreversible swelling capacity owing to water adsorption.[29,30] The effect of montmorillonite on initial and final setting times and expansion was negligible.

Other chemical compounds have been proposed by earlier investigations to modify the setting time and the expansion and to improve the biological properties of different cements.[17,31-38]

The experimental materials containing strontium chloride (TC-Sr) and apatite (TC-HA) had shorter setting times, whereas the cements containing tricalcium phosphate (TC-TCP) and calcium hydrogen phosphate (TC-CaP) had slightly longer initial setting times, although much lower than MTA. Interestingly, the inclusion of NaF substantially increased the initial setting time of cement.

The hygroscopic linear expansion of cement samples was investigated after 30 minutes of setting before immersion in the different solutions (deionized water, PBS, 80% PBS-20% FBS, and hexadecane oil). Our clinical experience suggested that 30 minutes is the time required for MTA preparation, its insertion in a suitable consistency, and periapical surgical flaps replacement. Storm et al.[39] measured the linear constrained expansion by LVDT and reported a slight linear expansion of 0.47% for gray MTA (GMTA), 0.04% for white MTA (WMTA), and 0.24% for portland cement when the specimen were submerged in water immediately after mixing. The linear expansion values of our experimental cements are within the same order of magnitude of those obtained by Storm et al.[39] except for TC-F that showed a 6.7% linear expansion in water. This expansion may explain the optimal sealing ability demonstrated by this cement in a microleakage study.[16] Water-soluble F increased the water-penetrability of cement paste. Fluorine may cause the hardened cement paste by promoting the formation of a porous structure with increased total pore volume and volume of large capillary pores. A likely explanation for the retardation of setting by F may be (1) fluorine that dissolves from NaF during hydration, precipitates as fine crystals of CaF_2; (2) the formation of water-insoluble protective film of CaF_2 on the surface of cement minerals suppressing the water penetration inside minerals and their dissolution/hydration and of movement of ions; (3) the formation of calcium-silica-fluorine complexes (containing SiF_6 groups) by reacting silicate ions with F dissolved from NaF additive.

Water was used as a control because calcium-silicate Portland cements set by reacting with water. During hydration and setting, these cements can react with phosphate ions present in solutions to form hydroxyapatite crystals on their surface, as recently proposed by different studies.[40-44] We expected this may occur on the cement immersed in PBS. Most biological fluids such as blood and plasma contain a complex mixture of proteins that can adsorb to cement surfaces. FBS was used because of its similar biochemical composition to human serum to simulate a more in vivo-like condition.[45] We mixed 20% FBS with 80% PBS to simulate body fluids. Others previously used pure bovine serum albumin.[45]

Expansion of calcium-silicate Portland cements is thought to be because of water and fluid sorption or other hydrolytic events. This can not occur in oil (water-free soaking solution). We used hexadecane as an example of a very pure oil to act as a negative control.

The immersion in FBS/PBS significantly reduced the expansion of TC-F, WPC, and MTA compared with the immersion in PBS. It is likely that the serum proteins adsorbed to the cements and reduced the dimensions of their surface porosities.[46]

The significant positive correlation between constrained linear expansion in water and initial setting time was observed in samples stored in water and in PBS. The longer it takes a cement to rigidify sufficient to support the lighter Gilmore needle, the more expansion occurs. A delayed water uptake may be responsible for longer setting time and higher expansion. After the initial setting time, it is unlikely that more dimensional change can occur by water uptake because the increasing stiffness of the cement opposes further dimensional changes.

The water-free hexadecane oil was used to determine if the expansion of these cements was a result of water. The slight expansion showed by the cements in the presence of water and the slight shrinkage detected in presence of hexadecane indicates the expansion was a result of the consequence of water uptake suggesting a water-dependent mechanism. The slight shrinkage of the cements immersed in hexadecane was probably because of dehydration of the cement surface by oil.

CONCLUSIONS

All the experimental accelerated calcium-silicate cements showed setting time values suitable for root-end filling surgical procedures (30-40 minutes) and for other clinical applications where short setting time is required, such as in root perforations.

A correlation between setting time and expansion was demonstrated in water and PBS.

The expansion is a water-dependent mechanism attributable to water uptake, because no expansion occurred in cements immersed in oil.

The expansion may occur inside the surgical sites in presence of physiological fluids and may play a positive role in improving the sealing ability, an essential property for the endodontic filling materials. Only fluoride-containing cement showed a significant expansion.

The inclusion of additional chemical compounds produced small changes in setting time and expansion,

so they may be added in the composition to improve the biological properties of the cements.

The authors express their gratitude to Fabiola D'Amato and Michelle Barnes for providing secretarial support.

REFERENCES

1. Torabinejad M, Watson TF, Pitt Ford TR. Sealing ability of a mineral trioxide aggregate when used as a root-end filling material. J Endod 1993;19:591-5.
2. Sluyk SR, Moon PC, Hartwell GR. Evaluation of setting properties and retention characteristics of mineral trioxide aggregate when used as a furcation perforation repair material. J Endod 1998;24:768-71.
3. Walker MP, Diliberto A, Lee C. Effect of setting conditions on mineral trioxide aggregate flexural strength. J Endod 2006;32: 334-6.
4. Ber BS, Hatton JF, Stewart GP. Chemical modification of ProRoot MTA to improve handling characteristics and decrease setting time. J Endod 2007;33:1231-4.
5. Camilleri J, Montesin FE, Di Silvio L, Pitt Ford TR. The chemical constitution and biocompatibility of accelerated Portland cement for endodontic use. Int Endod J 2005;38:834-42.
6. Camilleri J, Montesin FE, Juszczyk AS, Papaioannou S, Curtis RV, Donald FM, et al. The constitution, physical properties and biocompatibility of modified accelerated cement. Dent Mater 2008;24:341-50.
7. Camilleri J. Modification of mineral trioxide aggregate. Physical and mechanical properties. Int Endod J 2008;41:843-9.
8. Gandolfi MG, Sauro S, Mannocci F, Watson TF, Zanna S, Capoferri M, et al. New tetrasilicate cements as retrograde filling material: an in vitro study on fluid penetration. J Endod 2007; 33:742-5.
9. Gandolfi MG, Perut F, Ciapetti G, Mongiorgi R, Prati C. New Portland cement-based materials for endodontics mixed with articaine solution: a study of cellular response. J Endod 2008; 34:39-44.
10. Gandolfi MG, Pagani S, Perut F, Ciapetti G, Baldini N, Mongiorgi R, et al. Innovative silicate-based cements for endodontics: a study of osteoblast-like cell response. J Biomed Mater Res A 2008;87:477- 46.
11. Wiltbank KB, Schwartz SA, Schindler WG. Effect of selected accelerants on the physical properties of mineral trioxide aggregate and Portland cement. J Endod 2007;33:1235-8.
12. Kogan P, He J, Glickman GN, Watanabe I. The effect of various additives on setting properties of MTA. J Endod 2006;32:569-72.
13. Ding SJ, Kao CT, Shie MY, Hung C Jr, Huang TH. The physical and cytological properties of white MTA mixed with NA_2HPO_4 as an accelerant. J Endod 2008;34:748-51.
14. Dos Santos AD, Araujo EB, Yukimitu K, Barbosa JC, Moraes JCS. Setting time and thermal expansion of two endodontic cements. Oral Surg Oral Med Oral Pathol Oral Radiol Endod 2008;106:77-9.
15. Gandolfi MG, Prati C. Bio-Sealers derived from modified Portland cement. Apical sealing longitudinal study. J Dent Res 2008; 87c(Spec Issue):PEF-Division Abstr 743.
16. Gandolfi MG, Iacono F, Pirani C, Chersoni S, Prati C. Marginal adaptation and SEM-EDX analyses of Portland-based cement. J Dent Res 2008;87c(Spec Issue):PEF-Division Abstr 762.
17. Taddei P, Tinti A, Gandolfi MG, Rossi PL, Prati C. Vibrational study on the bioactivity of Portland cement-based materials for endodontic use. J Mol Struct 2009;924-926:548-54.
18. Budig CG, Eleazer PD. In vitro comparison of the setting of dry ProRoot MTA by moisture absorbed through the root. J Endod 2008;34:712-4.
19. ASTM standard C-266-07 Standard test method for time of setting of hydraulic-cement paste by Gilmore needles. Annual book of ASTM standards. ASTM International, West Conshokocken, PA: 2007.
20. Torabinejad M, Hong CU, McDonald F, Pitt Ford TR. Physical and chemical properties of a new root-end filling material. J Endod 1995;21:349-53.
21. Islam I, Chng HK, Yap AU. Comparison of the physical and mechanical properties of MTA and portland cement. J Endod 2006;32:193-7.
22. Huang TH, Shie MY, Kao CT, Ding SJ. The effect of setting accelerator on properties of mineral trioxide aggregate. J Endod 2008;34:590-3.
23. Chng HK, Islam I, Yap AUJ, Tong YW, Koh ET. Properties of a new root-end filling material. J Endod 2005;31:665-8.
24. Ylmén R, Jaglid U, Steenari BM, Panas I. Early hydration and setting of Portland cement monitored by IR, SEM and Vicat techniques. Cem Concr Res 2009;39:433-9.
25. Abdullah D, Ford TR, Papaioannou S, Nicholson J, McDonald F. An evaluation of accelerated Portland cement as a restorative material. Biomaterials 2002;23:4001-10.
26. Dowling AH, Stamboulis A, Fleming GJP. The influence of montmorillonite clay reinforcement on the performance of a glass ionomer restorative. Dent Mater 2006;34:802-10.
27. Kwon SY, Cho EH, Kim SS. Preparation and characterization of bone cements incorporated with montmorillonite. J Biomed Mater Res Part B: Appl Biomater 2007;83B:276-84.
28. Peethamparan S, Olek J, Diamond S. Mechanism of stabilization of Na-montmorillonite clay with cement kiln dust. Cem Concr Res 2009;39:580-9.
29. Laird DA. Model for the crystalline swelling of 2:1 layer phyllosilicates. Clays Clay Minerals 1996;44:553-9.
30. Bray HJ, Redfern SAT. Kinetics of dehydration of Ca-montmorillonite. Phys Chem Minerals 1999;26:591-600.
31. LeGeros RZ. Properties of osteoconductive biomaterials: calcium phosphates. Clin Orthop Relat Res 2002;395:81-98.
32. Bohner M. New hydraulic cements based on -tricalcium phosphate-calcium sulphate dehydrate mixtures. Biomaterials 2004; 25:741-9.
33. Padilla S, Roman J, Carenas A, Vallet-Regi M. The influence of the phosphorus content on the bioactivity of sol-gel glass ceramics. Biomaterials 2005;26:475-83.
34. Panzavolta S, Torricelli P, Sturba L, Bracci B, Giardino R, Bigi A. Setting properties and in vitro bioactivity of strontium-enriched gelatin-calcium phosphate bone cements. J Biomed Mater Res Part A 2008;84A:965-72.
35. Jegou Saint-Jean S, Camire' CL, Nevsten P, Hansen S, Ginebra MP. Study of the reactivity and in vitro bioactivity of Sr-substituted and alfa-TCP cements. J Mater Sci Mater Med 2005;16: 993-1001.
36. Ben-Dor L, Rubinsztain Y. The influence of phosphate on the hydration of cement minerals studied by TDA and TG. Thermochim Acta 1979;30:9-14.
37. Taddei P, Tinti A, Gandolfi MG, Rossi PL, Prati C. Ageing of calcium silicate cements for endodontic use in simulated body fluids: a micro-Raman study. J Raman Spectrosc 2009, in press.
38. Gandolfi MG, Taddei P, Tinti A, Siboni F, Prati C. Bio-coating formation on bio-active endodontic materials derived from portland cement. J Dent Res 2008;87c(Spec Issue):PEF-Division Abstr 733.
39. Storm B, Eichmiller FC, Tordik PA, Goodell GG. Setting ex

pansion of gray and white mineral trioxide aggregate and Portland cement. J Endod 2008;34:80-2.
40. Sarkar NK, Caicedo R, Ritwik P, Moiseyeva R, Kawashima I. Physicochemical basis of the biologic properties of mineral trioxide aggregate. J Endod 2005;31:97-100.
41. Bozeman TB, Lemon RR, Eleazer PD. Elemental analysis of crystal precipitates from gray and white MTA. J Endod 2006; 32:425-8.
42. Coleman NJ, Nicholson JW, Awosanya K. A preliminary investigation of the in vitro bioactivity of white Portland cement. Cem Concr Res 2007;37:1518-23.
43. Tay FR, Pashley DH, Rueggeberg FA, Loushine RJ, Weller RN. Calcium phosphate phase transformation produced by the interaction of the Portland cement component of white mineral trioxide aggregate with a phosphate-containing fluid. J Endod 2007;33:1347-51.
44. Huffman BP, Mai S, Pinna L, Weller RN, Primus CM, Gutmann JL, et al. Dislocation resistance of ProRoot Endo Sealer, a calcium silicate- based root canal sealer, from radicular dentine. Int Endod J 2009;42:34-46.
45. Tingey MC, Bush P, Levine MS. Analysis of mineral trioxide aggregate surface when set in the presence of fetal bovine serum. J Endod 2008;34:45-9.
46. Rößler C, Eberhardt A, Kucerova H, Möser B. Influence of hydration on the fluidity of normal Portland cement pastes. Cem Concr Res 2008;38:897-906.

Reprint requests:

Maria Giovanna Gandolfi, PhD
Department of Odontostomatological Sciences
Alma Mater Studiorum
University of Bologna
Via San Vitale 59
40125 Bologna, Italy
mgiovanna.gandolfi@unibo.it

Push-out strength of modified Portland cements and resins

FRANCESCO IACONO , DDS, MS, MARIA GIOVANNA GANDOLFI , MBIOL, DSC, MBIO, PHD, BRADFORD HUFFMAN , BS, J EREMY SWORD , BS, KELLI AGEE , BS, FRANCESCO SIBONI , DDS, FRANKLIN TAY, BDSC (HONS), PHD, CARLO PRATI , MD, DDS, PHD & DAVID PASHLEY , DMD, PHD

ABSTRACT : Purpose: Modified calcium-silicate cements derived from white Portland cement (PC) were formulated to test their push-out strength from radicular dentin after immersion for 1 month. Methods: Slabs obtained from 42 single-rooted extracted teeth were prepared with 0.6 mm diameter holes, then enlarged with rotary instruments. After immersion in EDTA and NaOCl, the holes were filled with modified PCs or ProRoot MTA, Vitrebond and Clearfil SE. Different concentrations of phyllosilicate (montmorillonite-MMT) were added to experimental cements. ProRoot MTA was also included as reference material. Vitrebond and Clearfil SE were included as controls. Each group was tested after 1 month of immersion in water or PBS. A thin-slice push-out test on a universal testing machine served to test the push-out strength of materials. Results were statistically analyzed using the least squares means (LSM) method. Results: The modified PCs had push-out strengths of 3-9.5 MPa after 1 month of immersion in water, while ProRoot MTA had 4.8 MPa. The push-out strength of PC fell after incubation in PBS for 1 month, while the push-out strength of ProRoot MTA increased. There were no significant changes in Clearfil SE Bond or Vitrebond after water or PBS storage. (Am J Dent 2010;23:43-46).

CLINICAL SIGNIFICANCE : Incorporation of phyllosilicate in the experimental Portland cements did not improve the pushout strength compared to the commercially available ProRoot MTA. PBS immersion decreased the push-out strength of modified Portland cements while ProRoot MTA exhibited higher push-out strength after immersion in PBS.

: Dr. Francesco Iacono, Department of Oral Sciences, Alma Mater Studiorum, University of Bologna, Via San Vitale 59, 40125 Bologna, Italy. E- : francesco.iacono@hotmail.it

Introduction

Modified Portland cements (PCs) like mineral trioxide aggregate (MTA) have multiple uses in dentistry.[1-4] These materials contain tricalcium and dicalcium silicate, and consist of a powder of fine hydrophilic particles that sets in water. Several studies are available on the chemical and physical properties of these materials.[5-7] Many authors agree that a significant feature of these materials is their ability to create an adequate seal.[8-10] Evidence of the interaction of Portland cements with phosphate buffered saline (PBS) resulting in the formation of hydroxyapatite (HA) crystals[11,12] indicates that these cements can create HA in physiological tissue fluids.[13]

Although PC-based cements fulfill most of the requirements for an endodontic filling material, their working properties are less than ideal. When these cements are mixed with water, the resulting cement pastes are difficult to handle and the setting times are long. Calcium chloride has often been incorporated in PC-based cements as an accelerator to shorten the setting time with a minimal impact on their physical properties or leakage.[14-16] Calcium chloride and phyllosilicate[a] (montmorillonite)-containing materials based on Portland cement were recently developed for endodontics to improve handling and physical characteristics and extend the clinical applications. The new materials showed improved in vitro properties such as marginal adaptation and sealing ability[9,17] and biocompatibility.[18,19] These studies used phyllosilicate clay as a plasticizing agent to improve the handling characteristics and dimension stability of the PC-based cements.

The ability of endodontic materials to resist deformation of established seals via micromechanical retention or friction is essential to the survival of the material-dentin interface during intraoral tooth flexure.[20]

This study assessed the push-out strength of modified PCs. A dentin adhesive and a resin-modified glass-ionomer cement were used as control materials. All the materials were evaluated after 1 month of incubation in water or PBS. The null hypothesis was that the push-out strength does not differ in the modified PCs and ProRoot MTA.

Materials and Methods

Sample preparation - Forty-two single-rooted teeth extracted for orthodontic/periodontal reasons were collected under a protocol reviewed and approved by the Human Assurance Committee of the Medical College of Georgia. For each tooth, a 0.90 ± 0.10 mm thick longitudinal slab was prepared by making buccolingual cuts perpendicular to the longitudinal axis of the tooth using a slow-speed diamond saw[b] under water-cooling. A 0.6 mm drill bit was used to prepare pilot holes in the radicular dentin. Each pilot hole was carefully drilled so that it was equidistant from the cementum and the canal wall. Six pilot holes were prepared for each tooth. Each hole was then enlarged using a size 40, 25 mm long 0.04 taper Profile nickel titanium rotary instrument.[c] A miniature drill press was configured so that the Profile files penetrated to the D16 diameter of the rotary instrument along the surface of the tooth slab. This permitted preparation of 252 truncated holes that simulated standardized circular defects. The tooth slabs were immersed in 17% EDTA and ultrasonicated for 5 minutes to remove the smear layer created during the hole-shaping procedures. The slabs were then immersed in 6.15% sodium hypochlorite (NaOCl) and ultrasonicated for 5 minutes to dissolve organic debris.

The 42 root slabs containing 252 holes were divided into seven groups, each containing 36 holes: Group I was filled with white PC (CEM I[d]) mixed with anhydrous calcium sulphate and calcium chloride (PC1); Groups II, III and IV (PC2, PC3, PC4, Table 1) were filled with the same modified

Table 1. Composition of tested materials..

Code	Composition
PC1	White Portland cement (thermally and mechanically treated), calcium sulphate, calcium chloride
PC2	Same as PC1 but with addition of 1% phyllosilicate
PC3	Same as PC1 but with addition of 2% phyllosilicate
PC4	Same as PC1 but with addition of 5% phyllosilicate
ProRoot MTA	Same as PC1 but with addition of bismuth oxide for radiopacity sterilization and sieving to narrow particle size.
Vitrebond	Polyacrylic acid with pendent vinyl goups and diphenyliodonium chloride to make it light curable, plaus acid-susceptable glass fillers.
Clearfil SE	Primer: hydroxyethyl methacrylate (HEMA), water, ethanol, 10-methacryloyloxydecamethylene phosphotic acid (MDP); Adhesive: HEMA, MDP, dimethacrylates.

Portland cement but mixed with 1, 2 and 5 wt% of phyllosilicate.[a] The experimental modified PCs are patented formulations (University Patent EP 07425074.7 and USA US60/900.467; extension PCT/EP2008/051583) designed and prepared at the Centre of Biomineralogy, Crystallography and Biomaterials.[e] Group V holes were filled with ProRoot MTA,[c] Group VI holes were filled with Vitrebond[f] and Group VII holes were filled with Clearfil SE Bond.[g] The PCs and ProRoot MTA were mixed with a powder/liquid ratio of 3/1. Vitrebond and Clearfil SE Bond were used according to the manufacturer's recommendations, and cured with a LED light-curing unit (Elipar FreeLight 2[f]) with an output intensity of 600 mW/cm^2. All cavities from one tooth slab were filled with one type of cement or adhesive. Each tooth slab was placed over a Mylar strip,[h] which in turn was placed over a microscope glass slide. The cement material was forced into the cavities with a small spatula so that each hole was filled to excess with the material. The surface of the tooth slab was then covered with another Mylar strip and a glass slide. The assembly was secured with binder clips so that excess material was expressed laterally from the surface and bottom Mylar strips. The assemblies were transferred to a humidity chamber to be stored under 100% relative humidity for 48 hours. The surfaces of each tooth slab were polished with 800-grit silicon paper under water to remove excess material.

Push-out strength - The push-out strength of the material was investigated after 1 month of incubation in water or in phosphate buffered saline (PBS). To prevent microbial growth, 0.02% sodium azide was included in the solutions.

The push-out strength of the set root canal sealers was evaluated using a thin-slice push-out test design according to the method of Chandra & Ghonem.[21] Prior to testing, the thickness of each tooth slab was measured using a pair of calipers. A 0.7 mm diameter carbon steel cylindrical plunger was used for the push-out test. The plunger was attached to a 100 N load cell connected to a universal testing machine (Vitrodyne, Model V1000 Universal Tester[i]). All specimens were loaded at a cross-head speed of 0.6 mm/minute.

The push-out device consisted of a clear Plexiglas platform with a vertical cylindrical channel, which served as the support for the tooth slab and provided space for the vertical movement of the plunger through the truncated hole (Fig. 1). To ensure optimal alignment of the plunger with the sealer-filled hole, a horizontal channel was drilled through the Plexiglas platform into the vertical channel (Fig. 1). A fiber optic light guide was inserted into the horizontal channel to provide high intensity illumination of the restored truncated hole during the alignment procedure.

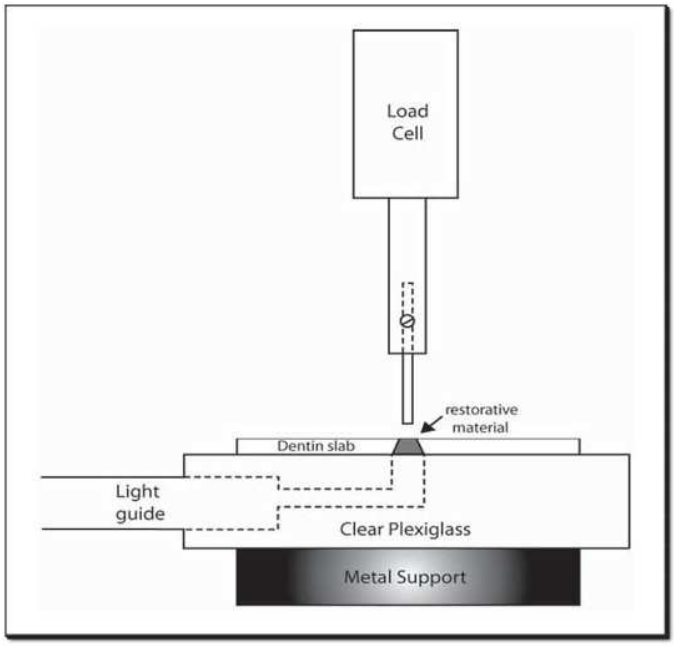

Fig. 1. Diagram of the clear plastic push-out platform mounted below the 0.7 mm diameter steel plunger that in turn was mounted on a 100 N load cell. Note the hole in the platform is directly beneath the plunger. A fiber-optic light guide inserted into a horizontal channel in the plastic plate provides high intensity illumination of the restored truncated hole during alignment procedures.

Statistical analysis of strength tests - Push-out strength of the materials was computed by dividing the maximum load (N) derived from the load displacement curve by the material-dentin interfacial area (mm^2) and expressed in megaPascals (MPa). Initial attempts to analyze the data with a two-way ANOVA (material vs. storage media) revealed that the data were not distributed normally, had unequal variances and had significant interactions. Therefore, the data were analyzed using the least square means (LSM) method. Least square means are the expected value of group means that one expects for a balanced design involving the group variable, with all covariates held at their mean value. The variance in the LSM value are given in standard error of the mean (SEM) instead of standard deviation (SD). Multiple comparisons of the LSM were performed by the Holm-Sidak method. Statistical significance was set in advance at = 0.05. The power of the LSM test was 1.0 for material, 0.9 for storage media and 0.85 for material vs. storage media.

Results

The push-out strength results are shown in Fig. 2. The mean 1-month push-out strength of PC1 was 10 MPa regardless of the storage solution (water or PBS). By contrast, PC2 had a very low push-out strength after 1 month of storage. When PC3 specimens were tested, although their mean values were lower than those of PC1 due to their relatively high variance, they were not significantly different from PC1, and they did not change in water or PBS. Portland cement 4 (PC4) 1-month push-out strengths in water or PBS did not significantly differ from those of PC1-2. ProRoot MTA

Table 2. Push-out strength of test materials in PBS or water.

Material	Time	Storage	Push-out strength (MPa)*
PC1 + 0% ps	1 month	PBS	12.3 ± 1.5 c
PC2 + 1% ps	1 month	PBS	1.3 ± 1.2 a
PC3 + 2% ps	1 month	PBS	7.0 ± 1.3 b
PC4 + 5% ps	1 month	PBS	8.4 ± 1.4 b
Pro Root MTA	1 month	PBS	11.6 ± 1.6 c
Vitrebond	1 month	PBS	24.2 ± 1.2 d
Clearfil SE Bond	1 month	PBS	21.2 ± 1.6 d
PC1 + 0% ps	1 month	Water	9.5 ± 1.4 c
PC2 + 1% ps	1 month	Water	3.1 ± 1.5 a
PC3 + 2% ps	1 month	Water	6.5 ± 1.2 b
PC4 + 5% ps	1 month	Water	5.1 ± 1.2 b
Pro Root MTA	1 month	Water	4.8 ± 1.4 b
Vitrebond	1 month	Water	19.7 ± 1.2 d
Clearfil SE Bond	1 month	Water	25.4 ± 1.1 d

*Values are least squares ± standard error of the mean. PC = Portland cement, ps = phyllosilicate.
Values identified by different letters are significantly different (P< 0.05).

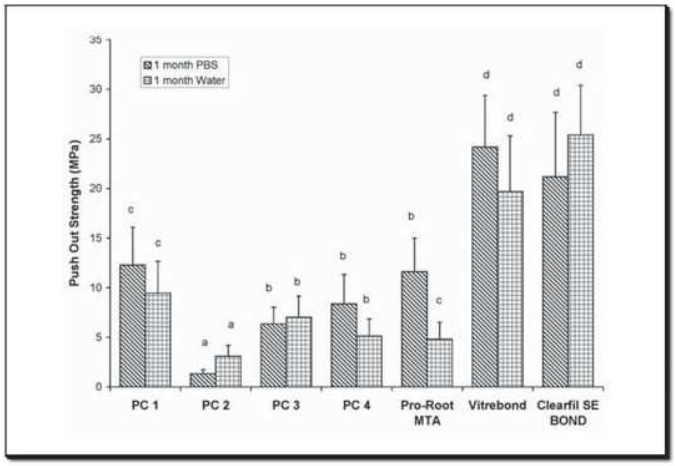

Fig. 2. Push-out strength (MPa) of modified Portland cements PC1-PC4, ProRoot MTA, Vitrebond and Clearfil SE Bond. The height of each bar represents the mean value of 10 specimens. Half brackets indicate plus one standard deviation. Different lower case letters indicate significant differences (P< 0.05) between groups tested after 1 month of immersion in water or phosphate buffered saline (PBS).

push-out strength was twice as high (P< 0.05) in PBS as in water (Table 2).

The two resin-based restoratives, Vitrebond and Clearfil SE Bond had significantly (P< 0.05) higher push-out strengths than those of the modified PCs, and their bond strengths were unaffected by time or storage solution (Fig. 2).

Discussion

The present study assessed the 1-month push-out strength of phyllosilicate-modified Portland-based cements formulated to improve their handling characteristics. Montmorillonite is a phyllosilicate mineral (deriving from deposits of weathered volcanic ash) formed by stacked silicate sheets (two silica-oxygen tetrahedral sheets sandwiching an aluminium or magnesium octahedral sheet) interposed by water and exchangeable interlayer cations (charge-balancing counterions). Montmorillonite is characterized by high cation exchange ability, swelling capacity and strong adsorption. Because of its hydrophilic nature the montmorillonite swells with the addition of water and may expand considerably due to water penetrating the interlayer molecular spaces and concomitant adsorption. Swelling produces an increase in the 001 interlayer d-spacing.[22] Crystalline swelling of 2:1 layer phyllosilicates is a thermodynamically irreversible process[23,24] and dehydration (removal of interlayer water) is an endothermic reaction starting below 150°C.[22] Previous studies included montmorillonite in the composition of glass-ionomer and bone substitute cements.[25,26]

Shrinkage is a detrimental problem affecting many cements and is responsible for gap formation and marginal sealing reduction. The irreversible swelling of montmorillonite may counteract the shrinkage and enhance dimensional stability over time. With the exception of PC2 in water and PBS, push-out strength did not differ among the modified PCs and ProRoot MTA. Thus, the null hypothesis is accepted, except for PC2.

The use of 1 mm thick root slabs perforated by standardized truncated cone holes made all holes for rinsing identical, rinsing with EDTA/NaOCl lasted exactly the same time, and all specimens were tested with the same-sized plunger. We previously found that there were no regional differences in the dislocation resistance of modified PCs among the coronal, middle and apical thirds of the radicular dentin, so that data from all regions, including the sclerotic dentin along the apical thirds of the root canal, could be pooled.[27]

Several studies have used thin slice push-out tests to evaluate the dislocation resistance of root filling materials.[28-35] Our study adopted a modified push-out protocol specifically designed to examine the retentive potential of pure sealer materials in radicular dentin.[27] Gancedo-Caravia & Garcia-Barbero[36] demonstrated that humidity increased the push-out strength of ProRoot MTA. Huffman et al[27] compared the push-out strength of an experimental calcium silicate-based root canal sealer, AH Plus Jet and Pulp Canal Sealer. They demonstrated a higher push-out strength of the calcium silicate-based cements, particularly after storage in PBS wherein carbonated apatites may be formed along the material-radicular dentin interface,[37] improving the frictional resistance[38] of the cement to dislocation.

Modified PCs resist displacement from dentin due to the intrinsic roughness of EDTA/NaOCl treated radicular dentin, the intrinsic roughness of the cements, and their intrinsic cohesive strength. There is some micromechanical retention due to interfacial friction and the cohesive shear strength of cement particles extending into microscopic undercuts in the dentin. As displacement force is applied to these cements vertically, it creates shear stress on the cement particles within dentin undercuts. When these shear stresses exceed the cohesive strength of the material, the bulk cement is vertically displaced slightly but may stop as another cement particle encounters another dentin undercut.

The effect of immersing calcium-silicate cements in PBS on a push-out test was first tested by Huffman et al[27] and then in the present study. Neither the resin-based material nor those of the PC-based materials Clearfil SE Bond and Vitrebond push-out strengths were significantly different when stored in water vs. PBS, except for Pro-Root MTA. Pro-Root MTA stored in water gave lower push-out strengths (P< 0.05) than those stored in PBS (Table 2, Fig. 2). The biocoating of apatite formed on the surface of Pro-Root MTA after immersion in PBS[12,27] may modify the retention and friction of cements on dentin walls. ProRoot MTA showed results not statistically different from white Portland cement

the active ingredient in white ProRoot MTA.[39] The incorporation of phyllosilicate (MMT) in white Portland cements (PCs) did not improve the push-out strength of these materials compared to commercially available ProRoot MTA. The push-out strength of ProRoot MTA was significantly higher ($P < 0.05$) after immersion in phosphate buffered solution, suggesting that simulated body fluids play an important role in increasing its mechanical properties. Further investigations are necessary to evaluate the chemical and mechanical transformation of white MTAs induced by PBS.

a. Montmorillonite-MMT, CNR, Italy.
b. Isomet, Buehler Ltd., Lake Bluff, IL, USA.
c. Dentsply Tulsa Dental Specialties, Tulsa, OK, USA.
d. CEM I, Aalborg White, Denmark.
e. Department of Earth Science, University of Bologna, Italy.
f. 3M ESPE, St. Paul, MN, USA.
g. Kuraray Medical Inc., Tokyo, Japan.
h. Angst & Pfister, Geneva, Switzerland.
i. Liverco, Inc., Burlington, VT, USA.

Acknowledgements:To Michelle Barnes for secretarial support.

Disclosure statement: All authors have no conflict of interest.

Dr. Iacono is an Instructor, Master of Clinical Endodontics, Mr. Siboni is a graduate student, Dr. Prati is Professor and Chair, Department of Dental Sciences, Endodontic Clinical Section; Dr. Gandolfi is a Researcher, Centre of Biomineralogy, Crystallography and Biomaterials (Dept. of Earth Sciences), Alma Mater Studiorum, University of Bologna, Bologna, Italy. Mr. Huffman is a dental student; Mr. Sword is a PhD graduate student; Ms Agee is a Research Associate; Dr. Tay is Associate Professor, Department of Endodontics, School of Dentistry, Dr. Pashley is Regent's Professor, Department of Oral Biology; Medical College of Georgia, Augusta, GA, USA.

References

1. Main C, Mirzayan N, Shabahang S, Torabinejad M. Repair of root perforations using mineral trioxide aggregate:A long-term study. J Endod 2004;30:80-83.
2. Gaitonde P, Bishop K. Apexification with mineral trioxide aggregate:an overview of the material. Eur J Prosthodont Restor Dent 2007;15:41-45.
3. Nair PN, Duncan HF, Pitt Ford TR, Luder HU. Histological, ultrastructural and quantitative investigations on the response of healthy human pulps to experimental capping with mineral trioxide aggregate:A randomized controlled trial. Int Endod J 2008;41:128-150.
4. Saunders WP. A prospective clinical study of periradicular surgery using mineral trioxide aggregate as a root-end filling. J Endod 2008;34:660-665.
5. Camilleri J, Montesin FE, Brady K, Sweeney R, Curtis RV, Ford TR. The constitution of mineral trioxide aggregate. Dent Mater 2005;21:297-303.
6. Islam I, Chng HK, Yap AU. Comparison of the physical and mechanical properties of MTA and Portland cement. J Endod 2006;32:193-197.
7. Camilleri J. Hydration mechanisms of mineral trioxide aggregate. Int Endod J 2007;40:462-470.
8. Matt GD, Thorpe JR, Strother JM, McClanahan SB. Comparative study of white and gray mineral trioxide aggregate (MTA) simulating a one- or two-step apical barrier technique. J Endod 2004;30:876-879.
9. Gandolfi MG, Sauro S, Mannocci F, Watson TF, Zanna S, Capoferri M, Prati C, Mongiorgi R. New tetrasilicate cements as retrograde filling material:An in vitro study on fluid penetration. J Endod 2007;33:742-745.
10. Martin RL, Monticelli F, Brackett WW, Loushine RJ, Rockman RA, Ferrari M, Pashley DH, Tay FR. Sealing properties of mineral trioxide aggregate orthograde apical plugs and root fillings in an in vitro apexification model. J Endod 2007;33:272-275.
11. Sarkar NK, Caicedo R, Ritwik P, Moiseyeva R, Kawashima I. Physicochemical basis of the biologic properties of mineral trioxide aggregate. J Endod 2005;31:97-100.
12. Tay FR, Pashley DH, Rueggeberg FA, Loushine RJ, Weller RN. Calcium phosphate phase transformation produced by the interaction of the Portland cement component of white mineral trioxide aggregate with a phosphate-containing fluid. J Endod 2007;33:1347-1351.
13. Tay FR, Pashley DH. Guided tissue remineralisation of partially demineralised human dentine. Biomaterials 2008;29:1127-1137.
14. Antunes Bortoluzzi E, Juárez Broon N, Antonio Hungaro Duarte M, de Oliveira Demarchi AC, Monteiro Bramante C. The use of a setting accelerator and its effect on pH and calcium ion release of mineral trioxide aggregate and white Portland cement. J Endod 2006;32:1194-1197.
15. Wiltbank KB, Schwartz SA, Schindler WG. Effect of selected accelerants on the physical properties of mineral trioxide aggregate and Portland cement. J Endod 2007;33:1235-1238.
16. Hong ST, Bae KS, Baek SH, Kum KY, Lee W. Microleakage of accelerated mineral trioxide aggregate and Portland cement in an in vitro apexification model. J Endod 2008;34:56-58.
17. Gandolfi MG, De Carlo B, Zanna S, Sauro S, Prati C, Mongiorgi R. Chemical and physical characterization of a tetrasilicate-based mineral cement. It J Oper Dent 2006;4:80-84.
18. Gandolfi MG, Pagani S, Perut F, Ciapetti G, Baldini N, Mongiorgi R, Prati C. Innovative silicate-based cements for endodontics:A study of osteoblast-like cell response. J Biomed Mater Res A 2008;87:477-486.
19. Gandolfi MG, Perut F, Ciapetti G, Mongiorgi R, Prati C. New Portland cement-based materials for endodontics mixed with articaine solution:A study of cellular response. J Endod 2008;34:39-44.
20. Panitvisai P, Messer HH. Cuspal deflection in molars in relation to endodontic and restorative procedures. J Endod 1995;21:57-61.
21. Chandra N, Ghonem H. Interfacial mechanics of push-out tests:Theory and experiments. Composites Part A:Applied Science and Manufacturing 2001;32:578-584.
22. Bray HJ, Redfern SAT. Kinetics of dehydration of Ca-montmorillonite. Phys Chem Miner 1999;26:591-600.
23. Laird DA, Shang C, Thompson ML. Hysteresis in crystalline swelling of smectites. J Colloid Interface Sci 1995;171:240-245.
24. Laird DA. Model for the crystalline swelling of 2:1 layer phyllosilicates. Clays Clay Miner 1996;44:553-559.
25. Dowling AH, Stamboulis A, Fleming GJ. The influence of montmorillonite clay reinforcement on the performance of a glass ionomer restorative. J Dent 2006;34:802-810.
26. Kwon SY, Cho EH, Kim SS. Preparation and characterization of bone cements incorporated with montmorillonite. J Biomed Mater Res B 2007;83:276-284.
27. Huffman BP, Mai S, Pinna L, Weller RN, Primus CM, Gutmann JL, Pashley DH, Tay FR. Dislocation resistance of ProRoot Endo Sealer, a calcium-silicated-based root canal sealer, from radicular dentin. Int Endod J 2009;42:34-46.
28. Gesi A, Raffaelli O, Goracci C, Pashley DH, Tay FR, Ferrari M. Interfacial strength of Resilon and gutta-percha to intraradicular dentin. J Endod 2005;31:809-813.
29. Skidmore LJ, Berzins DW, Bahcall JK. An in vitro comparison of the intraradicular dentin bond strength of Resilon and gutta-percha. J Endod 2006;32:963-966.
30. Ungor M, Onay EO, Orucoglu H. Push-out bond strengths:The Epiphany-Resilon endodontic obturation system compared with different pairings of Epiphany, Resilon, AH Plus and gutta-percha. Int Endod J 2006;39:643-647.
31. Bouillaguet S, Bertossa B, Krejci I, Wataha JC, Tay FR, Pashley DH. Alternative adhesive strategies to optimize bonding to radicular dentin. J Endod 2007;33:1227-1230.
32. Fisher MA, Berzins DW, Bahcall JK. An in vitro comparison of bond strength of various obturation materials to root canal dentin using a push-out test design. J Endod 2007;33:856-858.
33. Jainaen A, Palamara JE, Messer HH. Push-out bond strengths of the dentine-sealer interface with and without a main cone. Int Endod J 2007;40:882-890.
34. Nagas E, Cehreli ZC, Durmaz V, Vallittu PK, Lassila LV. Regional push-out bond strength and coronal microleakage of Resilon after different light-curing methods. J Endod 2007;33:1464-1468.
35. Sly MM, Moore BK, Platt JA, Brown CE. Push-out bond strength of a new endodontic obturation system (Resilon/Epiphany). J Endod 2007;33:160-162.
36. Gancedo-Caravia L, Garcia-Barbero E. Influence of humidity and setting time on the push-out strength of mineral trioxide aggregate obturations. J Endod 2006;32:894-896.
37. Weller RN, Tay KCY, Garrett LV, Mai S, Primus CM, Gutmann JL, Pashley DH, Tay FR. Microscopic appearance and apical seal of root canals filled with gutta-percha and ProRoot Endo Sealer after immersion in a phosphate-containing fluid. Int Endod J 2008;41:977-986.
38. Goracci C, Fabianelli A, Sadek FT, Papacchini F, Tay FR, Ferrari M. The contribution of friction to the dislocation resistance of bonded fiber posts. J Endod 2005;31:608-612
39. Primus CM. Dental Material. United States Patent Office 2005;Patent Application 20050263036.

International Endodontic Journal
doi:10.1111/j.1365-2591.2010.01774.x

Dynamic sealing ability of MTA root canal sealer

J. Camilleri[1], M. G. Gandolfi[2], F. Siboni[2] & C. Prati[2]

[1]Department of Building and Civil Engineering, Faculty for the Built Environment, University of Malta, Malta; and[2]Department of Oral Sciences, Endodontic Clinical Section, Laboratory of Biomaterials, University of Bologna, Bologna, Italy

Abstract

Camilleri J, Gandolfi MG, Siboni F, Prati C. Dynamic sealing ability of MTA root canal sealer. International Endodontic Journal, 44, 9-20, 2011.

Aims To evaluate (i) the sealing ability of two sealers, mineral trioxide aggregate sealer (MTAS) and Pulp Canal Sealer (PCS), used with gutta-percha utilizing the fluid filtration method, (ii) leaching and surface characteristics in Hank's balanced salt solution (HBSS) over a period of time.

Methodology Surface characteristics in HBSS were evaluated under the scanning electron microscope after 1 and 28 days, and the leaching of both sealers were assessed by inductively coupled plasma atomic absorption spectrometry (ICP-AAS). In addition, 24 single rooted extracted teeth were root filled using warm vertical compaction with either MTAS or PCS used as sealers with gutta-percha. Four teeth were used as positive and negative controls. Sealing ability was evaluated after 1 or 28 days using the fluid filtration method.

Results Mineral trioxide aggregate sealer exhibited crystalline deposits rich in calcium and phosphorus on its surface when in contact with a physiological solution. These crystalline deposits were absent in PCS and on MTAS stored at 100% humidity. The sealing ability of MTAS was similar to that of PCS.

Conclusions The novel sealer based on mineral trioxide aggregate had comparable sealing ability to a proprietary brand sealer cement. In contact with a simulated body fluid, the MTA sealer released calcium ions in solution that encouraged the deposition of calcium phosphate crystals.

Keywords: endodontic sealer, fluid filtration, inductively coupled plasma, mineral trioxide aggregate, Portland cement, Pulp Canal Sealer, scanning electron microscopy.

Received 27 March 2010; accepted 13 May 2010

Introduction

Mineral trioxide aggregate (MTA) is used primarily to seal lateral root perforations (Lee et al. 1993, Pitt Ford et al. 1995) and as a root-end filling material (Torabinejad et al. 1995, 1997, Chong et al. 2003, Saunders 2008). MTA can also be used for a variety of other applications (Schwartz et al.1999, Torabinejad & Chivian 1999) including pulp capping (Pitt Ford et al. 1996, Bakland 2000, Aeinehchi et al. 2003, Faraco Junior & Holland 2004) and as a dressing over pulpotomies in permanent teeth (Holland et al. 2001) and during apexification procedures (Witherspoon et al. 2008). It is a bioactive material that produces calcium hydroxide (Camilleri 2007, 2008a), which is released in solution (Fridland & Rosado 2003, Tanomaru-Filho et al. 2009) and induces formation of hydroxyapatite structures in simulated body fluid (Sarkar et al. 2005, Bozeman et al. 2006). Newer developments of MTA include its use as a root canal sealer. Currently, three MTA sealer formulations are available; Endo-CPM-Sealer (EGEO srl, Buenos Aires, Argentina), MTA Obtura (Angelus, Soluçoˇes Odontológicas, Londrina PR, Brazil) and ProRoot Endo Sealer (Dentsply Maillefer, Ballaigues, Switzerland). The composition of CPM sealer after mixing is reported to be 50% MTA (SiO_2, K_2O, Al_2O_3, SO_3, CaO and Bi_2O_3), 7% SiO_2, 10% $CaCO_3$, 10% Bi_2O_3, 10% $BaSO_4$,

Correspondence: Dr. Josette Camilleri Ph.D., Department of Building and Civil Engineering, Faculty for the Built Environment, University of Malta, Msida MSD 2080, Malta (Tel.: 00356 2340 2870; fax: 00356 21330190; e-mail: josette.camilleri@um.edu.mt).

1% propylene glycol alginate, 1% propylene glycol, 1% sodium citrate and 10% calcium chloride (Gomes-Filho et al. 2009). MTA-Obtura is a mixture of white MTA with a proprietary viscous liquid (Monteiro Bramante et al. 2008). ProRoot Endo Sealer is calcium silicate-based endodontic sealer. The major components of the powder of ProRoot Endo Sealer are tricalcium silicate and dicalcium silicate, with inclusion of calcium sulphate as setting retardant, bismuth oxide as radiopacifier and a small amount of tricalcium aluminate. Tricalcium aluminate is necessary for the initial hydration reaction of the cement. The liquid component consists of viscous aqueous solution of a water-soluble polymer (Weller et al. 2008, Huffman et al. 2009). The use of water-soluble polymers mixed with materials based on Portland cement added to the water to improve the workability has been reported (Camilleri et al. 2005a, Camilleri 2008b,c,d,e). The polymer did not seem to affect the biocompatibility of the materials (Camilleri et al. 2005a, Camilleri 2008e), and the hydration characteristics were similar to those reported for MTA (Camilleri 2009).

Sealers based on MTA have been reported to be biocompatible, stimulate mineralization (Gomes-Filho et al. 2009), and encourage apatite-like crystalline deposits along the apical and middle thirds of canal walls (Weller et al. 2008). These materials exhibited higher push-out strengths than Pulp Canal Sealer (PCS) particularly after storage in simulated body fluid (Huffman et al. 2009) and had similar sealing properties to epoxy resin-based sealer when evaluated using the fluid filtration system (Weller et al. 2008).

Root canal sealers are used in conjunction with gutta-percha to fill root canals in various methods, namely cold lateral condensation, warm vertical compaction or carrier-based techniques. The function of the sealer is to obliterate discrepancies such as grooves and lateral depressions (Zielinski et al. 2008) that cannot be filled with gutta-percha, to improve the marginal adaptation to the dentinal walls (Cobankara et al. 2006) and to fill lateral canals (Venturi et al. 2005). The final root filling should prevent microleakage and bacterial contamination (Siqueira & Rocas 2007). Gutta-percha is impermeable; thus, any leakage occurs at the sealer to gutta-percha and sealer to tooth interfaces (Hovland & Dumsha 1985). Microleakage is routinely assessed by leakage to tracers, namely dyes (Beckham et al. 1993, Zaia et al. 2002), bacteria (Barthel et al. 1999) and endotoxin (Trope et al. 1995). Alternatively, the assessment can be performed using a fluid filtration device (Wu et al. 1998a, Bouillaguet et al. 2008). The fluid filtration method has already been used to evaluate the sealing ability of ProRoot MTA used for root-end filling with (Bates et al. 1996, Tang et al. 2002) and without (Pelliccioni et al. 2007) the use of water for hydration, furcation repair (Weldon et al. 2002, Hardy et al. 2004), and orthograde plugs (Martin et al. 2007). It has also been used for MTA Angelus (De-Deus et al. 2007) and MTA Bio, a laboratory-controlled water-based cement (De-Deus et al. 2007, 2008). The sealing ability of sealers based on MTA namely ProRoot Endo Sealer (Weller et al. 2008), other variants of MTA (Gandolfi et al. 2007) have also been evaluated with this method.

The aim of this study was to evaluate the sealing ability of two sealers, MTA sealer and PCS, used with gutta-percha utilizing the fluid filtration method as well as leaching and surface characteristics in Hank's balanced salt solution (HBSS) over a period of time.

Methodology

Materials used in this study included PCS (Kerr-Hawe S.A., Bioggio, Switzerland) and mineral trioxide aggregate sealer (MTAS). The MTAS consisted of a mixture of 80% white Portland cement (Aalborg white, Aalborg, Denmark) and 20% bismuth oxide (Fischer Scientific, Leicester, UK). The PCS was mixed according to manufacturer's instructions, whilst the MTAS was mixed in water to powder ratio of 0.30 with an addition of 20 lL $g^{)1}$ of cement of water soluble polymer (Degussa Construction Chemicals, Manchester, UK) added to the mixing water (Camilleri 2009). The materials were tested after immersion in a simulated body fluid namely Hank's Balanced salt solution (HBSS H6648; Sigma-Aldrich, Gillingham, UK). The composition of the HBSS was (g $L^{)1}$) 0.4 KCl, 0.06 KH_2PO_4 anhydrous, 0.35 $NaHCO_3$, 8.0 NaCl, 0.05 Na_2HPO_4 anhydrous and 1.0 d-glucose.

Scanning electron microscopy of the cements

Diskettes 10 mm in diameter and 1 mm high of PCS and MTAS were prepared. Half the diskettes were cured at 100% humidity and the other half were cured in HBSS for either 1 or 28 days. Surface morphology was evaluated after 1 and 28 days under the environmental scanning electron microscope (ESEM Zeiss EVO 50; Carl Zeiss, Oberkochen, Germany) and X-ray energy dispersive analysis (EDX) at an accelerating voltage of 20 kV was performed using a secondary electron detector (EDAX, Oxford INCA 350 EDS detector). The

elemental analysis (weight % and atomic %) of the specimens was performed applying ZAF correction method. The powders of each cement type were also analysed by EDX.

Evaluation of leaching

The chemical analysis of the cement products released into simulated body fluid was performed using inductively-coupled plasma atomic absorption spectroscopy (Varian Medical Systems, Palo Alto, CA, USA). The PCS and MTAS were mixed in a similar way as the previous experiments producing diskettes 10 mm in diameter and 1 mm high. Six diskettes for every material tested were prepared. The specimens were cured for 24 h at 37 C and 100% humidity after which they were weighed to an accuracy of 0.0001 g and immersed in either 3 mL water or HBSS in closed sterile containers (Labplex, Birmingham, UK). The specimens were removed after 1, 14 and 28 days. Containers filled with water and HBSS were used as controls. The leachates were analysed for aluminium, bismuth, calcium, silicon, silver and zinc. The amount of leachate was calculated in lg $g^{)1}$ by using the following formula:

$$\text{Amount of leachate per weight of cement} = \frac{\text{amount of leachate per litre} \quad 0{:}003 \quad 1000}{\text{weight of cement pellet}}$$

Evaluation of sealing ability

Sample preparation

Twenty-four single-rooted teeth extracted for periodontal reasons were used. The study was performed on two experimental groups consisting of 10 teeth in each group. Four teeth were used as positive and negative controls. The teeth selected had similar dimension of root-apex namely a size 30 K-file, a similar diameter of root canal, no sclerotic dentine, circular cross-section of canal and no elliptic section, absence of caries and previous root fillings, absence of lateral canals and root curvature.

Radiographs were taken in the bucco-lingual and mesio-distal directions to establish the canal shape (circularity of cross-section) and to determine the presence of any root curvature and lateral canals. The teeth were decoronated, and the root length was standardized to 12 mm. The root canals were accessed, and canal patency was established using a size 15 K-file. Instrumentation was performed to 0.5 mm short of the radiographic apex using the crown-down technique with ProTaper rotary nickel-titanium instruments (Dentsply Maillefer). The apical preparation was performed to a size 30 master apical file. The diameter of root-apex was standardized in all samples with a size 30 K-file. The canal was irrigated with 10 mL of 5% NaOCl (Ogna, Milano, Italy) between instruments followed by 2 mL EDTA (Glyde file prep; Dentsply Maillefer, Montigny de Bretonneux, France) to remove the smear layer. The canals were dried with paper points and a master Gutta-percha cone (Dentsply Maillefer) was fitted to length and checked for tug-back. The canals were coated with the sealers under study using a size 20 reamer rotated anticlockwise. The master cone was coated with sealer and placed in the canal to working length. The cone was cut to the orifice and compacted with System B plugger (Sybron Endo, Orange, CA, USA) leaving a space of 2 mm coronally. Each root was radiographed to establish the adequacy of filling. An 18-gauge needle inserted across a plexiglass platform was introduced in the canal orifice and the root samples were attached to the platform with cyanoacrylate glue. The external root surface was coated with two layers of nail varnish (Paris, Bellure, Belgium) to seal the surfaces. For the positive control, the root canals of two teeth were cleaned and shaped as described earlier and filled with a master cone and no sealer. The negative control was prepared as described earlier, filled with gutta-percha and PCS and the apex was sealed off with bonding agent (Scotchbond; 3M ESPE, Milan, Italy) and nail varnish. The plexiglass support and tooth assembly was placed in 10 mL of HBSS keeping the free end of the needle un-immersed to mimic the clinical situation, where the coronal end of the tooth is not in contact with biological fluids. The samples were stored at 37 C in sealed containers.

Leakage evaluation

The set-up was connected to a fluid conductive system working at a hydraulic pressure of 6.9 kPa to measure fluid movement (Fig. 1); the system used was as reported previously (Gandolfi et al. 2007, Pelliccioni et al. 2007) The fluid filtration rate was measured over three 4-min periods at 1-min intervals and the mean calculated. The results were expressed as lL $min^{)1}$. The following procedure was repeated after 1 and 28 days following root filling. The specimens were kept at 37 C and the HBSS was changed weekly.

Figure 1 Set-up for determination of sealing ability using a fluid conductive system.

Statistical analysis

The data was evaluated using spss (Statistical Package for the Social Sciences) software (SPSS Inc., Chicago, IL, USA). Analysis of Variance (anova) with P = 0.05 was used to perform multiple comparison tests.

Results

Scanning electron microscopy of the cements

The results for the scanning electron microscopy for both MTAS and PCS are shown in Fig. 2. The MTAS powder had a granular surface appearance with elongated bismuth oxide particles interspersed within the structure (Fig. 2A1). EDX analysis showed the material to be composed of calcium, silicon, aluminium and bismuth (Fig. 2A2). The PCS had a larger particle size distribution (Fig. 2A3) and was composed of zinc and silver (Fig. 2A4). Immersion of MTAS in HBSS resulted in a crystalline deposition over the cement surface after 7-day immersion (Fig. 2B3, B5) and also after 28-day immersion (Fig. 2C3) in HBSS. These crystalline deposits were not present in the MTAS cured at 100% humidity (Fig. 2B1, C1). The crystalline deposits were mainly composed of calcium and phosphorus (Fig. 2B4, B6) initially, with sodium and chlorine peaks at later curing times (Fig. 2C4). The pulp canal sealer surface demonstrated considerable porosity (Fig. 2B7, B9, C5, C7). The curing method did not affect the PCS surface and its chemical composition (Fig. 2B8, B10) at an early age. At 28 days, however, a chlorine peak was observed in the PCS cured at 100% humidity (Fig. 2C8).

Evaluation of leaching

The results for leaching of both sealers in water and in HBSS are shown in Table 1a,b, respectively. The levels of sodium and phosphorus ions in HBSS blank solution and the ions detected in both materials are shown in Table 2. MTAS leached a high level of calcium ions in both soaking solutions. The calcium ion release increased with time and the levels were higher in water than in HBSS. Bismuth was also released in solution with more bismuth being released in HBSS than in water. PCS leached zinc and silica in solution. This leaching was more marked in water. Both sealers had high levels of sodium when soaked in HBSS, but the levels of phosphorus were high for PCS but much lower and reducing to practically below detection limits at 28 days for MTAS.

Evaluation of sealing ability

The sealing ability of the two sealers evaluated using the fluid filtration method is shown in Fig. 3. There was no difference between the two sealers both at 7 days

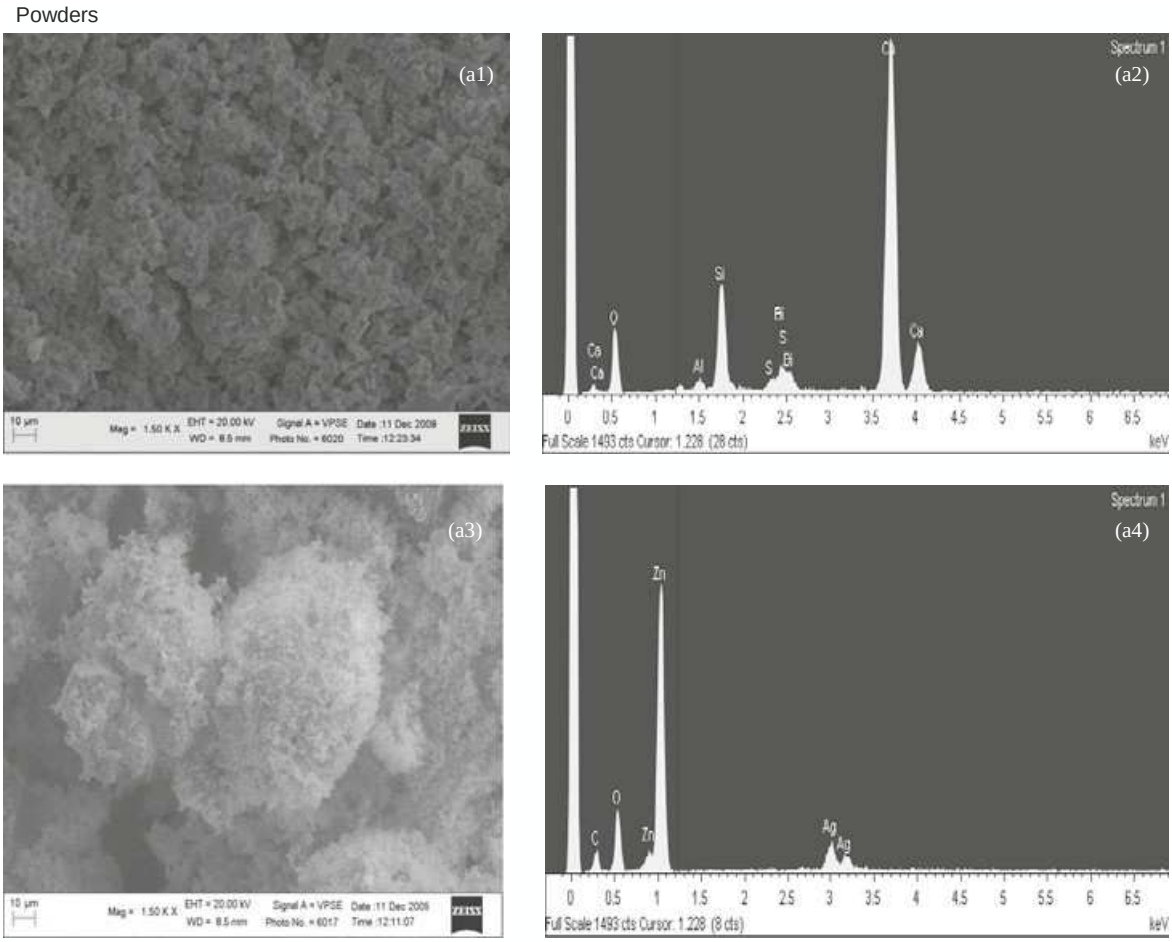

Figure 2 Scanning electron micrographs and X-ray energy dispersive analysis of A: powders (1,2): mineral trioxide aggregate sealer (MTAS), (3, 4): pulp canal sealer (PCS); B: materials cured for 7 days, (1-6): MTAS, (7-10): PCS, (1,2,7,8): cured at 100% humidity, (3-6,9,10): cured in Hank's balanced salt solution (HBSS); C: materials cured for 28 days, (1-4): MTAS, (5-8): PCS, (1,2,5,6): cured at 100% humidity, (3,4,7,8): cured in HBSS; (·1.5K magnification).

(P = 0.301) and at 28 days (P = 0.381). The negative control exhibited little or no leakage, whilst the positive control demonstrated a high level of leakage that increased over the 28-day period.

Discussion

In this study, a new material based on MTA was investigated. This novel material was composed of Portland cement and bismuth oxide, which were mixed with water and a water-soluble polymer. PCS was used as control. This material was chosen because it had a powder and liquid formulation and has been used for a long time in clinical dentistry. The PCS powder was reported to be composed of 34% ZnO, 25% Ag, 30% resins, 11% thymol iodide and the liquid of Canada balsam and eugenol (Kerr data sheet). The peaks for zinc and silver were also demonstrated in this study. MTA powder is constituted of tricalcium and dicalcium silicate, tricalcium aluminate and bismuth oxide (Camilleri 2007, 2008a). Elemental composition of MTAS reported in this study is similar to the elemental composition published for ProRoot MTA (Camilleri et al. 2005b, Asgary et al. 2006). Pulp canal sealer was characterized by a porous structure as demonstrated by the environmental scanning electron microscope. Contact of PCS with a simulated body fluid had no effect on the surface characteristics of this material. On the other hand, a crystalline deposit consisting of calcium and phosphorus was present on the MTAS

7 day curing

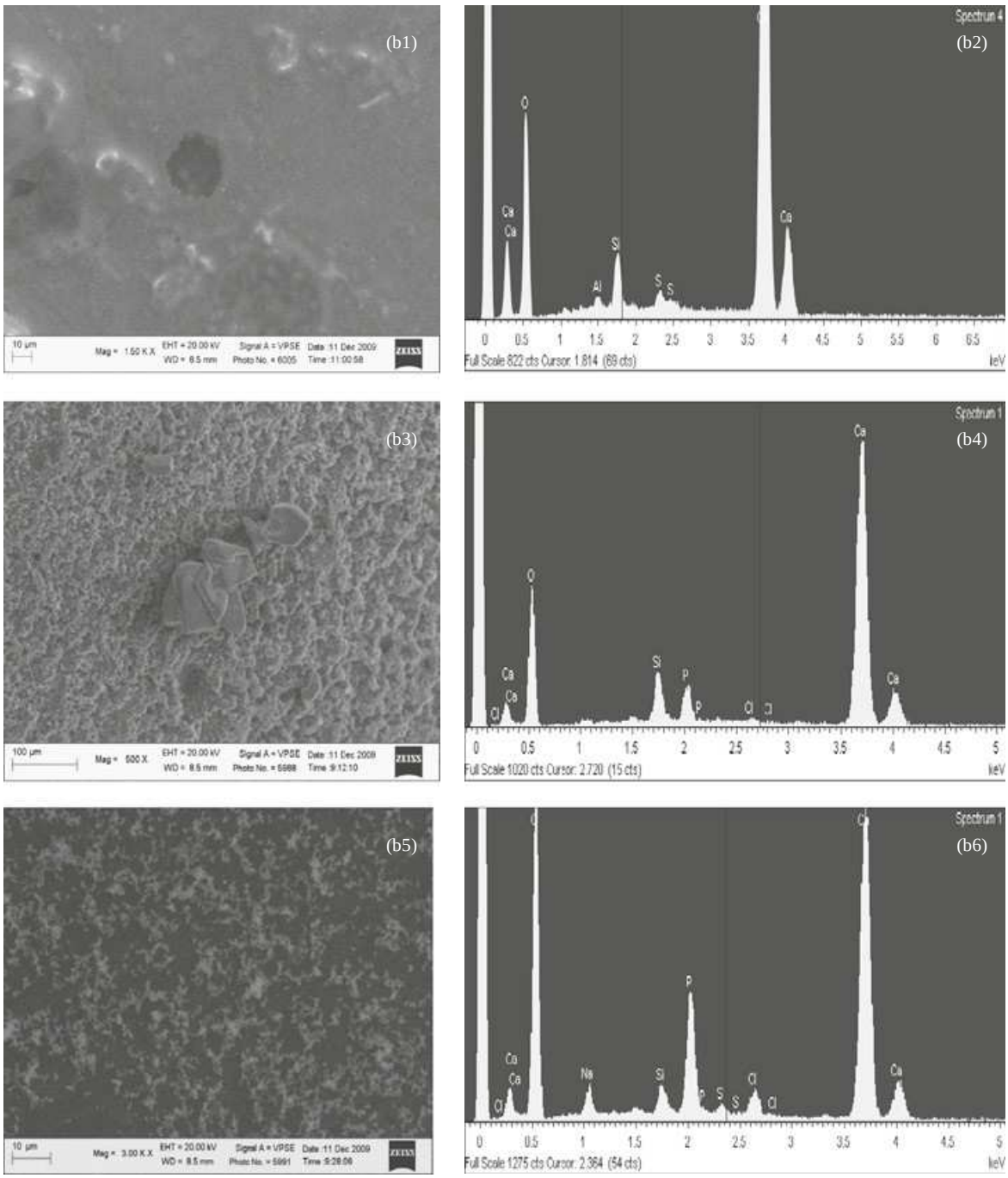

Figure 2b(1-6) (Continued).

surface when the MTA sealer was in contact with a simulated body fluid. MTAS released a high level of calcium ions in solution as indicated by the results of leaching. These calcium ions bind to the phosphates that are present within the simulated body fluid. This again was verified from the ICP results, where the

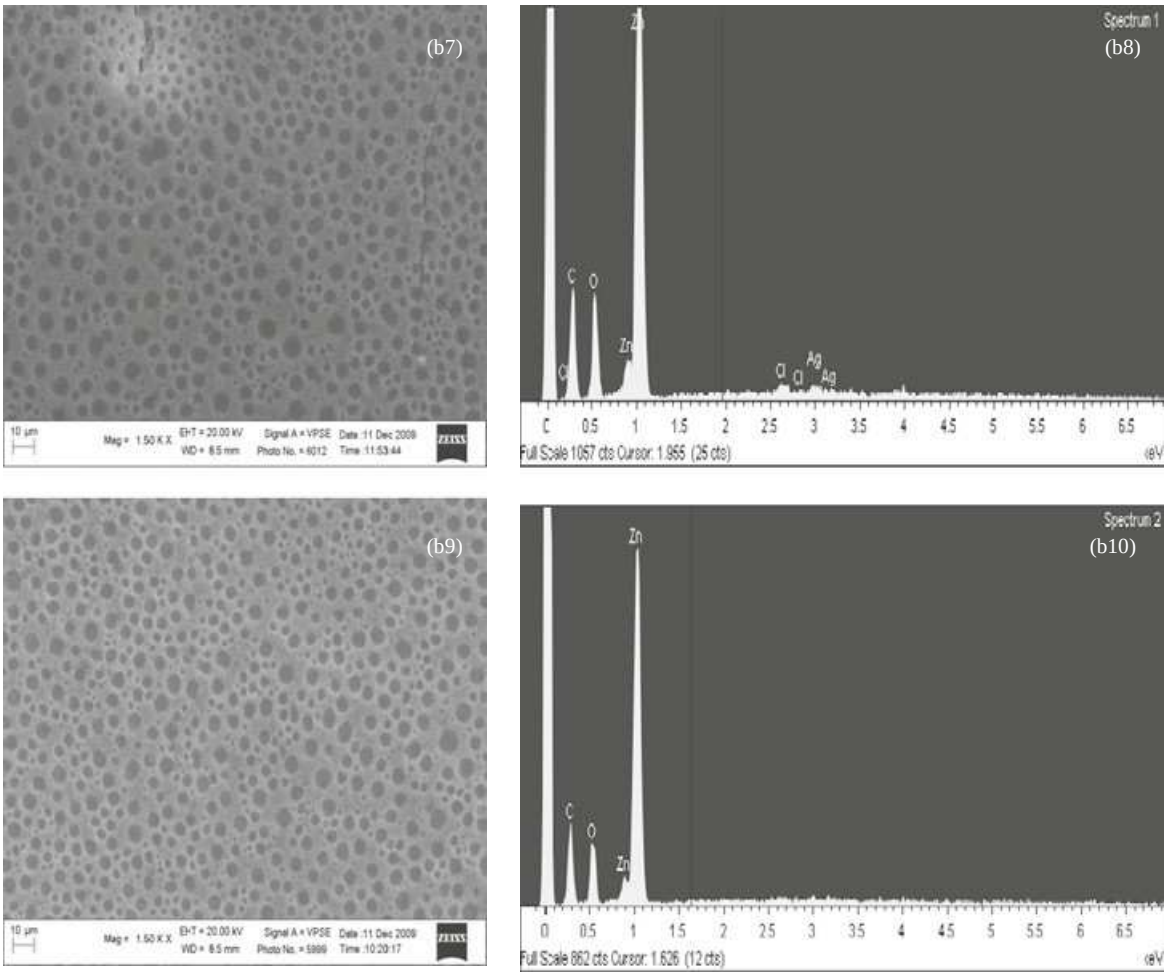

Figure 2b(7-10) (Continued).

phosphate ions were depleted over the 28-day period for MTAS but higher levels were registered for PCS. The deposition of calcium phosphates in the form of apatite and carbonated apatite has already been reported for MTA (Sarkar et al. 2005, Bozeman et al. 2006, Tay et al. 2007, Reyes-Carmona et al. 2009, Taddei et al. 2009, Gandolfi et al. 2010) and Portland cement (Coleman et al. 2007) in contact with simulated body fluids.

The sealing ability of the two sealers used in conjunction with gutta-percha was assessed using fluid filtration. This method is an established method used for the determination of permeability of dentine (Pashley et al. 1983, Tao et al. 1991) and has also been adapted to be used for the evaluation of sealing ability of dental materials including MTA used as a root-end filling material (Bates et al. 1996, Tang et al. 2002) and as a root canal sealer cement in conjunction with gutta-percha (Weller et al. 2008). It is superior to the other methods of evaluation of coronal microleakage; it is nondestructive and allows long-term evaluation of the filling. The results of sealing ability obtained using the fluid penetration method are similar to other test methods (Souza et al. 2008) and assessment of root fillings using bidirectional radiographs (Wu et al. 2009). This method does not employ the use of tracers, which may affect the sealers under test (Ahlberg et al. 1995, Wu et al. 1998b, Camilleri & Pitt Ford 2008). Fluid filtration is more reliable than the standard dye penetration method of evaluating sealing ability of root canal sealers (Camps & Pashley 2003). A pressure of 1 psi (6.895 kPa) was used in this study instead of the

28 day curing

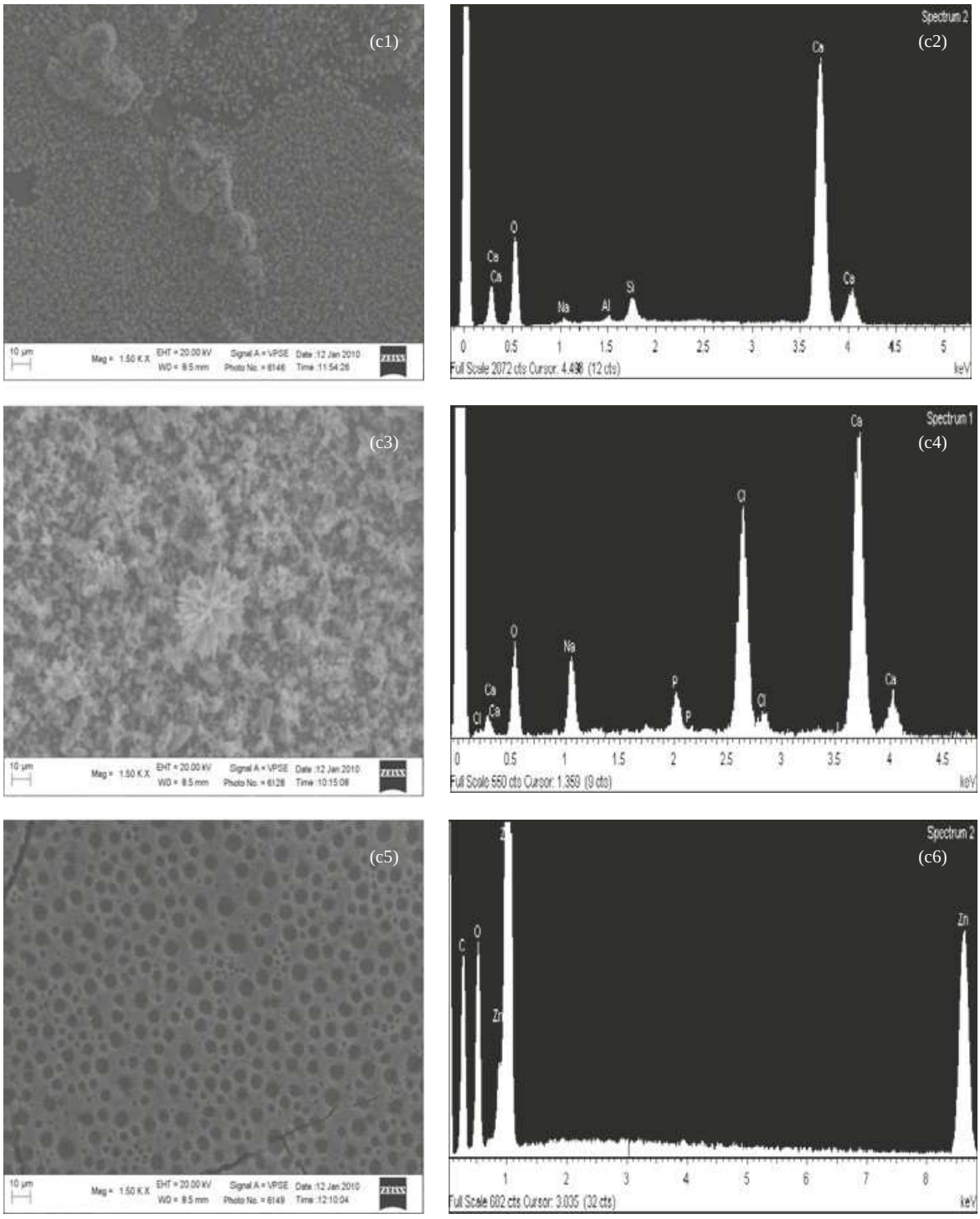

Figure 2c(1-6) (Continued).

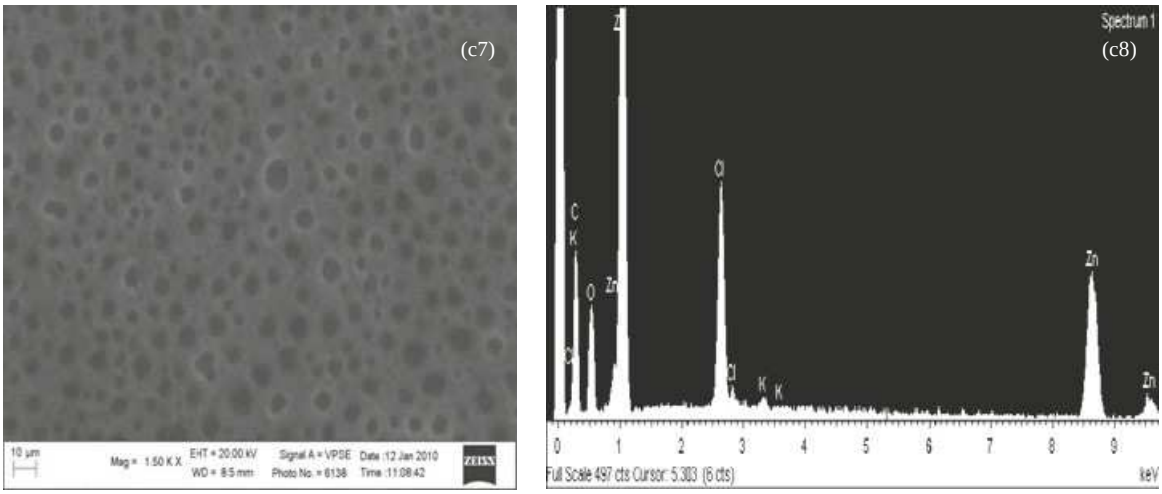

Figure 2c(7-8) (Continued).

Table 1 Elements leached out in lg g)1 of Pulp Canal Sealer (PCS) and mineral trioxide aggregate sealer (MTAS) after 1, 14 and 28 days in water (a), Hank's balanced salt solution (HBSS) (b)

Element detected	PCS			MTAS		
	1 day	14 days	28 days	1 day	14 days	28 days
(a)						
Ag	0.0	0.0	0.0	0.0	0.0	0.0
Al	0.0	0.0	0.0	2.1	0.2	0.0
Bi	0.0	0.0	0.0	3.7	5.6	3.9
Ca	0.0	0.0	0.0	4904	6867	7050
Si	102.9	101.0	79.3	0.0	0.0	0.0
Zn	0.8	68.6	179.4	0.0	0.0	0.0
(b)						
Ag	0.0	0.0	0.0	0.0	0.0	0.0
Al	0.0	0.0	0.0	0.5	0.0	0.0
Bi	0.0	0.0	0.0	27.2	7.4	58.9
Ca	0.0	0.0	0.0	2619	5597	5939
Si	0.0	2.2	54.1	37.2	0.0	43.4
Zn	0.0	0.0	0.0	0.0	0.0	0.0

physiological pressure through dentine, which is 1.3 kPa (Camps et al. 1997) to enhance apical leakage and to obtain detectable leakage values.

In this study, nickel-titanium rotary instruments were used to prepare the root canals in conjunction with gutta-percha cones that matched the taper of the canals. It has been demonstrated that the apical sealing ability of matched-taper single-cone root fillings was comparable with that of lateral condensation and Thermafil techniques (Inan et al. 2009). A number of publications have reported the sealing ability of PCS using the fluid filtration method (Yared & Bou Dagher 1996, Dagher et al. 1997, Pommel et al. 2003, Bouillaguet et al. 2008). All the different sealers tested did not fully prevent fluid flow (Bouillaguet et al. 2008). The sealing ability was reported to reduce with time (Bouillaguet et al. 2008) and also to increase with time (Dagher et al. 1997). PCS was also reported to have a similar or better sealing ability to resin-based sealers (Yared & Bou Dagher 1996, Pommel et al. 2003) and conversely in other studies using the same testing methodology it performed worse than the resin-based sealers (Adanir et al. 2006, Bouillaguet et al. 2008). In this study, the novel sealer MTAS has a sealing ability similar to PCS and the sealing ability decreased with time, whilst that of PCS showed the trend to increase with time. Conversely, research conducted on a novel

Table 2 Solution concentration of ions in parts per million (ppm) detected in Hank's balanced salt solution (HBSS) and Pulp canal Sealer (PCS) and mineral trioxide aggregate sealer (MTAS) after 1, 14 and 28 days

Element detected	HBSS	PCS			MTAS		
		1 day	14 days	28 days	1 day	14 days	28 days
Na	3289	3755.6	3725.2	3495.8	3929.3	3477.3	3303.3
P	25.4	26.1	28.7	17.1	5.1	0.0	0.37

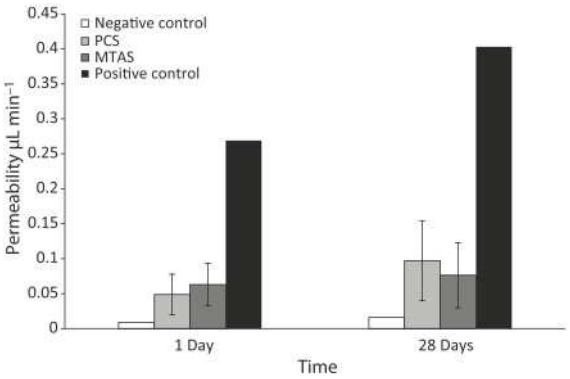

Figure 3 Permeability measurement of teeth obturated with gutta-percha and either Pulp Canal Sealer or mineral trioxide aggregate sealer immersed in HBSS after 1 and 28 days from obturation ±SD.

sealer based on MTA namely ProRoot Endo Sealer demonstrated the superior sealing ability of this material comparable to resin-based sealers and better than PCS (Weller et al. 2008).

Conclusions

The novel sealer based on mineral trioxide aggregate had comparable sealing ability to a proprietary brand sealer cement. In contact with a simulated body fluid, the MTAS released calcium ions in solution and encouraged the deposition of calcium phosphate crystals.

Acknowledgements

The authors thank The University of Malta Research Grant Committee for funding. Matteo Cesari and Ing. Iuri Boromei are acknowledged for their help with the experiments.

References

Adanir N, Cobankara FK, Belli S (2006) Sealing properties of different resin-based root canal sealers. Journal of Biomedical Material Research B; Applied Biomaterials 77, 1-4.

Aeinehchi M, Eslami B, Ghanbariha M, Saffar AS (2003) Mineral trioxide aggregate (MTA) and calcium hydroxide as pulp-capping agents in human teeth: a preliminary report. International Endodontic Journal 36, 225-31.

Ahlberg KM, Assavanop P, Tay WM (1995) A comparison of the apical dye penetration patterns shown by methylene blue and india ink in root-filled teeth. International Endodontic Journal 28, 30-4.

Asgary S, Parirokh M, Eghbal MJ, Stowe S, Brink F (2006) A qualitative X-ray analysis of white and grey mineral trioxide aggregate using compositional imaging. Journal of Materials Science Materials in Medicine 17, 187-91.

Bakland LK (2000) Management of traumatically injured pulps in immature teeth using MTA. Journal of the California Dental Association 28, 855-8.

Barthel CR, Strobach A, Briedigkeit H, Gobel UB, Roulet JF (1999) Leakage in roots coronally sealed with different temporary fillings. Journal of Endodontics 25, 731-4.

Bates CF, Carnes DL, del Rio CE (1996) Longitudinal sealing ability of mineral trioxide aggregate as a root-end filling material. Journal of Endodontics 22, 575-8.

Beckham BM, Anderson RW, Morris CF (1993) An evaluation of three materials as barriers to coronal microleakage in endodontically treated teeth. Journal of Endodontics 19, 388-91.

Bouillaguet S, Shaw L, Barthelemy J, Krejci I, Wataha JC (2008) Long term sealing ability of Pulp Canal Sealer, Ah-Plus, GuttaFlow and Epiphany. International Endodontic Journal 41, 219-26.

Bozeman TB, Lemon RR, Eleazer PD (2006) Elemental analysis of crystal precipitate from gray and white MTA. Journal of Endodontics 32, 425-8.

Camilleri J (2007) Hydration mechanisms of mineral trioxide aggregate. International Endodontic Journal 40, 462-70.

Camilleri J (2008a) Characterization of hydration products of mineral trioxide aggregate. International Endodontic Journal 41, 408-17.

Camilleri J (2008b) The physical properties of accelerated Portland cement for endodontic use. International Endodontic Journal 41, 151-7.

Camilleri J (2008c) Characterization and chemical activity of the Portland cement and two experimental cements with potential for use in dentistry. International Endodontic Journal 41, 791-9.

Camilleri J (2008d) Modification of MTA. Physical and mechanical properties. International Endodontic Journal 41, 843-9.

Camilleri J (2008e) The biocompatibility of modified experimental Portland cement with potential for use in dentistry. International Endodontic Journal 41, 1107-14.

Camilleri J (2009) Evaluation of selected properties of MTA sealer cement. Journal of Endodontics 35, 1412-7.

Camilleri J, Pitt Ford TR (2008) Evaluation of the effect of tracer pH on the sealing ability of glass ionomer cement and mineral trioxide aggregate. Journal of Materials Science; Materials in Medicine 19, 2941-8.

Camilleri J, Montesin FE, Brady K, Sweeney R, Curtis RV, Pitt Ford TR (2005a) The constitution of mineral trioxide aggregate. Dental Materials 21, 297-303.

Camilleri J, Montesin FE, Di Silvio L, Pitt Ford TR (2005b) The constitution and biocompatibility of accelerated Portland cement for endodontic use. International Endodontic Journal 38, 834-42.

Camps J, Pashley D (2003) Reliability of the dye penetration studies. Journal of Endodontics 29, 592-4.

Camps J, Giustiniani S, Dejou J, Franquin JC (1997) Low versus high pressure for in vitro determination of hydraulic conductance of human dentine. Archives of Oral Biology 42, 293-8.

Chong BS, Pitt Ford TR, Hudson MB (2003) A prospective clinical study of Mineral Trioxide Aggregate and IRM when used as root-end filling materials in endodontic surgery. International Endodontic Journal 36, 520-6.

Cobankara FK, Orucoglu H, Sengun A, Belli S (2006) The quantitative evaluation of apical sealing of four endodontic sealers. Journal of Endodontics 32, 66-8.

Coleman NJ, Awosanya K, Nicholson JW (2007) A preliminary investigation of the in vitro bioactivity of white Portland cement. Cement and Concrete Research 37, 1518-23.

Dagher FB, Yared GM, Machtou P (1997) Microleakage of a new and an old Kerr root canal sealers. Journal of Endodontics 23, 442-3.

De-Deus G, Reis C, Branda˜o C, Fidel S, Fidel RA (2007) The ability of Portland cement, MTA, and MTA Bio to prevent through-and-through fluid movement in repaired furcal perforations. Journal of Endodontics 33, 1374-7.

De-Deus G, Audi C, Murad C, Fidel S, Fidel R (2008) Similar expression of through-and-through fluid movement along orthograde apical plugs of MTA Bio and white Portland cement. International Endodontic Journal 41, 1047-53.

Faraco Junior IM, Holland R (2004) Histomorphological response of dogs' dental pulp capped with white mineral trioxide aggregate. Brazilian Dental Journal 15, 104-8.

Fridland M, Rosado R (2003) Mineral trioxide aggregate (MTA) solubility and porosity with different water-powder ratios. Journal of Endodontics 29, 814-7.

Gandolfi MG, Sauro S, Mannocci F et al. (2007) New tetrasilicate cement as retrograde filling material: an in vitro study on fluid penetration. Journal of Endodontics 33, 1082-5.

Gandolfi MG, Taddei P, Tinti A, Dorigo De Stefano E, Rossi PL, Prati C (2010) Kinetics of apatite formation on a calcium-silicate cement for root-end filling during ageing in physiological-like phosphate solutions. Clinical Oral Investigations DOI: 10.1007/s00784-009-0356-3.

Gomes-Filho JE, Watanabe S, Bernabé PF, de Moraes Costa MT (2009) A mineral trioxide aggregate sealer stimulated mineralization. Journal of Endodontics 35, 256-60.

Hardy I, Liewehr FR, Joyce AP, Agee K, Pashley DH (2004) Sealing ability of One-Up Bond and MTA with and without a secondary seal as furcation perforation repair materials. Journal of Endodontics 30, 658-61.

Holland R, de Souza V, Murata SS et al. (2001) Healing process of dog dental pulp after pulpotomy and pulp covering with mineral trioxide aggregate and Portland cement. Brazilian Dental Journal 12, 109-13.

Hovland EJ, Dumsha TC (1985) Leakage evaluation in vitro of the root canal sealer cement Sealapex. International Endodontic Journal 18, 179-82.

Huffman BP, Mai S, Pinna L et al. (2009) Dislocation resistance of ProRoot Endo Sealer, a calcium silicate-based root canal sealer, from radicular dentine. International Endodontic Journal 41, 34-46.

Inan U, Aydin C, Tunca YM, Basak F (2009) In vitro evaluation of matched-taper single-cone obturation with a fluid filtration method. Journal of the Canadian Dental Association 75, 123.

Kerr Pulp Canal Sealer website: http://www.kerrdental.com

Lee SJ, Monsef M, Torabinejad M (1993) Sealing ability of a mineral trioxide aggregate for repair of lateral root perforations. Journal of Endodontics 19, 541-4.

Martin RL, Monticelli F, Brackett WW et al. (2007) Sealing properties of mineral trioxide aggregate orthograde apical plugs and root fillings in an in vitro apexification model. Journal of Endodontics 33, 272-5.

Monteiro Bramante C, Demarchi AC, de Moraes IG et al. (2008) Presence of arsenic in different types of MTA and white and gray Portland cement. Oral Surgery Oral Medicine Oral Pathology Oral Radiology and Endodontics 106, 909-13.

Pashley DH, Kepler EE, Williams EC, Okabe A (1983) Progressive decrease in dentine permeability following cavity preparation. Archives of Oral Biology 28, 853-8.

Pelliccioni GA, Vellani CP, Gatto MR, Gandolfi MG, Marchetti C, Prati C (2007) Proroot mineral trioxide aggregate cement used as a retrograde filling without addition of water: an in vitro evaluation of its microleakage. Journal of Endodontics 33, 1082-5.

Pitt Ford TR, Torabinejad M, McKendry DJ, Hong CU, Kariyawasam SP (1995) Use of mineral trioxide aggregate for repair of furcal perforations. Oral Surgery Oral Medicine Oral Pathology Oral Radiology and Endodontics 79, 756-63.

Pitt Ford TR, Torabinejad M, Abedi HR, Bakland LK, Kariyawasam SP (1996) Using mineral trioxide aggregate as a pulp-capping material. Journal of the American Dental Association 127, 1491-4.

Pommel L, About I, Pashley D, Camps J (2003) Apical leakage of four endodontic sealers. Journal of Endodontics 29, 208-10.

Reyes-Carmona JF, Felippe MS, Felippe WT (2009) Biomineralization ability and interaction of mineral trioxide aggregate and white portland cement with dentin in a phosphate-containing fluid. Journal of Endodontics 35, 731-6.

Sarkar NK, Caicedo R, Ritwik P, Moiseyeva R, Kawashima I (2005) Physicochemical basis of the biologic properties of mineral trioxide aggregate. Journal of Endodontics 31, 97-100.

Saunders WP (2008) A prospective clinical study of periradicular surgery using mineral trioxide aggregate as a root-end filling. Journal of Endodontics 34, 660-5.

Schwartz RS, Mauger M, Clement DJ, Walker WA III (1999) Mineral trioxide aggregate: a new material for endodontics. Journal of the American Dental Association 130, 967-75.

Siqueira JF, Rocas IN (2007) Bacterial pathogenesis and mediators in apical periodontites. Brazilian Dental Journal 18, 267-80.

Souza EM, Wu MK, Shemesh H, Bonetti-Filho I, Wesselink PR (2008) Comparability of results from two leakage models. Oral Surgery Oral Medicine Oral Pathology Oral Radiology and Endodontics 106, 309-13.

Taddei P, Tinti A, Gandolfi MG, Rossi PL, Prati C (2009) Ageing of calcium silicate cements for endodontic use in simulated body fluids: a micro-Raman study. Journal of Raman Spectroscopy 40, 1858-66.

Tang HM, Torabinejad M, Kettering JD (2002) Leakage evaluation of root end filling materials using endotoxin. Journal of Endodontics 28, 5-7.

Tanomaru-Filho M, Faleiros FBC, Sacake JN, Duarte MAH, Guerreiro-Tanomaru JM (2009) Evaluation of pH and calcium ion release of root end filling materials containing calcium hydroxide or mineral trioxide aggregate. Journal of Endodontics 35, 1418-21.

Tao L, Anderson RW, Pashley DH (1991) Effect of endodontic procedures on root dentin permeability. Journal of Endodontics 17, 583-8.

Tay FR, Pashley DH, Rueggeberg FA, Loushine RJ, Weller RN (2007) Calcium phosphate phase transformation produced by the interaction of the portland cement component of white mineral trioxide aggregate with a phosphate-containing fluid. Journal of Endodontics 33, 1347-51.

Torabinejad M, Hong CU, Lee SJ, Monsef M, Pitt Ford TR (1995) Investigation of mineral trioxide aggregate for root-end filling in dogs. Journal of Endodontics 21, 603-8.

Torabinejad M, Pitt Ford TR, McKendry DJ, Abedi HR, Miller DA, Kariyawasam SP (1997) Histologic assessment of mineral trioxide aggregate as a root-end filling in monkeys. Journal of Endodontics 23, 225-8.

Torabinejad M, Chivian N (1999) Clinical applications of mineral trioxide aggregate. Journal of Endodontics 25, 197-205.

Trope M, Chow E, Nissan R (1995) In vitro endotoxin penetration of coronally unsealed endodontically treated teeth. Endodontics and Dental Traumatology 1, 90-4.

Venturi M, Di Lenarda R, Prati C, Breschi L (2005) An in vitro model to investigate filling of lateral canals. Journal of Endodontics 31, 877-81.

Weldon JK Jr, Pashley DH, Loushine RJ, Weller RN, Kimbrough WF (2002) Sealing ability of mineral trioxide aggregate and super-EBA when used as furcation repair materials: a longitudinal study. Journal of Endodontics 28, 467-70.

Weller RN, Tay KC, Garrett LV et al. (2008) Microscopic appearance and apical seal of root canals filled with gutta-percha and ProRoot Endo Sealer after immersion in a phosphate-containing fluid. International Endodontic Journal 41, 977-86.

Witherspoon DE, Small JC, Regan JD, Nunn M (2008) Retrospective analysis of open apex teeth obturated with mineral trioxide aggregate. Journal of Endodontics 34, 1171-6.

Wu MK, Kontakiotis EG, Wesselink PR (1998a) Long term seal provided by some root-end filling materials. Journal of Endodontics 24, 557-60.

Wu MK, Kontakiotis EG, Wesselink PR (1998b) Decoloration of 1% methylene blue in contact with dental filling materials. Journal of Dentistry 26, 585.

Wu MK, Bud MG, Wesselink PR (2009) The quality of single cone and laterally compacted gutta-percha fillings in small and curved root canals as evidenced by bidirectional radiographs and fluid transport measurements. Oral Surgery Oral Medicine Oral Pathology Oral Radiology and Endodontics 108, 946-51.

Yared GM, Bou Dagher F (1996) Sealing ability of the vertical condensation with different root canal sealers. Journal of Endodontics 22, 6-8.

Zaia AA, Nakagawa R, De Quadros I et al. (2002) An in vitro evaluation of four materials as barriers to coronal microleakage in root-filled teeth. International Endodontic Journal 35, 729-34.

Zielinski TM, Baumgartner C, Marshall JG (2008) An evaluation of GuttaFlow and gutta-percha in the filling of lateral grooves and depressions. Journal of Endodontics 34, 295-8.

dental materials 27 (2011) e134-e157

available at www.sciencedirect.com

ScienceDirect

journal homepage: www.intl.elsevierhealth.com/journals/dema

Development of the foremost light-curable calcium-silicate MTA cement as root-end in oral surgery. Chemical-physical properties, bioactivity and biological behavior

Maria Giovanna Gandolfi[a,*], Paola Taddei[b], Francesco Siboni[a], Enrico Modena[b], Gabriela Ciapetti[c], Carlo Prati[a]

[a] Laboratory of Biomaterials and Oral Pathology, Department of Odontostomatological Sciences, University of Bologna, Via San Vitale 59, 40125 Bologna, Italy

[b] Department of Biochemistry, University of Bologna, Bologna, Italy

[c] Laboratory for Orthopaedic Pathophysiology and Regenerative Medicine, Istituto Ortopedico Rizzoli, Bologna, Italy

article info

Article history:
Received 2 September 2010
Received in revised form
11 February 2011
Accepted 28 March 2011

Keywords:
Light-curable resin-modified calcium-silicate cement
Endodontic cement
Endosseous cement
HEMA-TEGDMA
Mineral trioxide aggregate (MTA)
Apatite-forming ability
Calcium release

abstract

Aim. An innovative light-curable calcium-silicate cement containing a HEMA-TEGDMA-based resin (lc-MTA) was designed to obtain a bioactive fast setting root-end filling and root repair material.

Methods. lc-MTA was tested for setting time, solubility, water absorption, calcium release, alkalinizing activity (pH of soaking water), bioactivity (apatite-forming ability) and cell growth-proliferation. The apatite-forming ability was investigated by micro-Raman, ATR-FTIR and ESEM/EDX after immersion at 37° C for 1-28 days in DPBS or DMEM + FBS. The marginal adaptation of cement in root-end cavities of extracted teeth was assessed by ESEM/EDX, and the viability of Saos-2 cell on cements was evaluated.

Results. lc-MTA demonstrated a rapid setting time (2 min), low solubility, high calcium release (150-200 ppm) and alkalinizing power (pH 10-12). lc-MTA proved the formation of bone-like apatite spherulites just after 1 day. Apatite precipitates completely filled the interface porosities and created a perfect marginal adaptation. lc-MTA allowed Saos-2 cell viability and growth and no compromising toxicity was exerted.

Signi“cance. HEMA-TEGDMA creates a polymeric network able to stabilize the outer surface of the cement and a hydrophilic matrix permeable enough to allow water absorption. SiO^-/Si-OH groups from the mineral particles induce heterogeneous nucleation of apatite by sorption of calcium and phosphate ions. Oxygen-containing groups from poly-HEMA-TEGDMA provide additional apatite nucleating sites through the formation of calcium chelates. The strong novelty was that the combination of a hydraulic calcium-silicate powder and a poly-HEMA-TEGDMA hydrophilic resin creates the conditions (calcium

Abbreviations: HEMA, 2-hydroxyethyl methacrylate; TEGDMA, triethyleneglycol dimethacrylate; DMEM, Dulbecco's modified eagle medium; FBS, fetal bovine serum; DPBS, Dulbecco's phosphate buffered saline; MTA, mineral trioxide aggregate; ESEM with EDX, environmental scanning electron microscope with energy dispersive X-ray analysis; FTIR, Fourier transform infrared spectroscopy; ATR, attenuated total reflectance; SBF, simulated body fluid.

* Corresponding author . Tel.: +39 0512088184.
E-mail address: mgiovanna.gandolfi@unibo.it (M.G. Gandolfi).

doi:10.1016/j.dental.2011.03.011

release and functional groups able to chelate Ca ions) for a bioactive fast setting light-curable material for clinical applications in dental and maxillofacial surgery. The first and unique/exclusive light-curable calcium-silicate MTA cement for endodontics and root-end application was created, with a potential strong impact on surgical procedures.

1. Introduction

Bacteria penetration into root canal is responsible for pulpitis and periapical tissue inflammation which may evolve in apical granuloma, cystic lesions and large bone defect [1]. These lesions require the removal of infected dentin root-apex and large portions of periapical bone tissue [2] and the filling of the root-apex cavity with a root-end sealing material preferably biocompatible, osteoconductive or osteoinductive. The failure rate of surgical root-end therapy with conventional materials, such as zinc-oxide cements and silver-amalgam, was reported approximately as 8-24% [3-6]. The consequences are bone resorption and tooth extraction. Millions of persons are surgically treated for endodontic diseases. The success of the endodontic treatment allows to keep the tooth functionality.

Calcium-silicate hydraulic cements conventionally defined MTA (mineral trioxide aggregate) cements have been clinically proposed as root-end materials [2,7,8], and prospective studies have reported a failure of 9.8-16% at 1 year [3,9] and 8% at 2 years [4,9].

The biological behavior and the apatite-forming ability (i.e. bioactivity) of MTA cements have been recently adequately documented [10-22].

The main clinical limitation of MTA cements is the long setting time [23-25] and the consequent risk for a fast dissolution and removal of the cement and wash-out of the fresh (not-set) cement [25] from the surgical site of root-end obturation due to the blood and fluid contamination at the apical region of root canal. The incorporation of light-curable resins has been proposed for many materials, such as the resin-modified glass-ionomer cements, to improve mechanical properties and reduce setting time. The reduced setting time of MTA materials may extend their clinical use and make their application advisable in extremely wet and blood-contaminated surgical sites.

HEMA (2-hydroxyethyl methacrylate) is a hydrophilic monovinyl monomer (i.e. it contains a single C—C double bond, Fig. 1). Its polymer poly-HEMA is a hydrogel widely used together with other methacrylic resins in biomedical applications. Poly-HEMA can imbibe large amounts of water (from 10 to 600%) by swelling without dissolving, due to the hydrophilic pendant groups of the molecule (Fig. 1); it has been extensively tested for bioactivity [26-29] and biocompatibility [30].

TEGDMA (triethyleneglycol dimethacrylate, Fig. 1) is a hydrophobic monomer that contains two C—C double bonds; its introduction into the resin formulation allows the formation of covalent crosslinks after curing and thus tight networks and solid structures [31].

Bioactivity of calcium-silicate Portland cements and other MTA materials such as ProRoot MTA has been recently demonstrated [10-16]. An essential requirement for a bioactive material is the formation of a biologically active bone-like apatite layer on its surface in a biological environment [32]. The concept of bioactivity is closely correlated with biointeractivity, i.e. the ability to exchange information within a biological system [33]. This means that a bioactive material reacts chemically with body fluids in a manner compatible with the repair processes of the tissue.

The examination of apatite formation on a material in a simulated body fluid (SBF) is a commonly accepted method to predict the in vivo bone bioactivity of a specific material [34].

The aim of the study was to characterize an innovative light-curable resin-modified calcium-silicate cement (lc-MTA), containing a HEMA-TEGDMA-based anphiphilic resin as organic light-curable matrix and a calcium-silicate powder, specifically designed for applications in contact with bone and dentin for oral surgery and dentistry. The goal was to obtain a material with more adequate characteristics and properties for applications in wet apical cavities contaminated by blood during the preparation of a bone window, as it occurs during root-end surgery procedures and root repair procedures. Chemical-physical properties, i.e. setting time, solubility, water absorption, calcium release, alkalinizing activity were evaluated. The in vitro apatite-forming ability was assessed by ESEM/EDX, micro-Raman and ATR-FTIR techniques after soaking in phosphate-containing solutions. Osteoblast-like cells (Saos-2) were used to estimate the biological compatibility of solid cements and cement extracts.

2. Materials and methods

2.1. Sample preparation

The light-curable resin-modified calcium-silicate cement (lc-MTA) was prepared by mixing a calcium-silicate cement powder (wTC-Ba) and an anphiphilic light-curable resin liquid phase (Gandolfi MG & Prati C, patent of the University of Bologna).

The wTC-Ba powder was constituted by di- and tricalcium-silicates, tricalcium aluminate, barium sulfate, calcium sulfate and calcium chloride; it was prepared by a conventional melt-quenching technique [35]. The liquid phase contained 2-hydroxyethyl methacrylate (HEMA), triethyleneglycol dimethacrylate (TEGDMA), camphorquinone (CQ) and ethyl-4-(dimethylamino)benzoate (EDMAB).

To obtain the wTC-Ba cement, the wTC-Ba powder was mixed with Dulbecco's phosphate buffer solution (DPBS, Lonza, Lonza Walkersville Inc., Walkersville, MD, USA, cat. no. BE17-512) for 30 s in a powder/liquid ratio of 3:1.

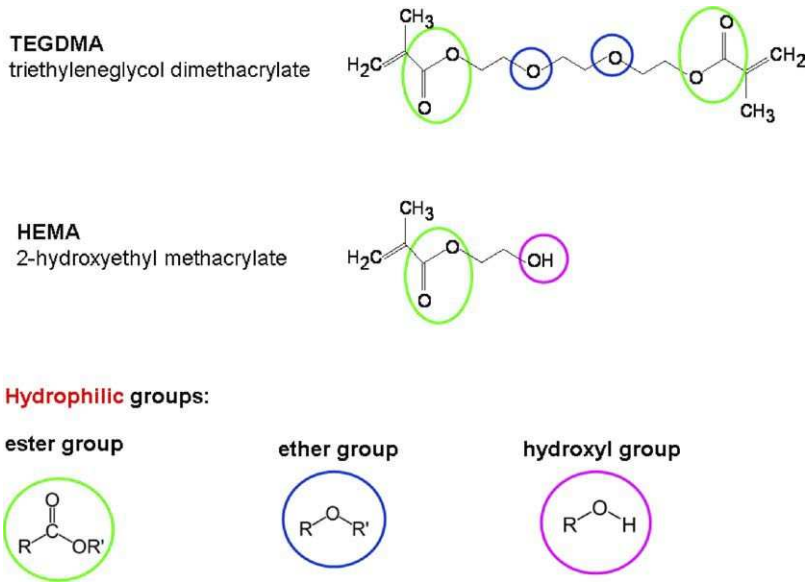

Fig. 1 - Chemical structure, name and acronym of the used monomers.

To obtain the lc-MTA cement, the wTC-Ba powder was mixed with the liquid phase for 30 s in a powder/liquid ratio of 4:1 and light-cured for 120 s with a halogen lamp (T-LED elca, Anthos Cefla, Imola, Italy).

A commercial hydraulic calcium-aluminosilicate Portland cement named ProRoot MTA (white ProRoot MTA, Dentsply Maillefer, Tulsa, Ok, USA—lot no. 08003395) was used as reference (a reference material is required by ISO 7405 clause 3) [36] since biocompatible osteoconductive material [7,37]. ProRoot MTA powder was mixed with the supplied deionized water for 30 s in a powder/liquid ratio of 3:1.

Vitrebond (3M ESPE AG, Dental Products, St.Paul, MN, USA—lot. no. 70-2010-2611-2) is a resin-modified glass-ionomer cement and was used as light-curable control (a positive control is required by both ISO 7405 and ISO 10993-5 clause 3) [36,38] since is a material able to evoke a positive or reactive response (i.e. cytotoxic material) [39]. The cement was prepared according to the manufacturer directions and light-cured for 30 s with a halogen lamp. As stated by the manufacturer, Vitrebond is composed by a fluoro-aluminosilicate powder (constituted by SiO_2, AlF_3, ZnO, SrO, Na_3AlF_6 (criolite), NH_4F, MgO, and P_2O_5) mixed with a light-curable liquid (containing polyacrylic acid with pendant methacrylate groups (PAA), 2-hydroxyethylmethacrylate (HEMA), water and photoinitiator camphorquinone) [40].

Standard cell culture plastic surface (Tissue Culture Polystyrene, TCPS) was used as negative control since a material that proved a non-reactive response in the test system as required by both ISO 7405 and ISO 10993-5 clause 3 [36,38].

Once mixed, all cements were compacted to the excess into PVC molds (8 mm in diameter and 1.6 mm thick). The wTC-Ba and ProRoot MTA were cured at 37°C and 98% relative humidity. For solubility, calcium release and alkalinizing activity tests, the samples were cured (at 37°C and 98% relative humidity) for a period corresponding to 70% of final setting time, i.e. 40 min for wTC-Ba and 117 min for ProRoot MTA (period of time 50% longer than the setting time stated by the manufacturer, according with ISO6876 clause 7.7.2.) [41] and then demolded.

The lc-MTA and Vitrebond specimens were light-cured through a mylard streep (Directa Matrix Strips, Directa AB, Upplands Vasby, Sweden) and immediately demolded.

The obtained cylindrical specimens (8 mm in diameter, 1.6 mm thick and 0.3 g of weight) exposed an exchange surface of 90.43 ± 0.01 mm^2 (upper surface r^2 = 50.24 mm^2 and lateral surface 2r h = 40.19 mm^2).

2.2. Setting times

The initial and final setting times of the cements were evaluated using Gilmore needles according to ASTM C266-03 and ADA specifications [42,43]. Briefly, the Gilmore initial setting time was the elapsed time (min) between the mixing of the cement with liquid and the first penetration measurement that does not mark the specimen surface with a complete circular impression. As the initial or final setting times approached (i.e. no indentation), the specimens were tested every minute to determine the exact Gilmore setting time. The initial setting time needle was 113.4 g in weight and 2.12 mm in tip diameter. After the initial setting time was measured, the specimens were tested every 5 min with the final setting time needle with a tip diameter of 1.06 mm and a weight of 453.6 g.

The wTC-Ba and ProRoot MTA samples were removed from the curing chamber (37°C and 98% relative humidity) and immediately tested for setting time to prevent the dehydration of cement surface. The lc-MTA and Vitrebond samples were light-cured (for 120 or 60 s, respectively) and immediately tested for setting time to standardize the polymerization level and to prevent any polymerization progress. Each sample was used only for one penetration/indentation test and then discarded. A large number of samples were used to find the approximate initial and final setting times of the cements.

Their exact evaluation was performed on three replicates for each material.

2.3. Solubility

The solubility of the materials was determined using the method described in ISO 6876 [41]. The mass of the cements was measured gravimetrically using an analytical balance (Bel Engineering series M, Monza, Italy) with an accuracy of 0.001 g after 1, 14 and 28 days of soaking in deionized water or in DMEM + FBS, i.e. Dulbecco's modified eagle medium (DMEM, Lonza, Lonza Walkersville Inc., Walkersville, MD, USA, cat. no. 12-604) added with 10% fetal bovine serum (FBS, Lonza, Lonza Walkersville Inc., Walkersville, MD, USA, cat. no. DE14-801E). Each weight measurement was repeated three times.

The specimens (n = 5 for each material) were weighed (Initial weight) and placed in sealed cylindrical polystyrene holders (3 cm high and 4 cm in diameter) containing 5 mL of deionized water or DMEM + FBS, at 37°C. At the pre-determined intervals, the samples were removed from the solutions, blotted dry at 37°C for 48 h, i.e. till the weight was stable and then weighed and finally discarded.

The solubility (percentage weight variation, W%) at each time t was calculated according to the following equation:

$$W\% = \frac{\text{dry weight at time } t - \text{initial weight}}{\text{initial weight}} \times 100$$

2.4. Water absorption

The water uptake was determined gravimetrically. The specimens (n = 5 for each material) were placed in sealed containers containing 5 mL of deionized water and maintained in a cabinet at 37°C under static conditions. The wet weight was recorded throughout a 24-h time period. At pre-determined intervals (1, 6h and 1 day) the specimens were carefully removed from water, wiped free from any visible surface moisture (blotted on filter paper for 3 s to remove the surface water) and immediately weighed (within 30 s to eliminate the influence of desiccation). After the last endpoint (24 h) the samples were dried at 37°C until the weight was stable and then the dry weight was recorded. Each weight measurement was repeated three times using an analytical balance (Bel Engineering series M, Monza, Italy).

The water absorption at each time t was calculated according to the following equation:

$$\text{water absorption} = \frac{\text{wet weight at time } t - \text{dry weight at } 24\,h}{\text{dry weight at time } 24\,h} \times 100$$

2.5. Alkalinizing activity and calcium release

Cement specimens (n = 5 for each material) were prepared as previously described and immersed in 10 mL of deionized water (pH 6.8) in polypropylene sealed containers stored at 37°C. After 3 and 24 h and 7, 14 and 28 days soaking water was collected and renewed.

A multi-parameter laboratory meter (inoLab 750 WTW, Weilheim, Germany) previously calibrated with standard solutions was used. The pH of soaking water was measured using a selective temperature compensated electrode (Sen Tix Sur WTW, Weilheim, Germany). Calcium release was measured using a calcium probe (Calcium ion electrode, Eutech instruments Pte Ldt, Singapore) after addition of 0.200 mL (2%) of ionic strength adjuster (ISA, 4 mol/L KCl, WTW, Weilheim, Germany) to the collected soaking medium (10 mL).

The probes were inserted into the soaking media at room temperature (24°C) under magnetic stirring. Each measurement was repeated three times.

The obtained results (setting time, solubility, water absorption, calcium release and pH) were statistically analyzed. The 1-way analysis of variance (ANOVA) was used to test for differences among the groups. Tukey's HSD (honestly significant differences) test was used in conjunction with ANOVA to determine the statistical significance of the differences.

2.6. In vitro apatite-forming ability (bioactivity)

The ability of the different materials to form apatite on their surface was tested in vitro as an index of bioactivity [33,34]. Bioactivity tests were carried out in DPBS [12-16]. DPBS is a physiological-like buffered (pH 7.4) Ca- and Mg-free solution with the following composition (mM): K^+ (4.18), Na^+ (152.9), Cl^- (139.5), PO_{43-} (9.56, sum of H_2PO_{4-} 1.5 mM and HPO_{42-} 8.06 mM).

Each specimen (0.3 g weight) was immersed in 5 mL of DPBS (DPBS/cement ratio 17 mL/g) [10] in a sealed cylindrical polystyrene holder (3 cm high and 4 cm in diameter) and was maintained at 37°C until the pre-determined endpoint time (1, 7, 14, and 28 days). The storage media were renewed at each endpoint.

Additional samples were soaked in DMEM + FBS (i.e. the same medium used for cell culture) for 1 and 7 days, as control specimens for cell culture studies. DMEM is a cell culture medium containing salts (calcium chloride, potassium chloride, magnesium sulfate, sodium chloride, sodium bicarbonate and monosodium phosphate) and rich in vitamins (folic acid, nicotinamide, riboflavin and B-12), amino acids and glucose.

At the established endpoint times, the disks were analyzed by micro-Raman, ATR/FTIR spectroscopy and ESEM/EDX.

To evaluate the possible bioactivity of poly-HEMA, poly-TEGDMA and poly-HEMA-TEGDMA polymers, a still debated subject [44 and references cited therein] additional resin samples composed of pure poly-HEMA or pure poly-TEGDMA or pure poly-HEMA-TEGDMA were prepared by light-curing under the same experimental conditions used for lc-MTA. The specimens were soaked for 4 weeks in a metastable calcifying medium at pH 7.3 containing Ca^{2+} and PO_{43-} ions in a Ca/P ratio of 1.67, according to Chirila et al. [45] and analyzed by FTIR.

2.6.1. Micro-Raman spectroscopy

Micro-Raman spectra were obtained using a Jasco NRS-2000C instrument (Jasco Inc., Easton, MD, USA) connected to a microscope with 20× magnification. In these conditions the laser spot size (i.e. the excitation source) was a few microns. All the spectra were recorded in back-scattering conditions with 5 cm^{-1} spectral resolutions using the 488 nm blue line (Innova 70, Coherent Inc., Santa Clara, CA, USA) with a power of 50 mW.

A 160 K frozen CCD detector from Princeton Instruments Inc. (Trenton, NJ, USA) was used. To minimize the variability deriving from possible sample inhomogeneity, at least five spectra were recorded on five different points of both the upper surface and inner fractured side of each specimen. Due to the high fluorescence of Vitrebond upon excitation in the visible range (i.e. at 488 nm), the Raman spectra were recorded using a Nd^{3+}-YAG laser emitting in the near-infrared region (1064 nm) with a Bruker MultiRam Fourier Transform FT-Raman spectrometer (Bruker Optik GmbH, Ettlingen, Germany) equipped with a cooled Ge-diode detector. The focused laser beam diameter was about 100 m, the spectral resolution 4 cm^{-1}, and the laser power at the sample about 300 mW. The Raman spectra were recorded on wet cement samples (i.e. when maintained in their storage media) as well as on unhydrated cement powders and poly-HEMA-TEGDMA resin polymerized under the same conditions used for lc-MTA samples.

2.6.2. ATR/FTIR spectroscopy

IR spectra were recorded on a Nicolet 5700 FTIR (Thermo Fisher Scientific Inc., Waltham, MA, USA), equipped with a Smart Orbit diamond attenuated total reflectance (ATR) accessory and a DTGS detector; the spectral resolution was 4 cm^{-1} and the number of scans was 64 for each spectrum. The ATR area had a 2 mm diameter. The IR radiation penetration was about 2 microns. To minimize the variability deriving from possible sample inhomogeneity, at least five spectra were recorded on five different points of both the upper surface and inner fractured side of each specimen. IR spectra were also recorded on unhydrated cement powders and poly-HEMA-TEGDMA resin polymerized under the same conditions used for lc-MTA.

To evaluate the presence of interactions between the resin and the silicate component, unhydrated samples composed of wTC-Ba (20%) and resin (80%) were prepared and analyzed.

Before IR analysis, the poly-HEMA, poly-TEGDMA and poly-HEMA-TEGDMA samples tested for bioactivity were dried.

2.6.3. ESEM/EDX surface analysis

The samples were examined with an Environmental Scanning Electron Microscope ESEM (ESEM Zeiss EVO 50, Carl Zeiss, Oberkochen, Germany) connected to a secondary electron detector for Energy Dispersive X-ray analysis EDX (Oxford INCA 350 EDS, Abingdon, Oxfordshire, UK) computer-controlled software Inca Energy Version 18, using an accelerating voltage of 20-25 kV. The elemental analysis (weight % and atomic %) of the samples was performed applying ZAF correction method. At 25 kV acceleration, the X-ray electron beam penetration of ESEM/EDX (inside a material with a density of about 3 g/cm^3) proved to be 2.98 m and consequently the volume excited and involved in the emission of characteristic X-rays from the constituting elements must be considered 10 m^3. The disks were placed directly onto the ESEM stub and examined without any form of preparation (the specimens were not coated for this analysis) and then inspected under wet conditions by ESEM/EDX as previously described [15].

2.6.4. Marginal adaptation

To evaluate the morphology and the marginal adaptation of materials to dentin, freshly extracted single-rooted human teeth were instrument and a root-end cavity was prepared at apical area, according to previous studies [46] and filled with lc-MTA (n = 6) or ProRoot MTA (n = 4) or wTC-Ba (n = 6) or Vitrebond (n = 4). After preparation, the filled roots were immersed in DPBS at 37°C and inspected in wet conditions under ESEM/EDX after 10 min, 24 h and 28 days of storage. EDX was used to evaluate the formation of calcium phosphate deposits or any surface change. Optical microscopy (Motic, Motic Incorporation Ltd., Hong Kong) was also used to observe the restoration of filled roots.

2.7. Cell culture and testing

Each material was layered on a 13 mm diameter Thermanox™ Plastic coverslip (Nalgene, Nunc International, NY, USA) to obtain disks. Mechanical vibrations were used to make the surface flat and regular. The surface area of each disk was 1.9 ± 0.1 cm^2, the weight was 0.3 ± 0.02 g.

The sample disks of wTC-Ba and ProRoot MTA were left to cure at 100% humidity and 37°C for 2 h, to obtain a partial setting of the cements, before their immersion in culture medium for the in vitro experiments.

The biological compatibility of the new silicate-based cements has been tested in vitro by challenging Saos-2 osteoblast-like cells (Istituto Zooprofilattico Brescia, Italy) with cements as solids and with cement extracts [20,38].

2.7.1. Test on extracts (indirect toxicity test)

The indirect toxicity evaluation was performed by extraction method. The extracts were obtained using extract conditions (24 h at 37°C) and extraction vehicle (culture medium with serum) in accordance with ISO recommendations (ISO 7405 clause 6, ISO 10993-5 clause 4 and ISO 10993-12 clause 10) [36,38,47]. A higher extraction ratio (1.9 cm^2/mL expressed as surface area of the sample/extractant volume or 0.3 g sample/mL expressed as mass of the sample/extractant volume) higher than that suggested by ISO 10993-12 clause 10 [47] was used.

Saos-2 cells (5×10^3 per well) were seeded in 96-well flat-bottom microplate. After 5 h at 37°C to allow cell adhesion, 0.2 mL of pure extract was added to the wells. Cell viability of four replicate samples (n = 4) was assessed by Alamar Blue test at 1 and 3 days.

2.7.2. Test on solid materials (direct-contact toxicity test)

Each cement disk was placed in a well of a 24-well polystyrene plates (Costar, Cambridge, MA, USA). Pre-wetting of the cement surfaces was obtained by covering the cements with 1 mL of complete culture medium for 24 h at 37°C. At 24 h the medium was collected and stored at −80°C to be used as an extract of the material [38].

The culture medium was a modification of Eagle's medium (DMEM, Sigma-Aldrich Corp., St. Louis, MO, USA) containing 10% fetal bovine serum (Sigma-Aldrich Corp.) and 1% penicillin/streptomycin (10,000 U penicillin, 10 g streptomycin, 25 g amphotericin B/mL, Sigma-Aldrich Corp.).

Cells were inoculated on cement surface at a plating density of 20×10^3 cells/cm^2. After an adhesion time of 30 min, the cells were carefully covered with the complete medium and incubated at 37°C, 5% CO_2 and saturated humidity.

Three samples for each cement were used in replicate experiments, with cells seeded on polystyrene plates (TCPS) without cement used as negative controls. The viability of cells was assessed by Alamar Blue assay in six replicate samples (n = 6) and by Neutral red test in three replicates (n = 3) after 1, 3 and 7 days of culture.

2.7.3. Cell viability and proliferation

Alamar blue (intracellular redox status, i.e. the metabolic activity) and neutral red (membrane integrity) non-destructive tests were performed to measure cell vitality and proliferation, i.e. as indicators of the degree of cytotoxicity caused by the test material.

Alamar blue assay provides measures of the metabolic rate and the maximal functional capacity of mitochondrial respiratory-chain and was used for quantifying in vitro viability of cells and as an indicator of cell health. The nontoxic and stable nature of the Alamar blue dye allows continuous monitoring of cultures over time and permits long-term exposure of cells without negative impact.

Alamar blue assay is quantitative with respect to time providing information on the ability of metabolically active cells to convert the reagent into a fluorescent and colorimetric indicator. The amount of fluorescence or absorbance is proportional to the number of living cells and corresponds to the cell metabolic activity. Damaged and nonviable cells have lower innate metabolic activity and thus generate a proportionally lower signal than healthy cells.

Alamar blue assay uses a visible blue fluorogen probe resazurin, which is reduced to a red fluorescent compound (resorufin) by cellular redox enzymes of the mitochondrial respiratory-chain. Viable cells continuously convert resazurin to resorufin, thereby generating a quantitative measure of viability and cytotoxicity.

At pre-determined intervals of culture (1, 3, and 7 days), 200 L of Alamar blue dye (BioSource International, Camarillo, CA, USA) was added to the culture wells (1:10 v/v). After 4 h of incubation at 37°C, 100 L of culture medium (supernatant) of each well was transferred to a 96 well-plate, and fluorescence (oxidation of Alamar blue) in the sample and control wells were read at 490 excitation-540 emission wavelengths using a Cytofluor 2350 fluorimeter (Millipore Corporation, Bedford, MA, USA).

The results of replicate samples (n) were recorded as relative fluorescence units (RFU) and expressed mean ± standard deviation. Statistical analysis was performed by the nonparametric one-way ANOVA test (with a p value <0.05 considered as significant).

Neutral red uptake cytotoxicity assay , recommended by the ISO 10993-5 annex A [38] is based on incorporation of the supravital neutral red dye into living cells with storage of the neutral red dye in the lysosomes of viable, uninjured cells. Alterations of the cell surface or the sensitive lysosomal membrane lead to lysosomal fragility. Such changes produced by toxic substances cause decreased uptake and binding of neutral red dye, making it possible to distinguish among viable, damaged or dead cells. This test provides a sensitive signal of both cell integrity and growth inhibition.

Viable cells take up the dye by active transport and incorporate the dye into lysosomes, whereas non-viable cells do not take up the dye. The incorporated dye is then liberated fro the cells in an acidified solution. Ai increase of decrease in the number of cells of their physiological state results in a concomitant change in the amount of dye incorporated by the cells in the culture.

Following culture onto cements the cells were incubated for 2h with neutral red medium, i.e. neutral red dye (100 g/mL) dissolved in serum free medium (DMEM). Cells were then washed with phosphate buffered saline (PBS) and added with of 1 mL of elution medium (EtOH/AcCOOH, 50%/1%) followed by gentle shaking for 10 min to achieve complete dissolution. Aliquots of the resulting solutions were transferred to 96-well plates and absorbance at 540 nm was recorded using the microplate spectrophotometer system (Spectra III Tecan, Austria).

The results, recorded as optical density, were expressed as mean ± standard deviation of replicate samples (n) and statistically analyzed with the nonparametric one-way ANOVA test with a p value <0.05 considered as significant.

Table 1 - Initial and final setting times (mean ± standard deviation, n = 3 for each material) determined by Gilmore needles [42,43] at 37°C and 98% relative humidity. lc-MTA and Vitrebond were light cured for 120 and 30 s, respectively. Data with the same superscript letter do not differ significantly (p > 0.01).

Materials	Initial setting time (min)	Final setting time (min)
lc-MTA	2±0[a]	2±1[a]
wTC-Ba	31 ± 3[b]	57 ± 3[c]
ProRoot MTA	36 ± 3[b]	168 ± 5[d]
Vitrebond	1±0[a]	1±0[a]

3. Results

3.1. Setting times

Table 1 shows the initial and final setting times of the cements determined using Gilmore needles.

The lc-MTA cement showed statistically shorter initial and final setting times than both conventional calcium-silicate MTA cements (wTC-Ba and ProRoot MTA), i.e. 120 s of light curing exposition were enough to create an external polymerized layer able to resist to the Gilmore needles. Vitrebond, the control light-curable material, exhibited a setting time of 60 s.

wTC-Ba showed a statistically shorter final setting time than ProRoot MTA (57 ± 3 vs 168 ± 5 min).

3.2. Solubility

Table 2A reports the solubility, i.e. the % weight variation (W%) of the tested cements (ISO 6876 [41]) after 1, 14 and 28 days of soaking in deionized water. All the cements displayed a loss of material (a weight loss, i.e. W% < 0) increasing over soaking time. lc-MTA showed the statistically lowest solubility at all times. wTC-Ba and ProRoot MTA proved higher weight loss than lc-MTA and Vitrebond. No statistically significant differences were found comparing ProRoot MTA vs wTC-Ba while statistically significant differences were measured comparing Vitrebond vs both wTC-Ba and ProRoot MTA.

Table 2 - Solubility (mean ± standard deviation, n = 5 for each material) expressed as percentage weight variation (W%) after different times of soaking at 37°C in (A) deionized water (ISO6876) [41] and (B) DMEM + FBS. Different superscript letters denote significant differences ($p < 0.01$).

Materials	W% at 1 day	W% at 14 days	W% at 28 days
(A)			
lc-MTA	-5.2 ± 1.13^{a}	-6.34 ± 0.85^{a}	$-7.38 \pm 1.39^{a,b}$
wTC-Ba	-17.17 ± 1.69^{d}	$-20.16 \pm 3.33^{d,e,f}$	$-22.02 \pm 2.85^{e,f}$
ProRoot MTA	$-18.34 \pm 0.51^{d,e}$	$-20.65 \pm 1.72^{d,e,f}$	-22.54 ± 1.49^{f}
Vitrebond	$-9.44 \pm 0.44^{b,c}$	$-11.04 \pm 0.82^{b,c}$	-11.42 ± 1.51^{c}
(B)			
lc-MTA	-3.64 ± 1.51^{a}	6.25 ± 2.91^{d}	6.67 ± 1.36^{d}
wTC-Ba	-11.52 ± 1.22^{c}	$-5.22 \pm 3.48^{a,b}$	3.94 ± 3.26^{d}
ProRoot MTA	-11.50 ± 2.81^{c}	-4.06 ± 0.48^{a}	3.62 ± 1.12^{d}
Vitrebond	$-9.20 \pm 2.59^{b,c}$	-4.19 ± 0.43^{a}	-3.30 ± 0.23^{a}

A different trend of weight variation was observed when the samples were immersed in DMEM + FBS (Table 2B). After 1 day, lc-MTA, wTC-Ba and ProRoot MTA showed a lower weight loss in DMEM + FBS than in deionized water while Vitrebond showed the same weight loss in both media. lc-MTA displayed a loss of material only after 1 day of immersion in DMEM + FBS while wTC-Ba and ProRoot MTA specimens showed a reduction of weight till 14 days. lc-MTA showed an increment of weight since 14 days, while wTC-Ba and ProRoot MTA displayed an analogous behavior only at 28 days. Vitrebond underwent weight loss over all the period.

3.3. Water absorption

The results of water uptake (n = 5 for each material) are shown in Table 3. All the materials revealed an increase of water uptake from 1 h to 1 day. lc-MTA absorbs more water (weight increase of approx 3%) than the other materials.

3.4. Alkalinizing activity and calcium release

Table 4 shows the pH of soaking water after immersion of the cements. The pH values of water increased from 6.5 to approximately 11.0 already after 3 h of immersion of lc-MTA, wTC-Ba and ProRoot MTA samples. This time of analysis was selected because it corresponds to the final setting time of ProRoot MTA. After 14 days of immersion, ProRoot MTA showed a significant reduction of the alkalinizing activity (pH 7.8), while wTC-Ba and lc-MTA were still able to noticeably basify the soaking water after 28 days (pH values of 9.2 and 9.8, respectively). Differently, Vitrebond slightly acidified the soaking medium until 1 day, and then the pH increased to 7.0 after 7 days and decreased again to 6.4 after 28 days.

Calcium release and cumulative calcium release are shown in Table 5 and Fig. 2, respectively. Table 5 reports the calcium release at 3 h (immediately after final setting of ProRoot MTA) and 1, 7, 14 and 28 days. Early release of calcium was very high for lc-MTA (211 ppm) and wTC-Ba (271 ppm) while statistically lower for ProRoot MTA (32 ppm). Vitrebond did not release calcium ions, according to its composition devoid of calcium. Calcium release (Table 5) showed a different trend in the first 7 days of soaking. lc-MTA still showed a high calcium release after 7 days of soaking (145 ppm), wTC-Ba showed a drastic reduction of calcium release after 1 day (77 ppm) and ProRoot MTA showed a low calcium release (35-16 ppm) during the whole soaking time. Cumulative calcium release (Fig. 2) was significantly higher for lc-MTA (537 ppm) than wTC-Ba (437 ppm) and ProRoot MTA (121 ppm).

3.5. In vitro bioactivity tests

3.5.1. Micro-Raman analyses

Fig. 3 reports the Raman spectra of the cements aged in DPBS. Band assignments have been given according to the literature ([13,14, and references cited therein].

The spectra of unhydrated wTC-Ba and ProRoot MTA revealed the presence of calcium carbonate as calcite and/or aragonite, calcium sulfate (as gypsum and/or anhydrite), alite, belite as well as barium sulfate in the former and bismuth oxide in the latter. If compared with the wTC-Ba powder, ProRoot MTA powder showed a higher amount of calcite and/or aragonite and lower quantities of calcium sulfate, prevalently as anhydrite; moreover, the silicate component was more crystalline, as revealed by the higher resolution of the alite and belite bands.

The Raman spectra recorded on the surface of the lc-MTA, wTC-Ba and ProRoot MTA cements after one day of aging in DPBS showed with different relative intensities the marker band of apatite at about 960 cm^{-1}; in the same spectral range, no spectral changes were observed for Vitrebond. The spectrum of the lc-MTA surface displayed the bands typical of

Table 3 - Water absorption (mean ± standard deviation, n = 5 for each material) after different times of soaking in deionized water. Different superscript letters indicate statistical significant differences ($p < 0.01$).

Materials	1h	6h	1 day
lc-MTA	$9.61 \pm 1.14^{a,b}$	$11.96 \pm 1.27^{a,b}$	12.94 ± 1.60^{a}
wTC-Ba	$12.07 \pm 1.61^{a,b}$	$12.26 \pm 1.69^{a,b}$	13.87 ± 1.63^{a}
ProRoot MTA	$11.67 \pm 3.90^{a,b}$	$12.11 \pm 3.45^{a,b}$	13.96 ± 3.92^{a}
Vitrebond	8.17 ± 0.47^{b}	$9.57 \pm 0.63^{a,b}$	$10.77 \pm 0.36^{a,b}$

Table 4 - Values of pH (mean ± standard deviation, n = 5 for each material) of soaking water after immersion of the cements for different times. No coincidence in the superscript letters indicates significant differences ($p < 0.01$).

Materials	3h	1 day	7 days	14 days	28 days
lc-MTA	10.6 ± 0.1^{c}	11.7 ± 0.2^{a}	$10.5 \pm 1.0^{c,d}$	9.6 ± 1.0^{e}	9.8 ± 0.7^{e}
wTC-Ba	$11.5 \pm 0.2^{a,b}$	$11.4 \pm 0.1^{a,b}$	$10.8 \pm 0.6^{b,d}$	93 ± 05^{f}	9.2 ± 0.7^{f}
ProRoot MTA	$11.5 \pm 0.1^{a,b}$	$11.5 \pm 0.4^{a,b}$	$11.2 \pm 0.8^{a,b,c}$	75 ± 0.1^{g}	$8.2 \pm 0.2^{f,g}$
Vitrebond	5.9 ± 0.1^{l}	$6.0 \pm 0.1^{h,i}$	7.0 ± 0.2^{i}	$6.7 \pm 0.1^{h,i}$	$6.4 \pm 0.4^{i,l}$
Deionized water	6.8 ± 0.4^{i}	7.0 ± 0.1^{i}	7.1 ± 0.1^{i}	6.6 ± 0.1^{i}	6.9 ± 0.1^{i}

Table 5 - Calcium released (mean ± standard deviation, expressed as ppm, n = 5 for each material) in soaking water after immersion of the samples for different times. Superscript letters indicate statistical significance ($p < 0.01$).

Materials	3h	1 day	7 days	14 days	28 days
lc-MTA	211 ± 20.7	134 ± 4.0^{c}	145 ± 13.2^{c}	$28 \pm 4.6^{a,b}$	$19 \pm 11.9^{a,d}$
wTC-Ba	271 ± 57.9	77 ± 9.1	49 ± 38.0^{b}	$28 \pm 8.6^{a,d}$	$12 \pm 8.6^{a,d}$
ProRoot MTA	$32 \pm 4.5^{a,b}$	$35 \pm 2.3^{b,d}$	$24 \pm 3.8^{a,b}$	$14 \pm 2.7^{a,d}$	16 ± 2.9^{a}
Vitrebond	1 ± 0.9^{a}	0 ± 0.5^{a}	1 ± 0.9^{a}	1 ± 0.5^{a}	0 ± 0.4^{a}
Deionized water	1 ± 1.0^{a}	1 ± 0.6^{a}	2 ± 0.6^{a}	1 ± 0.6^{a}	1 ± 0.6^{a}

a B-type carbonated apatite (in particular the component at 1070 cm^{-1}) superimposed to those weaker due to the cement components and calcite; the lc-MTA cement appeared to form the thickest deposit, as revealed by the highest intensity ratio between the bands of apatite and belite (at about 960 and 855 cm^{-1}, respectively).

At increasing storage times, the deposit became progressively thicker on all the calcium-silicate cements: the bands of the cement components progressively weakened while the bands typical of a B-type carbonated apatite progressively appeared. After 28 days of aging, ProRoot MTA appeared to be characterized by less mature apatite deposits than the experimental cements, as revealed by its HPO_{42-} ion band at about 1000 cm^{-1}. No changes were observed in the spectrum recorded on the surface of Vitrebond after 28 days of aging in DPBS.

The portlandite (i.e. $Ca(OH)_2$) band at 360 cm^{-1} was never detected on the surface of the cements, due to its release into the storage medium which increased its pH (data not reported). However, the portlandite component was revealed in the inner area of all the lc-MTA and wTC-Ba cements until 28 days of aging. No portlandite component was detected either in ProRoot MTA (due to the overlapping of the strong bands of bismuth oxide) or Vitrebond. The spectra recorded in the interior of ProRoot MTA clearly showed the formation of ettringite, as hydration product of calcium sulfate and tricalcium aluminate. In the experimental cements this component was not spectroscopically revealed due to the interference of barium sulfate; however, ettringite was observed since the early stages of hydration in both wTC cement (i.e. the corresponding cement free from barium sulfate) [13-15] and in its composite with poly-HEMA-TEGDMA.

The CSH phase (i.e. the hydration product of alite and belite), which shows a broad and very weak Raman band, was detected with higher intensity in the experimental cements than in ProRoot MTA.

3.5.2. ATR/FTIR analyses

Figs. 4 and 5 report the IR spectra of the cements aged in DPBS and DMEM + FBS, respectively. Band assignments have been given according to the literature [13 and references cited therein].

IR spectroscopy confirmed the Raman findings on the composition of the unhydrated powders. In ProRoot MTA, calcium carbonate was prevalently present in its aragonite form.

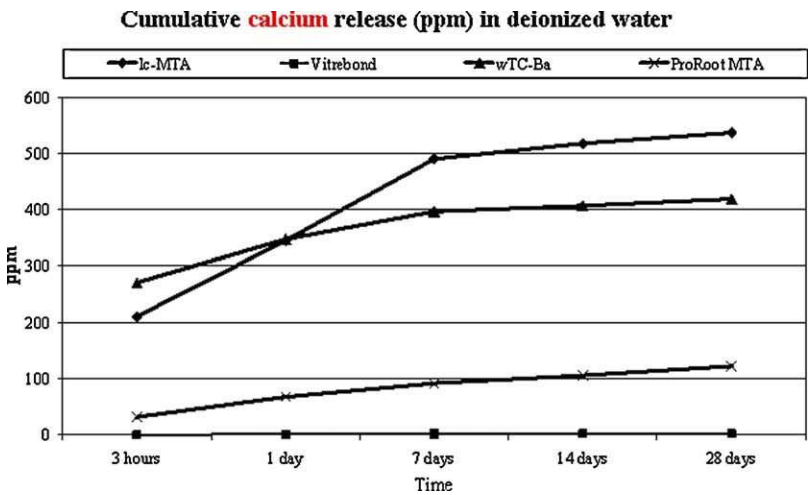

Fig. 2 - Cumulative calcium release (ppm) in deionized water.

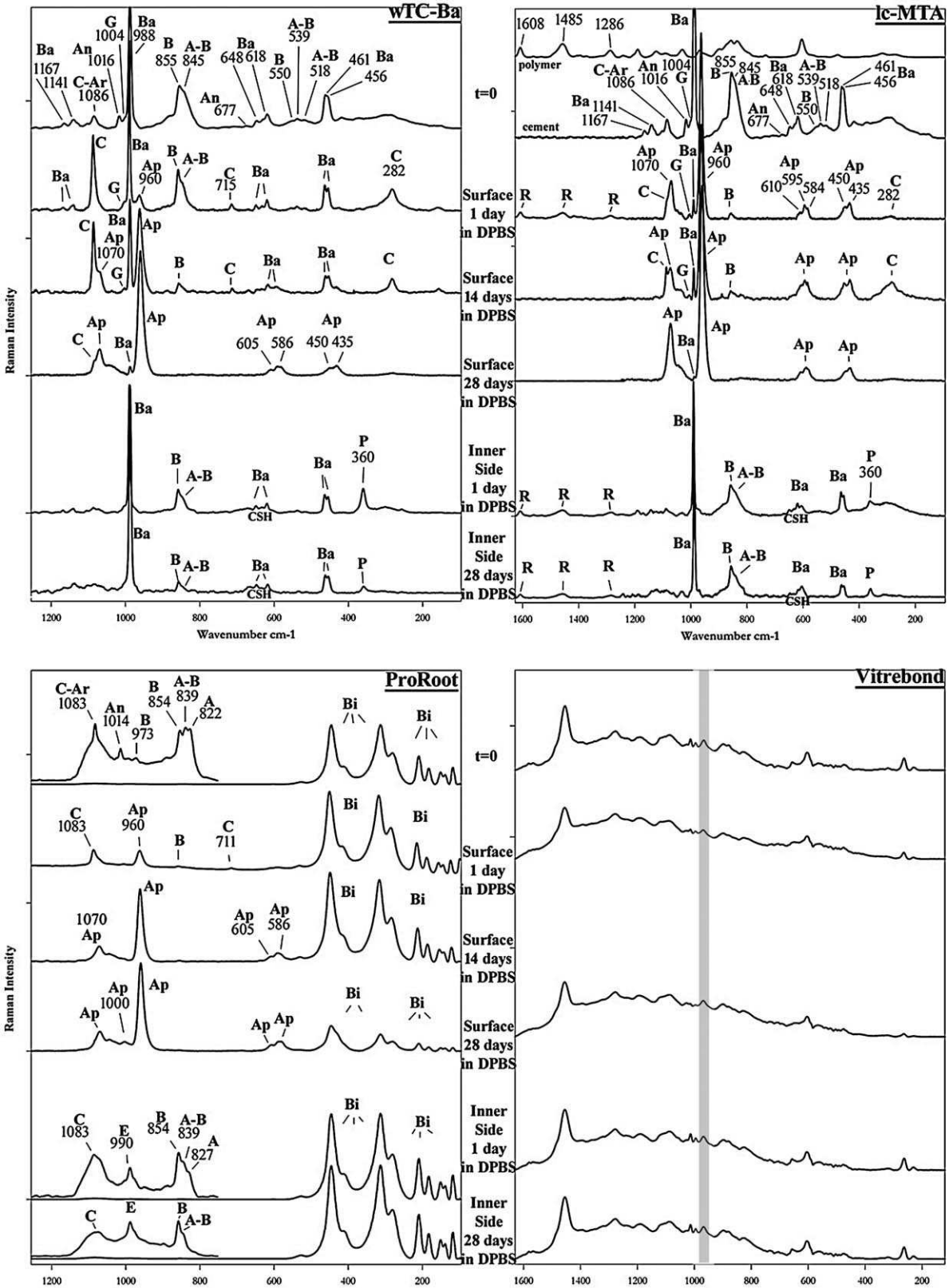

Fig. 3 - Raman spectra of lc-MTA, wTC-Ba, ProRoot MTA and Vitrebond after different times of aging in DPBS. The spectra of the unhydrated cements and resin are reported for comparison. The bands assignable to barium sulfate (Ba), calcite (C), aragonite (Ar), anhydrite (An), gypsum (G), belite (B), alite (A), ettringite (E), resin (R), apatite (Ap), bismuth oxide (Bi), and portlandite (P) are indicated.

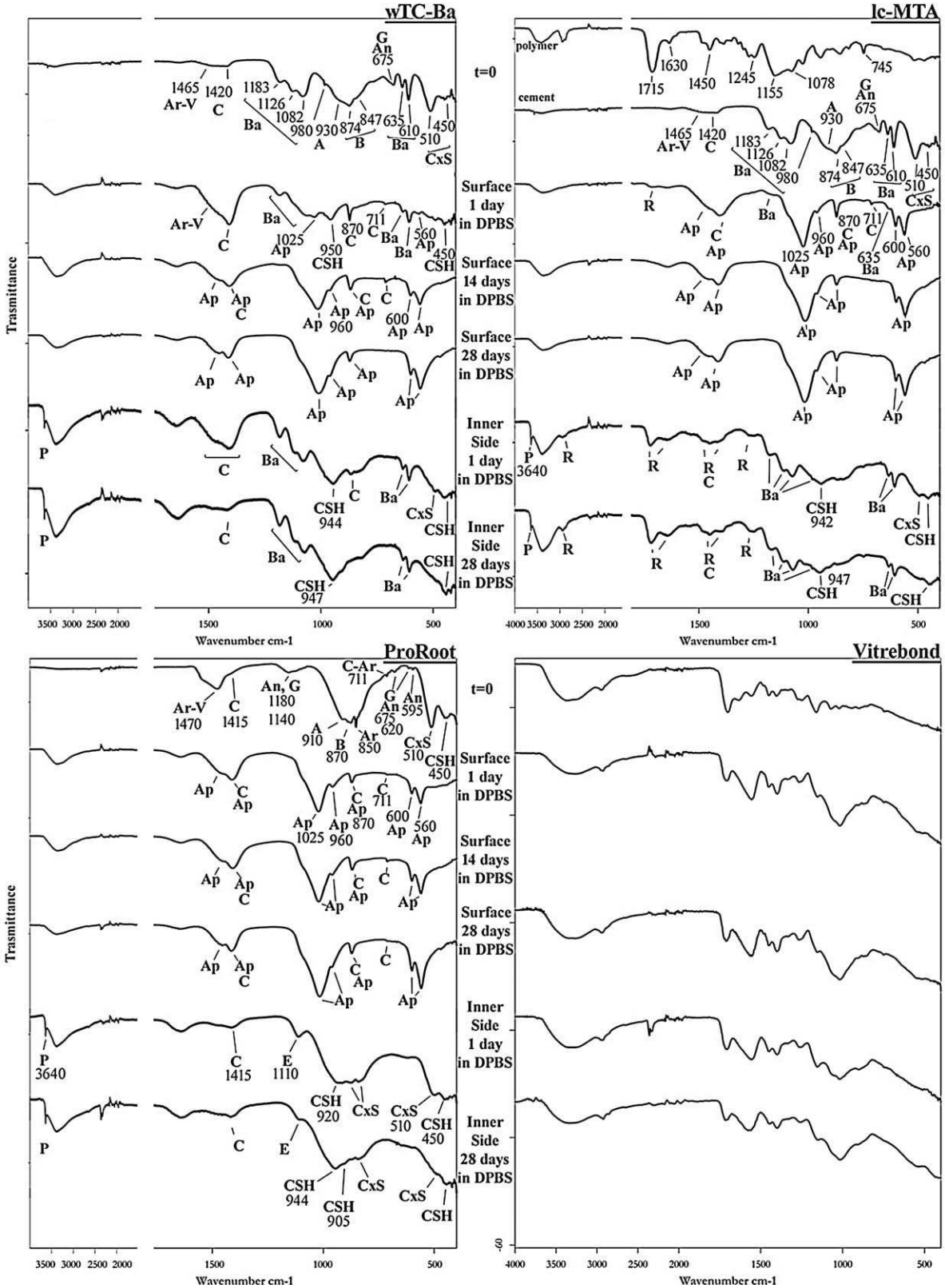

Fig. 4 - IR spectra of lc-MTA, wTC-Ba, ProRoot MTA and Vitrebond after different times of aging in DPBS. The spectra of the unhydrated cements and resin are reported for comparison. The bands due to portlandite (P), barium sulfate (Ba), calcite (C), aragonite (Ar), anhydrite (An), gypsum (G), ettringite (E), hydrated calcium silicate gel (CSH), newly polymerized silicates (CxS), belite (B), alite (A), resin (R), and apatite (Ap) are indicated.

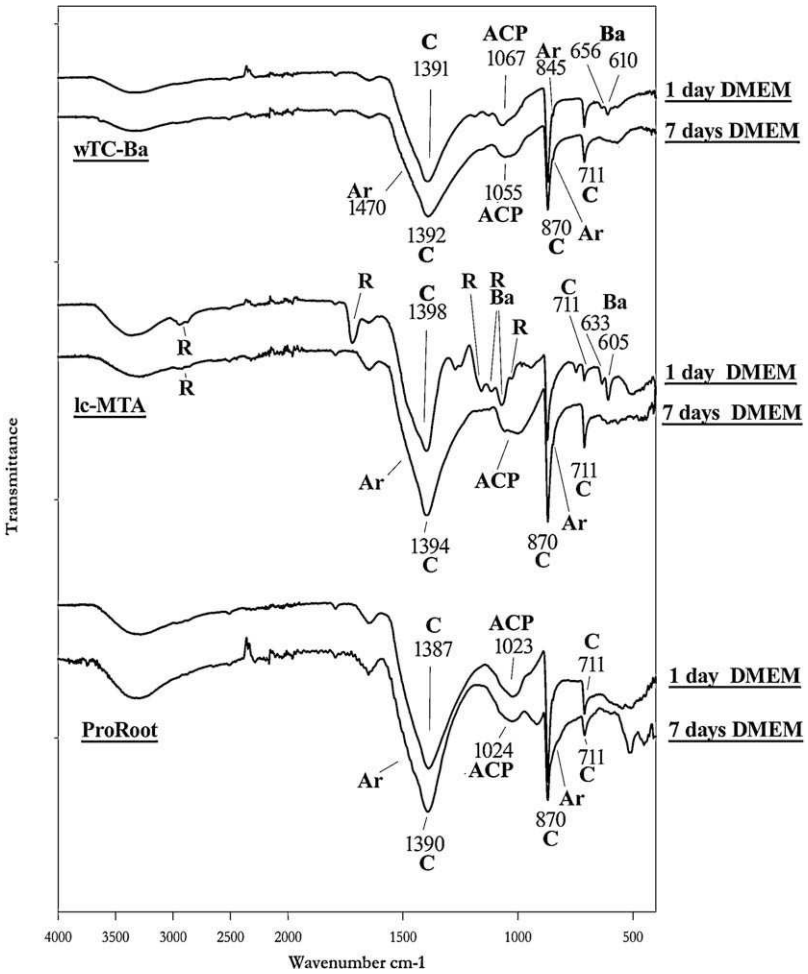

Fig. 5 - IR spectra recorded on the surface of lc-MTA, wTC-Ba and ProRoot MTA after 1 and 7 days of aging in DMEM + 10% FBS. The bands due to barium sulfate (Ba), calcite (C), aragonite (Ar), resin (R), and amorphous calcium phosphate (ACP) are indicated.

After one day of aging in DPBS, the IR spectra of lc-MTA and ProRoot MTA surfaces showed the presence of an apatite and calcite/aragonite deposit about 2 microns thick: no bands of the underlying cement were observable for ProRoot MTA, while for lc-MTA weak bands due the resin and barium sulfate components were visible. On wTC-Ba, the apatite deposit appeared thinner than on the other calcium-silicate cements, as revealed by the lower intensity of the apatite bands, and the detection of prominent components due to calcite/aragonite, CSH silicate phase and barium sulfate.

After aging in DPBS for 14 and 28 days, the surface spectra of ProRoot MTA, lc-MTA and wTC-Ba showed the presence of a B-type carbonated apatite and a small quantity of calcite. No bands of the underlying cement were observed.

With regard to Vitrebond, the spectral changes observed on the surface of the cement were analogous to those detected in its interior and thus not ascribable to the formation of an apatite deposit, according to the chemical composition of the cement lacking in calcium.

The IR spectra recorded until 28 days of aging in the internal region of the experimental cements and ProRoot MTA showed the presence of portlandite, ettringite (observable only for ProRoot MTA according to Raman results) and CSH phase, in addition to belite and calcite/aragonite. No portlandite was observed for Vitrebond, according to its chemical composition. After one day of aging, cement polymerization appeared more advanced for the experimental cements than ProRoot-MTA, as revealed by the higher wavenumber of the CSH band observed for the former.

The IR spectra of lc-MTA, wTC-Ba and ProRoot MTA surfaces after 1 and 7 days in DMEM + FBS showed the presence of a high quantity of calcite/aragonite deposit, together with lower amounts of amorphous calcium phosphate; after one day of aging, the spectrum of the lc-MTA surface still showed bands due to the resin and barium sulfate.

To assess the occurrence of resin-mineral ions interactions, a just-prepared lc-MTA cement was analyzed and its IR spectrum is shown in Fig. 6; the spectra of the just polymerized poly-HEMA-TEGDMA resin and unhydrated wTC-Ba powder are reported for comparison. As can be easily seen, in the spectrum of lc-MTA (Fig. 6, spectrum c), the 1640 cm^{-1} band due to the C—C group of the HEMA and TEGDMA monomers (Fig. 1) is significantly weaker than in the spectrum of the resin (Fig. 6, spectrum a); this result suggests that in lc-MTA the

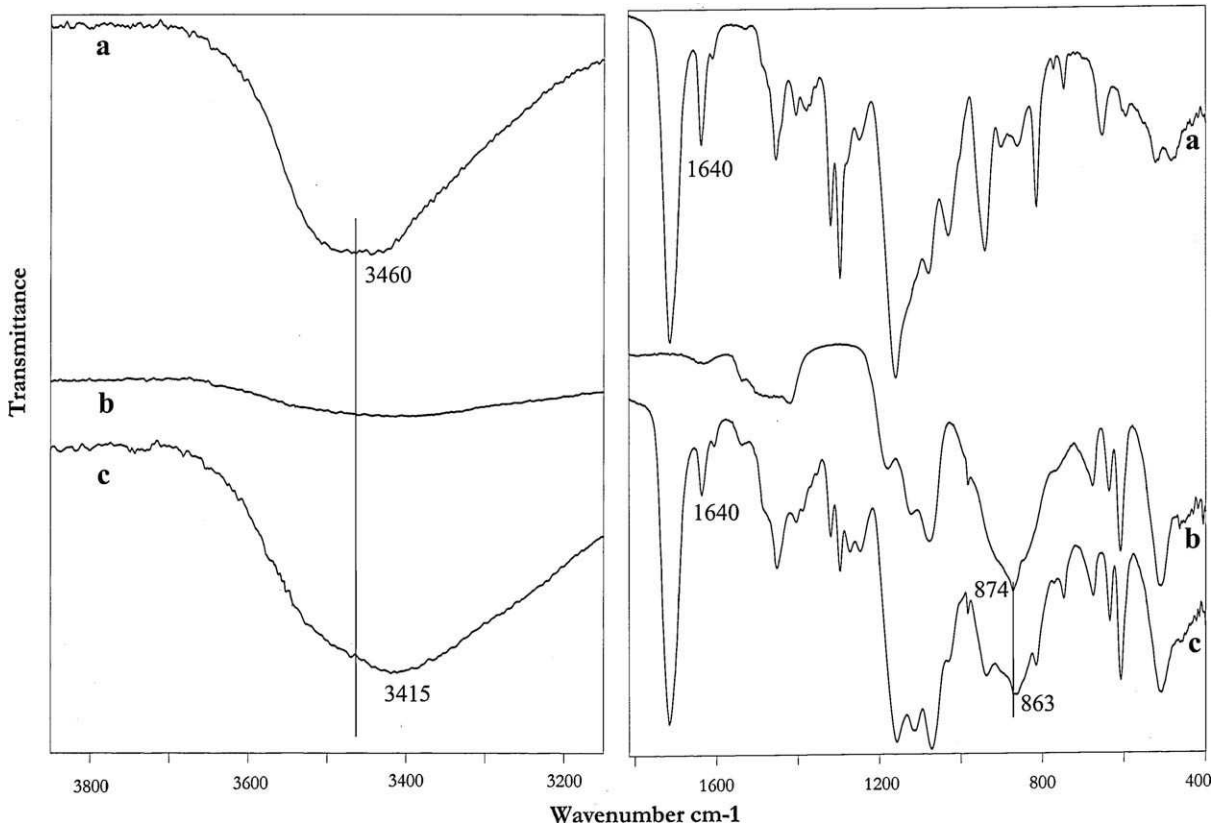

Fig. 6 - IR spectra of the just polymerized poly-HEMA-TEGDMA resin (a), unhydrated wTC-Ba powder (b) and just-prepared lc-MTA cement (c).

resin attained a higher polymerization degree than in the pure poly-HEMA-TEGDMA resin.

In lc-MTA, the band due to the OH group (prevalently attributable to the OH stretching vibration of HEMA component, Fig. 1) is shifted to lower wavenumber values with respect to the pure resin (from 3460 to 3415 cm^{-1}); also the band due to silicate groups (SiO_{44-} stretching vibration) shifted downwards with respect to the wTC-Ba unhydrated powder (from 874 to 863 cm^{-1}). Both these trends indicate the presence of hydrogen bond interactions between silicate and OH groups of HEMA.

The possible formation of Si-O-C covalent bonds has been taken into account. These groups are characterized by strong absorptions near 1100 cm^{-1} [48], i.e. in a spectral range covered by strong bands due to barium sulfate. Therefore, to clarify this aspect, a composite containing wTC (i.e. cement free from barium sulfate) and poly-HEMA-TEGDMA was prepared and analyzed (spectrum not reported): no spectral features ascribable to the formation of Si-O-C bonds were observed, in agreement with other authors [44].

To evaluate the possible bioactivity of pure poly-HEMA, pure poly-TEGDMA and poly-HEMA-TEGDMA polymers, the resins were soaked for 4 weeks in a metastable calcifying medium, according to Chirila et al. [44,45]. At this time, the samples that were transparent at the beginning, appeared slightly opaque (the most opaque sample was poly-HEMA); their IR spectra are reported in Fig. 7. The bands at about 1025, 600 and 560 cm^{-1} revealed that all the samples were covered by an apatite deposit that appeared inhomogeneous and of different thicknesses on the various samples, but always thinner than 2 m (due to the detection of the bands of the polymeric components). On the basis of the relative intensity of the apatite bands, it can be deduced that the thickness of the deposit decreased along the series: poly-HEMA (the 963 cm^{-1} band was also detectable) > poly-HEMA-TEGDMA > poly-TEGDMA.

The spectra corresponding to poly-HEMA (Fig. 7A) appeared particularly interesting. Upon apatite deposition, some polymer bands underwent wavenumber shifts and/or intensity changes. As reported in the figure, the most significant changes involved the bands at about 3350 cm^{-1} (OH stretching vibration), 1700 cm^{-1} (C—O stretching vibration), 1270-1248-1150 cm^{-1} (C-O-C stretching vibrations), 1070 cm^{-1} (C—O stretching vibration). Since control and soaked samples were characterized by similar polymerization degrees, these changes can be ascribed to the chelation of calcium ions.

Similar changes have been observed also for poly-TEGDMA and poly-HEMA-TEGDMA (Fig. 7B and C); however, for these polymers, the polymerization degree of control and soaked samples appeared different, so that spectral changes could be due to both calcium chelation and polymerization progress.

3.5.3. In vitro dentin marginal adaptation: ESEM…EDX and OM analyses

The morphology of cement-dentin interface in fresh restorations soaked 10 min in DPBS (Figs. 8 and 9a and b) was analyzed

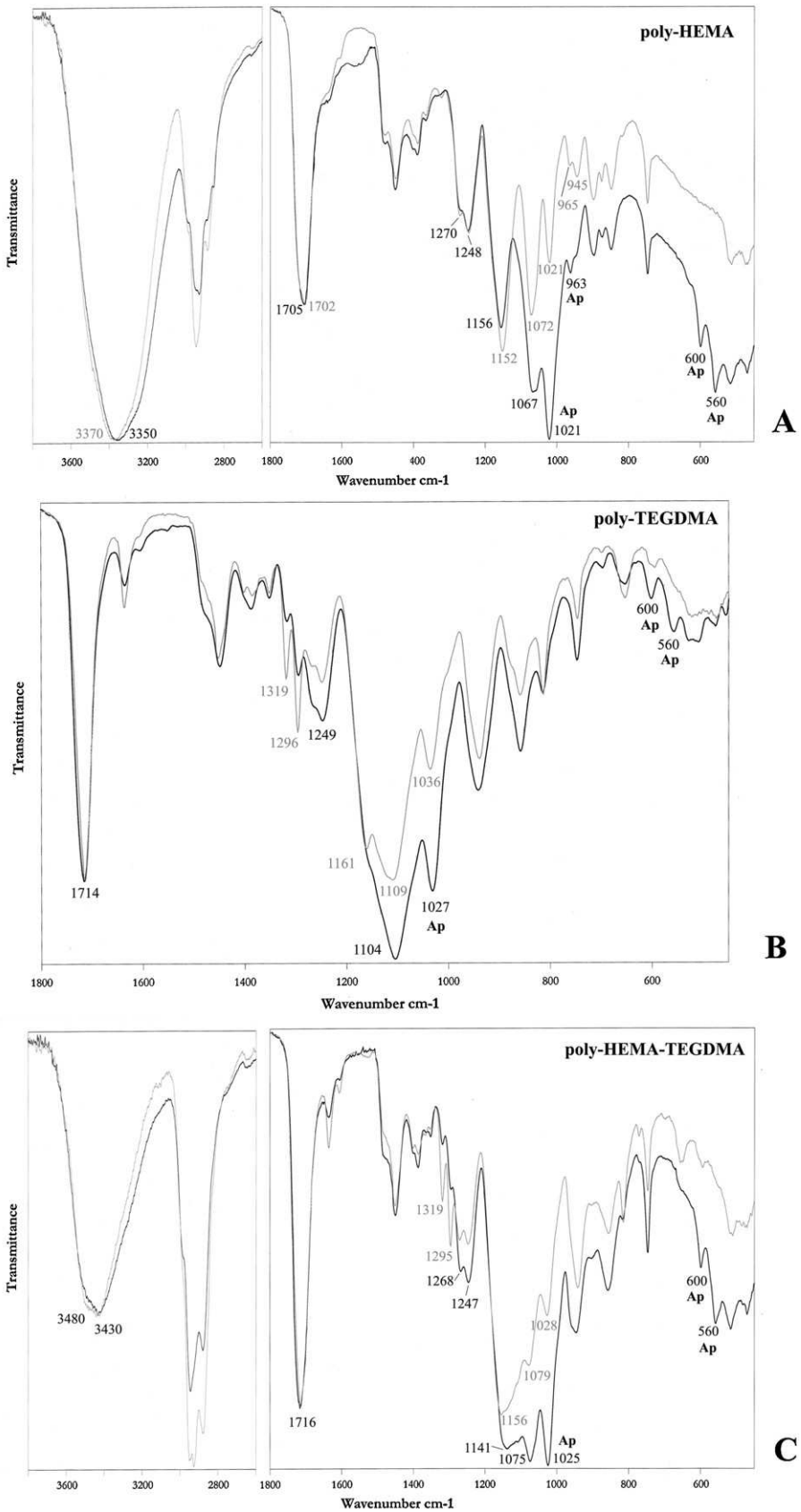

Fig. 7 - IR spectra of poly-HEMA (A), poly-TEGDMA (B) and poly-HEMA-TEGDMA (C) resins after soaking for 4 weeks according to Chirila et al. (black). The spectra of control samples are reported for comparison (gray).

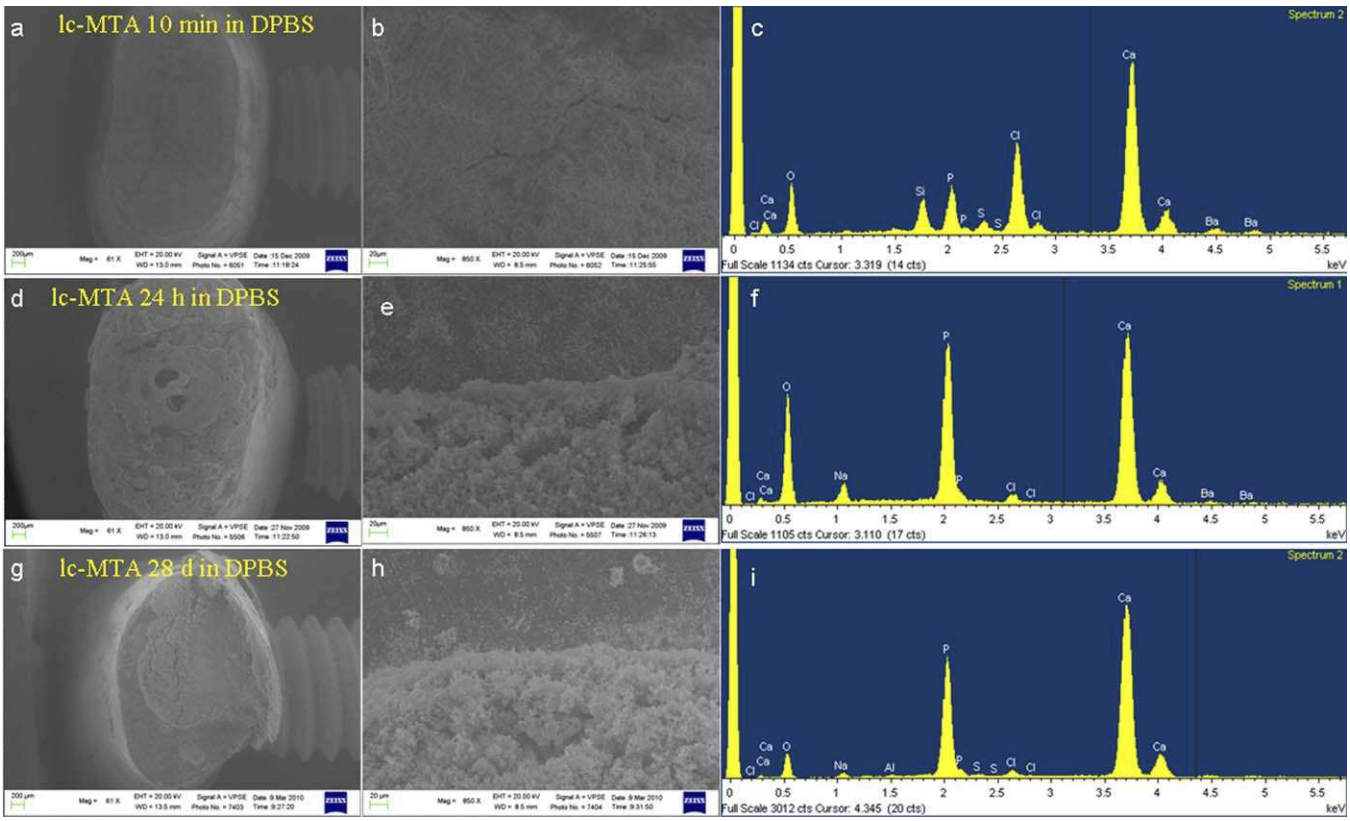

Fig. 8 - Morphology and chemical composition and marginal adaptation of lc-MTA filling human roots after 10 min (a-c), 24 h (d-f) and 28 days (g-i) of soaking in DPBS at 37°C.

using ESEM/EDX. A first evaluation was made immediately after restoration. The margins of all cements resulted free from porosities or gaps, suggesting the optimal adaptation to dentinal cavity walls of all cements. EDX on lc-MTA, wTC-Ba and ProRoot MTA (not shown) revealed calcium (Ca), silicon (Si) and phosphorous (P) peaks (Figs. 8 and 9c) while on Vitrebond aluminum (Al), Si, zinc (Zn) and fluorine (F) peaks were detected (not shown).

After 24 h of immersion in DPBS a great amount of precipitates completely covered the surface, the margin and partially also the peripheral dentin surface of lc-MTA (Fig. 8d and e), wTC-Ba (Fig. 9d and e) and ProRoot MTA (Fig. 10a and b). All margins resulted filled and crowded by apatite deposits. EDX revealed Ca and P peaks, while Si was completely absent on the surface of lc-MTA and wTC-Ba (Figs. 8 and 9f) and still detected on ProRoot MTA (Fig. 10c). The lc-MTA, wTC-Ba and ProRoot MTA displayed similar morphology at the cement/dentin interface-margin; lc-MTA showed a thicker apatite layer. Vitrebond surface showed irregular precipitates and EDX displayed Al, Si, Zn and F, and also traces of Ca and P (Fig. 10f-h).

Additional apicected, root-filled maxillary roots soaked for 24 h in DPBS were observed by optical microscopy; they showed the presence of a thick layer formed on the apex (Fig. 11a-d).

After 28 days in DPBS a thick layer of apatite was detected on lc-MTA (Fig. 8g and h), wTC-Ba (Fig. 9g and h) and ProRoot MTA (Fig. 10d), either on their surface, or at the cement-dentin interface, or on the adjacent dentin. All margins resulted filled and covered by apatite deposits. EDX revealed Ca and P peaks (Figs. 8, 9i, and 10e). Vitrebond showed the presence of irregular deposits and EDX revealed the presence of Al, Si, Zn, F, and detected weak Ca and P peaks (Fig. 10i and l).

3.5.4. ESEM/EDX analysis of cement disks

The ESEM/EDX inspection of freshly prepared samples of lc-MTA, wTC-Ba and ProRoot MTA revealed the presence of a water film when evaluated at 9.9 Torr pressure, 100% RH and 4°C. The water film completely masked the cement surface. At 3.9-2.9 Torr and 40-0% RH the cement surface appeared completely smooth with few nanosized porosities. Cements observed at 2.9 Torr in wet environment showed many randomly oriented needle-like crystalline formations immersed and embedded in a sort of gel matrix.

EDX analyses of freshly prepared lc-MTA and wTC-Ba revealed the presence of Ca and Si peaks and traces of barium (Ba), Al and sulfur (S). ProRoot MTA displayed Ca, bismuth (Bi) and Si peaks while Vitrebond showed Al, Si, Zn and F peaks.

After 24 h in DPBS the surface of all lc-MTA, wTC-Ba and ProRoot MTA samples was covered by a newly formed calcium phosphate layer consisting of aggregated apatite spherulites (0.5-1 m diameter). Little porosities were observed on the surface.

EDX on lc-MTA and wTC-Ba surface revealed the presence of Ca and phosphorus (P), chlorine (Cl) and sodium (Na) peaks and the disappearance of Si, S, Ba and Al peaks, suggesting the formation of a deposit thick enough to mask the dense

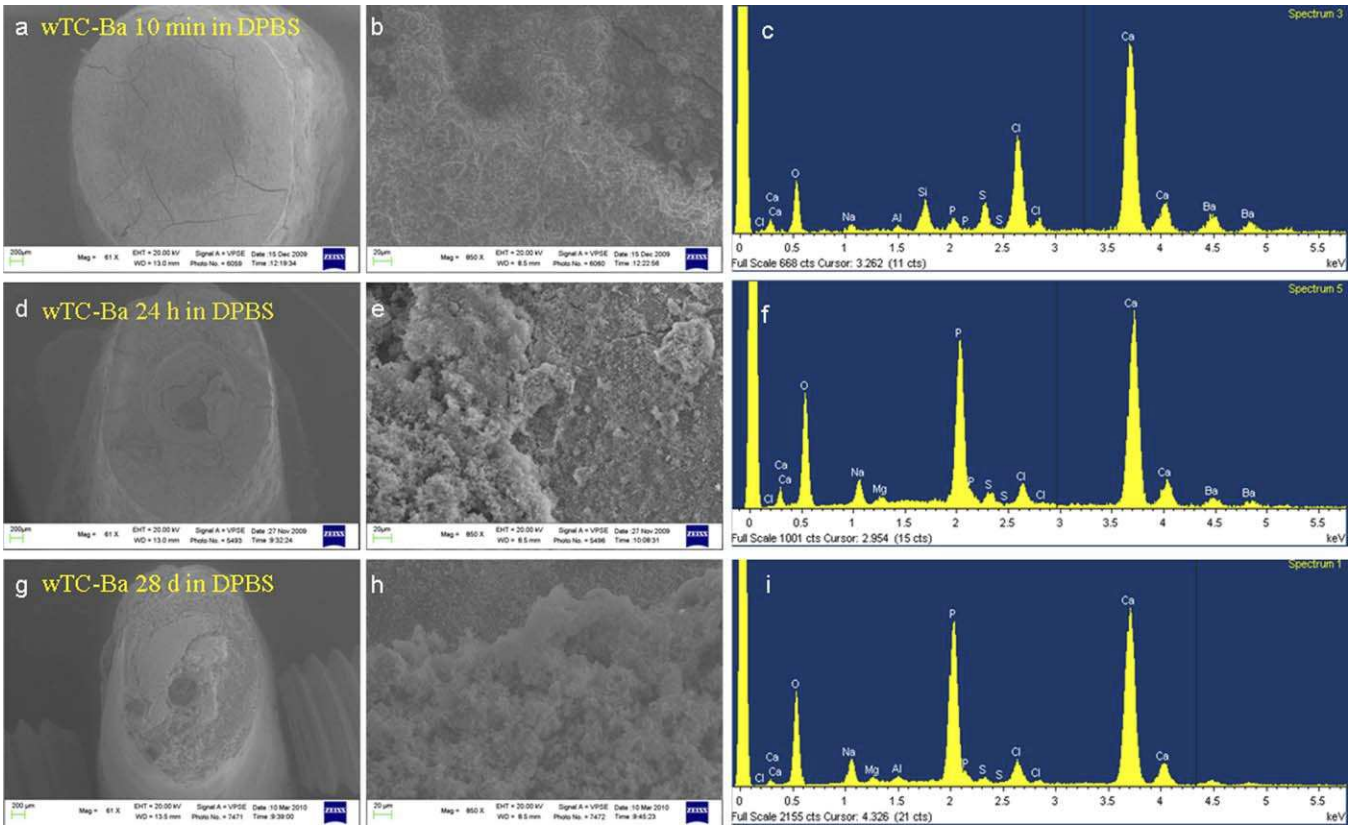

Fig. 9 - Morphology and chemical composition and marginal adaptation of wTC-Ba filling human roots after 10 min (a-c), 24 h (d-f) and 28 days (g-i) of soaking in DPBS at 37°C.

surface of the cement. EDX analysis of inner area of fractured samples showed the presence of Ca, Ba, Si and S. The surface of ProRoot MTA displayed Ca, P, Cl and Na while the inner area of fractured samples showed Ca, Si, S, Bi and Al peaks. Vitrebond surface showed Al, Si, Zn and F peaks.

After 28 days the entire surface of lc-MTA cement (Fig. 12a and b) resulted covered by a thick porous apatite deposit consisting of large spherulites (1-2 m in diameter), so that the dense cement surface was completely hidden. EDX showed Ca and P, traces of Na and Cl. Similar results were obtained for wTC-Ba (Fig. 12c and d) and ProRoot MTA (Fig. 12e and f) surfaces.

Differently, Vitrebond disks soaked for 28 days in DPBS (Fig. 12g and h) showed the absence of apatite precipitates. EDX revealed Si, Al, Zn, F and traces of Mg and Cl.

3.6. Cell viability

3.6.1. Response to the extract exposure

Alamar blue assay uses a visible blue fluorogen probe resazurin, which is reduced to a red fluorescent compound (resorufin) by cellular redox enzymes. Viable cells continuously convert resazurin to resorufin, thereby generating a quantitative measure of viability and cytotoxicity. The amount of fluorescence is estimated proportional to the number of living cells and corresponds to the cell metabolic activity.

The exposure of Saos-2 cells to the extracts showed the increase of the cell viability and number with time for all the materials' extracts (Fig. 13A).

No statistical differences were detected at 24 h in the viability of cells exposed to the extracts of any calcium-silicate

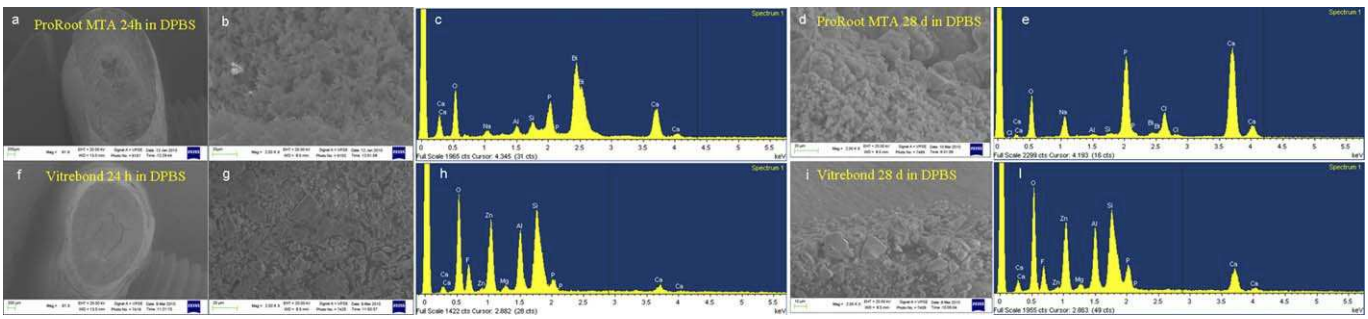

Fig. 10 - Morphology and chemical composition and marginal adaptation of ProRoot MTA (a-e) and Vitrebond (f-l) cements filling human roots after 24 h and 28 days of soaking in DPBS at 37°C.

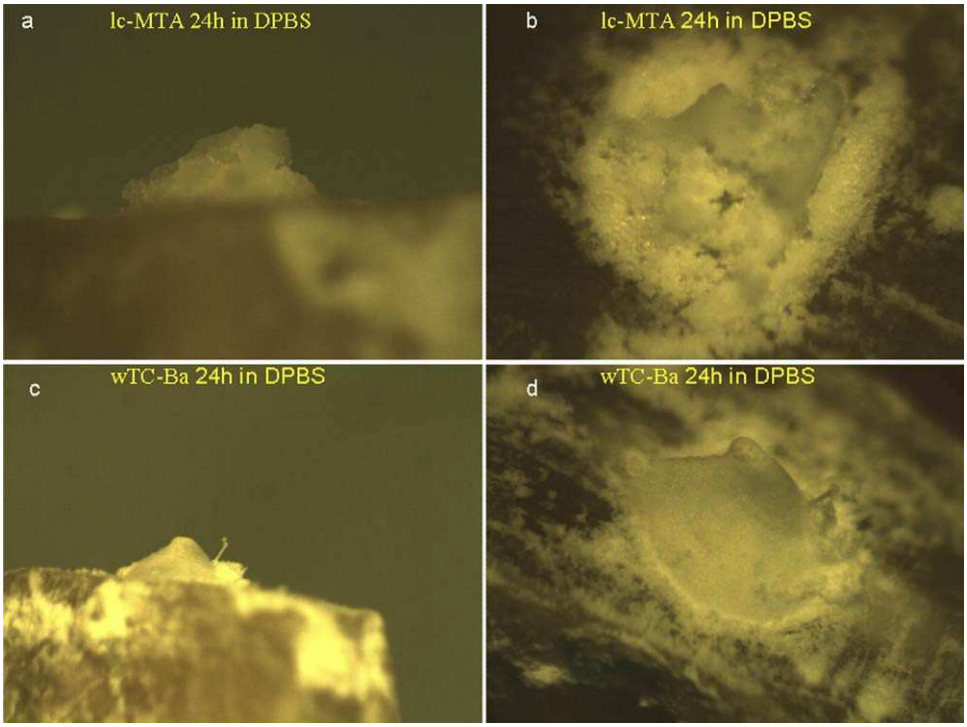

Fig. 11 - Optical microscopy observation of the morphology of retro-filled roots surface, obturated with lc-MTA (a and b) or wTC-Ba (c and d) and soaked in DPBS for 24 h. Apatite deposits are visible on the surface of cements and on adjacent dentin.

material and controls, while the exposure to the extracts of Vitrebond allowed a statistically lower cell viability, suggesting the presence of damaged and nonviable cells. The data of lc-MTA, wTC-Ba and ProRoot MTA were all statistically different from Vitrebond at 1 day.

Statistically lower viability value was detected after 3 days of exposure to the extracts of lc-MTA compared to wTC-Ba and ProRoot MTA extracts. No statistical differences were obtained between lc-MTA and Vitrebond at 3 days.

3.6.2. Response to the solid cements

All the materials showed a statistically reduced viability and cell number compared to the control TCPS. However, cell response on TCPS was measured to check the viability and proliferation of Saos-2 along the experiments, and was not used as control surface against the cement surface since the reaction of cells to the chemistry and to the (smooth) surface area of the culture plastic cannot be compared with the response to the 3D rough surface of the cements.

Similar results were obtained using two different assays of cell cytotoxicity, i.e. Alamar blue reduction (metabolic activity, Fig. 13B) and neutral red uptake (membrane integrity, Fig. 13C).

The viability and cell number increased with time for Saos-2 cultured onto wTC-Ba and ProRoot MTA (Fig. 13B and C).

At 24 h and 3 days the viability on the calcium-silicate cements was similar while was statistically lower on Vitrebond (Fig. 13B).

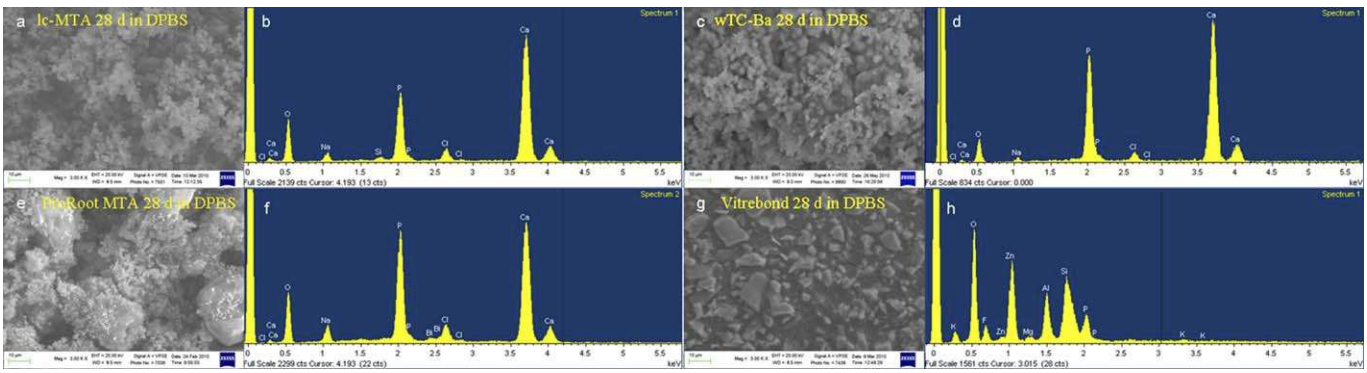

Fig. 12 - ESEM/EDX analyses of sample disks soaked 28 days in DPBS at 37°C showing the formation of apatite (bioactivity) on the surface of lc-MTA (a and b), wTC-Ba (c and d) and ProRoot MTA (e and f) and the complete lack of bioactivity of Vitrebond (g and h).

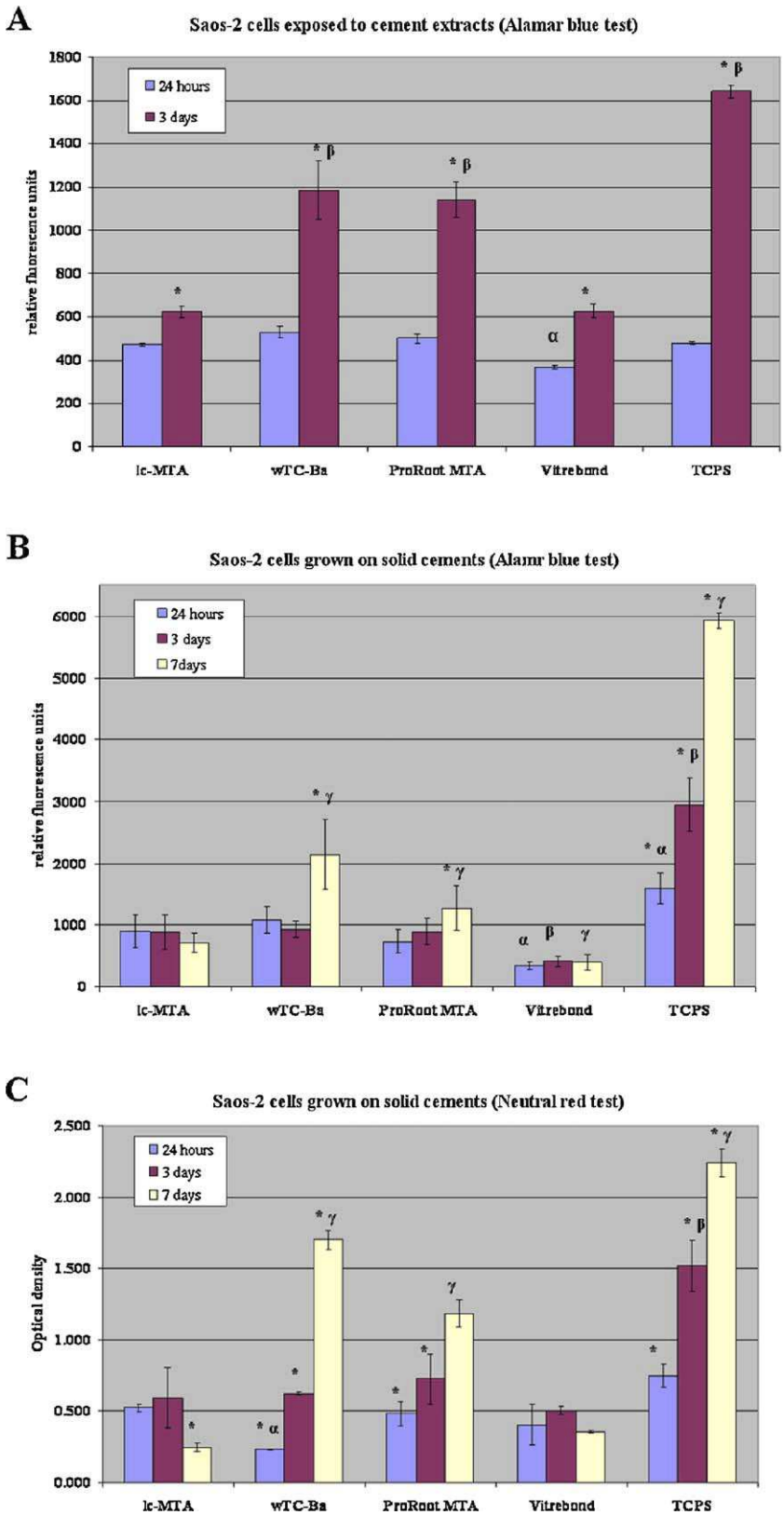

Fig. 13 - Viability of Saos-2 cells: evaluation of the health state of cells (metabolic activity and cell integrity). The diagrams include the one-way ANOVA results (*significant difference per $p < 0.05$ within each material group (3 days vs 24 h); is the significant difference per $p < 0.05$ vs lc-MTA at 24 h; is the significant difference for $p < 0.05$ vs lc-MTA at 3 days; is the significant difference per $p < 0.05$ vs lc-MTA at 7 days). (A) Alamar blue cytotoxicity assay showing the viability (metabolic rate and functional capacity of mitochondria) of cells exposed to the materials' extracts (n = 4). The metabolic activity of cells statistically increased over time for all the materials' extracts. No statistical differences were detected at 24 h in the

A decrease in viability and cell number was observed at 7 days for lc-MTA (Fig. 13B and C). At this time the viability on lc-MTA was statistically lower than on wTC-Ba and ProRoot MTA but statistically higher than on Vitrebond (Fig. 13C).

4. Discussion

Blood contamination is inevitable through all clinical procedures in oral and root-end apical surgery and may increase the risk for a complete washout of the materials during their setting phase. Moreover, the materials can take up more water than might be ideal [50,51] and may change their physical properties [52] when in moist environment.

The setting time of calcium-silicate MTA cements is 30-70 min [53,54], but is longer when in presence of serum and blood [54,55]. The presence of serum proteins increases the setting time and modifies the expansion of calcium silicate cements [54,55]. So, the use of fast setting light-curable materials to fill root-end cavities represents an innovative approach to prevent the cement wash-out and to ensure the clinical success.

The present study demonstrated that lc-MTA possesses improved chemical-physical properties (fast setting, bioactivity) mainly due to the presence of calcium-silicate mineral particles and poly-HEMA polychelating amphiphilic material. After 120 s of light-curing the surface of the cement was hard enough to support both the initial and final Gilmore needles. Differently, the setting time of the commercial available control cement ProRoot MTA was 170 min, in agreement with previous studies [54,56,57].

The surface structure of the experimental lc-MTA cement, observed by ESEM/EDX, resulted pore-free and more homogeneous than the surface of both wTC-Ba and ProRoot MTA cements.

A complex setting mechanism is proposed for lc-MTA:

(i) After light-curing the presence of HEMA and TEGDMA monomers creates a polymeric network able to stabilize the outer surface of the cement.
(ii) Hydrogen bond interactions occur between the OH groups of HEMA and silicate groups of the mineral powder (poly-HEMA-Si bond, Fig. 14A).These chemical interactions may confer to the cement bulk fast hardness and early consistency and stability.
(iii) Once immersed into aqueous media, the designed resin matrix is permeable enough to absorb water due to the hydrophilicity of HEMA, and to keep it entrapped inside the cement. Consequently, the inclusion of a HEMA/TEGDMA-based resin into a calcium-silicate powder resulted in a HEMA/TEGDMA-Si hybrid showing hydrophilic nature, in agreement with previous studies [49,58].
(iv) After the initial polymerization of the resin matrix induced by light-curing, a second setting reaction is triggered by the absorbed free water and involves the hydration and polymerization reactions of calcium-silicate mineral particles (CSH formation).It is possible to affirm that despite the external light-cured set coating layer, the cement is permeable enough to absorb water (confirmed by water uptake tests) due to its hydrophilicity. The permeability and water sorption of HEMA-based systems has been previously proved [49].

ESEM/EDX, Raman and FTIR analyses demonstrated that upon soaking in DPBS, the exposed external surface of lc-MTA is a reactive substrate that is rapidly covered by calcium-phosphate spherulites forming a biocoating mainly composed of carbonated apatite. The apatite-forming ability of calcium-silicate MTA cements has been recently demonstrated [12,15,16]. The study proved that the experimental lc-MTA cement is more bioactive than conventional calcium-silicate MTA cements; upon aging in DPBS, the lc-MTA cement appeared to form the thickest carbonated apatite deposit, suggesting that the incorporation of poly-HEMA-TEDGMA into the cement increased its bioactivity.

Many different chemical reactions may explain the improved bioactivity of lc-MTA.

4.1. Release of calcium ions

Calcium-silicate MTA cements were able to release calcium ions. Calcium ions released by calcium-silicate cements favor the ability to form apatite deposits [59] and increase the number of pores inside the cement [59,60].

Calcium-silicate MTA cements are porous media, partially or completely saturated with a pore solution. Due to this porosity, material-environment mass exchanges occur, in particular ion diffusion through the porosity. Calcium release of ProRoot MTA was in agreement with previous studies [61,62]. lc-MTA, although less soluble than ProRoot MTA and wTC-Ba, was characterized by calcium release and alkalinizing power statistically higher than the others. It can be hypothesized that the hydrophilicity of lc-MTA allows water mobility (inward-outward flux) and penetration into the cement bulk through the meshes of the resin molecular net; these processes are responsible for the high calcium release from the

mitochondrial function of cells exposed to the extracts of any calcium-silicate material and controls, while the exposure to the extracts of Vitrebond allowed a statistically lower viability of cells. Statistically lower number of cells was detected after 3 days of exposure to the extracts of lc-MTA compared to wTC-Ba and ProRoot MTA extracts. (B) Alamar blue cytotoxicity assay of cells cultured on solid cements (n = 6). The viability increased with time for Saos-2 cultured onto wTC-Ba and ProRoot MTA. At 24 h and 3 days the mitochondrial function of cells cultured on the calcium-silicate cements was similar while was statistically lower on Vitrebond. A non-significant decrease of metabolic activity was observed at 7 days for lc-MTA; at this time the viability on lc-MTA was statistically lower than on wTC-Ba and ProRoot MTA but statistically higher than on Vitrebond. (C) Neutral red cytotoxicity assay (cell surface integrity and lysosome viability) of cells grown on solid cements (n = 3). The trend of the Neutral red assay was similar to the Alamar blue. A significant decrease of metabolic activity was observed at 7 days for lc-MTA.

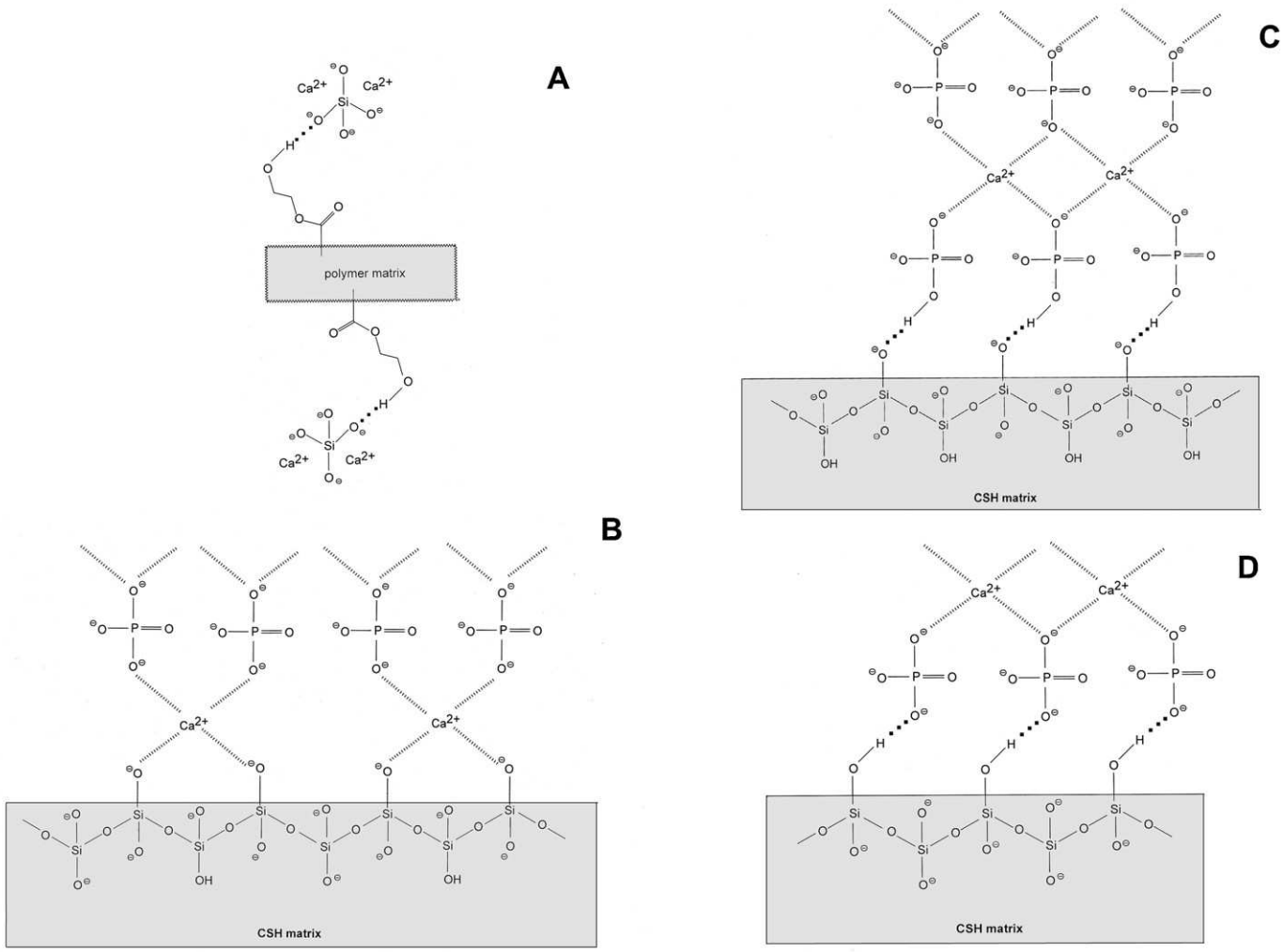

Fig. 14 - (A) Hydrogen bonding interactions between silicate ions and the resin. (B) Ionic interactions between the CSH matrix and Ca^{2+} ions and the subsequent nucleation of an apatite phase. (C) Hydrogen bonding interactions between the CSH matrix and HPO_{42-} ions and the subsequent nucleation of an HPO_{42-}-containing apatite phase. (D) Hydrogen bonding interactions between the CSH matrix and PO_{43-} ions and the subsequent nucleation of an apatite phase.

lc-MTA cement. The water absorption inward the hydrogel structure promotes the solubilization of mineral ions (Ca^{2+}) and the formation of portlandite and CSH; the water mobility favors the calcium release from the cement bulk. Differently, the formation of a sheath protective layer [63] on the surface of hydraulic calcium-silicate cements (and similarly on wTC-Ba and ProRoot MTA) reduces the inward flux of water into the cement bulk after the first stages of the hydration reaction and consequently decreases the material-environment mass exchanges and leaching (outward flux of calcium from the cement).

The initial high calcium release detected after 3 h could be explained by the surface hydration and dissolution of calcium-silicate particles due to their high reactivity with water. The formation of portlandite (calcium hydroxide) in the early hydration stages of lc-MTA (as well as of other MTA cements) has been confirmed by both the strong increase in pH of soaking water and by Raman and FTIR analyses. Further apatite-formation ability is related to calcium ions supplied by both $CaCl_2$ and calcium sulfate present in wTC-Ba formulation. Calcium chloride has been demonstrated able to increase the bioactivity of HEMA-based hybrid materials [64].

As expected on the basis of its chemical composition, Vitrebond was absolutely unable to produce calcium hydroxide, to release calcium and to increase pH. High calcium release is a requisite for a material to be bioactive [59].

4.2. Mineral component: sorption of Ca^{2+} and phosphate ions

After hydration of calcium-silicate particles, a solid-liquid interface forms on the mineral particles and ion dissolution occurs almost immediately. Ca^{2+} ions are rapidly released (calcium hydroxide formation) and migrate into the solution. Silicates are attacked by OH^- ions (hydrolysis of SiO_{44-} groups in alkaline environment) and a CSH phase forms on mineral particles. CSH is a porous, fine-grained and highly disorganized hydrated silicate gel layer containing Si-OH silanol

groups and negative surface charges. Actually, at alkaline pH, the deprotonation of silanol groups should predominate [65] with the consequent formation of SiO^- negative groups. The attraction between CSH particles has been reported as a consequence of the very high negative charge density of the CSH particles and the presence of Ca^{2+} ions [66].

The SiO^- negative groups induce heterogeneous nucleation of apatite by bonding calcium ions from the mineral particles on the silica-rich CSH surface (Fig. 14B), according to:

$$\equiv Si\text{-}O^- + Ca^{2+} \rightarrow -Si\text{-}O^- \cdots Ca^{2+}$$

The sorption of phosphate (PO_{43-}) and monohydrogenphosphate (HPO_{42-}) ions may occur through hydrogen bonding (Fig. 14C and D), according to:

$$\equiv Si\text{-}O^- + HPO_{42-} \rightarrow -Si\text{-}O^- \cdots HPO_4^{2-}$$

$$\equiv Si\text{-}OH + PO_{43-} \rightarrow \equiv Si\text{-}OH \cdots PO_4^{3-}$$

Alternatively, the HPO_{42-} ions can enter the apatite structure through the formation of $PO_{43-} \cdots HPO_{42-}$ hydrogen bond interactions.

4.3. Organic phase: oxygen atoms present in the resin (hydroxyl, ester and ether groups, see Fig. 1) are able to chelate calcium ions

Bioactivity experiments showed that poly-HEMA, poly-TEGDMA and poly-HEMA-TEGDMA polymers are able to induce apatite deposition after a 4-week immersion in a metastable calcifying medium. IR spectroscopy showed that the thickness of the deposit decreased along the series: poly-HEMA > poly-HEMA-TEGDMA > poly-TEGDMA. In other words, the most hydrophilic polymer is also the most bioactive.

The IR spectra corresponding to poly-HEMA showed that upon apatite deposition (Fig. 7A), the bands assignable to OH, C–O, C-O-C and C-O groups underwent wavenumber shifts and intensity changes. This trend can be explained by considering that oxygen atoms from hydroxyl and ester groups may chelate calcium ions released by mineral particles and induce apatite deposition (Fig. 15A). This process occurs on poly-TEGDMA thanks to analogous interactions between calcium ions and oxygen atoms from hydroxyl, ester and ether groups (Fig. 15B). Apatite deposition on poly-HEMA-TEGDMA can be explained consequently.

In other words, the hydroxyl, ester and ether chelating groups (Fig. 1) of HEMA and TEGDMA exposed on the surface of the polymer are the coordination sites for chelating calcium ions acting as nanotemplates for the growing of apatite nanoparticles. So, the calcium ions bonded by both HEMA and TEGDMA contribute to the formation of additional apatite nucleating sites.

The formation of a HEMA-calcium chelate complex is in agreement with previous in vitro investigations, which demonstrated that poly-HEMA-based materials [67-70] and silica gel-HEMA hybrid nanocomposites [26,27] possess bioactivity and that poly-HEMA increases the reactivity of a calcium phosphate bone cement [28,29].

So, calcium ions incorporated into the HEMA/TEGDMA calcium-silicate cement hybrid bind the SiO^- groups to form Si-O-Ca bonds, in agreement with a previous study [71].

It has been previously demonstrated that negatively charged polar groups must be present at the surface for a catalytic effect on apatite nucleation [72]. In lc-MTA negatively charged $Si\text{-}O^-$ groups from CSH (derived from the hydrolysis of silica groups of calcium-silicate particles [70,71]) may exert this catalytic action. At the same time, the combination of calcium-silicate particles with a HEMA-TEGDMA-based resin enhances the bioactivity of the cement.

Silanol groups are responsible for the apatite nucleation in acellular simulated body fluid [73]. The bioactivity of calcium-silicate cements and ProRoot MTA has been recently demonstrated [12-16], but conventional MTA cements have only CSH groups available for apatite nucleation. This study is in agreement with previous investigations which demonstrated that hydrated silica gel is crucial for the formation of bone-like apatite and consequent bone bonding [11,19,20,32,74].

4.4. Environmental alkalinity

The increase of environmental pH would accelerate the apatite nucleation, since apatite solubility decreases at basic pH values [75] and OH^- may be a component of apatite [59,60].

Therefore, when exposed to a phosphate-containing solution such as DPBS, the silanol groups of the silica-rich CSH surface induce heterogeneous nucleation of apatite through the adsorption of calcium from the mineral particles and phosphate from the solution (due to local supersaturation); an HPO_{42-}-containing apatite precipitates and matures into a B-type carbonated apatite phase at increasing storage times.

The nucleation of apatite is triggered by the catalytic effect of SiO^-/Si-OH groups from mineral particles and oxygen-containing groups from HEMA and TEGDMA present on the cement surface. This process is accelerated by the high pH and the release of calcium ions from the mineral component of the cement (calcium-silicate particles, calcium chloride, calcium sulfate, portlandite, and CSH) that increase the ionic activity with respect to apatite. Among the above mentioned factors, the high calcium release of lc-MTA seems the predominant in determining the highest bioactivity.

Interestingly, lc-MTA was statistically less soluble than the other MTA cements. lc-MTA showed a low weight loss in deionized water at all times (1-28 days) demonstrating a low solubility in water. Differently, when immersed in DMEM-FBS, lc-MTA samples showed a moderate weight loss only at 1 day, but a significant weight increment after 14 and 28 days. This trend of weight increase may be explained by the precipitation of calcite and/or aragonite and Ca-P mineral phases, after an initial release of Ca and Si from the cement due to the hydration reaction of calcium-silicate mineral particles. The formation of this deposit is due to the precipitation reaction between calcium ions (released by the cement) and phosphate and carbonate ions originating from DMEM.

Actually, the hydration reaction of calcium-silicate particles (involving the hydration, surface dissolution and decalcification of mineral particles) occurs in depth inside the cement matrix (sub-surface areas), as proved by the formation

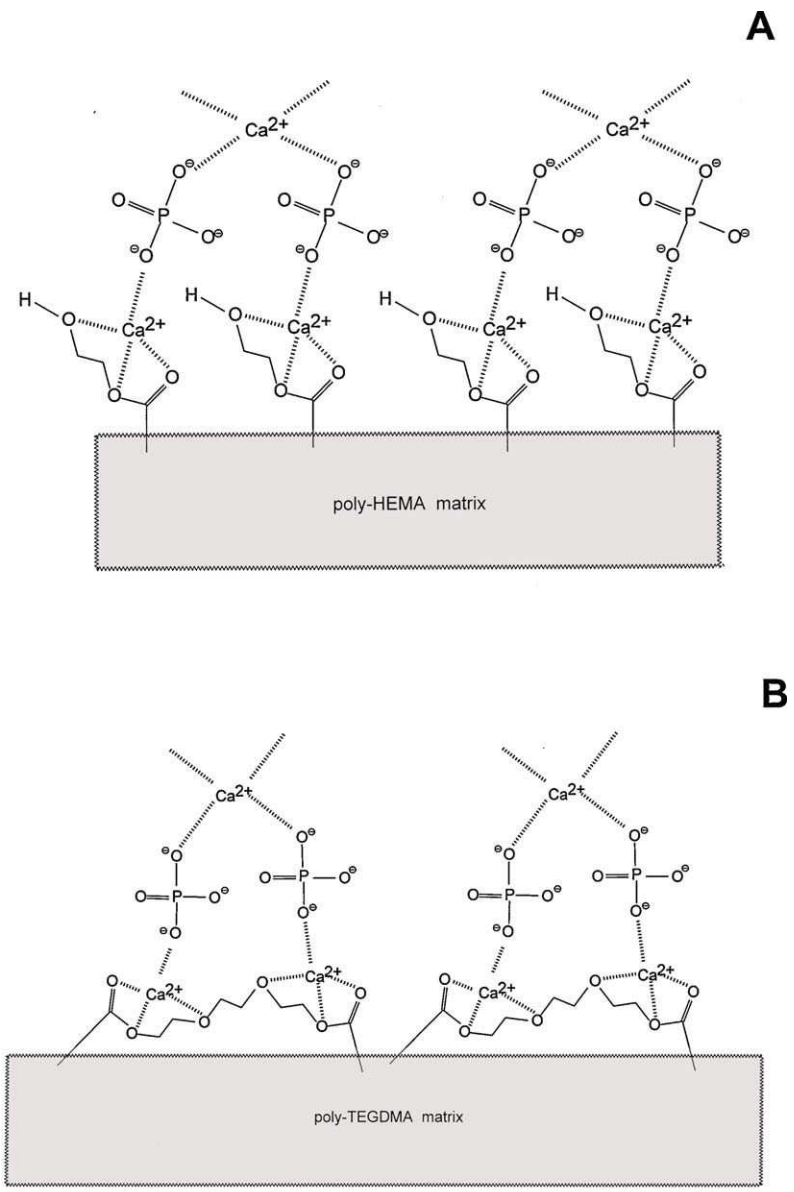

Fig. 15 - (A) Chelation of calcium ions by hydroxyl, ester and ether groups from poly-HEMA and the subsequent nucleation of an apatite phase; (B) Chelation of calcium ions by ester and ether groups from poly-TEGDMA and the subsequent nucleation of an apatite phase.

of portlandite and CSH (typical hydration products of Portland-derived cements) demonstrated by Raman and FTIR bands.

Previous studies demonstrated that calcium-silicate MTA cements are good substrates for osteoblast growth [19,20,37] and are able to induce cell proliferation mainly when they are freshly prepared [21,22]. Their biological activity is mainly related to calcium release, to the presence of silicon ions on their surface and to the formation of bone-like apatite [12-16,21,22,37]. Calcium-silicate MTA cements proved to be more biocompatible compared to the previous root-end filling materials such as SuperEBA, IRM and amalgam [19,20,37,76-78]. Calcium-silicate MTA cements allow osteoblast growth and differentiation [37] despite these materials provoked a strong alkalinization of the surrounding medium/fluids (pH 11 or more) due to the formation of calcium hydroxide. In the present study both the conventional calcium-silicate MTA cements (wTC-Ba and ProRoot MTA) did not induce any compromising cytotoxicity on Saos-2 cells, according to previous studies [37] and Saos-2 cell viability was good mainly at 7 days.

Unexpectedly, the presence of the HEMA/TEGDMA-based resin in lc-MTA cement did not reduced the viability and the number of cells with respect to both calcium-silicate cements (wTC-Ba and ProRoot), as demonstrated by the in vitro cytotoxicity tests at 1 and 3 days. The fast formation of a bone-like apatite layer probably reduced the expected negative effect of the resin. Moreover, polymer-protein interactions (poly-HEMA interacts with proteins) [58] and the presence of silica gel (CSH) may improve the cell viability and adhesion [21,22]. As expected [20,39,79,80], Vitrebond showed some cytotoxic

effect on exposed cells. Vitrebond, is composed by an alumino-fluoro-silicate mineral powder mixed with a HEMA-containing light-curable liquid, proved a complete lack of bioactivity upon soaking in DPBS, according to its chemical composition; under these conditions, no formation of apatite and calcium hydroxide was observed, due to the lack of calcium in the formulation.

It has to be underlined that the direct application of cells on materials, as reproduced in this study, represents an extreme challenge, because of the static conditions and the lack of defensive mechanisms able to moderate the injury imposed to the cells, such as biological fluids and reactive molecules in vivo. Therefore, it is reasonable to believe that the response of these cells in this type of experiment overestimates the outcome expected in a clinical situation.

The effect of cement extracts used as culture medium on cell viability was carried out to test the presence of cytotoxic chemicals (extractables or leachables) leached out in the medium from the material. In the present study an high extraction ratio, i.e. surface area of the material/volume of extractant medium (higher than that suggested by ISO 10993-12 clause 10) was used to attain the maximum amount of extractables. Exaggerated extraction is appropriate for hazard identification (ISO 10993-12 annex C [47]). Actually, many authors used extraction ratio [81-83] different from those recommended by the ISO 10993-12 [47] to test resin dental materials, and obtained reliable and probable results.

The data of cell viability in presence of lc-MTA extracts showed that the leachables released in the medium allow cell proliferation, with no differences with respect to wTC-Ba, ProRoot or control TCPS.

To verify the clinical use of the new material, restorations were prepared in root-end cavities and ESEM/EDX was used to evaluate marginal adaptation. All cements displayed adequate marginal adaptation to dentin, i.e. no gaps and no porosities were observed along the margin either in freshly prepared restorations or in 24-h aged restorations. However, all lc-MTA restorations were coated by a thick layer of Ca-P precipitates which demonstrated the high reactivity of the new material. The restorations with the experimental wTC-Ba displayed similar adequate marginal adaptation, but thinner Ca-P coatings. Finally, Vitrebond restorations showed the absence of marginal gaps and the presence on the surface of calcium and phosphate peaks but not of apatite spherulites. This result can be explained by considering that dentin released calcium under the acidic conditions (pH of about 3) attained in the early stages of cement mixing.

5. Conclusion

The study demonstrated that it is possible to develop a light-curable calcium-silicate MTA cement able to set in 2 min through the combination of a HEMA/TEGDMA-based hydrophilic resin and a calcium-silicate powder. This innovative material displayed high bioactivity, as demonstrated by the early formation of an apatite deposit after immersion in phosphate-containing solutions. Poly-HEMA-TEGDMA creates a polymeric network able to stabilize the outer surface of the cement and a hydrophilic matrix permeable enough to absorb water. Heterogeneous nucleation of apatite occurs in nucleating sites (SiO^-/Si-OH groups from CSH and oxygen-containing groups from poly-HEMA-TEGDMA) through the sorption of calcium and phosphate ions. The formation of an apatite biocoating on the cement surface and the fast setting time represent extremely interesting properties for a material specifically designed for the applications in hard tissues in dental and maxillofacial surgery (root-end obturations and bone defects) and make it an attractive alternative to conventional calcium-silicate cements.

references

[1] Nair PNR. On the causes of persistent apical periodontitis: a review. Int Endod J 2006;39:249-81.

[2] Schulz M, von Arx T, Altermatt HJ, Bosshardt D. Histology of periapical lesions obtained during apical surgery. J Endod 2009;35:634-42.

[3] von Arx TJS, Hanni S, Jensen SS. Clinical results with two different methods of root-end preparation and filling in apical surgery: mineral trioxide aggregate and adhesive resin composite. J Endod 2010;36:1122-9.

[4] Saunders WP. A prospective clinical study of periradicular surgery using mineral trioxide aggregate as root-end filling. J Endod 2008;34:660-5.

[5] Kim E, Song JS, Jung IY, Lee SJ, Kim S. Prospective clinical study evaluating endodontic microsurgery outcomes for cases with lesions of endodontic origin compared with cases with lesions of combined periodontal-endodontic origin. J Endod 2008;34:546-51.

[6] Tsesis I, Faivishevsky V, Kfir A, Rosen E. Outcome of surgical endodontic treatment performed by a modern technique: a meta-analysis of literature. J Endod 2009;35:1505-11.

[7] Torabinejad M, White DJ. US Patent Number 5,769,638; May 1995.

[8] Bogen G, Kuttler S. Mineral trioxide aggregate obturation: a review and case series. J Endod 2009;35:777-90.

[9] Chong BS, Pitt Ford TR, Hudson MB. A prospective clinical study of mineral trioxide aggregate and IRM when used as root-end filling materials in endodontic surgery. Int Endod J 2003;36:520-6.

[10] Tay FR, Pashley DH, Rueggeberg FA, Loushine RJ, Weller RN. Calcium phosphate phase transformation produced by the interaction of the Portland cement component of white mineral trioxide aggregate with a phosphate-containing fluid. J Endod 2007;33:1347-51.

[11] Coleman NJ, Awosanya K, Nicholson JW. Aspects of the in vitro bioactivity of hydraulic calcium (alumino) silicate cement. J Biomed Mater Res 2009;90A:166-74.

[12] Gandolfi MG, Taddei P, Tinti A, Dorigo De Stefano E, Rossi PL, Prati C. Kinetics of apatite formation on a calcium-silicate cement for root-end filling during ageing in physiological-like phosphate solutions. Clin Oral Invest 2010;14:659-68.

[13] Taddei P, Tinti A, Gandolfi MG, Rossi PL, Prati C. Vibrational study on the bioactivity of Portland cement-based materials for endodontic use. J Mol Struct 2009;924-926:548-54.

[14] Taddei P, Tinti A, Gandolfi MG, Rossi PL, Prati C. Ageing of calcium silicate cements for endodontic use in simulated body fluids: a micro-Raman study. J Raman Spectrosc 2009;40:1858-66.

[15] Gandolfi MG, Van Landuyt K, Taddei P, Modena E, Van Meerbeek B, Prati C. ESEM-EDX and Raman techniques to study ProRoot MTA and calcium-silicate cements in wet conditions and in real-time. J Endod 2010;36:851-7.

[16] Gandolfi MG, Taddei P, Tinti A, Prati C. Apatite-forming ability of ProRoot MTA. Int Endod J 2010;43:917-29.
[17] Mitchell PJC, Pitt Ford TR, Torabinejad M, McDonald F. Osteoblast biocompatibility of mineral trioxide aggregate. Biomaterials 1999;20:167-73.
[18] Perez AL, Spears R, Gutmann JL, Opperman LA. Osteoblasts and MG-63 osteosarcoma cells behave differently when in contact with ProRoot MTA and white MTA. Int Endod J 2003;36:564-70.
[19] Gandolfi MG, Perut F, Ciapetti G, Mongiorgi R, Prati C. New Portland cement-based materials for endodontics mixed with articaine solution: a study of cellular response. J Endod 2008;34:39-44.
[20] Gandolfi MG, Pagani S, Perut F, Ciapetti G, Baldini N, Mongiorgi R, et al. Innovative silicate-based cements for endodontics: a study of osteoblast-like cell response. J Biomed Mater Res 2008;87A:477-86.
[21] Gandolfi MG, Ciapetti G, Perut F, Taddei P, Modena E, Rossi PL, et al. Biomimetic calcium-silicate cements aged in simulated body solutions. Osteoblasts response and analyses of apatite coating. J Appl Biomater Biomech 2009;7:160-70.
[22] Gandolfi MG, Ciapetti G, Taddei P, Perut F, Tinti A, Cardoso M, et al. Apatite formation on bioactive calcium-silicate cements for dentistry affects surface topography and human marrow stromal cells proliferation. Dent Mater 2010;26:974-92.
[23] Bogen G, Kuttler S. Mineral trioxide aggregate obturation: a review and a case series. J Endod 2009;35:777-90.
[24] Gomes-Filho JE, Rodriguez G, Watanabe S, Estrada Bernabe P, Lodi CS, Gomes AC, et al. Evaluation of the tissue reaction to fast endodontic cement (CER) and Angelus MTA. J Endod 2009;35:1377-80.
[25] Porter ML, Berto A, Primus CM, Watanabe I. physical and chemical properties of new-generation endodontic materials. J Endod 2010;36:524-8.
[26] Costantini A, Luciani G, Annunziata G, Silvestri B, Branda F. Swelling properties and bioactivity of silica gel/pHEMA nanocomposites. J Mater Sci: Mater Med 2006;17:319-25.
[27] Costantini A, Luciani G, Silvestri B, Tescione F, Branda F. Bioactive poly(2-hydroxyethylmethacrylate)/silica gel hybrid nanocomposites prepared by sol-gel process. J Biomed Mater Res Part B: Appl Biomater 2008;86B:98-104.
[28] Boesel LF, Cachinho SCP, Fernandes MHV, Reis RL. The in vitro bioactivity of two novel hydrophilic, partially degradable bone cements. Acta Biomater 2007;3:175-82.
[29] Boesel LF, Reis RL. A review on the polymer properties of hydrophilic, partially degradable and bioactive acrylic cements (HDBC). Prog Polym Sci 2008;33:180-90.
[30] Montheard JP, Chatzopoulos M, Chappard D. 2-hydroxyethyl-methacrylate HEMA; chemical properties and applications in biomedical fields. J Macromol Sci Macromol Rev 1992;32:1-34.
[31] Barszczewska-Rybarek IM. Structure-property relationship in dimethacrylate network based on Bis-GMA, UDMA and TEGDMA. Dent Mater 2009;25:1082-9.
[32] Kokubo T. Design of bioactive bone substitute based on biomineralization process. Mater Sci Eng C 2005;25: 97-104.
[33] PAS (Publicly Available Specification) 132. Terminology for the bio-nano interface. London, UK: BSI (British Standards Institution); 2007.
[34] Kokubo T, Takadama H. How useful is SBF in predicting in vivo bone bioactivity? Biomaterials 2006;27:2907-15.
[35] Odler I. Improving energy efficiency in Portland clinker manufacturing. In: Ghosh SN, editor. Cement and concrete science and technology, vol. 1. New Delhi: ABI Books; 1992. p. 188 [part 1].
[36] ISO 7405. Dentistry—evaluation of biological effects of medical devices used in dentistry; 2008.
[37] Torabinejad M, Parirokh M. Mineral Trioxide Aggregate: a comprehensive literature review. Part II. Leakage and biocompatibility investigations. J Endod 2010;36: 190-202.
[38] ISO 10993-5. Biological evaluation of medical devices. Part 5. Tests for in vitro cytotoxicity; 2009.
[39] Vajrabhaya L, Korsuwannawong S, Bosl C, Schmalz G. The cytotoxicity of self-etching primer bonding agents in vitro. Oral Surg Oral Med Oral Pathol Oral Radiol Endodontol 2009;107:e86-90.
[40] 3M Vitrebond product profile. http://multimedia.3m.com/mws/mediawebserver?66666UuZjcFSLXTtmxfX4Xs6EVuQEcuZgVs6EVs6E666666.
[41] ISO 6876. Dental root canal sealing materials; 2002. British Standard ISO 6876.
[42] ASTM International C266-07. Standard test method for time of setting of hydraulic cement paste by Gillmore needles; 2007.
[43] ADA specifications. Endodontic filling and sealing materials: laboratory testing materials; 2008.
[44] Chirila TV, Zainuddin Z, Hill DJT, Wittaker AK, Kemp A. Effect of phosphate groups on the calcification capacity of acrylic hydrogels. Acta Biomater 2007;3:95-102.
[45] Chirila TV, Morrison DA, Gridneva Z, Garcia AJ, Platten ST, Griffin BJ, et al. Crystallization patterns and calcium phosphate precipitated on acrylic hydrogels in abiogenic conditions. J Mater Sci Lett 2005;24:4987-90.
[46] Gandolfi MG, Prati C. MTA and F-doped MTA cements used as sealers with warm gutta-percha. Long-term sealing ability study. Int Endod J 2010;43:889-901.
[47] ISO 10993-12. Biological evaluation of medical devices. Part 12. Sample preparation and reference materials; 2007.
[48] Socrates G. Infrared characteristic group frequencies. Tables and charts. 2nd ed. New York: John Wiley and Sons; 1998.
[49] Bajpai AK, Mishra DD. Dynamics of blood proteins adsorption onto poly(2-hydroxyethyl methacrylate)-silica nanocomposites: correlation with biocompatibility. J Appl Polym Sci 2008;107:541-53.
[50] Boesel LF, Reis RL. The effect of water uptake on the behaviour of hydrophilic cements in confined environments. Biomaterials 2006;27:5627-33.
[51] Pelliccioni GA, Vellani CP, Gatto MR, Gandolfi MG, Marchetti C, Prati C. ProRoot mineral trioxide aggregate cement used as a retrograde filling without addition of water: an in vitro evaluation of its microleakage. J Endod 2007;33: 1082-5.
[52] Budig CG, Eleazer PD. In vitro comparison of the setting of dry ProRoot MTA by moisture absorbed through the root. J Endod 2008;34:712-4.
[53] Storm B, Eichmiller FC, Tordik PA, Goodell GG. Setting expansion of grey and white mineral trioxide aggregate and Portland cement. J Endod 2008;34:80-2.
[54] Gandolfi MG, Iacono F, Agee K, Siboni F, Tay F, Pashley DH, et al. Setting time and expansion in different soaking media of experimental accelerated calcium-silicate cements and ProRoot MTA. Oral Surg, Oral Med, Oral Pathol Oral Radiol Endod 2009;108:e39-45.
[55] Tingey MC, Bush P, Levine MS. Analysis of mineral trioxide aggregate when set in the presence of fetal bovine serum. J Endod 2008;34:45-9.
[56] Torabinejad M, Hong CU, McDonald F, Pitt Ford TR. Physical and chemical properties of a new root-end filling material. J Endod 1995;21:349-53.
[57] Islam I, Chng HK, Yap AU. Comparison of the physical and mechanical properties of MTA and Portland cement. J Endod 2006;32:193-7.

[58] Bajpai AK, Mishra DD. Adsorption of a blood protein on to hydrophilic sponges based on poly(2-hydroxyethyl methacrylate). J Mater Sci: Mater Med 2004;15:583-92.
[59] Ohtsuki C, Miyazaki T, Kamitakahara M, Tanihara M. Design of novel bioactive materials through organic modification of calcium silicate. J Eur Ceram Soc 2007;27:1527-33.
[60] Ohtsuki C, Kamitakahara M, Miyazaki T. Bioactive ceramic-based materials with designed reactivity for bone tissue regeneration. J R Soc Interf 2009;6:S349-360.
[61] De Vasconcelos BC, Bernardes RA, Cruz SM, Duarte MA, Padilha Pde M, Bernardineli N, et al. Evaluation of pH and calcium ion release of new root-end filling materials. Oral Surg Oral Med Oral Pathol Oral Radiol Endod 2009;108:135-9.
[62] Duarte MA, Demarchi AC, Yamashita JC, Kuga MC, Fraga Sde C. pH and calcium ion release of 2 root-end filling materials. Oral Surg Oral Med Oral Pathol Oral Radiol Endod 2003;95:345-7.
[63] Kamali S, Moranville M, Leclercq S. Material and environmental parameter effects on the leaching of cement pastes: experiments and modelling. Cem Concr Res 2008;38:575-85.
[64] Miyasaki T, Iamamura M, Ishida E, Ashizuka M, Otsuki C. Apatite formation abilities and mechanical properties of hydroxyethylmethacrylate-based organic-inorganic hybrids incorporated with sulfonic groups and calcium ions. J Mater Sci: Mater Med 2009;20:157-61.
[65] Sanchez F, Zhang L. Molecular dynamics modeling of the interface between surface functionalized graphitic structures and calcium-silicate-hydrate: interaction energies, structure, and dynamics. J Colloid Interf Sci 2008;323:349-58.
[66] Plassard C, Lesniewska E, Pochard I, Nonat A. Nanoscale experimental investigation of particle interactions at the origin of the cohesion of cement. Langmuir 2005;21:7263-70.
[67] Valles Llunch A, Gallego Ferrer G, Monleon Pradas M. Biomimetic apatite coating on P(EMA-co-HEA)/SiO_2 hybrid nanocomposites. Polymer 2009;50:2874-84.
[68] Zainuddin Z, Hill DJT, Whittaker AK, Chirila TV. In-vitro study of the spontaneous calcification of PHEMA-based hydrogels in simulated body fluid. J Mater Sci: Mater Med 2006;17:1245-54.
[69] Zainuddin Z, Hill DJT, Chirila TV, Whittaker AK, Kemp A. Experimental calcification of HEMA-based hydrogels in the presence of albumin and a comparison to the in vivo calcification. Biomacromolecules 2006;7:1758-65.
[70] Zainuddin Z, Hill DJT, Whittaker AK, Lambert L, Chirila TV. Preferential interactions of calcium ions in poly(2-hydroxyethyl methacrylate) hydrogels. J Mater Sci: Mater Med 2007;18:1141-9.
[71] Wan XH, Chang CK, Mao DL, Jiang L, Li M. Preparation and in vitro bioactivities of calcium silicate nanophase materials. Mater Sci Eng C 2005;25:455-61.
[72] Zhu P, Masuda Y, Yonezawa T, Koumoto K. Investigation of apatite deposition onto charged surfaces in aqueous solutions using a quartz-crystal microbalance. J Am Ceram Soc 2003;86:782-90.
[73] Leonor IB, Baran ET, Kawashita M, Reis RL, Kokubo T, Nakamura T. Growth of a bonelike apatite on chitosan microparticles after a calcium silicate treatment. Acta Biomater 2008;4:1349-59.
[74] Xue W, Bandyopadhyay A, Bose S. Mesoporous calcium silicate for controlled release of bovine serum albumin protein. Acta Biomater 2009;5:1686-96.
[75] Somasundaran P, Ofori Amankonah J, Ananthapadmabhan KP. Mineral-solution equilibria in sparingly soluble mineral systems. Colloids Surf 1985;15:309-33.
[76] Pelliccioni GA, Ciapetti G, Cenni E, Granchi D, Nanni M, Pagani S, et al. Evaluation of osteoblast-like cell response to ProRoot MTA (mineral trioxide aggregate) cement. J Mater Sci: Mater Med 2004;15:167-73.
[77] Chen CL, Huang TH, Ding SJ, Kao CT. Comparison of calcium and silicate cement and mineral trioxide aggregate biologic effects and bone markers expression in MG63 cells. J Endod 2009;35:682-5.
[78] Bonson S, Jeansonne BG, Lallier TE. Root-end filling materials alter fibroblast differentiation. J Dent Res 2004;83:408-13.
[79] Nicholson JW, Czarnecka B. The biocompatibility of resin-modified glass-ionomer cements for dentistry. Dent Mater 2008;24:1702-8.
[80] Geurtsen W, Spahl W, Leyhausen. Residual monomer/additive release and variability in cytotoxicity of light-curing glass-ionomer cements and compomers. J Dent Res 1998;77:2012-9.
[81] Labban N, Song FMS, Al-Shibani N, Windsor LJ. Effects of provisional acrylic resins on gingival fibroblast cytokine/growth factor expression. J Prosth Dent 2008;100:390-7.
[82] Konga N, Jiangb T, Zhouc Z, Fuc J. Cytotoxicity of polymerized resin cements on human dental pulp cells in vitro. Dent Mater 2009;25:1371-5.
[83] Al-Hiyasat AS, Tayyar M, Darmani H. Cytotoxicity evaluation of various resin based root canal sealers. Int Endod J 2010;43:148-53.

dental materials 27 (2011) 1055-1069

available at www.sciencedirect.com

ScienceDirect

journal homepage: www.intl.elsevierhealth.com/journals/dema

Biomimetic remineralization of human dentin using promising innovative calcium-silicate hybrid "smart" materials

Maria Giovanna Gandolfi[a,*], Paola Taddei[b], Francesco Siboni[a], Enrico Modena[b], Elettra Dorigo De Stefano[c], Carlo Prati[a]

[a] Laboratory of Biomaterials, Department of Odontostomatological Science, University of Bologna, Bologna, Italy [b] Department of Biochemistry, University of Bologna, Bologna, Italy

[c] Department of Biomedicine, Unit of Dental Sciences and Biomaterials, University of Trieste, Trieste, Italy

article info

Article history:
Received 7 February 2011
Received in revised form
6 April 2011
Accepted 13 July 2011

Keywords:
Calcium-silicate cements
Portland cement
Fluoride-containing calcium-aluminosilicate composites
Ions-leaching composites
Apatite-depleted dentin
Dentin remineralization
Biomimetic remineralization
Bioremineralization
Calcium release
Fluoride release
Apatite

abstract

Introduction. The hypothesis was that experimental ion-leaching bioactive composites enhance remineralization of apatite-depleted dentin.

Materials and methods. Calcium-aluminosilicate (wTC-Ba) or fluoride-containing calcium-aluminosilicate (FTC-Ba) Portland-derived mineral powders were mixed with HTP-M methacrylate HEMA/TEGDMA/PAA-based resin to prepare experimental composites. Controls were Vitrebond and Gradia Direct LoFlo.

Calcium- and fluoride-release, pH of soaking water, solubility and water uptake were evaluated in deionized water using material disks (8 mm diameter and 1.6 mm thick).

The apatite-formation ability (bioactivity) and the ability to remineralize previously demineralized dentin were assessed by ESEM-EDX and FTIR after soaking in a phosphate-containing solution.

Human dentin slices (0.8 mm thickness) were demineralized in EDTA 17% for 2 h, placed in close contact with the material disks and immersed in a phosphate-containing solution (Dulbecco's Phosphate Buffered Saline, DPBS) to assess the ability of the materials to remineralize apatite-depleted dentin.

Results. Only the experimental materials released calcium and basified the soaking water (released hydroxyl ions). A correlation between calcium release and solubility was observed. FTC-Ba composite released more fluoride than Vitrebond and formed calcium fluoride (fluorite) precipitates. Polyacrylate calcium complexes (between COO^- groups of polyacrylate and released calcium ions) formed at high pH.

Abbreviations: HEMA, 2-hydroxyethyl methacrylate; TEGDMA, triethyleneglycol dimethacrylate; UDMA, urethane dimethacrylate; EDMAB, ethyl 4-(dimethylamino)benzoate; CQ, camphorquinone; PAA, polyacrylic acid; DPBS, Dulbecco's Phosphate Buffered Saline; MTA, mineral trioxide aggregate; ESEM-EDX, Environmental Scanning Electron Microscope with Energy Dispersive X-ray analysis; FTIR, Fourier transform infrared spectroscopy; ATR-FTIR, attenuated total reflectance-Fourier transform IR spectroscopy; SBF, simulated body fluid.

* Corresponding author at : Laboratory of Biomaterials and Oral Pathology, Department of Odontostomatological Sciences, University of Bologna, Via S. Vitale 59, Bologna, Italy. Tel.: +39 0512094913.

E-mail address: mgiovanna.gandolfi@unibo.it (M.G. Gandolfi).

0109-5641/$ - see front matter
doi:10.1016/j.dental.2011.07.007

The formation of apatite was noticed only on the experimental materials, due to the combination of calcium ions provided by the materials and phosphate from the DPBS. Apatite deposits (spherulites showing Ca and P EDX peaks and IR bands due to phosphate stretching and bending) were detected early on the experimental material disks after only 24 h of soaking in DPBS.

Only the experimental composites proved to have the ability to remineralize apatite-depleted dentin surfaces. After 7 days in DPBS, only the demineralized dentin treated with the experimental materials showed the appearance of carbonated apatite (IR bands at about 1400, 1020, 600 cm^{-1}). EDX compositional depth pro“le through the fractured demineralized dentin slices showed the reappearance of Ca and P peaks (remineralization of dentin surface) to 30-50 m depth.

Conclusions. The ion-leachable experimental composites remineralized the human apatite-depleted dentin. Ion release promotes the formation of a bone-like carbonated-apatite on demineralized dentin within 7 days of immersion in DPBS.

The use of bioactive “smart” composites containing reactive calcium-silicate Portland-derived mineral powder as tailored filler may be an innovative method for the biomimetic remineralization of apatite-depleted dentin surfaces and to prevent the demineralization of hypomineralized/carious dentin, with potentially great advantage in clinical applications.

1. Introduction

Dentin is a complex tissue, which contains apatite as mineral phase, collagen and other proteins, and water [1,2]. Initial carious lesions affect the mineral phase of dentin and expose the collagen fibers creating the conditions for a fast destruction of the entire dentin network [2].

An important requirement for operative and preventive dentistry is the development of restorative “smart” materials able to induce the remineralization of hypomineralized carious dentin (demineralized/carious dentin). At present no restorative materials with proven capability to induce dentin remineralization are available on the market.

The remineralization of demineralized dentin (bioremineralization) is the process of restoring minerals through the formation of inorganic mineral-like materials [3].

Recently, experimental remineralizing resin-based calcium phosphate cements (ion-leaching composites) have been proposed as restorative materials to induce dentin remineralization [4-8].

Biomimetic remineralization (bioremineralization) of dentin has been investigated with different methods using ion-containing solutions or ion-leaching silicon-containing materials (mainly bioactive glasses): solutions containing Ca^{2+}, SiO_{44-}, F^{-} or PO_{43-} ions [9], bioactive glasses placed on dentin [10], remineralization solutions supplemented with a bioactive glass [11] and remineralizing solutions containing the ions leached from ultrafine bioactive glass particles [12], glass-ionomer cements containing a bioactive glass in dog restorations [13], MTA cement layered on the dentin surface [14], Portland cement blocks (as a source of calcium and hydroxyl ions) immersed in a biomimetic analog consisting of simulated body fluid added with polyacrylic acid and polyphosphonic acid) [15,16] or poly(vinyl phosphonic acid (PVPA) [17].

In most of these studies dentin was immersed in solutions containing ions leached from different silicate-based materials without dentin-material contact, and consequently long times (14 days to 1 month) are required to achieve the remineralization of dentin.

Calcium-silicate cements (conventionally termed mineral trioxide aggregate MTA cements, such as ProRoot MTA, MTA Angelus, Tech Biosealer) are Portland-derived cements that have been introduced in dentistry as materials for different endodontic clinical applications [18,19].

Calcium-silicate cements are hydrophylic materials able to tolerate moisture (hydraulic materials) and to polymerize and harden (setting) also in the presence of biological fluids (blood, plasma, saliva, dentinal fluid). They are ion-leaching materials able to release calcium and hydroxyl ions (alkalinizing activity) into the surrounding fluids, creating the conditions for apatite formation [20-23]. In detail, calcium-silicate particles hydrate and decalcify after mixing with water following the formation of CSH gel (calcium-silicates hydrates) and calcium hydroxide [22,24].

Calcium-silicate cements possess bioactive behavior i.e. stimulate the formation of new apatite-containing tissues, since they are biointeractive materials able to develop apatite on their surface in a short induction period [20-23] and able to elicit a positive response at the interface from the biological environment [3,19,25]. They showed excellent clinical results [19] possibly related to their biocompatibility and bioactivity (i.e. apatite-forming ability) properties [20-23,26].

The aim of this study was to develop bioactive calcium-releasing light-curable hydrophilic composites with tailored remineralizing properties, to be used as restorative base-liner materials in sandwich restorations. Moreover, to test the remineralization of dentin by the experimental composites, a new experimental set-up was proposed involving the dentin-material contact, with the aim to mimic clinical conditions.

2. Materials and methods

2.1. Materials

Two experimental composites (named wTC-Ba + HTP-M and FTC-Ba + HTP-M) containing calcium-silicate Portland-derived hydrophilic mineral fillers (2-20 m-sized particles) with tailored enhanced reactivity and a light-curable hydrophylic resin (1 g mineral powder/0.8 g of resin) were designed and prepared [Gandolfi, University of Bologna, Italy].

The experimental composite wTC-Ba + HTP-M was composed of a reactive calcium-aluminosilicate powder, wTC-Ba [containing tricalcium-silicate $3CaO{\cdot}SiO_2$, dicalcium-silicate $2CaO{\cdot}SiO_2$, tricalcium-aluminate $3CaO{\cdot}Al_2O_3$, calcium sulfate and barium sulfate], mixed with an experimental light-curable hydrophylic resin, HTP-M [containing HEMA, TEGDMA and polyacrylic-co-maleic acid, EDMAB and camphorquinone]. HEMA, TEGDMA and polyacrylic-co-maleic acid obtained from Sigma-Aldrich, Steinheim, Germany.

The experimental composite FTC-Ba + HTP-M was composed of a fluoride-containing calcium-aluminosilicate powder, FTC-Ba [i.e. wTC-Ba added to sodium fluoride], mixed with the light-curable hydrophylic resin HTP-M.

Vitrebond [3 M, St. Paul, MN, USA; lot 9NN] was used as HEMA-PAA-containing control base material. Vitrebond (resin-reinforced glass-ionomer cement) consisted of a fluoro-aluminosilicate powder [SiO_2, AlF_3, ZnO, SrO, Na_3AlF_6 (criolite), NH_4F, MgO, P_2O_5] and a light-curable liquid [PAA, HEMA, water and photoinitiator] [27]. Vitrebond was prepared following manufacturer directions [1 spoon (0.033 g)/1 drop (0.05 g)].

Gradia Direct LoFlo A3 [GC, Tokyo, Japan; lot 1001271] was used as light-cured flowable control composite/base material. Gradia contained a silica prepolymerized filler (0.85 m size) and UDMA methacrylate monomers.

The materials were prepared by mixing the mineral powder with the resin on a glass plate to form a homogeneous paste. PVC molds (8 mm diameter and 1.6 mm thick) were used to prepare material disks. Each disk was light-cured on each side using a LED unit (Anthos, Imola, Italy). Light-curing time was 30 s for the commercial materials and 100 s for the experimental composites.

The materials were characterized for their chemical-physical properties (setting times, solubility, water absorption, alkalinizing activity, calcium and fluoride release) and bio-properties (apatite forming ability, dentin remineralization).

2.2. Chemical…physical properties

2.2.1. Setting times

Gilmore setting times (initial and final setting times) were evaluated by the penetration measurements of specific needles (initial setting Gilmore needle weight 113.4 g and diameter 2.12 mm; final setting Gilmore needle weight 453.6 g diameter 1.06 mm). Setting times corresponded to the lack of a complete circular impression (i.e. no indentation mark) on the specimen surface [28,29].

2.2.2. Solubility

According to ISO 6876, 2002 [29], the specimens were weighed (Initial weight) and placed in sealed cylindrical polystyrene holders (3 cm high and 4 cm in diameter) containing 15 mL of deionized water, at 37°C. After 1 and 28 days, the samples were removed from the solutions and dried to constant weight.

The solubility (percentage weight variation, W %) at each time t was calculated according to the following equation:

$$W\% = \left[\frac{\text{Dry weight at time } t - \text{Initial weight}}{\text{Initial weight}}\right] \times 100$$

2.2.3. Water absorption

The water uptake at 1, 6 and 24 h was determined gravimetrically, upon aging in 15 mL of deionized water at 37°C. The water absorption at each time t was calculated according to the following equation:

$$\text{Water absorption} = \left[\frac{\text{Wet weight at time } t - \text{Dry weight at time } t}{\text{Dry weight at time } t}\right] \times 100$$

2.2.4. Alkalinizing activity, and calcium and ”uoride release

The alkalinizing activity (pH of soaking deionized water) and calcium release in soaking water were measured by potentiometric methods. A multiparameter laboratory meter (inoLab 750, WTW Weilheim, Germany) connected to specific electrodes was used. A temperature compensated electrode (Sen Tix Sur WTW, Weilheim, Germany) was used to measure the pH of soaking water. Selective probes (Calcium or Fluoride ion electrodes, Eutech instruments Pte Ldt., Singapore) were used for Ca^{2+} and F^- quantization in15 mL of deionized water at 37°C.

The Ca^{2+} and F^- ions released in the elapsed time between two consecutive analysis times were measured.

2.2.5. Statistical analysis

The data (expressed as mean and standard deviation of 10 samples for each material) were statistically analyzed using one-way ANOVA with Tukey's test ($p < 0.05$).

2.3. Bio-properties

2.3.1. Apatite deposition on the surface of material disks (apatite-forming ability test)

The apatite-forming ability (biointeractivity/bioactivity [3]) was investigated by evaluating the apatite formation on the material disks in the presence of a simulated body fluid [25].

Material disks (8 mm diameter × 1.6 mm thick, 0.3 g weight, surface area = $2(\pi r^2) + 2\pi rh = 2(3.14 \times 16) + (2 \times 3.14 \times 4 \times 1.6) = 140.672\ mm^2$) were prepared and soaked in 5 mL of DPBS (Dulbecco's Phosphate Buffered Saline) phosphate-containing solution in sealed cylindrical polystyrene holders (3 cm high and 4 cm in diameter) and maintained at 37°C until the pre-determined endpoint times (24 h and 7 days). A DPBS/cement ratio of 17 mL/g was used. The surface chemistry (surface composition and elemental

distribution of phases) and morphology of the disks after immersion in DPBS were studied in humid conditions using ESEM-EDX and ATR-FTIR methodologies for chemical characterization (ISO 10993-18:2005 clause 7) [30].

DPBS is a physiological-like buffered (pH 7.4) Ca- and Mg-free solution with the following composition (mM): K^+ (4.18), Na^+ (152.9), Cl^- (139.5), PO_{43-} (9.56, sum of H_2PO_{4-} 1.5 mM and HPO_{42-} 8.06 mM).

2.3.2. Dentin remineralization test (DRT Gandol“ technique)

The dentin-remineralization ability (bioremineralization of demineralized dentin) has been evaluated as the capability to induce the formation of apatite on previously demineralized human dentin. Human dentin slices (5 ± 2 mm side and 0.8 ± 0.1 mm thick, surface area 30 mm^2 + 24 mm^2 = 54 mm^2) from molar teeth extracted for orthodontic/surgical reasons were prepared and demineralized in 15 mL of EDTA 17% for 2h at room temperature (Fig. 1A).

Disks of set materials (8 mm diameter and 1.6 mm thick) were prepared using PVC rings as molds. An innovative set-up (DRT Gandol“ technique, Fig. 1B) was used for dentin remineralization: each material disk was maintained in close contact with a demineralized dentin slice using a tailored PVC support and soaked in 15 mL of DPBS at 37°C for 7 days. After this time, the dentin slice was removed from the support, rinsed with deionized water and then analyzed in wet conditions by ESEM-EDX and ATR-FTIR.

2.3.3. Environmental Scanning Electron Microscopy with Energy Dispersive X-ray analysis (ESEM-EDX)

Samples were examined with an Environmental Scanning Electron Microscope (ESEM Zeiss EVO 50, Carl Zeiss, Oberkochen, Germany) connected to a secondary electron detector for Energy Dispersive X-ray analysis EDX (Oxford INCA 350 EDS, Abingdon, Oxfordshire, UK) computer-controlled software Inca Energy Version 18, using an accelerating voltage of 20-25 kV. The elemental analysis (weight % and atomic %) of samples was performed applying the ZAF correction method.

EDX was carried out on the surface of the wet material disks and on the surface of the wet dentin slices. The samples were placed directly onto the ESEM stub and examined without preparation (the samples were not coated for this analysis).

Moreover, an EDX compositional depth profile analysis (depth pro“ling EDX analysis) was carried out through the cross-sectional sample of longitudinally fractured (perpendicular to the surface) dentin disks to scan/monitor the calcium (blue scan lines) and phosphorous (red scan lines) through the dentin thickness. Both the surfaces of dentin disks (surface in contact with the composite and opposite free surface) were analyzed. Sudden roughness of scan line profiles is imputable to the lack of smoothness of the fractured surface.

EDX spectra refer to the whole image and the EDX elements percentages are an average over the whole image.

2.3.4. ATR-FTIR spectroscopy

IR spectra were recorded on a Nicolet 5700 FTIR spectrometer, equipped with a Smart Orbit diamond attenuated total reflectance (ATR) accessory and a DTGS detector; the spectral resolution was 4 cm^{-1} and 64 the number of scans for each spectrum. The ATR area had a 2 mm diameter. The IR radiation penetration was about 2 m.

To minimize the variability deriving from possible sample inhomogeneity, at least five spectra were recorded at five different points on the upper surface of each specimen.

3. Results

3.1. Chemical…physical properties

3.1.1. Setting times

All the materials were set after light-curing: no circular impression was left by the light or the heavy Gilmore needles (Table 1).

3.1.2. Solubility

Experimental composites showed the highest solubility (Table 1), which did not show any significant increase over time (from 1 day to 28 days).

3.1.3. Water absorption

The amount of water absorption tended to increase over soaking time for all the materials (Table 1). Both the experimental composites absorbed statistically more water than the other materials. Gradia absorbed the statistically least amount of water.

3.1.4. Alkalinizing activity (pH of soaking water)

Both the experimental composites possessed significant alkalinizing activity throughout the whole soaking period (pH raised to 9-11) (Table 2). Gradia and Vitrebond did not cause any significant pH variation of the water.

3.1.5. Calcium release

High Ca^{2+} release was noticed from both the experimental composites, especially from wTC-Ba + HTP-M (Table 2). Gradia and Vitrebond did not release calcium.

3.1.6. Fluoride release

The experimental F-containing composite released statistically more fluoride than Vitrebond (Table 2). Gradia did not release fluoride.

3.2. Bio-properties

3.2.1. Apatite deposition on the surface of material disks (apatite-forming ability test)

- ESEM-EDX analysis

  Freshly prepared materials : ESEM-EDX analysis of the materials surface (Fig. 2) revealed the presence of their respective constituent elements. The P peak was detected only on Vitrebond, due to the P_2O_5 component. The strontium EDX peak (Sr L-alpha at 1.8 keV) was not detected due to interference from the silicon peak (Si K-alpha at 1.84 keV).

  Materials soaked for 24 h in DPBS: ESEM/EDX showed the presence of calcium phosphate deposits (Ca/P 1.89-2.04) on the surface of wTC-Ba + HTP-M and FTC-Ba + HTP-M. On these samples, EDX proved the appearance of the P peak (Fig. 2).

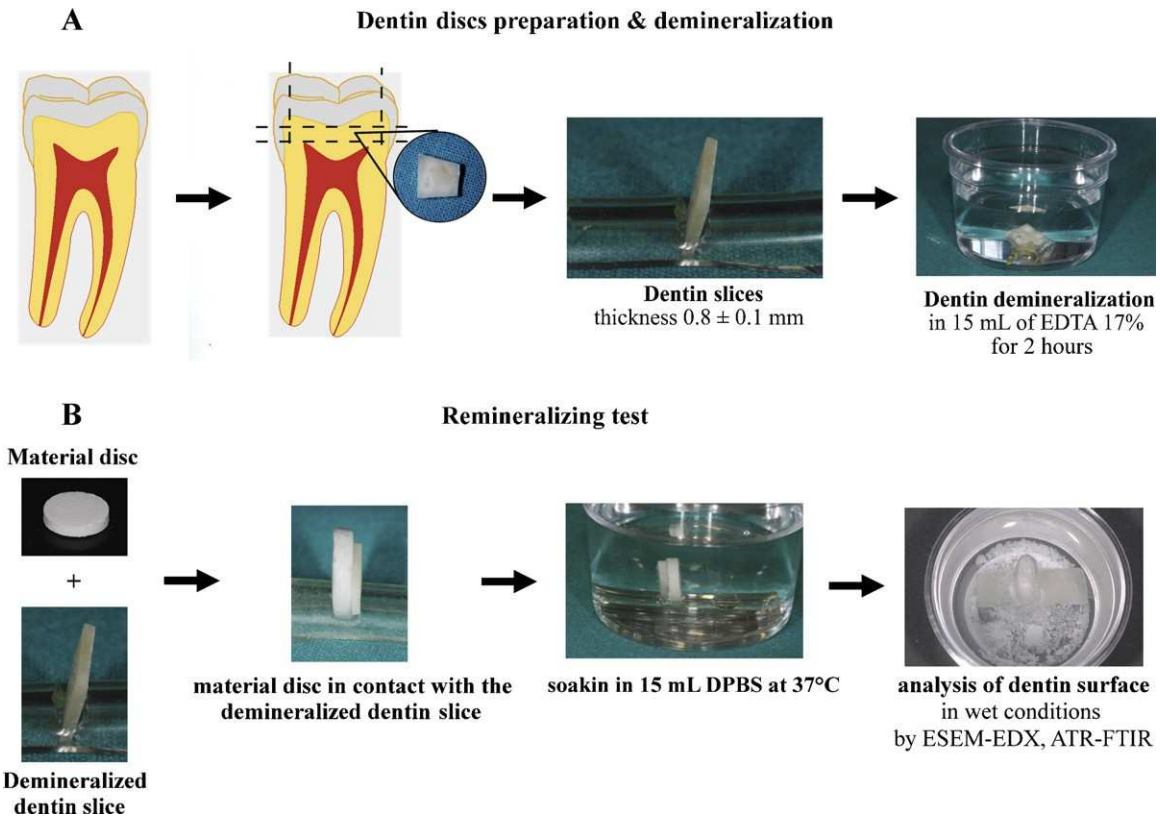

Fig. 1 - DRT Gandolfi technique: experimental set-up for Dentin remineralization tests (DRT). The innovation of the experimental set-up consists in the close contact between the sample disk and the dentin slice obtained by the PVC support. The DRT Gandolfi technique allows to the easy separation of the dentin slice from the material disk after soaking in DPBS. The debris present in the polystyrene container are precipitates of apatite.

The Vitrebond surface showed the presence of the P peak (possibly due to DPBS sorption, according to water absorption data), but was free from any Ca peak.

No calcium phosphate deposits (and no P peak) were detected on Gradia disks immersed in DPBS.

Materials soaked for 7 days in DPBS: After 7 days in DPBS, apatite formation was noticed only on calcium-silicate filled materials (Fig. 3). WTC-Ba + HTP-M displayed uniform calcium phosphate deposits and an increase in the P peak over soaking time (Ca/P 2.27). FTC-Ba + HTP-M showed diffuse calcium phosphate deposits and an increase in the P peak over time (Ca/P 2.28). Vitrebond proved the absence of calcium phosphate deposits and an increase in the P peak due to further DPBS absorption. Gradia proved the lack of calcium phosphate deposits (and in the P peak).

- FTIR spectroscopic analyses

Fig. 4 shows the IR spectra recorded on the surface of the cement disks after aging for 1 and 7 days in DPBS. Band assignments have been given according to the literature [23,31-33].

FTIR analyses proved:

(i) the presence of a carbonated apatite on both the experimental composites at both aging times (1 and 7 days), (Fig. 4A and B);

Table 1 - Polymerization time (seconds for side), solubility (percent variation of weight, W %) and water sorption.

	Polymerization time (seconds on each side)	Solubility		Water sorption		
		1 day	28 days	1h	6h	24 h
wTC-Ba + HTP-M	100	−24.70 (0.60)^{A,b}	−28.00 (3.00)^{A,b}	10.60 (1.90)^{A,c}	10.70 (1.90)^{A,c}	12.00 (2.00)^{A,b}
FTC-Ba + HTP-M	100	−23.00 (3.00)^{A,b}	−26.00 (3.00)^{A,b}	10.40 (0.70)^{A,c,d}	11.50 (0.60)^{A,c}	14.20 (0.90)^{B,c}
Vitrebond	30	−9.40 (0.40)^{A,c}	−11.30 (0.90)^{A,c}	8.20 (0.50)^{A,d}	9.60 (0.60)^{A,c}	10.80 (0.40)^{B,b}
Gradia	30	−0.57 (0.08)^{A,a}	−5.70 (0.60)^{B,a}	0.96 (0.11)^{A,b}	1.39 (0.13)^{A,b}	2.90 (0.30)^{A,a}

Samples disks (n = 10 for each material) were used. The data were expressed as mean and standard deviation and statistically analyzed using one-way ANOVA with Tukey's test ($p < 0.05$). Different CAPITAL superscript letters in the same row or different small superscript letters in the same column, mean statistically significant differences.

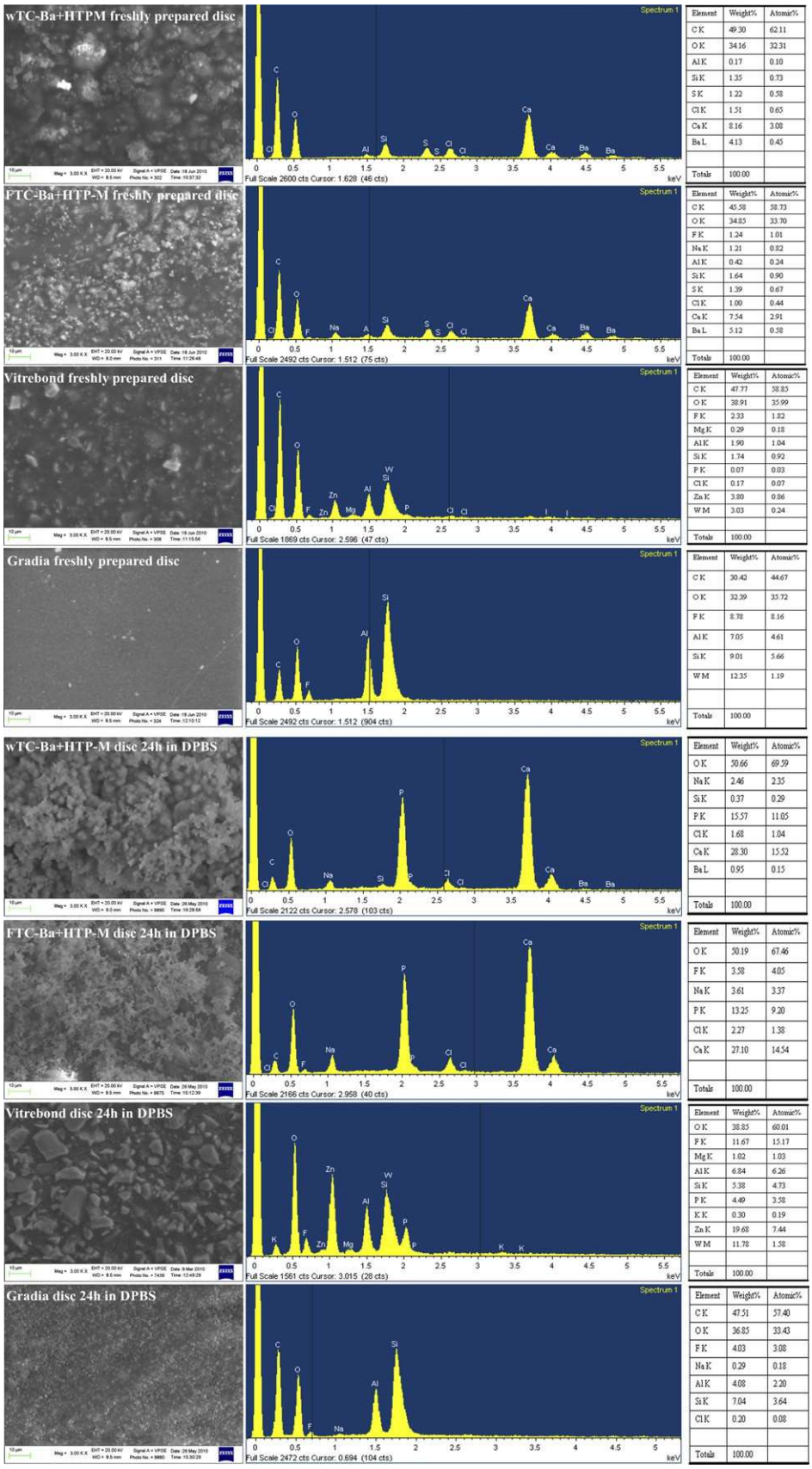

Fig. 2 - (Continued)

Table 2 - pH of soaking water, calcium and fluoride released in soaking water.

	3h	24 h	7 days	14 days	28 days
Calcium released (ppm) in soaking water					
wTC-Ba +HTP-M	500 (30)^{A,b}	207 (1.5)^{B,b}	160 (20)^{C,b}	60 (10)^{D,b}	66 (5)^{D,b}
FTC-Ba + HTP-M	112 (11)^{A,d}	79 (10)^{B,c}	150 (8)^{A,d}	65 (4)^{B,b}	69 (2)^{B,b}
Vitrebond	3.0 (2.00)^{A,e}	3.0 (1.20)^{A,d}	0.32 (0.01)^{A,c}	1.21 (0.01)^{A,c}	0.8 (0.60)^{A,c}
Gradia	2.1 (0.60)^{A,e}	1.0 (0.60)^{A,d}	1.12 (0.01)^{A,c}	0.32 (0.01)^{A,c}	0.36 (0.01)^{A,c}
Water	2.0 (0.60)^{A,e}	1.1 (0.60)^{A,d}	1.1 (0.60)^{A,c}	1.02 (0.01)^{A,c}	10.4 (0.60)^{A,c}
Fluoride released (ppm) in soaking water					
wTC-Ba + HTP-M	1.0 (0.1)^{A,a}	1.7 (0.1)^{A,a}	0.3 (0.5)^{A,a}	0.3 (0.1)^{A,a}	1.1 (0.1)^{A,a}
FTC-Ba + HTP-M	71 (5.0)^{A,c}	17 (2.0)^{B,c}	12.1 (0.5)^{C,b}	10.4 (0.5)^{C,b}	9.3 (0.5)^{C,}
Vitrebond	9.7 (1.1)^{A,d}	11 (3.0)^{A,B,d}	18 (6.0)^{C,c}	14.1 (1.5)^{B,C,d}	6.1 (1.0)^{D,b}
Gradia	1.4 (0.5)^{A,a}	0.1 (0.5)^{A,a}	0.3 (0.5)^{A,a}	1.6 (0.1)^{A,c}	0.3 (0.5)^{A,a}
Water	1.3 (0.5)^{A,a}	1.2 (0.5)^{A,a}	0.6 (0.5)^{A,a}	0.6 (0.5)^{A,a}	1.2 (0.5)^{A,a}
pH of soaking water					
wTC-Ba + HTP-M	8.58 (0.12)^{A,d}	9.44 (0.16)^{B,C,a}	9.65 (0.05)^{B,b}	9.3 (0.20)^{B,b}	8.98 (0.04)^{A,C,b,c}
FTC-Ba + HTP-M	9.3 (0.30)^{A,b}	10.82 (0.16)^{B,b}	9.8 (1.10)^{A,b}	9.8 (0.60)^{A,b}	9.3 (0.40)^{A,b,d}
Vitrebond	6.59 (0.03)^{A,c}	7.54 (0.18)^{B,c}	7.36 (0.16)^{B,c}	6.70 (0.16)^{C,c}	7.56 (0.04)^{B,c}
Gradia	6.80 (0.10)^{A,c}	7.87 (0.15)^{B,c}	6.99 (0.07)^{A,c}	7.3 (0.20)^{A,B,c}	6.7 (0.20)^{A,c}
Water	6.88 (0.04)^{A,c}	7.00 (0.02)^{A,c}	7.10 (0.11)^{A,c}	6.96 (0.06)^{A,c}	7.2 (0.40)^{A,c}

Samples disks (n = 10 for each material) were used. The data (expressed as mean and standard deviation) were statistically analyzed using one-way ANOVA with Tukey's test ($p < 0.05$). Different CAPITAL superscript letters in the same row or different small superscript letters in the same column mean statistically significant differences.
The Ca^{2+} and F^{-} release in the elapsed time between two consecutive analysis times was reported (i.e. not a cumulative release).

(ii) a more crystalline apatite phase on wTC-Ba + HTP-M at both aging times, as primarily revealed by the higher resolution of the phosphate bending bands at 598-556 cm^{-1} (Fig. 4A and B);

(iii) more prominent carboxylate bands (at about 1560 and 1410 cm^{-1}, due to calcium polyacrylate (PAA-Ca complexes) on FTC-Ba + HTP-M at both aging times (Fig. 4B);

(iv) the absence of apatite (lack of bioactivity) on Vitrebond and on Gradia at any aging time (Fig. 4C and D).

With regards to Vitrebond (Fig. 4C), the strengthening near 1000 cm^{-1} observed upon aging was not ascribable to the formation of an apatite deposit, since an analogous spectral feature was observed in the interior of the samples (spectra not shown). Moreover, it is interesting to note that the bands due to polyacrylate (PAA) were observed upon aging (Fig. 4C); in fact, at pH 6, the ionization degree of polyacrylic acid has already been reported to be 0.8 [34]; in other words, as confirmed by the IR spectra, most of the carboxyl groups of polyacrylic acid were in the COO^{-} form.

3.2.2. Dentin remineralization tests

• ESEM-EDX analysis

EDX compositional depth profile through the fractured demineralized dentin slices: EDX depth profile on fractured demineralized dentin sections proved that the treatment used (EDTA 17%, 2 h) completely removed the mineral phase of dentin to approx. 50 m depth. Actually, no Ca or P peaks were observed, suggesting that only the water and collagen/proteinaceous matrix were left in place (Fig. 5).

The EDTA-treated dentin immersed for 7 days in DPBS was analyzed to check that no dentin remineralization occurs when demineralized dentin is soaked in DPBS: indeed EDX data showed the lack of Ca and P on the dentin surface to a depth of approx. 50 m (Fig. 6).

Demineralized dentin after contact with wTC-Ba + HTP-M for 7 days in DPBS: On the demineralized dentin surface conditioned by the cement, Ca and P peaks were detected to a depth of 30-50 m (Fig. 6), meaning that dentin remineralization occurred on the surface in contact with the composite. On the other surface, no Ca and P peaks were revealed.

Demineralized dentin after contact with FTC-Ba + HTP-M for 7 days in DPBS: Traces of Ca and P were detected on the surface conditioned by the cement and some remineralization occurred on the surface in contact with the composite, while no Ca and P were displayed by the other surface (Fig. 6).

Demineralized dentin after contact with Gradia or Vitrebond for 7 days in DPBS in DPBS: No Ca and P were detected on the dentin surface to a depth of approx. 50 m meaning that no dentin remineralization occurred on the surface in contact with these materials (Fig. 6).

• FTIR analyses

Demineralized dentin: According to EDX data, FTIR analyses confirmed that the used EDTA treatment was able to remove the mineral phase of dentin; in fact, the spectrum recorded

Fig. 2 - ESEM-EDX of freshly prepared material disks and of the disks soaked in DPBS for 24 h. EDX spectra refer to the whole image and the EDX elements percentages are an average over the whole image. ESEM-EDX analysis of the freshly prepared materials revealed the presence of the P peak only for Vitrebond (due to the P_2O_5 component). After soaking in DPBS for 24 h in DPBS, the surface of wTC-Ba + HTP-M and FTC-Ba + HTP-M was covered by calcium phosphate deposits (apatite spherulites, Ca/P 1.89-2.04) and EDX proved the appearance of the P peak of calcium-phosphate deposits. Vitrebond surface showed P but no Ca peak. No calcium phosphate deposits (and no P peak) were detected on Gradia.

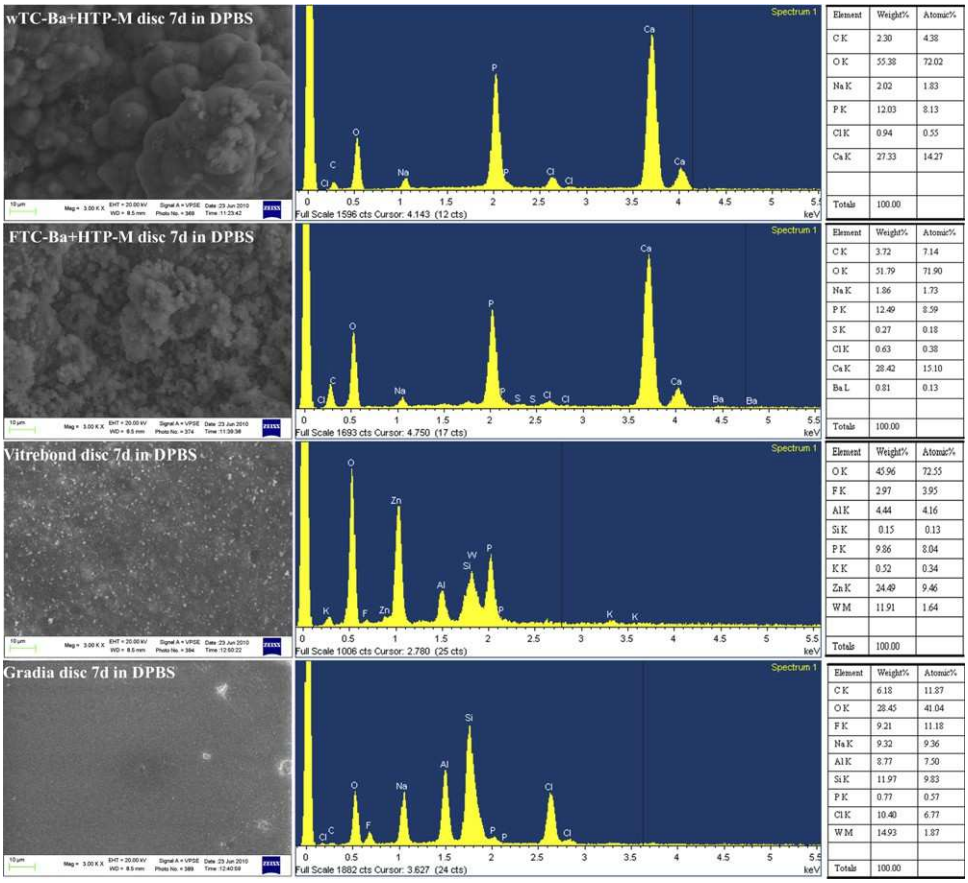

Fig. 3 - ESEM-EDX of the material disks soaked in DPBS for 7 days. EDX spectra refer to the whole image and the EDX elements percentages are an average over the whole image. Apatite formation was noticed only on calcium-silicate filled materials. WTC-Ba + HTP-M displayed a uniform calcium phosphate deposit (Ca/P 2.27) and evident P peak. FTC-Ba + HTP-M showed diffuse calcium phosphate deposits (Ca/P 2.28) and P peaks. Vitrebond proved the presence of P peak, the absence of calcium peak and of deposits. Gradia proved the lack of Ca and P peaks and of surface precipitates.

after the treatment (Fig. 5), showed only the bands due to collagen, while the spectral features typical of the apatite component were no longer observed.

Demineralized dentin after contact with experimental composites for 7 days in DPBS: The demineralized dentin samples treated with the experimental cements remineralized to different extents. After contact with wTC-Ba + HTP-M, the remineralization was more pronounced than after contact with FTC-Ba + HTP-M. In the spectrum corresponding to the former treatment, a carbonated apatite phase formed, as revealed by the appearance of the bands at about 1400, 1020 and 600 cm^{-1} (Fig. 7A); the band at about 1550 cm^{-1} increased in intensity with respect to the 1630 cm^{-1} band, due to the contribution of the carboxylate group of polyacrylate calcium complexes. This group can contribute also to the band at about 1400 cm^{-1}.

Analogous spectral changes were observed also on the dentin sample treated with FTC-Ba + HTP-M (Fig. 7B); however, the apatite component was detected in a significantly lower amount, according to calcium release data.

It is interesting to note that the apatite phase formed upon contact with wTC-Ba + HTP-M was significantly different from that typical of sound dentin as well as from the apatite powder isolated from the DPBS storage medium (Fig. 8); in fact, the phosphate asymmetric stretching mode in the above mentioned samples fell at different wavenumber values, i.e. at 1020, 1001 and 1014 cm^{-1}, respectively.

Demineralized dentin after contact with Vitrebond or Gradia: Minor or no significant spectral changes were observed after treatment with Vitrebond or Gradia, following the same trend as calcium release (Fig. 7C and D).

4. Discussion

The study demonstrated that the presence of the experimental calcium-silicate based composites in contact with demineralized dentin surfaces induced a significant remineralization of the demineralized dentin surface.

The inclusion of a reactive calcium-silicate powder as tailored filler in resin restorative materials enhanced (biocatalyzation) apatite formation. Interestingly, the remineralizing test in phosphate-containing solution demonstrated that the experimental materials placed in close contact with demineralized dentin are able to induce the remineralization of the phosphorous-depleted demineralized dentin surface down to

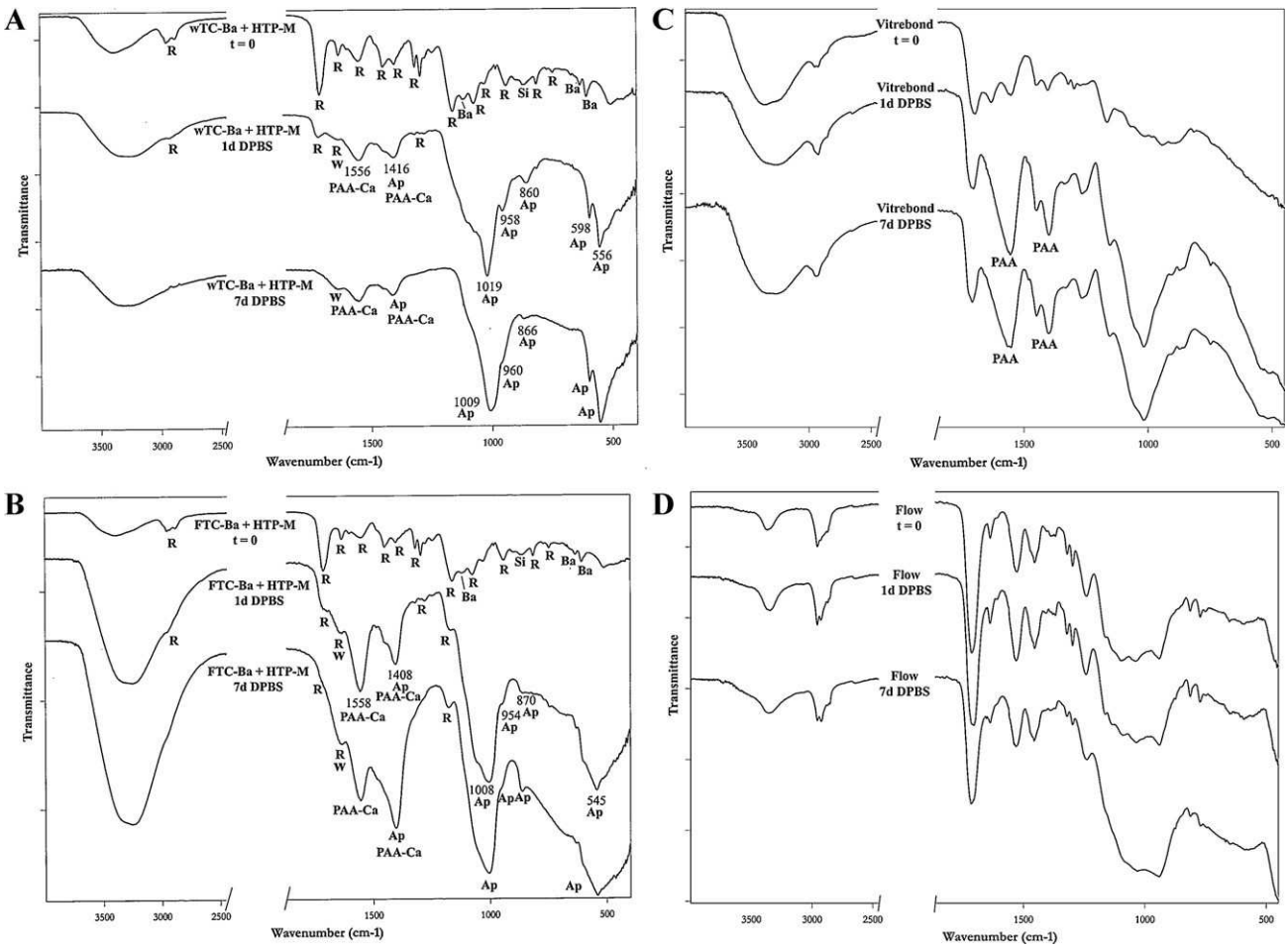

Fig. 4 - IR spectra recorded on the surface of the material disks before (t = 0) and after aging in DPBS for 1 and 7 days: (A) wTC-Ba + HTP-M, (B) FTC-Ba + HTP-M, (C) Vitrebond, and (D) Gradia. The bands prevalently due to calcium silicates (Si), barium sulfate (Ba), resin (R), water (w), polyacrylate (PAA), polyacrylate calcium complexes (PAA-Ca) and apatite (Ap) have been indicated.

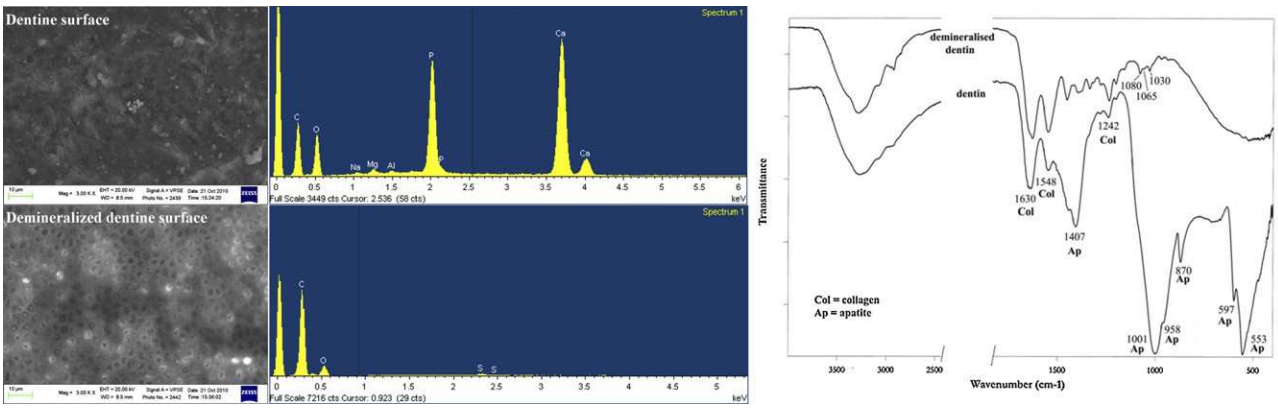

Fig. 5 - ESEM-EDX and IR analyses of whole dentin and demineralized dentin. EDX showed the complete disappearance of P peaks after demineralization in EDTA 17% for 2 h (phosphorous-depleted demineralized dentin surface). IR spectra recorded on the surface of a dentin slice before and after treatment with EDTA 17% for 2 h (apatite-depleted demineralized dentin). The bands prevalently due to collagen (Col) and apatite (Ap) mineral phases have been indicated.

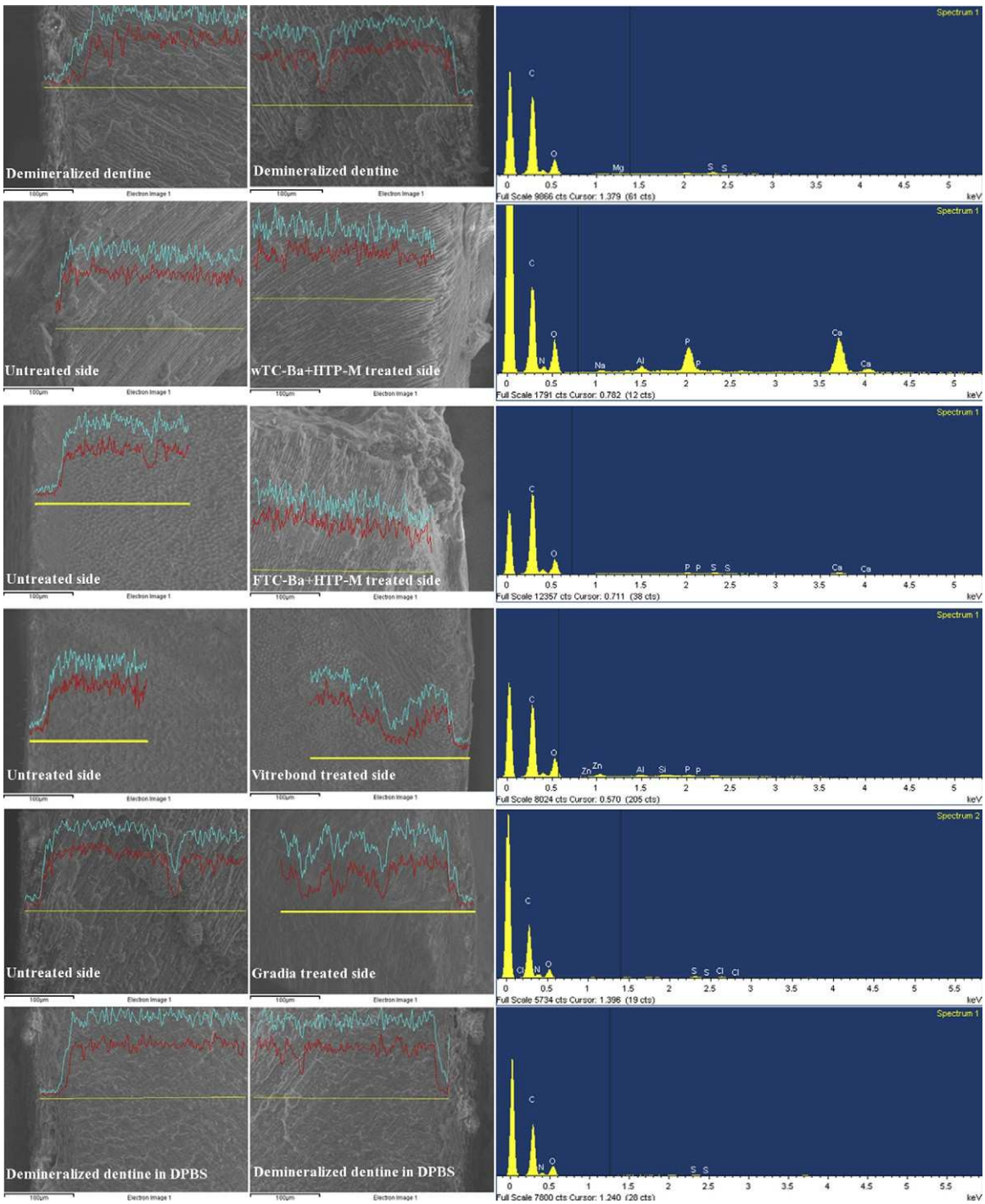

Fig. 6 - ESEM-EDX of treated and untreated dentin after 7 days in DPBS. EDX compositional depth profile analysis (depth pro“ling EDX analysis) trough the cross-sectional sample of longitudinally fractured dentin disks: calcium (blue scan lines) and phosphorous (red scan lines) contents through the dentin thickness are shown. No dentin remineralization occurred in demineralized EDTA-treated dentin soaked in DPBS: EDX data showed the lack of Ca and P on dentin surface till a depth of approx. 50 m. After contact/treatment of the demineralized dentin with wTC-Ba + HTP-M for 7 days in DPBS, dentin remineralization occurred: Ca and P peaks were detected on the dentin surface till a depth of 30-50 m. On the opposite untreated surface, no Ca and P peaks were revealed. Some remineralization occurred on the surface in contact with FTC-Ba + HTP-M: traces of Ca and P were detected on dentin surface, while no Ca and P were displayed by the untreated dentin side. No Ca and P were detected on dentin surface till a depth of approx. 50 m after contact with Gradia or Vitrebond, meaning that no dentin remineralization occurred on the surface in contact with each of these materials. (For interpretation of the references to color in this figure legend, the reader is referred to the web version of this article.)

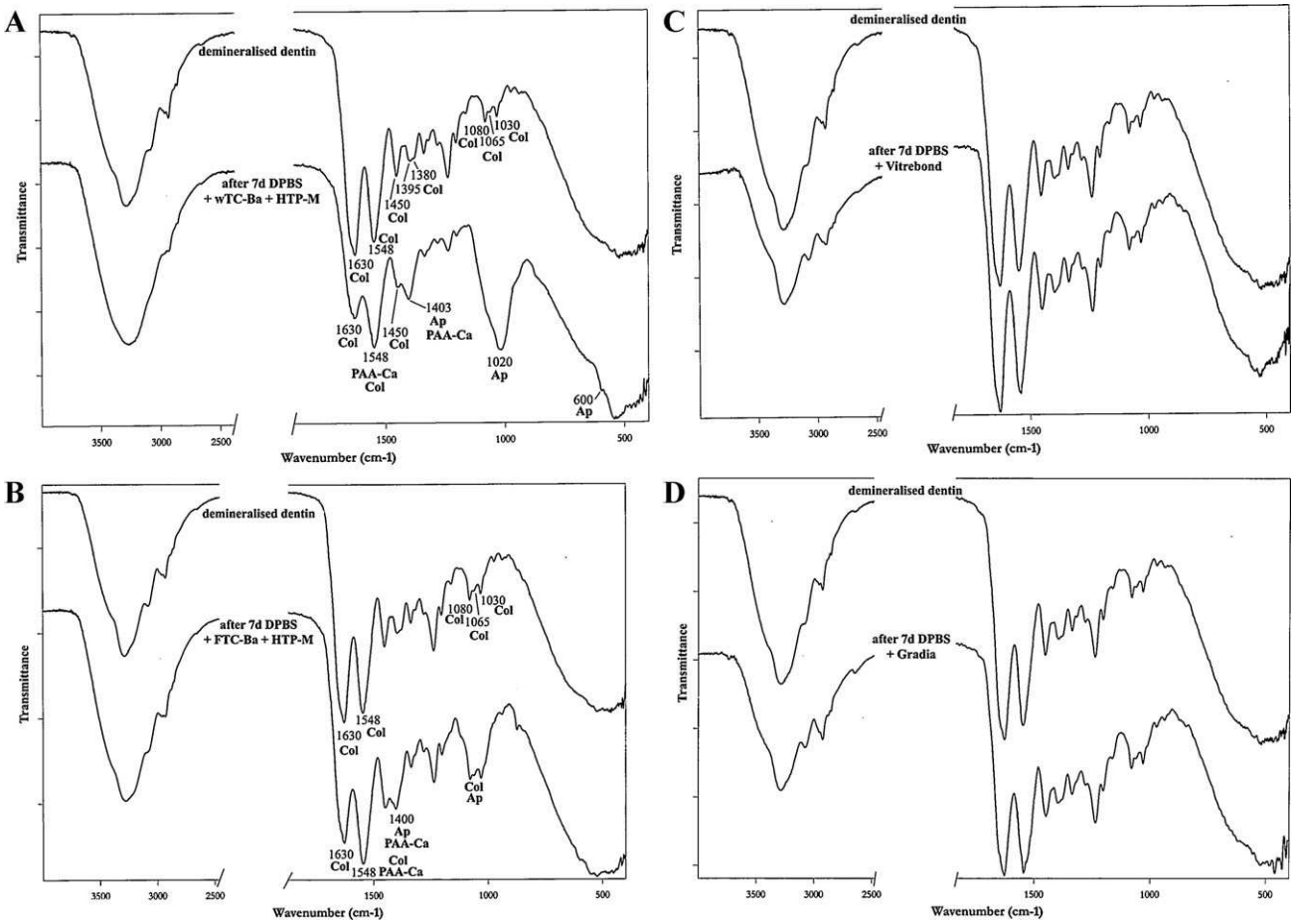

Fig. 7 - IR spectra recorded on the surface of demineralized dentin after contact with the four different materials for 7 days in DPBS: (A) wTC-Ba + HTP-M, (B) FTC-Ba + HTP-M, (C) Vitrebond, (D) Gradia. The bands prevalently due to collagen (Col), apatite (Ap) and polyacrylate calcium complexes (PAA-Ca) have been indicated.

a 30-50 mm depth within a period of 7 days, as proved by the EDX compositional depth pro“le and IR analyses. Differently, the HTP-M resin did not show any ability to enucleate an apatite phase from Ca^{2+}- and PO_{43-}-containing solutions (data not shown).

In this remineralizing process the bioavailability of mineral ions (calcium, fluoride) from restorative materials is the basic requirement to enhance the apatite formation and the mineralization of the dentinal tissue in the presence of phosphate-containing solutions. The mineral uptake in demineralized dentin was allowed by the detected high calcium release from the calcium-silicate filler in the experimental liners.

The concept of remineralization is based on the reincorporation of mineral (apatite) in dental tissues (dentin or enamel). Remineralization of demineralized/carious dentin occurs by incorporation of mineral ions (calcium, phosphate, fluoride) from the oral fluid or from external sources (specific treatments), through the growth of existing apatite crystals (belonging to remnant crystallites in the subsurface) [35,36]. The mineral precipitated may act as a constant site for further nucleation of mineral promoting a continuous remineralization over time when in presence of environmental mineral ions.

The capability of a material to induce the formation of apatite on demineralized dentin (remineralization ability) is strictly related to the biointeractivity and bioactivity, i.e. the ability to evoke a positive response from the biological environment.

Various methods have been used for evaluating the effectiveness of the remineralization procedure in dental tissues. Assessment methods can provide quantitative and qualitative information. Recent studies have assessed the reincorporation of mineral into demineralized dentin using indirect qualitative analysis, such as polarized light microscopy [37], semiquantitative analysis such as transverse microradiography [38,39], Transmission Electron Microscopy (TEM) [15] and spectroscopic analyses, such as Raman and Fourier transform infrared spectroscopy [40-42]. However, some limits are present in each method of analysis.

In polarized light microscopy analyses, the quantitative relationship between changes in mineral content and birefringence has not been fully established. TEM imaging provides information on crystal shape and structure; however, the analyzed tissue volume is very small and may not be representative of the material bulk; moreover, TEM does not allow any distinction between the mineral chemically bound to the organic matrix and that located close to it.

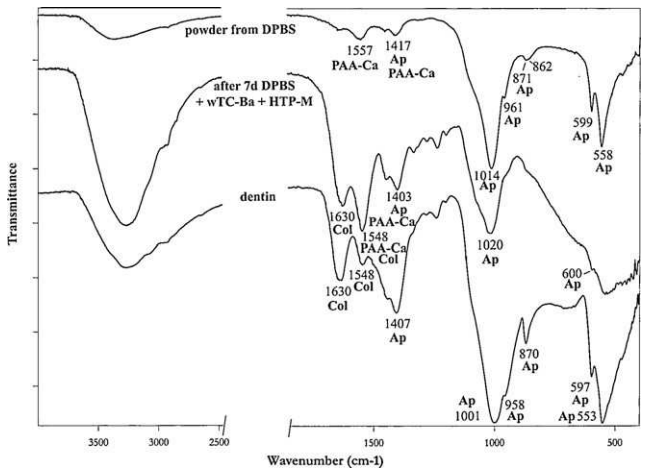

Fig. 8 - IR spectra recorded on the surface of demineralized dentin after contact with wTC-Ba + HTP-M for 7 days in DPBS. The spectra of the powder isolated from the DPBS storage medium and dentin are reported for comparison. The bands prevalently due to collagen (Col), apatite (Ap) and polyacrylate calcium complexes (PAA-Ca) have been indicated.

Spectroscopic analyses provide a lot of information in dentin remineralization studies. Vibrational techniques: (i) allow the determination of the nature of the mineral, (ii) provide quantitative information on the changes in the mineral and matrix compositions as mineralization proceeds and also (iii) supply separate responses on the mineral and the organic structures in the dentin matrix. Unfortunately, spectroscopic methods are not able to differentiate between the contributions of intra- and extrafibrillar mineral. The IR spectrum gives information on mineral content (i.e. collagen/apatite ratio) and mineral crystallinity.

In the present study, IR spectroscopy in the ATR technique has been used to non-destructively verify the efficiency of the demineralization procedure as well as the extent of the remineralization process. The same technique has been used to characterize the composition changes, which occurred on the surface of the cement disks aged in DPBS.

Remineralization of dentin can occur either by the simple precipitation of mineral into the loose demineralized dentin matrix between collagen fibrils (net remineralization) or by the chemical tight association of mineral to the dentin matrix structure (functional remineralization). The simple precipitation of mineral generates an increased mineral content, but may not necessarily provide an optimal interaction with the organic components of the dentin matrix.

In the present study, the position of the phosphate asymmetric stretching IR band at about 1000 cm^{-1} (Fig. 8) suggested that the newly formed apatite, although not perfectly coincident with that of sound dentin, had a different nature with respect to that isolated from the DPBS storage medium.

This result demonstrated that the apatite formed on dentin was intimately bound to it, and not simply a phase deposited on its surface. Moreover, it is interesting to note that the spectra reported in Fig. 7A and B showed the bands due to polyacrylate calcium complexes, as well as the spectrum recorded on the powder isolated from the storage medium (Fig. 8). On the contrary, the same bands were not observed in the spectrum of the dentin treated with Vitrebond (Fig. 7C). These data suggested that polyacrylate interacted with the calcium ions belonging to the apatite deposits, while no interaction occurred between polyacrylate and collagen from dentin. Actually, under alkaline conditions, both polyacrylic acid and collagen are negatively charged and repulsive forces prevent complex formation (i.e. no aggregate forms) [34].

Achieving remineralization of dentin remains one of the most difficult tasks in dentistry. There is a lack of commercially available composites with declared and proved remineralizing activity. Therefore, the development of new materials for remineralization of dentin should be encouraged. Remineralizing dental composites must be interactive materials able to release mineral ions that may encourage the formation of dentin-like apatite.

Calcium hydroxide-containing materials are currently used as liners. These materials dissolve in tissue fluids, are able to release calcium and hydroxyl ions, and exert an antibacterial action generally associated with their high pH.

Glass ionomer cements have been used as liner-base materials for their ability to release fluoride [43] available for the formation of a less soluble fluorapatite [2,44]. Despite the great mass of information on the positive effects of fluoride on enamel, no data have demonstrated the effectiveness of fluoride ions to induce new mineralization of demineralized dentin and no nucleation of new apatite crystallites within an apatite-free dentin has been identified in the demineralized dentin immersed in a calcium-and-phosphate-containing remineralization media in presence of a glass ionomer cement [45].

Resin-based calcium-phosphate cements have been proposed as potential restorative base-liner materials for their ability to induce the remineralization of hypo-/demineralized/carious (mineral-deficient) dentin [4-6,46]. These materials showed the ability to release either calcium or phosphate or fluoride, but no apatite formation on the dentin surface and into the thickness of demineralized dentin, has been evidenced.

In the present study designed reactive calcium-silicate mineral powders have been introduced in the experimental formulations to confer to the experimental composites the ability to release calcium ions and to form apatite. The bioavailability of calcium in the surrounding medium demonstrated a significant effect on dentin remineralization: the data showed that freshly placed experimental calcium-aluminosilicate composites had a significant impact on the processes occurring in their vicinity, and the formation of apatite deposits on the experimental composites or nearby dental tissues may occur in the intra-oral conditions. The presence of the experimental composites induced a significant remineralization of the hypomineralized adjacent dentin by calcium/mineral uptake, as demonstrated by FTIR and EDX data.

According to calcium release data (Table 2), the experimental composite containing wTC-Ba showed greater remineralization ability than that containing the FTC powder. The two calcium silicate fillers showed a different behavior also in the bioactivity tests: at all aging times, wTC-Ba + HTP-M showed

a more crystalline (i.e. more mature) apatite deposit than FTC-Ba + HTP-M. Interestingly, the latter composite showed more prominent bands than the former due to polyacrylate calcium complexes (Fig. 4A and B). This result can be explained in relation to the higher alkalinizing activity of FTC-Ba + HTP-M (Table 2); actually higher pH values favor the formation of higher amounts of COO^- groups (i.e. polyacrylate), able to interact with calcium ions forming polyacrylate calcium complexes. The lower calcium release observed for FTC-Ba + HTP-M (Table 2) can be partly related to the formation of such complexes, and partly to the formation of calcium fluoride (fluorite) as precipitate.

The detection of higher amounts of polyacrylate in FTC-Ba + HTP-M may also explain the slower bioactivity and the lower remineralization ability observed for this composite. Actually, several authors have reported that the presence of even a small quantity of PAA inhibits apatite deposition [33,47,48]. As confirmation, wTC-Ba and FTC-Ba cements (i.e. with no HTP-M addition) showed higher bioactivity and remineralization ability than the composites with HTP-M (data not shown).

In a pilot study [49] the calcium-silicate wTC-Ba and FTC-Ba designed powders have been inserted into Gradia Direct LoFlo A3 to assess if the ion-leaching experimental powders may confer some bioactivity to this commercial composite. Actually, calcium-silicate powders in combination with Gradia triggered calcium release, the alkalinization of the soaking solution, the formation of apatite and dentin remineralization, although to a lesser extent than in the composites with HTP-M.

A major drawback of dental composites is polymerization shrinkage with the subsequent negative effects on bonding integrity and formation of gaps at the composite-dentin interface, and increased possibility of restoration failure for bacterial microleakage and secondary caries formation.

In this study the selection of an adequate hydrophylic resin to prepare the experimental composites played a critical role to confer water absorption ability and bioactivity properties: the absorption of small amounts of water triggers the hydration reaction of calcium-silicate fillers, allows calcium release and apatite formation, and may help to reduce possible gap formation.

Moreover, hydroxyl ions are released during the hydration reaction and may create unfavorable conditions for bacterial survival and proliferation. Antibacterial properties are primarily required at the dentin-restoration interfacial region. Actually, the presence of residual bacteria within dentin further increases the risk of reinfection and secondary caries, in particular when using dental composites lacking any antimicrobial activity.

After light-curing, the presence of HEMA and TEGDMA monomers in the experimental HTP-M resin creates a polymeric network able to stabilize the material. Once immersed in aqueous media, the designed HTP-M resin matrix is permeable enough to absorb water due to the hydrophilicity of HEMA, and to keep it entrapped inside the cement. The hydrophilic nature of the experimental HEMA-containing resin allows the triggering and progression of the hydration reaction of the calcium-silicate powder [50], with following calcium and hydroxyl ion release (Tables 4 and 5). The weight reduction over time of the experimental composites immersed in water is correlated to the leaching of high amounts of calcium and hydroxyl ions.

5. Conclusions

Demineralized dentin may be remineralized by new composite materials with enhanced reactivity.

The inclusion of reactive calcium-silicate powders as tailored filler in hydrophylic resin confers to the composites the ability to release mineral ions.

The bioavailability of remineralizing ions is the basic requirement for the apatite formation (biocatalyzation) in presence of a phosphate-containing solution.

Innovative restorative base-liner hybrid composites with attractive basic properties have been produced, such as:

(i) light-curable materials with controlled solubility in water and oral fluids
(ii) hydrophylic nature to tolerate moisture during placement and to interact with oral fluids and moist tooth structures
(iii) ions-releasing filler
(iv) alkalinizing activity (hydroxyl ion release) to buffer the environmental acids, and antibacterial properties
(v) bioavailability of remineralizing ions (calcium and fluoride release)
(vi) bioactivity (apatite forming ability)
(vii) ability to enhance the natural remineralizing capability of dental structures (biocatalyzation) and to remineralize dentin (bioremineralization).

A new generation of “smart” materials able to induce apatite formation in demineralized dentin has been obtained as promising composites to be tested in clinical trials.

references

[1] Omelon SJ, Grynpas MD. Relationship between polyphosphate chemistry, biochemistry and apatite biomineralization. Chem Rev 2008;108:4694-715.
[2] Bertassoni LE, Habelitz S, Kinney JH, Marshall SJ, Marshall GW. Biomechanical perspective on the remineralization of dentin. Caries Res 2009;43:70-7.
[3] BSI (British Standards Institution). Terminology for the bio-nano interface. PAS132:2007, London, UK.
[4] Dickens S, Flaim G, Takagi S. Mechanical properties and biochemical activity of remineralizing resin-based Ca-PO_4 cements. Dent Mater 2003;19:558-66.
[5] Dickens SH, Eichmiller FC. Remineralizing dental cements. Patent WO2005002531 (A1) 2005-01-13 and US200520720 (A1) 2005-01-13.
[6] Peters MC, Fagundes TC, Navarro MFL, Dickens SH. In vivo dentin remineralization by calcium-phosphate cement. J Dent Res 2010;89:286-91.
[7] Xu HH, Sun L, Weir MD, Antonucci JM, Yakagi S, Chow LC. Nano DCPA-wisker composites with high strength and Ca and PO_4 release. J Dent Res 2006;85:722-7.
[8] Skrtic D, Antonucci JM, Eanes ED. Amorphous calcium phosphate-based bioactive polymeric composites for mineralized tissue regeneration. J Res Nat Inst Stand Technol 2003;108:167-82.

[9] Saito T, Toyooka H, Ito S, Crenshaw MA. In vitro study of remineralization of dentin: effects of ions on mineral induction by decalcified dentin matrix. Caries Res 2003;37:445-9.
[10] Efflandt SE, Magne P, Douglas WH, Francis LF. Interaction between bioactive glasses and human dentin. J Mater Sci Mater Med 2002;13:557-65.
[11] Forsback AP, Areva S, Salonen JI. Mineralization of dentin induced by treatment with bioactive glass S53P4 in vitro. Act Odontol Scand 2004;62:14-20.
[12] Vollenweider M, Brunner TJ, Knecht S, Grass RN, Zehnder M, Imfeld T, et al. Remineralization of human dentin using ultrafine bioactive glass particles. Acta Biomater 2007;3:936-43.
[13] Yli-Urpo H, Narhi M, Narhi T. Compound changes and tooth mineralization effects of glass ionomer cements containing bioactive glass (S53P4), an in vivo study. Biomaterials 2005;26:5934-41.
[14] Sarkar NK, Caicedo R, Ritwik P, Moiseyeva R, Kawashima I. Physicochemical basis of the biologic properties of mineral trioxide aggregate. J Endod 2005;31:97-100.
[15] Tay FR, Pashley DH. Guided tissue remineralisation of partially demineralised human dentine. Biomaterials 2008;29:1127-37.
[16] Kim YK, Gu LS, Bryan TE, Kim JR, Chen L, Liu Y, et al. Mineralization of reconstituted collagen using polyvinylphosphonic acid/polyacrylic acid templating matrix protein analogues in the presence of calcium, phosphate and hydroxyl ions. Biomaterials 2010;31:6618-27.
[17] Gu L, Kim YK, Liu Y, Takahashi K, Arun S, Wimmer CE, et al. Immobilization of a phosphonated analog of matrix phosphoproteins within cross-linked collagen as a templating mechanism for biomimetic mineralization. Acta Biomater 2011;7:268-77.
[18] Torabinejad M, White DJ. US Patent Number 5,769,638; May 1995.
[19] Parirokh M, Torabinejad M. Mineral trioxide aggregate: a comprehensive literature review—part III clinical applications, drawbacks and mechanism of action. J Endod 2010;36:400-13.
[20] Gandolfi MG, Taddei P, Tinti A, Dorigo De Stefano E, Rossi PL, Prati C. Kinetics of apatite formation on a calcium-silicate cement for root-end filling during ageing in physiological-like phosphate solutions. Clin Oral Invest 2010;14:659-68.
[21] Gandolfi MG, Van Landuyt K, Taddei P, Modena E, Van Meerbeek B, Prati C. ESEM-EDX Raman techniques to study ProRoot MTA and calcium-silicate cements in wet conditions and in real-time. J Endod 2010;36:851-7.
[22] Gandolfi MG, Taddei P, Tinti A, Prati C. Apatite-forming ability of ProRoot MTA. Int Endod J 2010;43:917-29.
[23] Taddei P, Modena E, Tinti A, Siboni F, Prati C, Gandolfi MG. Vibrational investigation on the in vitro bioactivity of commercial and experimental calcium-silicate cements for root-end endodontic therapy. J Mol Struct 2011;993:367-75.
[24] Parirokh M, Torabinejad M. Mineral trioxide aggregate: a comprehensive literature review—part I chemical, physical and antibacterial properties. J Endod 2010;36:16-27.
[25] ISO 23317. In vitro evaluation for apatite-forming ability of implant materials; 2007.
[26] Torabinejad M, Parirokh M. Mineral trioxide aggregate: a comprehensive literature review—part II leakage and biocompatibility studies. J Endod 2010;36:190-202. [27] 3M Vitrebond Liner/base. Technical Product Profile Update. http://multimedia.3m.com/mws/mediawebserver?66666UuZjcFSLXTtmxfX4Xs6EVuQEcuZgVs6EVs6E666666-.
[28] ASTM International C266-07. Standard test method for time of setting of hydraulic cement paste by Gillmore needles; 2007.
[29] ISO 6876, International Organization for Standardization. Specification for dental canal sealing materials: ISO 6876. Geneva, Switzerland: International Organization for Standardization; 2002.
[30] ISO 10993-18. Biological evaluation of medical devices part 18: chemical characterization of materials; 2005.
[31] Taddei P, Tinti A, Gandolfi MG, Rossi PL, Prati C. Vibrational study on the bioactivity of Portland cement-based materials for endodontic use. J Mol Structure 2009;924-926:548-54.
[32] Taddei P, Tinti A, Gandolfi MG, Rossi PL, Prati C. Ageing of calcium silicate cements for endodontic use in simulated body fluids: a micro-Raman study. J Raman Spectrosc 2009;40:1858-66.
[33] Girija EK, Yokogawa Y, Nagata F. Apatite formation on collagen fibrils in the presence of polyacrylic acid. J Mater Sci Mater Med 2004;15:593-9.
[34] Barbani N, Lazzeri L, Cristallini C, Cascone MG, Polacco G, Pizzirani G. Bioartificial materials based on blends of collagen and poly(acrylic acid). J Appl Polym Sci 1999;72:971-6.
[35] Featherstone JD. An updated understanding of the mechanism of dental decay and its prevention. Nutr Q 1990;14:5-11.
[36] ten Cate JM, Featherstone JD. Mechanistic aspects of the interactions between fluoride and dental enamel. Crit Rev Oral Biol Med 1991;2:283-96.
[37] Arnold WH, Bietau V, Renner PO, Gaengler P. Micromorphological and micronanalytical characterization of stagnating and progressing root caries lesions. Arch Oral Biol 2007;52:591-7.
[38] ten Cate JM. Remineralization of caries lesions extending into dentin. J Dent Res 2001;80:1407-11.
[39] Zaura E, Buijs MJ, ten Cate JM. Effects of ozone and sodium hypochlorite on caries-like lesions in dentin. Caries Res 2007;41:489-92.
[40] Kawasaki K, Ruben J, Tsuda H, Huysmans MC, Takagi O. Relationship between mineral distributions in dentine lesions and subsequent remineralization in vitro. Caries Res 2000;34:395-403.
[41] Rahiotis C, Vougiouklakis G. Effect of a CPP-ACP agent on the demineralization and remineralization of dentine in vitro. J Dent 2007;35:695-8.
[42] Boskey AL, Mendelsohn R. Infrared spectroscopic characterization of mineralized tissues. Vib Spectrosc 2005;38:107-14.
[43] Gandolfi MG, Chersoni S, Acquaviva GL, Piana G, Prati C, Mongiorgi R. Fluoride release and absorption at different pH from glass-ionomer cements. Dental Mater 2006;22:441-9.
[44] Wiegand A, Buchalla W, Attin T. Review on fluoride-releasing restorative materials—fluoride release and uptake characteristics, antibacterial activity and influence on caries formation. Dent Mater 2007;23:343-62.
[45] Kim YK, Yiu CKY, Kim JR, Gu L, Kim SK, Weller RN, et al. Failure of a glass ionomer to remineralize apatite-depleted dentin. J Dent Res 2010;89:230-5.
[46] Mehdawi I, Abou Neel EA, Valappil SP, Palmer G, Salih V, Pratten J, et al. Development of remineralizing, antibacterial dental materials. Acta Biomater 2009;5:2525-39.
[47] Kamitakahara M, Kawashita M, Kokubo T, Nakamura T. Effect of polyacrylic acid on the apatite formation of a bioactive ceramic in a simulated body fluid: fundamental examination of the possibility of obtaining bioactive glass-ionomer cements for orthopaedic use. Biomaterials 2001;22:3191-6.
[48] Liou S, Chen SY, Liu DM. Manipulation of nanoneedle and nanosphere apatite/poly(acrylic acid) nanocomposites. J Biomed Mater Res B Appl Biomater 2005;73B:117-22.

[49] Gandolfi MG, Siboni F, Taddei P, Rossi PL, Prati C, Dorigo De Stefano E. Biomimetic remineralization of human dentin using promising innovative calcium-silicates hybrid "Smart" materials. J Dent Res 2010;89B:138340. http://iadr.confex.com/iadr/arce/webprogramschedule/Paper138340.html.

[50] Gandolfi MG, Taddei P, Siboni F, Modena E, Ciapetti G, Prati C. Development of the foremost light-curable calcium-silicate MTA cement as root-end in oral surgery. Chemical-physical properties, bioactivity and biological behaviour. Dental Mater 2011;27:e134-57.

International Endodontic Journal
doi:10.1111/j.1365-2591.2011.01907.x

Fluoride-containing nanoporous calcium-silicate MTA cements for endodontics and oral surgery: early fluorapatite formation in a phosphate-containing solution

M. G. Gandolfi[1], P. Taddei[2], F. Siboni[1], E. Modena[2], M. P. Ginebra[3] & C. Prati[1]

[1]Laboratory of Biomaterials and Oral Pathology, Department of Odontostomatological Science, Endodontic, Clinical Section, University of Bologna, Bologna;[2]Department of Biochemistry, University of Bologna, Bologna, Italy; and[3]Division of Biomaterials, Bioceramics and Tissue Engineering, Department of Materials Science and Metallurgical Engineering, Technical University of Catalonia, Barcelona, Spain

Abstract

Gandolfi MG, Taddei P, Siboni F, Modena E, Ginebra MP, Prati C. Fluoride-containing nanoporous calcium-silicate MTA cements for endodontics and oral surgery: early fluorapatite formation in a phosphate-containing solution. International Endodontic Journal, 44, 938-949, 2011.

Aim To test the chemical-physical properties and apatite-forming ability of experimental fluoride-doped calcium silicate cements designed to create novel bioactive materials for use in endodontics and oral surgery.

Methodology A thermally treated calcium silicate cement (wTC) containing $CaCl_2$ 5%wt was modified by adding NaF 1%wt (FTC) or 10%wt (F10TC). Cements were analysed by environmental scanning electron microscopy with energy-dispersive X-ray analysis, IR and micro-Raman spectroscopy in wet conditions immediately after preparation or after ageing in a phosphate-containing solution (Dulbecco's phosphate-buffered saline). Calcium and fluoride release and pH of the storage solution were measured. The results obtained were analysed statistically (Tukey's HSD test and two-way anova).

Results The formation of calcium phosphate precipitates (spherulites) was observed on the surface of 24 h-aged cements and the formation of a thick bone-like B-type carbonated apatite layer (biocoating) on 28 day-aged cements. The rate of apatite formation was FTC > F10TC > wTC. Fluorapatite was detected on FTC and F10TC after 1 day of ageing, with a higher fluoride content on F10TC. All the cements released calcium ions. At 5 and 24 h, the wTC had the significantly highest calcium release ($P < 0.001$) that decreased significantly over the storage time. At 3-28 days, FTC and F10TC had significantly higher calcium release than wTC ($P < 0.05$). The F10TC had the significantly highest fluoride release at all times ($P < 0.01$) that decreased significantly over storage time. No significant differences were observed between FTC and wTC. All the cements had a strong alkalinizing activity (OH^- release) that remained after 28 days of storage.

Conclusions The addition of sodium fluoride accelerated apatite formation on calcium silicate cements. Fluoride-doped calcium silicate cements had higher bioactivity and earlier formation of fluorapatite. Sodium fluoride may be introduced in the formulation of mineral trioxide aggregate cements to enhance their biological behaviour. F-doped calcium silicate cements are promising bone cements for clinical endodontic use.

Keywords: apatite, bioactive materials, calcium hydroxide, calcium release, calcium-silicate cements, endodontic cements, fluorapatite, fluoride release, fluoride-doped MTA, mineral trioxide aggregate.

Received 1 February 2011; accepted 14 May 2011

Correspondence: Maria Giovanna Gandolfi, DBiol, DSc, MBiol, PhD, Head Laboratory of Biomaterials and Oral Pathology, Department of Odontostomatological Sciences, University of Bologna, Via San Vitale 59, 40125 Bologna, Italy (e-mail: mgiovanna.gandolfi@unibo.it).

Introduction

Calcium silicate cements, well known as mineral trioxide aggregate (MTA), are novel self-setting biomaterials for oral and endodontic surgery (Parirokh & Torabinejad 2010). The setting reaction of calcium silicate cements requires water, so that they are able to set in a wet environment through the formation of a nanoporous calcium silicate hydrate (CSH) gel.

Calcium silicate MTA cements are biointeractive bioactive materials, i.e. materials able to exchange information with a biological system (this encompasses a physicochemical interplay between the material surface and the biological environment) (biointeractivity) and materials able to evoke a positive response from the host body (bioactivity) (BSI, 2007). A number of investigations have demonstrated that when calcium silicate MTA cements are exposed to simulated extracellular fluids containing a phosphate source, they form calcium phosphates and apatite precipitates on their surface (Gandolfi et al. 2009a, 2010a-d, Taddei et al. 2009a, 2009b, Torrisi et al. 2010; Taddei et al. 2011). Calcium ions released from MTA react with phosphates provided by the simulated fluid causing apatite formation. The sealing ability, biocompatibility and dentinogenic activity of MTA cements may be improved and favoured by their bioactivity properties and the formation of apatite.

Fluoride-doped calcium silicate MTA cements have recently been designed and studied (Gandolfi et al. 2009b, Gandolfi & Prati 2010e, Colin et al. 2010). It has been reported that (i) the addition of sodium fluoride 1%wt to calcium silicate powders causes a delay in the setting time and increases expansion (Gandolfi et al. 2009b) and long-term apical sealing ability in the root canal (Gandolfi & Prati 2010e) and (ii) an increase in NaF content (from 0% to 10%wt) results in an enhanced solubility of F-doped MTA cements in water or in Dulbecco's modified eagle medium (DMEM) (Colin et al. 2010).

This study aimed to evaluate the effect of the sodium fluoride content in experimental MTA cements on the kinetics of apatite formation and ion release. The bioactivity of experimental fluoride-doped calcium silicate cements was investigated by environmental scanning electron microscopy coupled with energy-dispersive X-ray analysis (ESEM-EDX), micro-Raman and Fourier transform infrared spectroscopy (FTIR) analyses, after storage in a simulated extracellular fluid solution.

Materials and methods

Cement preparation

The experimental thermally treated calcium silicate cement (identified as wTC) composed of di- and tricalcium silicate, tricalcium aluminate, calcium sulphate, calcium chloride (setting accelerator) and bismuth oxide (radiopacifying agent) was prepared (Gandolfi et al. 2010d). Sodium fluoride 1% wt or 10% wt was added to wTC to produce two experimental fluoride-doped cements, identified as FTC and F10TC, respectively (Gandolfi, Laboratory of Biomaterials, University of Bologna, Bologna, Italy).

The cements were mixed with Dulbecco's phosphate-buffered saline (Dulbecco's phosphate-buffered saline (DPBS), cat. n.BE17-512; Lonza, Verviers, Belgium) as a source of phosphate ions, using a liquid/powder ratio of 0.3 to produce a homogeneous paste. After preparation, the cement pastes were placed in PVC moulds (8 mm diameter and 1.6 mm thick) to prepare standard discs.

In vitro apatite-forming ability (bioactivity)

The ability of the different materials to form apatite on their surface was tested in vitro as an index of bioactivity (BSI, 2007, Kokubo & Takadama 2006). Bioactivity tests were carried out in DPBS (Gandolfi et al. 2010a-d, Taddei et al. 2009a, 2009b, Taddei et al. 2010). DPBS is a physiological-like buffered (pH 7.4) Ca- and Mg-free solution with the following composition (mmol $L^{)1}$): K^+ (4.18), Na^+ (152.9), $Cl^{)}$ (139.5) and $PO_{43)}$ (9.56, sum of $H_2PO_{4)}$ 1.5 mmol $L^{)1}$ and $HPO_{42)}$ 8.06 mmol $L^{)1}$).

Each cement disc was placed in a hermetically sealed cylindrical polystyrene container (3 cm high and 4 cm in diameter) containing 5 mL DPBS (15 mL of medium for 1 g of cement paste) and was maintained at 37 C until the pre-determined end-point time (1, 7 and 28 days).

The phosphate ions (as $H_2PO_{4)}$ and $HPO_{42)}$) were continuously supplied by the DPBS solution that was renewed after 5 and 24 h and 7, 14 and 28 days.

The cements were analysed by ESEM/EDX, micro-Raman and FTIR spectroscopy immediately after preparation (fresh unset samples 10 min old) and after 1 and 28 days of ageing in DPBS (1 day-aged group and 28 day-aged group). The constituent cement powders (anhydrous powders) were also analysed.

Environmental scanning electron microscopy with energy-dispersive X-ray analysis

Samples were examined under an environmental scanning electron microscope (ESEM Zeiss EVO 50; Carl Zeiss, Oberkochen, Germany) connected to a secondary electron detector for energy-dispersive X-ray analysis EDX (INCA 350 EDS, Oxford Instruments, Abingdon, UK) computer controlled software INCA energy version 18 (Oxford Instruments, Abingdon, UK), using an accelerating voltage of 20-25 kV. The elemental analysis (weight % and atomic %) of samples was carried out applying the ZAF correction method. At 25 kV acceleration, the X-ray electron beam penetration of ESEM-EDX (inside a material with a density of about 3 g $cm^{)3}$) proved to be 2.98 lm and consequently the volume excited and involved in the emission of characteristic X-rays from the constituting elements was considered to be 10 lm^3. Cement discs were placed directly on the ESEM stub and examined without preparation (samples were not coated for this analysis).

Micro-Raman and ATR/FTIR spectroscopy

Micro-Raman spectra were obtained using a Jasco NRS-2000C instrument (Jasco Inc., Easton, MD, USA) connected to a microscope with 20· magnification. In these conditions, the laser spot size (i.e. the excitation source) was of the order of a few microns. All the spectra were recorded in back-scattering conditions with 5 $cm^{)1}$ spectral resolutions using the 488-nm line (Innova Coherent 70; Coherent Inc., Santa Clara, CA, USA)) with a power of 50 mW. A 160 K frozen Charge Coupled Device detector from Princeton Instruments Inc (Trenton, NJ, USA) was used.

IR spectra were recorded on a Nicolet 5700 FTIR spectrometer (Thermo Electron Scientific Instruments Corp., Madison, WI, USA) equipped with a Smart Orbit diamond attenuated total reflectance (ATR) accessory and a Deuterated Tri-Glycine Sulphate detector; the spectral resolution was 4 $cm^{)1}$, and 64 scans were made for each spectrum. The ATR area had a 2 mm diameter. The IR radiation penetration was about two microns.

To minimize the variability deriving from possible sample inhomogeneity, at least five spectra were recorded on five different points on the upper surface of each specimen. The Raman spectra were recorded on wet cement samples (i.e. when maintained in their storage media).

pH of storage solution and calcium and fluoride release

Each cement disc was placed in a hermetically sealed cylindrical polystyrene holder (3 cm high, 4 cm diameter) containing 10 mL water and was maintained at 37 C until the pre-determined end-point time (5 h, 24 h, 3, 7, 14 and 28 days). At each end-point time, the storage water was analysed for pH as well as calcium and fluoride content and renewed. The pH was measured using a (selective) temperature-compensated electrode (Sen Tix Sur WTW, Weilheim, Germany) connected to a multiparameter laboratory meter (inoLab 750; WTW).

For calcium quantization, 0.100 mL (2%) of ISA (4 mol $L^{)1}$ KCl; WTW) was added to 5 mL of storage medium, and the calcium content was evaluated using a calcium probe (Calcium ion electrode; Eutech instruments Pte Ldt, Singapore) connected to a multiparameter laboratory meter (inoLab 750; WTW).

For fluoride assessment, 5 mL of TISAB (sodium chloride 5.8% w/v, acetic acid 5.7% w/v, sodium hydroxide 3.0% (w/v), CDTA 0.4% (w/v) and water; WTW) was added to 5 mL of storage solution, and the fluoride content was evaluated using a fluoride probe (Fluoride ion electrode; Eutech instruments Pte Ldt) connected to a multiparameter laboratory meter (inoLab 750; WTW). The probes were inserted in the storage media at room temperature (24 C) under magnetic stirring. Each measurement was repeated three times.

The results obtained were analysed statistically. Tukey's HSD (honestly significant differences) test was used in conjunction with the two-way analysis of variance (two-way anova), to determine the statistical significance of the differences among the groups.

Results

Environmental scanning electron microscopy with energy-dispersive X-ray analysis

Starting cement powders (unhydrated cement powders) (Figs 1a, 2a and 3a) showed the reflexes of Ca (calcium), Si (silicon) and Al (aluminium) from the cement particles, Bi (bismuth) from the Bi_2O_3 radiopacifier, Cl (chlorine) from the $CaCl_2$ setting accelerator, O (oxygen) from the cement particles and the radiopacifier. In addition, the F-doped powders showed Na (sodium) and F (fluorine) from sodium fluoride.

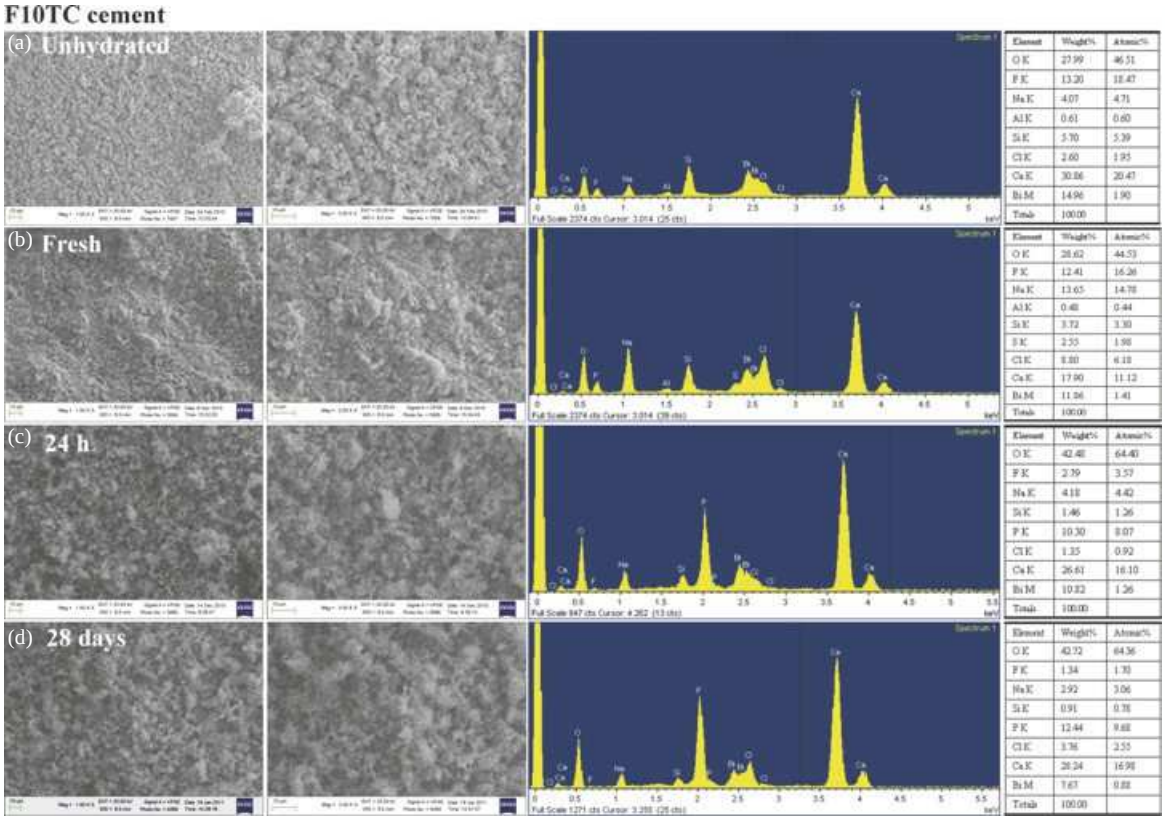

Figure 1 F10TC cement: environmental scanning electron microscopy with energy-dispersive X-ray analyses of unhydrated powder (a), freshly prepared (b), 24 h-aged (c) and 28 day-aged (d) samples.

The surface of fresh cements (Figs 1b, 2b and 3b) appeared rough/irregular and free from porosities. EDX showed prominent peaks because of Ca, Cl and O (from the cement particles, the radiopacifier and water), S (sulphur), Si (also from the silanol groups of CSH) and Bi.

The surface of 24 h-aged samples (Figs 1c, 2c and 3c) showed diffuse deposits with different size and shape, composed of globular precipitates (spherulites, 0.2-1 micron diameter). The deposit was more evident and thicker on F-containing cements (Figs 1c and 2c).

Energy-dispersive X-ray analysis microanalysis on the area (approximately 3000 l^2) displayed prominent Ca, P (phosphorous) and O reflexes and traces of Si, Bi and Cl components. The intensity of the typical elements of the cement (mainly silicon) decreased over storage time because of the formation of the calcium phosphate layer (biocoating).

FTC and F10TC samples displayed higher P peaks and lower Ca/P ratio approximately 2.2-2.5) than wTC (approximately 3.2): the Ca peak detected on the wTC cement originated from the calcium phosphate deposits, the calcium silicate component and the $CaCl_2$ ingredient.

Punctual EDX on spherulites showed only Ca and P peaks, suggesting the formation of calcium phosphate precipitates.

Environmental scanning electron microscopy observations of the surface of 28 day-aged samples (Figs 1d, 2d and 3d) showed a continuous irregular layer of deposits. No morphological differences were noted among the cements.

Energy-dispersive X-ray analysis detected prevalent Ca and P peaks and traces of typical elements of the cement, suggesting the formation of a thick calcium phosphate layer that is able to mask the underlying components of the cement. FTC and F10TC samples displayed lower Ca/P ratio than wTC.

Punctual EDX registered Ca and P with a Ca/P ratio (approximately 2) close to that of bone-like carbonated apatites.

The Ca/P ratio on the calcium phosphate layer decreased during immersion in DPBS (from

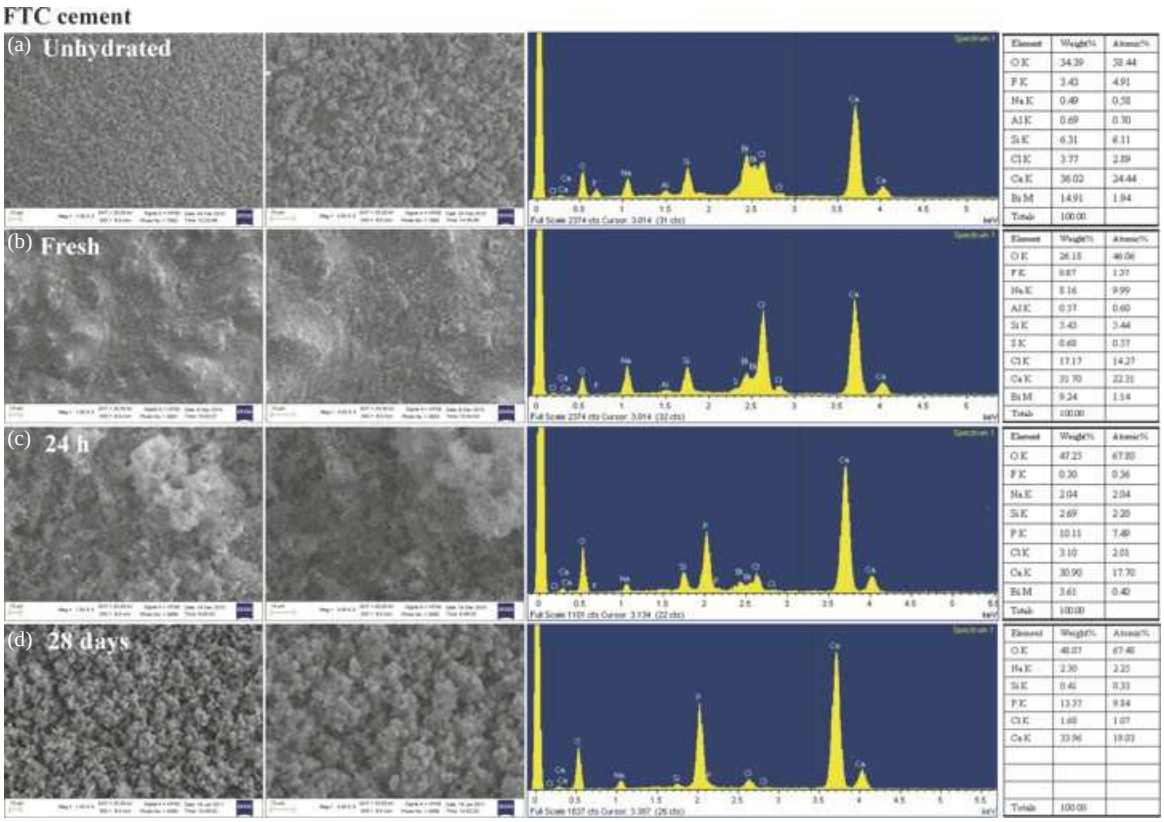

Figure 2 FTC cement: environmental scanning electron microscopy with energy-dispersive X-ray analyses of unhydrated powder (a), freshly prepared (b), 24 h-aged (c) and 28 day-aged (d) samples.

approximately 2.5-3.0 at 24 h to approximately 2 at 28 days) for all the cements. The presence of $CaCl_2$ may have slightly affected the Ca/P ratio detected on the samples covered by a calcium phosphate layer thinner than the X-ray electron beam penetration, i.e. approximately 2.98 lm. The contribution of $CaCl_2$ to the observed Ca/P ratio decreased at increasing deposit thickness, i.e. at increasing ageing time.

Micro-Raman analyses

Figure 4 reports the micro-Raman spectra recorded on the cements. Bands were assigned according to the literature (Taddei et al. 2009a,b, 2011 and references cited therein).

The spectra of the unhydrated powders practically coincided and disclosed calcium carbonate (band at 1087-1088 $cm^{)1}$), calcium sulphate as both anhydrite (band at 1017 $cm^{)1}$) and gypsum (band at 1002-1003 $cm^{)1}$), alite (band at 845 $cm^{)1}$), belite (bands at 855 and 845 $cm^{)1}$) and bismuth oxide (bands below 600 $cm^{)1}$).

The freshly prepared samples revealed the appearance of the marker band of ettringite (i.e. the hydration product of the reaction between anhydrite/gypsum and tricalcium aluminate) at about 990 $cm^{)1}$, particularly strong on the F10TC cement.

After 1 day of ageing in DPBS, all the cements showed an apatite + calcite/aragonite deposit. Apatite was revealed by the appearance of the band at 960 $cm^{)1}$, and the bands at 1000, 1045 and 1070 $cm^{)1}$ (typical of a B-type carbonated apatite) and 607 and 590 $cm^{)1}$ (FTC) were also detected on the F-doped cements. The intensity ratio between the bands of apatite and belite (at about 960 and 855 $cm^{)1}$, respectively) was taken as a marker of the thickness of the apatite deposit. This ratio was higher on the F-doped cements than on wTC. The 960 $cm^{)1}$ apatite band was broader on F10TC than on FTC, and an analogous trend was observed after 7 days of ageing.

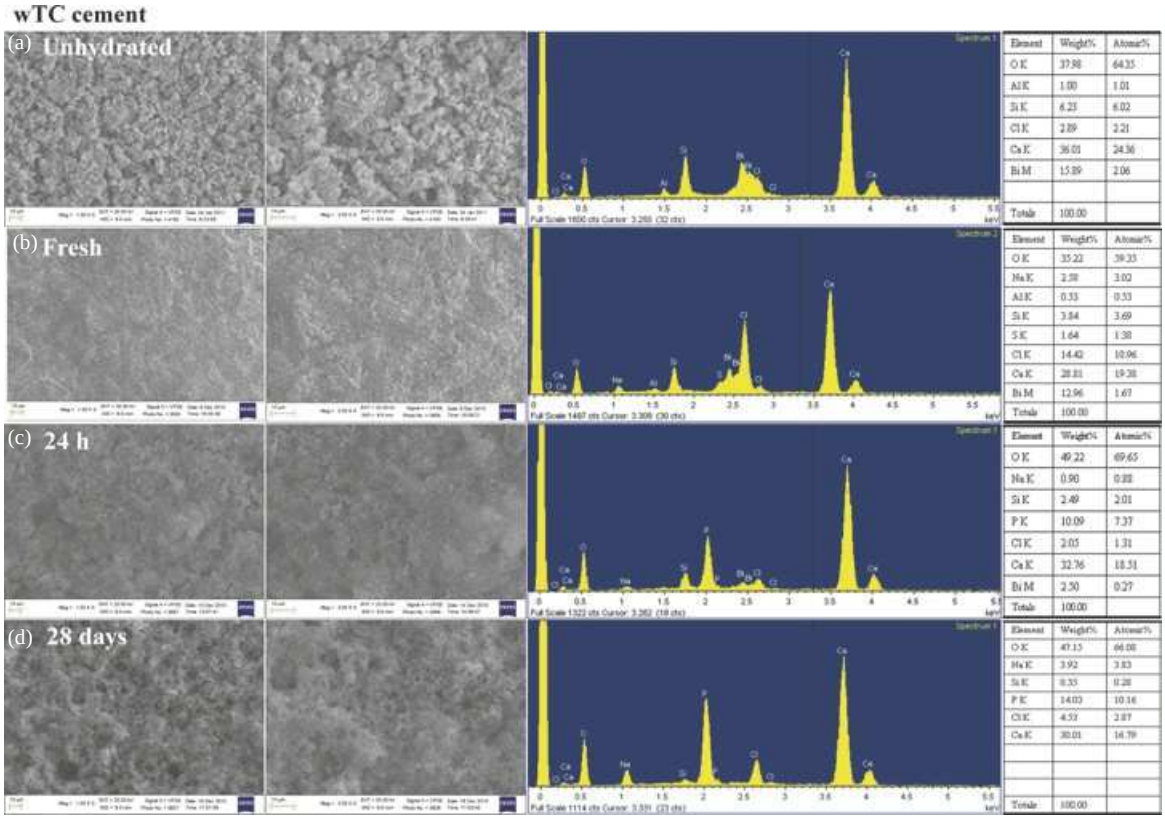

Figure 3 wTC cement: environmental scanning electron microscopy with energy-dispersive X-ray analyses of unhydrated powder (a), freshly prepared (b), 24 h-aged (c) and 28 day-aged samples (d).

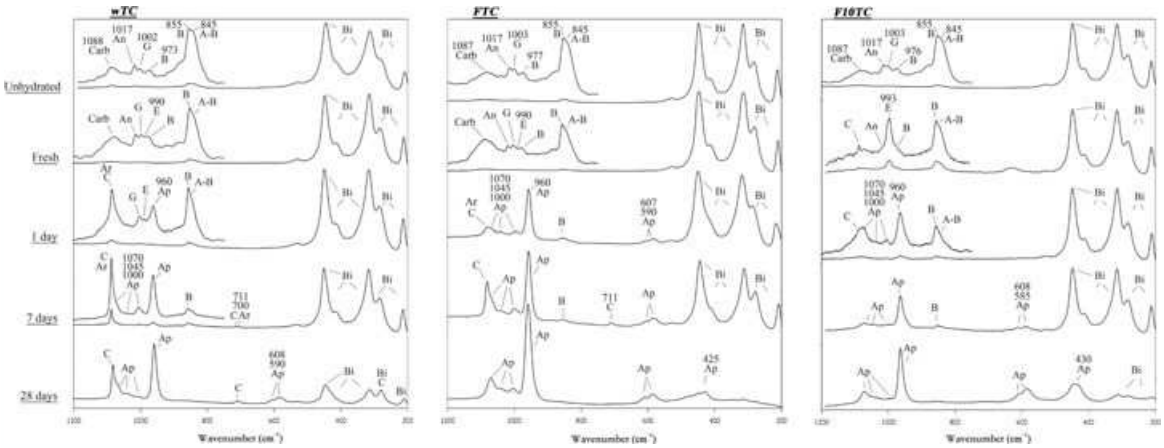

Figure 4 Micro-Raman spectra recorded on the surface of the three cements: freshly prepared (after 10 min) and after 1 and 28 days of ageing in Dulbecco's phosphate-buffered saline. The bands owing to calcium carbonate (Carb), calcite (C), aragonite (Ar), anhydrite (An), gypsum (G), ettringite (E), belite (B), alite (A), apatite (Ap) and bismuth oxide (Bi) are indicated. The spectra of the unhydrated cement powders are reported for comparison.

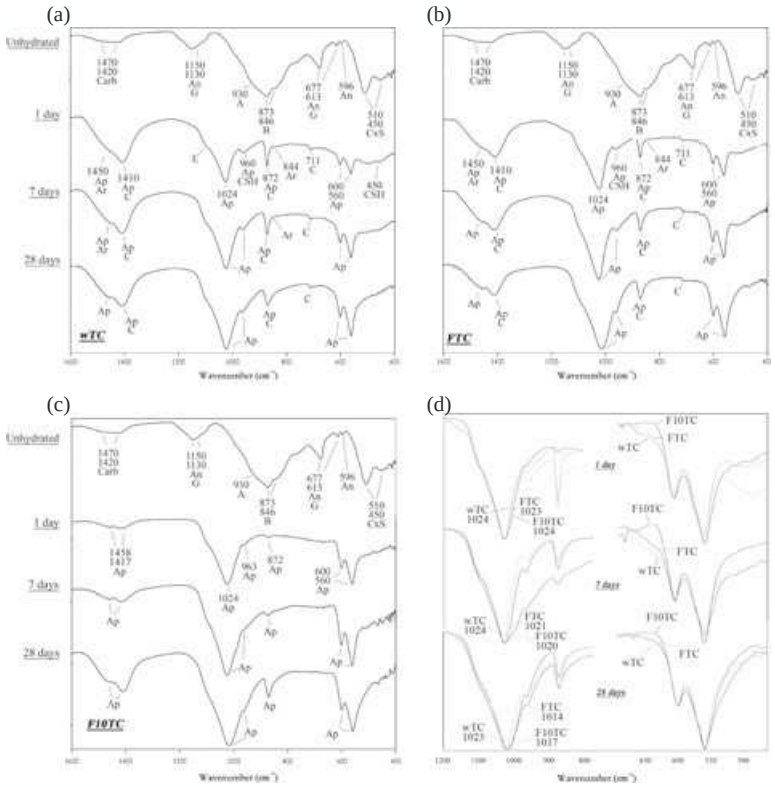

Figure 5 (a-c) IR spectra recorded on the surface of the three cements after 1 and 28 days of ageing in Dulbecco's phosphatebuffered saline (DPBS). The bands owing to calcium carbonate (Carb), calcite (C), aragonite (Ar), anhydrite (An), gypsum (G), ettringite (E), hydrated calcium silicate gel, slightly polymerized silicates (CxS), belite (B), alite (A) and apatite (Ap) are indicated. The spectra of the unhydrated cement powders are reported for comparison. (D) IR spectra recorded on the powders isolated from the DPBS storage media after 1, 7 and 28 days of ageing.

At increasing storage times, the bands of the cement progressively weakened, while the bands typical of a B-type carbonated apatite progressively strengthened. After 7 days of ageing in DPBS, the intensity ratio between the bands of apatite and belite had decreased along the series: FTC > F10TC > wTC. An analogous result was obtained after 28 days of ageing: the bands of bismuth oxide were observed with a progressively increasing intensity going from FTC to F10TC and wTC.

ATR/FTIR analyses

Figure 5 reports the IR spectra recorded on the cements. Bands were assigned according to the literature (Taddei et al. 2009a, 2011 and references cited therein).

The IR spectra of the unhydrated cements coincided and confirmed the presence of calcium carbonate (bands at 1420 and 1470 $cm^{)1}$), anhydrite (bands at 1150, 1130, 677, 613 and 596 $cm^{)1}$), gypsum (bands at 1150, 1130, 677 and 613 $cm^{)1}$) and slightly polymerized silicate groups (bands at 510 and 450 $cm^{)1}$) in the alite (marker band at 930 $cm^{)1}$) and belite (marker bands at 873 and 846 $cm^{)1}$) forms.

After 1 day of ageing in DPBS, all the cements had a B-type carbonated apatite deposit varying in thickness on the different samples, according to the Raman results. The spectra recorded on the surface of FTC and F10TC surfaces did not show any band of the underlying cement, and the deposit was mainly constituted by B-type carbonated apatite (bands at about 1450, 1410, 1024, 960, 872, 600 and 560 $cm^{)1}$) and calcite/aragonite indicating that the deposit was thicker than 2 lm.

The apatite bands on F10TC were broader than on FTC (in particular those at 1024 and 963 $cm^{)1}$), according to the Raman findings. Besides B-type carbonated apatite and calcite/aragonite, the spectrum recorded on the surface of wTC showed the components

owing to the hydration of the cement (CSH and ettringite), suggesting that the deposit was thinner than 2 lm (i.e. thinner than on the F-doped cements).

After 7 days of ageing, the cement components also became undetectable on wTC, owing to the increased thickness of the deposit. After 7 and 28 days, the apatite bands on F10TC were also broader than on FTC. The same trend was observed in the spectra recorded on the powders isolated from the ageing media (Fig. 5d). These spectra showed a different trend for the different cements also in the range near 630 $cm^{)1}$, where the OH bending mode falls. At all the ageing times, the prominent feature observed for wTC progressively weakened going to FTC and F10TC. According to a previous study (Amberg et al. 1974), this trend suggests that the apatite deposit on FTC and F10TC contained increasing amounts of fluoride in the lattice.

pH of storage water and calcium and fluoride release

The pH of storage water after immersion of the cements is reported in Table 1a. All the cements had a strong alkalinizing activity (ability to release hydroxyl ions): the pH of the deionized storage water (approximately pH 6.8) increased significantly up to pH 12 during the first 5 h of immersion and decreased significantly over time.

NaF-doped cements caused a statistically higher increase of the pH at all end-points, and the pH rise (alkalinizing activity) of F10TC was stronger than FTC. The addition of fluoride increased the pH mainly at short storage times.

The alkalinizing activity of all the cements remained after 28 days of storage.

The calcium release of cements when soaked in deionized water is shown in Table 1b. All the cements released calcium ions. The calcium release from wTC decreased statistically over the storage time. At 5 and 24 h, the wTC had the significantly highest calcium release ($P < 0.001$), but at 3-28 days, FTC and F10TC had significantly higher calcium release than wTC ($P < 0.05$).

The fluoride release of cements when soaked in deionized water is shown in Table 1c. The F10TC showed the statistically highest fluoride release at all times ($P < 0.01$). The fluoride release statistically decreased over time. No significant differences were proved between FTC and wTC.

Discussion

Bioactive calcium silicate cements precipitate hydroxy-carbonated apatite onto their surface (Gandolfi et al. 2010a-c, Taddei et al. 2009a, 2009b) on dentine and inside the dentinal tubules (Gandolfi et al. 2008a).

It has been demonstrated that silanol groups form from hydrated calcium silicate upon cement powder hydration (after mixing with water). Phosphate ions from DPBS are absorbed by the silanol groups allowing the formation/nucleation of small round-shaped calcium phosphate precipitates named apatite spherulites (Gandolfi et al. 2010c).

Calcium silicate MTA cements for endodontic surgery (root-end filling materials and endodontic sealers) are used directly in contact with alveolar bone: a

Table 1 (a) pH of soaking water, (b) calcium and (c) fluoride released (ppm) in soaking water. Samples disks (n = 10 for each material) were used. The data (expressed as mean and standard deviation) were statistically analyzed using one-way anova with Tukey test ($P < 0.05$). Different CAPITAL superscript letters in the same row or different small superscript letters in the same column mean statistically significant differences.

Material	5h	1 day	3 days	7 days	14 days	28 days
(a)						
F10TC	$12.49 \pm 0.04^{A,a}$	$11.80 \pm 0.10^{B,a}$	$9.74 \pm 0.22^{C,a}$	$9.63 \pm 0.42^{C,a}$	$8.81 \pm 0.50^{D,a}$	$8.93 \pm 0.34^{D,a}$
FTC	$11.82 \pm 0.08^{A,b}$	$11.24 \pm 0.16^{B,b}$	$10.37 \pm 0.31^{c,b}$	$8.96 \pm 0.16^{D,b}$	$8.95 \pm 0.07^{D,ab}$	$8.84 \pm 0.12^{D,a}$
wTC	$11.73 \pm 0.11^{A,b}$	$11.23 \pm 0.12^{B,b}$	$9.52 \pm 0.26^{c,a}$	$9.26 \pm 0.06^{CD,c}$	$9.05 \pm 0.21^{D,b}$	$8.50 \pm 0.11^{E,b}$
(b)						
F10TC	$21.13 \pm 4.40^{A,a}$	$6.57 \pm 4.70^{B,a}$	$35.80 \pm 5.47^{C,a}$	$23.10 \pm 2.25^{A,a}$	$11.23 \pm 0.93^{B,a}$	$24.35 \pm 1.52^{A,a}$
FTC	$21.88 \pm 7.65^{A,a}$	$8.12 \pm 1.45^{B,a}$	$32.30 \pm 0.94^{C,a}$	$29.77 \pm 1.19^{C,b}$	$19.71 \pm 1.63^{A,b}$	$18.40 \pm 1.06^{A,a}$
wTC	$440.22 \pm 17.10^{A,b}$	$193.92 \pm 16.95^{B,b}$	$25.21 \pm 0.96^{C,b}$	$11.56 \pm 1.40^{D,c}$	$10.14 \pm 3.04^{D,a}$	$12.89 \pm 1.72^{D,b}$
(c)						
F10TC	$9.33 \pm 3.13^{A,a}$	$3.78 \pm 0.66^{B,a}$	$1.89 \pm 0.24^{C,a}$	$1.71 \pm 0.25^{C,a}$	$1.51 \pm 0.16^{C,a}$	$2.35 \pm 0.35^{C,a}$
FTC	$1.24 \pm 0.19^{A,b}$	$0.50 \pm 0.08^{B,b}$	$0.35 \pm 0.03^{B,b}$	$0.58 \pm 0.10^{B,b}$	$0.58 \pm 0.07^{B,b}$	$0.52 \pm 0.08^{B,b}$
wTC	$0.48 \pm 0.19^{A,b}$	$0.37 \pm 0.4^{A,b}$	$0.22 \pm 0.02^{A,b}$	$0.26 \pm 0.03^{A,b}$	$0.27 \pm 0.08^{A,b}$	$0.25 \pm 0.04^{A,b}$

root-end filling material is positioned in the root-end cavity to seal the resected apex, and an endodontic sealer is frequently extruded from the apex in clinical practice. Therefore, osteoconductive activity is an essential property to support an adequate biological response and new bone tissue formation.

It is well known that sodium fluoride possesses good biological activity on bone/osteoblast cells and dental pulp cells (Lau & Baylink 1998, Nakade et al. 1999, Abdullah et al. 2002) and may be introduced in the formulation of MTA cements to improve their biological behaviour (Gandolfi et al. 2008b). Moreover, fluorapatite $Ca_{10}(PO_4)_6OH\text{-}F$ is more active on osteoblast activity and bone formation than hydroxyapatite $Ca_5(PO_4)_3OH$ (Qu & Wei 2006). The introduction of fluoride into apatite has been shown to improve osteoblast response in terms of adhesion (Qu & Wei 2006), differentiation (Qu & Wei 2006), proliferation (Yoon et al. 2005, Qu et al. 2008) and mineralization processes (Zhang et al. 1998) when compared to pure hydroxyapatite. The incorporation of fluorapatite into implant coatings improves implant integration into bone (Bhadang et al. 2010).

Sodium fluoride has been added to bone cements to speed up the early formation of bone at the interface and thereby improve fixation (Sundfeldt et al. 2002, Cartmell 2009). A recent study (Lin et al. 2009) investigated the effects of CaF_2 (0, 1, 2 and 3 wt%) on the apatite formation ability of tricalcium silicates (Ca_3SiO_5) and the mechanism of apatite formation in simulated body fluid. CaF_2-doped tricalcium silicates showed a better bioactivity than Ca_3SiO_5 owing to the formation and stability of F-substituted apatite (Lin et al. 2009). Fluoride-containing tricalcium silicates (Xu et al. 2008, Lin et al. 2009) or bioactive glasses (Brauer et al. 2008, 2010)) doped with CaF_2 have been studied for their ability to form F-substituted apatite. However, CaF_2 has a only limited solubility (K_{sp} $3.9 \cdot 10^{)11}$), which decreases in an alkaline environment. Therefore, NaF was selected in the present study for its greater solubility.

The results demonstrated that the NaF-doped calcium silicate cements were able to increase strongly the pH of storage water up to pH 12 during the first day of immersion. The addition of fluoride enhanced this pH rise mainly for short storage times. This result showed that NaF has a significantly different (i.e. opposite) effect from that exerted by CaF_2 (Lin et al. 2009), which has been reported to decrease cement hydration resulting in a lower alkalinizing activity (i.e. lower pH values).

F-containing cements released significantly lower amounts of calcium ions into the storage water than wTC (Table 1b). This result was not surprising because the F-containing cements allow the precipitation of calcium fluoride (fluorite) because of the presence of $F^{)}$ ions. This phase was detected (data not shown) on the surface of the F-doped cements aged in water.

Raman and IR spectroscopies have been used to investigate the thickness of the deposit as well as its chemical nature. Both techniques revealed that in DPBS, FTC and F10TC had a more pronounced apatite-forming ability than wTC. Because of its low sampling depth, ATR/FTIR spectroscopy was able to yield information on the relative thickness of the deposits only at 1 day of ageing when the bands of the underlying cement were observed only for wTC. This behaviour suggested that the deposit was thinner on wTC than on the F-doped cements. Because of its higher sampling depth, Raman spectroscopy was able to discriminate among the three cements at all ageing times. The intensity ratio between the bands of apatite and belite differed significantly among the three cements and showed that bioactivity decreased along the series: FTC > F10TC > wTC.

Vibrational Raman and IR spectroscopy also yielded information on the chemical composition of the deposits. Both techniques showed that for all the cements, the apatite lattice contained carbonate in B-site (i.e. carbonate substitutes the phosphate ion in the lattice), as revealed by the marker bands of B-type carbonated apatites at about 1070 $cm^{)1}$ (Raman), 1450-1410 and 870 $cm^{)1}$ (IR). The broadening of the phosphate bands observed for F10TC in both the Raman and IR spectra suggested that on this cement, the apatite deposit was less crystalline than on the other cements. IR spectroscopy appeared more sensitive than Raman spectroscopy in the analysis of the fluoridation degree of the apatite formed on F-doped cements. It is well known that the fluoridation mechanism involves a hydroxyl substitution and a subsequent adjacent hydroxyl rearrangement. As a consequence, the intensity of the OH bending mode at about 630 $cm^{)1}$ has been reported to decrease as the extent of fluoridation increases (Amberg et al. 1974). As shown in Fig. 5d, at all ageing times, the spectral feature at about 630 $cm^{)1}$ appeared with decreasing intensity along the series wTC > FTC > F10TC. On this basis, it can be affirmed that the cements under study formed different apatite phases upon ageing in DPBS: a hydroxy-carbonated apatite formed on the surface of wTC, while from 1 day of ageing, the apatite

phase on FTC and F10TC contained increasing amounts of fluoride ions in the lattice. The incorporation of fluoride ions into the lattice can explain the higher bioactivity of the F-doped cements in DPBS, because F-substituted apatites have a lower K_{sp} than hydroxy-carbonate apatite.

The trend of the micro-Raman spectra suggested that FTC should have a higher bioactivity than F10TC. In other words, the increase in the fluoride content up to 10%wt did not lead to an improvement in the apatite-forming ability. This finding was not surprising in the light of a previous study (Lin et al. 2009) who reported that among the tricalcium silicate samples doped with 1, 2 and 3 wt% of CaF_2, the specimen with the intermediate fluoride content (i.e. 2%wt) had the highest bioactivity.

The mechanism of apatite formation on NaF-doped calcium silicate MTA cements may be proposed in the following stages:

- Stage I: when the calcium silicate powder reacts with water, CSH gel and $Ca(OH)_2$ are the main products; $Ca(OH)_2$ was detected in the IR spectra recorded in the interior of the cement discs (not shown). As Ca^{2+} and OH^- were rapidly released into the storage solution, the pH values increased. In addition, NaF-doped cement pastes can release F^- (Table 1c).
- Stage II: before the apatite formation, the surface layer of CSH gel formed in the calcium silicate pastes mainly consists of silanol groups $Si(OH)_4$, whose presence can be inferred from the IR band at 960 cm^{-1} (Lin et al. 2009). This band was observed in the IR spectra recorded in the interior of the cement discs (not shown).
- Stage III: the CSH gel layer provides the negatively charged sites for the migration of Ca^{2+} and PO_4^{3-} ions to the paste surface, followed by growth of an F-substituted apatite (Fig. 5d) layer by the incorporation of soluble F^- because F-substituted apatite has a lower K_{sp} ($6.5 \cdot 10^{-65}$) than that of hydroxy-apatite $Ca_5(PO_4)_3OH$ ($K_{sp} = 7.36 \cdot 10^{-60}$).
- Stage IV: the F-substituted apatite acts as a new nucleation centre promoting the crystallization of the $CaO\text{-}P_2O_5$ layer by the incorporation of Ca^{2+}, PO_4^{3-}, CO_3^{2-} and F^- to form an apatite layer.

The study demonstrated that fluoride-doped calcium silicate cements are biointeractive materials able to release calcium and hydroxyl ions and form fluorapatite on their surface.

The calcium released by these cements affects osteoblast viability, proliferation and differentiation (Maeno et al. 2005, Sun et al. 2009a,b) and may have several biologically important functions in many clinical applications such as pulp capping procedures (Nair et al. 2008, Tuna & Olmez 2008) and apexogenesis (Holden et al. 2008). Apatite formation represents a biological substrate for all clinical applications in bone tissue and may have a clinical effect on damaged tissues where new bone formation is required (Nair 2006). These data may explain the positive reports on the use of calcium silicate cements such as ProRoot MTA, MTA Angelus and Tech Biosealer in clinical situations (Saunders 2008, Pace et al. 2008, Parirokh & Torabinejad 2010).

Conclusions

Fluoride-doped calcium silicate cements form fluorapatite in phosphate-containing solutions. These cements are better able to form apatite (bioactivity) and are more reactive than conventional calcium silicate cements. The improved bioactivity can be attributed to the formation of F-substituted apatites, which have a K_{sp} lower than hydroxy-carbonate apatite. F-doped calcium silicate cements are promising materials for use in contact with bone in endodontics and oral surgery.

References

Abdullah D, Ford TR, Papaioannou S, Nicholson J, McDonald F (2002) An evaluation of accelerated Portland cement as a restorative material. Biomaterials 23, 4001-10.

Amberg CH, Luk HC, Wagstaff KP (1974) The fluoridation of nonstoichiornetric calcium hydroxyapatite. An infrared study. Canadian Journal of Chemistry 52, 4001-6.

Bhadang KA, Holding CA, Thissen H, McLean KM, Forsythe JS, Havnes DR (2010) Biological responses of human osteoblasts and osteoclasts to flame-sprayed coatings of hydroxyapatite and fluorapatite blends. Acta Biomaterialia 6, 1575-83.

Brauer DS, Karpukhina N, Seah D, Law RV, Hill RG (2008) Fluoride-containing bioactive glasses. Advanced Materials Research 39-40, 299-304.

Brauer DS, Mneimne M, Lynch E, Gillam DG, Hill RG (2010) Fluorapatite-forming bioactive glasses for use in dentifrices treating dentine hypersensitivity. Journal of Dental Research 89A, 3758.

BSI, British Standards Institution (2007) Terminology for the bio-nano interface. PAS (Publicly Available Specification) 132, 2.

Cartmell S (2009) Controlled release scaffolds for bone tissue engineering. Journal of Pharmacological Sciences 98, 430-41.

Colin A, Prati C, Pelliccioni GA, Gandolfi MG (2010) Solubility in water or DMEM of F-doped MTA cements with increasing F-content. Dental Materials 26S, e67.

Gandolfi MG, Farascioni S, Pashley DH, Gasparotto G, Prati C (2008a) Calcium silicate coating derived from Portland cement as treatment for hypersensitive dentine. Journal of Dentistry 36, 565-78.

Gandolfi MG, Perut F, Ciapetti G, Mongiorgi R, Prati C (2008b) New Portland cement-based materials for endodontics mixed with articaine solution: a study of cellular response. Journal of Endodontics 34, 39-44.

Gandolfi MG, Ciapetti G, Perut F et al. (2009a) Biomimetic calcium-silicate cements aged in simulated body solutions. Osteoblasts response and analyses of apatite coating. Journal of Applied Biomaterials & Biomechanics 7, 160-70.

Gandolfi MG, Iacono F, Agee K et al. (2009b) Setting time and expansion in different soaking media of experimental accelerated calcium-silicate cements and ProRoot MTA. Oral Surgery, Oral Medicine, Oral Pathology, Oral Radiology & Endodontics 108, e39-45.

Gandolfi MG, Taddei P, Tinti A, Dorigo De Stefano E, Rossi PL, Prati C (2010a) Kinetics of apatite formation on a calcium-silicate cement for root-end filling during ageing in physiological-like phosphate solutions. Clinical Oral Investigations 14, 659-68.

Gandolfi MG, Van Landuyt K, Taddei P, Modena E, Van Meerbeek B, Prati C (2010b) ESEM-EDX and raman techniques to study MTA calcium-silicate cements in wet conditions and in real-time. Journal of Endodontics 36, 851-7.

Gandolfi MG, Taddei P, Tinti A, Prati C (2010c) Apatite-forming ability of ProRoot MTA. International Endodontic Journal 43, 917-29.

Gandolfi MG, Ciapetti G, Taddei P et al. (2010d) Effect of ageing on bioactivity and in vitro biological properties of calcium silicate-cements for dentistry. Dental Materials 26, 974-92.

Gandolfi MG, Prati C (2010e) MTA and F-doped MTA cements used as sealers with warm gutta-percha. Long-term sealing ability study. International Endodontic Journal 43, 889-901.

Holden DT, Schwartz SA, Kirkpatrick TC, Schindler WG (2008) Clinical outcomes of artificial root-end barriers with mineral trioxide aggregate in teeth with immature apices. Journal of Endodontics 34, 812-7.

Kokubo T, Takadama H (2006) How useful is SBF in predicting in vivo bone bioactivity? Biomaterials 27, 2907-15.

Lau KHW, Baylink DJ (1998) Molecular mechanism of action of fluoride on bone cells. Journal of Bone and Mineral Research 13, 1660-7.

Lin Q, Li Y, Lan X, Lu C, Chen Y, Xu Z (2009) The apatite formation ability of CaF_2 doping tricalcium silicates in simulated body fluid. Journal of Biomedical Materials Research 4, 1-6.

Maeno S, Niki Y, Matsumoto H et al. (2005) The effect of calcium ion concentration on osteoblast viability, proliferation and differentiation in monolayer and 3D culture. Biomaterials 26, 4847-55.

Nair PNR (2006) On the causes of persistent apical peridontitis: a review. International Endodontic Journal 39, 249-81.

Nair PNR, Duncan HF, Pitt Ford TR, Luder HU (2008) Histological, ultrastructural and quantitative investigations on the response of healthy human pulps to experimental capping with mineral trioxide aggregate: a randomized controlled trial. International Endodontic Journal 41, 128-50.

Nakade O, Koyama H, Arai J, Ariji H, Takada J, Kaku T (1999) Stimulation by low concentrations of fluoride of the proliferation and alkaline phosphatase activity of human dental pulp cells in vitro. Archives of Oral Biology 44, 89-92.

Pace R, Giuliani V, Pagavino G (2008) Mineral trioxide aggregate as repair material for furcal perforation: case series. Journal of Endodontics 34, 1130-3.

Parirokh M, Torabinejad M (2010) Mineral trioxide aggregate: a comprehensive literature review - Part III: clinical applications, drawbacks, and mechanism of action. Journal of Endodontics 36, 400-13.

Qu H, Wei M (2006) The effect of fluoride contents in fluoridated hydroxyapatite on osteoblast behaviour. Acta Biomaterialia 2, 113-9.

Qu WJ, Zhong DB, Wu PF, Wang JF, Han B (2008) Sodium fluoride modulates caprine osteoblast proliferation and differentiation. Journal of Bone and Mineral Metabolism 26, 328-34.

Saunders WP (2008) A prospective clinical study of periradicular surgery using mineral trioxide aggregate as a root-end filling. Journal of Endodontics 34, 660-5.

Sun J, Wei L, Liu X et al. (2009a) Influence of ionic dissolution products of dicalcium silicate coating on osteoblastic proliferation, differentiation and gene expression. Acta Biomaterialia 5, 1284-93.

Sun J, Li J, Liu X, Wei L, Wang G, Meng F (2009b) Proliferation and gene expression of osteoblasts cultured in DMEM containing the ionic products of dicalcium silicate coating. Biomedicine & Pharmacotherapy 63, 650-7.

Sundfeldt M, Persson J, Swanpalmer J et al. (2002) Does sodium fluoride in bone cement affect implant fixation Part II: evaluation of the effect of sodium fluoride additions to acrylic bone cement and the fixation of titanium implants in ovariectomized rabbits. Journal of Materials Science: Materials in Medicine 13, 1045-50.

Taddei P, Tinti A, Gandolfi MG, Rossi PL, Prati C (2009a) Vibrational study on the bioactivity of portland cement-based materials for endodontic use. Journal of Molecular Structure 924-926, 548-54.

Taddei P, Tinti A, Gandolfi MG, Rossi PL, Prati C (2009b) Ageing of calcium silicate cements for endodontic use in simulated body fluids: a micro-Raman study. Journal of Raman Spectroscopy 40, 1858-66.

Taddei P, Modena E, Tinti A, Siboni F, Prati C, Gandolfi MG (2011) Vibrational investigation on the in vitro bioactivity of commercial and experimental calcium-silicate cements for root-end endodontic therapy. Journal of Molecular Structure 993, 367-75.

Torrisi A, Torrisi V, Tuccitto N, Gandolfi MG, Prati C, Licciardello A (2010) Tof SIMS images and spectra of biomimetic calcium-silicate based cements after storage in solutions simulated the human biological fluid effects. International Journal of Mass Spectrometry 289, 150-61.

Tuna D, Olmez A (2008) Clinical long-term evaluation of MTA as a direct pulp capping material in primary teeth. International Endodontic Journal 41, 273-8.

Xu Z, Lin Q, Li Y, lan X, Lu C (2008) An evaluation of CaF2 doping tricalcium silicate as dental restorative materials. Advanced Materials Research 47-50, 1339-42.

Yoon BH, Kim HW, Lee SH, Bae CJ, Koh YH (2005) Stability and cellular responses to fluorapatite-collagen composites. Biomaterials 26, 2957-63.

Zhang WG, Wang LZ, Liu Z (1998) The influence of fluoride on the development of the osteoblast phenotype in rat calvarial osteoblasts: an in vitro study. Shanghai Kou Qiang Yi Xue 7, 88-93.

International Endodontic Journal
doi:10.1111/j.1365-2591.2012.02013.x

Chemical-physical properties of TheraCal, a novel light-curable MTA-like material for pulp capping

M. G. Gandolfi, F. Siboni & C. Prati

Laboratory of Biomaterials and Oral Pathology, Department of Odontostomatological Sciences, University of Bologna, Bologna, Italy

Abstract

Gandolfi MG, Siboni F, Prati C. Chemical-physical properties of TheraCal, a novel light-curable MTA-like material for pulp capping. International Endodontic Journal, 45, 571-579, 2012.

Aim To evaluate the chemical-physical properties of TheraCal, a new light-curable pulp-capping material composed of resin and calcium silicate (Portland cement), compared with reference pulp-capping materials (ProRoot MTA and Dycal).

Methodology Calcium (Ca) and hydroxyl (OH) ion release over 28 days, solubility and water uptake (weight percentage variation, D%) at 24 h, cure depth and radiopacity of TheraCal, ProRoot MTA and Dycal were evaluated. Statistical analysis ($P < 0.05$) of release of ion was carried out by two-way repeated measures anova with Tukey, whilst one-way anova with Tukey test was used for the other tests.

Results TheraCal released significantly more calcium than ProRoot MTA and Dycal throughout the test period. TheraCal was able to alkalinize the surrounding fluid initially to pH 10-11 (3 h-3 days) and subsequently to pH 8-8.5 (7-14 days). TheraCal had a cure depth of 1.7 mm. The solubility of TheraCal (D)1.58%) was low and significantly less than that of Dycal (D)4.58%) and ProRoot MTA (D)18.34%). The amount of water absorbed by TheraCal (D +10.42%) was significantly higher than Dycal (D +4.87%) and significantly lower than ProRoot MTA (D +13.96%).

Conclusions TheraCal displayed higher calcium-releasing ability and lower solubility than either ProRoot MTA or Dycal. The capability of TheraCal to be cured to a depth of 1.7 mm may avoid the risk of untimely dissolution. These properties offer major advantages in direct pulp-capping treatments.

Keywords: calcium and hydroxyl ion release, calcium hydroxide, Dycal, ProRoot MTA, pulp capping materials, resin-modified calcium silicate, TheraCal.

Received 14 July 2011; accepted 29 December 2011

Introduction

Direct pulp capping involves the application of a dental material to the exposed pulp in an attempt to act as a barrier, protect the dental pulp complex and preserve its vitality (European Society of Endodontology 2006).

Calcium hydroxide [$Ca(OH)_2$]-based and calcium oxide (CaO)-based materials are the most popular agents for direct and indirect pulp capping, given their ability to release hydroxyl (OH) and calcium (Ca) ions upon dissolution (Horsted-Bindslev & Lovshall 2002, Desai & Chandler 2009, Mohammadi & Dummer 2011). Unfortunately, these materials are soluble and raise local pH with the formation of a necrotic layer at the material-pulp interface.

Dycal (Dentsply, Milford, DE, USA) (Dougherty 1962) is a self-setting (2.5-3.5 min) (Shen et al. 2010) radiopaque calcium hydroxide-based material employed in direct and indirect pulp capping procedures and as a liner under restorations, cements and other base materials. Its alkaline pH (pH 9-11) stimulates the formation of secondary dentine when the material is in direct contact with the pulp. Its toxicity to pulp cells is well documented (Furey et al. 2010, Shen et al. 2010).

Correspondence: Maria Giovanna Gandolfi, Head Laboratory of Biomaterials and Oral Pathology, Department of Odontostomatological Sciences, University of Bologna, Via San Vitale 59, 40125 Bologna, Italy (e-mail: mgiovanna.gandolfi@unibo.it).

Radiopaque Portland cements, commonly named mineral trioxide aggregate (MTA) cements (such as ProRoot MTA, MTA-Angelus, Tech Biosealer and others), are therapeutic, endodontic repair calcium silicate materials introduced at first as a grey cement (Torabinejad & White 1995). MTA cements exhibit calcified tissue-conductive activity and facilitate the differentiation of human orofacial mesenchymal stem cells (Gandolfi et al. 2011a) and the mineralization process in human dental pulp cells; they also have the potential to be used as pulp capping materials (Min et al. 2009).

White ProRoot MTA (Dentsply, Johnson City, TN, USA) is a bioactive (Gandolfi et al. 2009, 2010a,b,c, 2011b,c, Taddei et al. 2009), biocompatible (Torabinejad & Parirokh 2010) and self-setting hydrophilic calcium silicate cement (Gandolfi et al. 2008, Parirokh & Torabinejad 2010a) now successfully used for direct pulp capping (Tuna & Olmez 2008, Parirokh & Torabinejad 2010b). MTA is more effective and better than calcium hydroxide materials, as it has an enhanced interaction with dental pulp tissue (Takita et al. 2006) with limited pulp tissue necrosis (less caustic effect) shortly after its application and less pulp inflammation (Moghaddame-Jafari et al. 2005). MTA facilitated the proliferation/differentiation of human dental pulp cells (Takita et al. 2006, Sawicki et al. 2008) and exhibited calcified tissue-conductive activity with the ability to stimulate more/faster complete dentine bridge formation and new hard tissue formation (Moghaddame-Jafari et al. 2005, Bogen et al. 2008, Okiji & Yoshiba 2009).

TheraCal (Bisco Inc, Schamburg, IL, USA) is a new light-cured resin-modified calcium silicate-filled base/liner material designed with direct and indirect pulp capping containing approximately 45% wt mineral material (type III Portland cement), 10% wt radiopaque component, 5% wt hydrophilic thickening agent (fumed silica) and approximately 45% resin (Suh et al. 2008). The patent stated that the resin consists of a hydrophobic component (comprising hydrophobic monomers) such as urethane dimethacrylate (UDMA), bisphenol A-glycidyl methacrylate (BisGMA), triethylene glycol dimethacrylate (TriEDMA or TEGDMA) and a hydrophilic component (containing hydrophilic monomers) such as hydroxyethyl methacrylate (HEMA) and polyethylene glycol dimethacrylate (PEGDMA) (Suh et al. 2008). TheraCal has good sealing capabilities (Suh et al. 2008) and was well-tolerated by immortalized odontoblast cells (Hebling et al. 2009).

The aim of this study was to evaluate calcium and hydroxyl ions release, cure depth, solubility, water absorption and radiopacity of TheraCal compared with reference pulp capping materials (ProRoot MTA and Dycal).

Materials and methods

Materials

TheraCal (Bisco Inc, lot. 603-189-A) consists of a single paste containing CaO, calcium silicate particles (type III Portland cement), Sr glass, fumed silica, barium sulphate, barium zirconate and resin containing Bis-GMA and PEGDMA (Suh et al. 2008).

White ProRoot MTA (Dentsply, lot. 09001920) is composed of white Portland cement and bismuth oxide (Parirokh & Torabinejad 2010a). ProRoot MTA was prepared following the manufacturer's instructions by mixing a 3 : 1 powder-to-liquid ratio.

Dycal (Dentsply, lot. 081007), a two-paste system made of a base paste (1,3-butylene glycol disalicylate, zinc oxide, calcium phosphate, calcium tungstate, iron oxide pigments) and a catalyst paste (calcium hydroxide, N-ethyl-o/p-toluene sulphonamide, zinc oxide, titanium oxide, zinc stearate, iron oxide pigments) (Shen et al. 2010), was prepared following the manufacturer's instructions by mixing equal amounts of catalyst paste and base paste.

Calcium ions (ppm) and hydroxyl ions (pH) release test

The different cement pastes were compacted to excess into PVC moulds (8 mm in diameter and 1.6 mm thick).

Each filled mould was placed on the bottom of a cylindrical polystyrene-sealed container (3 cm high and 4 cm in diameter) in 10 mL of deionized water at 37 C. The exposed surface area of each sample was 50.24 ± 0.01 mm^2 (upper surface). The storage water was collected (for Ca and pH analyses) and replaced after 3 and 24 h, and 7, 14, 28 days.

Calcium ions (ppm) and hydroxyl ions (pH) were analysed in deionized water with a magnetic stirrer using a multiparameter laboratory meter (inoLab 750 WTW, Weilheim, Germany) connected to a calcium probe (Calcium ion electrode; Eutech instruments Pte Ldt, Singapore) or a (selective) temperature-compensated pH probe/electrode (Sen Tix Sur WTW, Weilheim, Germany).

For calcium quantization, 0.200 mL (2%) of 4 mol $L^{)1}$ KCl (ISA WTW, Weilheim, Germany) was added to 10 mL of deionized water. The results were recorded when the data had stabilized to the second decimal place

Solubility and water absorption: weight percentage variation (D%) after storage in water

The different cement pastes were compacted to excess into PVC moulds (8 mm in diameter and 1.6 mm thick). ProRoot MTA and Dycal samples were cured (at 37 C and 98% relative humidity) for a period equal to 70% of the final setting time, that is, 2 min for Dycal and 117 min for ProRoot MTA (a period 50% longer than the time stated by the manufacturer, according to ISO 6876 clause 7.7.2. Dental root canal sealing materials) (ISO 6876 2002) and then removed from the mould.

TheraCal specimens were light-cured for 20 s on both surfaces using a 1700-mW $cm^{)2}$ LED lamp (T-LED elca, Anthos, Italy) through a polyester strip (Directa Matrix Strips; Directa AB, Upplands, Vasby, Sweden) and removed from the mould.

Each cylindrical specimen was placed in a cylindrical polystyrene-sealed container (3 cm high and 4 cm in diameter) in 20 mL of deionized water at 37 C. The lower surface of the samples was not in contact with the container but inclined, so the entire surface of the sample was in contact with the water. The exposed surface area of each sample was 140.67 ± 0.01 mm^2 (upper and lower surface 2 (pr^2) = 100.48 mm^2 and lateral surface 2 prh = 40.19 mm^2).

Solubility and water absorption were assessed by gravimetric determination as the percentage weight variation (D%) using an analytical balance (Bel Engineering series M, Monza, Italy, 0.001 g accuracy). Each weight measurement was repeated three times. The solubility of the materials was calculated using the method described in ISO 6876 (ISO 6876 2002).

The cylindrical specimens were weighed before immersion in water (Initial weight). After 24 h of soaking, the samples were removed from the deionized water and blotted dry at 37 C for 48 h, that is, until the weight was stable and then re-weighed (Dry weight) and finally discarded. Solubility (percentage weight variation, DW%) was calculated as follows:

Solubility ¼½ðDry weight at time t Initial weightÞ

Initial weight 100

The solubility of the set materials should not exceed 3% mass fraction (ISO 6876 clause 4.3.6.). For water absorption (water uptake), the specimens were immersed in deionized water for 24 h (Wet weight) and blotted dry at 37 C for 48 h, that is, until weight stabilization (Dry weight). Water absorption was calculated as follows:

Water absorbtion ¼ ½ðWet weight at time t

Dry weight at 24 hÞ= Dry weight at time 24 h 100

Depth of cure

The depth of cure (DOC) was evaluated following ISO 4049 (ISO 4049 2000 Dentistry - Polymer-based filling, restorative and luting materials) (ISO 4049 2000).

TheraCal samples were placed in a mould (4 mm diameter, 9 mm thick) and light-cured for 20 s on the upper surface and demoulded. The noncured/uncured material at the bottom was removed using a spatula, and the thickness of the cured material was measured with a digital micrometer (0.01 mm accuracy). The measurement was repeated in three different positions in each sample, and these data were recorded as mean value. ISO 4049 requirement suggests a DOC >1.5 mm.

Radiopacity

In accordance with ISO 6876 (ISO 6876 clause 7.8 for Dental root canal sealing materials) (ISO 6876 2002), completely set samples (10 ± 0.1 mm diameter; 1.0 ± 0.1 mm height) were radiographed using a radiographic unit (Myray Cefla, Imola, Italy) with reference aluminium step wedge (60 mm long, 10 mm wide). Operative conditions were as follows: 3 cm distance, 0.13 s exposure at 70 KVp and 8 mA. The film (Kodak dental film, Eastman Kodak Company, Carestream Health Inc., Rochester, New York, NY, USA) was processed (automatic developer, 4 min at 30 C) and scanned. The radiographic density (colour intensity) data were converted (software Image J) into aluminium step-wedge equivalent thickness (mm Al). A radiopacity ‡3 mm Al is suggested by ISO 6976.

Statistical analysis

The data are reported as mean ± standard deviation. The results of the Ca and OH release were analysed using two-way repeated measures anova with Tukey.

The data on solubility and water absorption were analysed by one-way anova with Tukey test. On the table, different capital letters represent statistically significant differences ($P < 0.05$) in the same line, whilst different small letters represent differences in the same column.

Results

TheraCal released significantly more calcium than either ProRoot MTA or Dycal throughout the tested period (Table 1). The amount of leached calcium decreased with the time for all the materials. The release of calcium by ProRoot MTA fluctuated during the first 3 days.

TheraCal was able to alkalinize the surrounding fluid initially to approximately pH 10-11 (3 h-3 days) and subsequently to pH 8-8.5 (7-28 days). The pH of the medium conditioned by ProRoot MTA was significantly higher than either TheraCal or Dycal up to 7 days. Dycal maintained the pH at a constant value (pH approximately 10) throughout the experimental period (Table 2), but the pH of Dycal was not stable and showed a significant decrease at 7 and 14 days.

The solubility of TheraCal was significantly lower than Dycal and ProRoot MTA (Table 3). TheraCal absorbed significantly more water than Dycal and significantly less than ProRoot MTA (Table 3).

After irradiation for 20 s, TheraCal was cured to an approximately 1.7 mm thickness (Table 3). The DOC of Dycal and ProRoot MTA was not tested as they are not light-activated materials (ISO 4049, clause 7.10).

Dycal and TheraCal were weakly radiopaque (Table 3). ProRoot MTA had a nonhomogeneous radiopacity inside the samples (showing the highest standard deviation amongst the materials); however, only the ProRoot cement had a radiopacity in line with ISO 6876.

Discussion

Direct pulp capping is the treatment of the exposed vital pulp by sealing the pulpal wound with a dental material to induce a reparative dentinogenic response

Table 1 Ca ions release test. TheraCal released statistically more calcium than either ProRoot MTA or Dycal throughout the tested period.

Calcium (ppm) leaked soaking water (n = 10)						
Material	3h	1 day	3 days	7 days	14 days	28 days
ThearCal	74.74 ± 9.20^{Aa}	37.41 ± 4.54^{Ba}	25.18 ± 6.54^{Ca}	24.56 ± 1.96^{Ca}	24.13 ± 1.12^{Ca}	19.63 ± 3.06^{Ca}
Dyal	34.25 ± 9.74^{Ab}	14.76 ± 5.33^{Bb}	12.50 ± 1.40^{Bb}	12.83 ± 4.27^{Bb}	$17.08 \pm 0.81^{Ba,b}$	12.93 ± 3.93^{Bb}
ProRoot MTA	$32.21 \pm 4.52^{A,Ba}$	$29.82 \pm 3.51^{Aa,b}$	35.44 ± 2.33^{Bc}	24.51 ± 3.85^{Aa}	14.32 ± 2.73^{Cb}	$16.11 \pm 2.94^{Ca,b}$
Water	1.66 ± 0.57^{Ac}	1.33 ± 0.57^{Ac}	1.33 ± 0.10^{Ad}	0.33 ± 0.57^{Bc}	0.24 ± 0.34^{Bc}	0.54 ± 0.21^{Ac}

Table 2 OH ions release test. The pH of the medium conditioned by ProRoot MTA was statistically higher than either TheraCal or Dycal till 7 days.

pH of soaking water (n = 10)						
Material	3h	1 day	3 days	7 days	14 days	28 days
ThearCal	10.96 ± 0.03^{Aa}	10.19 ± 0.24^{Ba}	9.28 ± 0.41^{Ca}	8.32 ± 0.06^{Da}	8.63 ± 0.15^{Ea}	8.04 ± 0.18^{Da}
Dyal	10.83 ± 0.44^{Aa}	10.99 ± 0.51^{Ab}	$10.14 \pm 0.28^{A,Bb}$	9.60 ± 0.38^{Bb}	9.94 ± 0.16^{Bb}	10.25 ± 0.49^{Ab}
ProRoot MTA	11.52 ± 0.75^{Ab}	10.91 ± 0.13^{Ab}	11.52 ± 0.41^{Ac}	11.25 ± 0.82^{Ac}	7.84 ± 0.13^{Bc}	8.25 ± 0.24^{Ba}
Water	6.88 ± 0.04^{Ac}	7.00 ± 0.02^{Ac}	7.07 ± 0.09^{Ad}	7.10 ± 0.10^{Ad}	6.96 ± 0.06^{Ac}	7.22 ± 0.12^{Ac}

Table 3 Solubility, water absorption, depth of cure, radiopacity. The solubility of TheraCal was very low, statistically less than that of Dycal and much less than ProRoot MTA. TheraCal absorbed statistically more water than Dycal and statistically less than ProRoot MTA. Dycal and ProRoot did not polymerize after a light-curing. TheraCal and ProRoot MTA shower less radiopacity than ProRoot MTA.

	Solubility (n = 10)	Water absorption (n = 10)	Depth of curve (mm, n = 3)	Radiopacity (mm of Al, n = 6)
ThearCal	$)1.58 \pm 0.35^{a}$	10.42 ± 0.34^{a}	1.69 ± 0.04	1.07 ± 0.06^{a}
Dyal	$)4.58 \pm 1.11^{b}$	4.87 ± 0.61^{b}	-	2.30 ± 0.10^{b}
ProRoot MTA	$)18.34 \pm 0.51^{c}$	13.96 ± 3.92^{c}	-	4.34 ± 0.64^{c}

(Horsted-Bindslev & Lovshall 2002, Goldberg & Smith 2004, Desai & Chandler 2009, Modena et al. 2009) and is one of the most important endodontic modalities for maintaining dental pulp vitality. A liner must act as a barrier to protect the dental pulpal complex and induce the formation of new dentine bridge or dentine-like bridge between the pulp and restorative material.

The bioavailability of calcium (Ca) ions plays a key role in the various biological events on cells involved in the new formation of mineralized hard tissues. Ca ions stimulate the expression of bone-associated proteins mediated by calcium channels (Jung et al. 2010), and large quantities of Ca ions could activate ATP, which plays a significant role in the mineralization process (Torneck et al. 1983).

Ca-releasing materials accelerate osteoblast differentiation: a 2-4 mmol $L^{)1}$ (80-160 ppm) concentration of calcium ions had a stimulatory effect on mouse primary osteoblasts, whilst 6-8 mmol $L^{)1}$ induced differentiation and >10 mmol $L^{)1}$ showed a cytotoxic effect (Maeno et al. 2005), considering normal extracellular calcium concentration is approximately 2 mmol $L^{)1}$ (80 ppm) (Clapham 1995).

Ca ions are necessary for the differentiation and mineralization of pulp cells (Schroder 1985), and a Ca-rich medium induces both proliferation and differentiation into odontoblast-like cells (Lopez-Cazaux et al. 2006). The eluted Ca ions increase the proliferation of human dental pulp cells in a dose-dependent manner (Clapham 1995, Takita et al. 2006). In addition, Ca ions specifically modulate osteopontin and bone morphogenetic protein-2 levels during pulp calcification (Rashid et al. 2003), and the release of Ca enhances the activity of pyrophosphatase, which helps to maintain dentine mineralization and the formation of a dentine bridge (Estrela & Holland 2003).

In view of this, the continuous release of Ca ions from a pulp capping material is likely the main reason for a material-induced proliferation and differentiation of human dental pulp cells. All the pulp capping materials tested in the present study proved to be calcium-releasing formulations. Unexpectedly, TheraCal proved to be an ion-leaching material able to release calcium and hydroxyl ions for a period of at least 28 days, and it released significantly more calcium than either ProRoot MTA or Dycal throughout the test period. Some calcium ion release from Dycal occurred during the 28-day experimental period, in agreement with other studies (Shubich et al. 1978, Tamburic et al. 1993), but ProRoot MTA released significantly more calcium ions than Dycal throughout the experimental period, in accordance with other studies (Takita et al. 2006). However, it is difficult to compare directly the findings of calcium release when the experimental protocols are different. The high amount of calcium provided by ProRoot MTA was in agreement with other studies (Takita et al. 2006, Gandolfi et al. 2011d).

It has been suggested that the positive effect of MTA cements on proliferation of human dental pulp cells is enhanced potentially by the continuous and constant release of calcium ions: the elution components such as calcium ions (approximately 0.3 mmol $L^{)1}$) from MTA increased the proliferation of human dental pulp cell in a dose-dependent manner compared with Dycal and the control (Takita et al. 2006).

Interestingly, in the present study, the amount of calcium ions released from TheraCal was in the concentration range with potential stimulatory activity for bone-forming cells (Maeno et al. 2005), dental pulp cell (Takita et al. 2006) and odontoblasts (Rashid et al. 2003, Lopez-Cazaux et al. 2006).

The findings of this study suggest that the resin portion of TheraCal (comprising hydrophobic and hydrophilic monomers) is able to promote/sustain Ca and OH ion release within the wet surgical site (on the tooth pulp and/or dentine) and could favour the interaction of the formulation with the hydrophilic tooth dentine. The results of the water absorption test showed that the hydrophilic resin in TheraCal formulation allows some water absorption that is likely responsible for the initiation of the hydration reaction of the Portland cement particles with subsequent formation of portlandite or calcium hydroxide. The occurrence of similar chemical-physical events in a light-curable MTA-based material containing an amphiphilic resin was recently reported (Gandolfi et al. 2011d).

The ability of TheraCal and ProRoot MTA to release calcium and alkalinize the surrounding fluids is correlated to the formation of calcium hydroxide $Ca(OH)_2$ that separates into calcium and hydroxl ions, resulting in Ca and OH ion release and increased pH. The alkalinizing power of a pulp capping material represents a key property for different alkaline-related biological properties. The release of hydroxyl ions during the hydration reaction creates an adverse environment for bacterial survival and proliferation. These antibacterial properties are primarily required at the dentine/restoration interface where residual bacteria could further increase the risk of re-infection and

secondary caries, in particular when using dental composites lacking any antimicrobial activity. In addition, alkaline pH is known to cause an inflammatory reaction with the formation of reparative dentine (Horsted-Bindslev & Lovshall 2002, Okiji & Yoshiba 2009) and also favours the formation of hydroxyapatite (Meyer & Eanes 1978, Lazic 1995).

The decrease in hydroxyl ion release from TheraCal after 7-14 days approaching the physiological pH may create a favourable environment for pulp cell viability and metabolic activity with the formation of new/reparative tertiary dentine.

The present study showed that Ca and OH ion release from the pulp capping materials would continue over time, and the action of these ions on vital tissue could induce the deposition of hard tissue and have an antibacterial effect. The chemical dissociation occurs in the presence of fluids, and the free calcium and hydroxyl ions dissociated from calcium hydroxide could likely penetrate the surrounding dentine (Tronstad et al. 1981, Hosoya et al. 2001). In a clinical situation, it is possible to speculate that a wet environment/surgical site (presence of exudates and dentinal fluid) may maintain the dissociation constant because of the presence of fluid in contact with the material.

One of the major drawbacks of the traditional self-cure $Ca(OH)_2$-based and CaO-based materials is high solubility and dissolution over time (within 1-2 years after application) in tissue fluids. This leads to the disappearance of the material and the formation of tunnel defects/patencies in reparative dentine underneath the capping, thereby failing to provide a permanent seal against bacterial invasion (Horsted-Bindslev & Lovshall 2002, Desai & Chandler 2009). In the present study, TheraCal showed low solubility values, whereas the high solubility of ProRoot MTA was likely related to its long setting time, with consequent disintegration of unset material, rather than its real solubility.

There is a criticism on the ISO definition of solubility as the test measures the elution of water-soluble material. The physicochemical definition of solubility for a solid involves/implies a situation where a pure chemical compound is in thermodynamic equilibrium with its solution, but equilibrium is not attained for a dental cement (Wilson 1976).

Moreover, the ISO tests (ISO 6876 clause 7.7.2.) are not ideal, as often the methods to perform the test are different from the clinical situation and the results obtained are far from the clinical outcomes. In confirmation of this, the high solubility of ProRoot MTA is not consistent with its excellent clinical performances.

Unfortunately, there is a lack of an international standard and test methods for both conventional and resin-modified calcium silicate MTA-like cements. This deficiency has been also mentioned by others (Nekoofar et al. 2007). There is a need for a standard requirement for the aforementioned materials in relationship to their specific clinical application (root end filling materials, endodontic sealers, pulp capping materials, etc.). The tests suggested in the available specifications are often inappropriate/unfeasible and inapplicable to MTA materials.

ISO 6876 for dental root canal sealing materials was used for the solubility test (ISO 6876 clause 7.7.2.) as it is commonly used on MTA materials. However, this specification has been conceived and refers to 'root canal sealing materials which set with or without the assistance of moisture and are used for permanent obturation of the root canal … applicable only to sealers intended for orthograde use, i.e. root filling placed from the coronal aspect of a tooth' (ISO 6876 comma 1). It does not concern specifically pulp capping materials and does not comply its test to the effective clinical conditions such as the setting in the presence of biological fluids.

ISO 4049 Dentistry - Polymer-based restorative materials refer/intend to materials 'for use in the cementation or fixation of restorations and appliances such as inlays, onlays, veneers, crown and bridges' and includes luting materials of class 1 (self-curing), class 2 (external-energy-activated) or class 3 (dual cure) materials. However, some suggested tests are inadequate for MTA-like materials such as water sorption and solubility testing (clause 7.12.2.1 for class 1 materials) that suggest to use specimens after 60 min at 37 C, that is, MTA samples completely dried with sure alteration of the hydration, setting and hardening reactions that require several hours and humidity.

ISO 9917 Dentistry - Water-based cements concern cement 'for use as a luting agent, a base or liner or as a restorative material' (clause 1), but does not include the specifications for many tests such as solubility or water sorption.

ProRoot MTA is a water-based cement, and Dycal is a polymer-based cement, although both are class 1 materials, that is, 'materials in which the setting reaction of the polymerizable component is activated chemically following mixing components' (ISO 9917 part 2 clause 4.1.). TheraCal is a resin-modified MTA-like material and a class 2 material 'in which the setting reaction of the polymerizable component is light-activated' (ISO 9917 part 2 clause 4.1.). Unfor-

tunately, appropriate standard specifications for the solubility and water absorption test of calcium hydroxide-releasing hydrophilic pulp capping materials do not exist. ISO 9917 for water-based cements does not include these tests, and ISO 4049 for polymer-based restorative materials does not consider hydrophilic materials that require water/moisture to set and/or need to absorb water to release bioactive ions as occur for the studied cements. For this reason, the ISO 6876 has been partly followed for the solubility and the water absorption tests, in agreement with previous studies on ProRoot MTA (Danesh et al. 2006, Islam et al. 2006). The solubility after 24 h of soaking was tested, in agreement with ISO 6876 and with previous studies on ProRoot MTA (Danesh et al. 2006, Islam et al. 2006, Gandolfi et al. 2011d) and Dycal (Shen et al. 2010).

Some modifications to ISO 6876 methodology because of the different typology of the test materials have been introduced. In this study, the internal diameter of the mould (8 mm, instead of 15 mm) was the same diameter as the LED light tip, in order that all the sample surface was exposed. Moreover, the weight loss of the test samples instead of the disintegrated material recovered in the soaking containers was considered/recorded, in agreement with previous studies (Danesh et al. 2006, Gandolfi et al. 2011d) and with ISO 4049. Finally, as in direct pulp-capping, the higher risk of dissolution of Dycal and mainly of ProRoot MTA is during the first hours, before setting and hardening has been completed, and the samples were immersed after a few minutes of being prepared.

Adequate specifications to test the radiopacity of hydrophilic calcium hydroxide-releasing MTA-based materials do not exist. The radiopacity data mismatch the ISO 6876 (Dental root canal sealing materials) requirement of a radiopacity ‡3 mm Al; however, the data of all the materials complied the ISO 9917 item 5.6. (Water-based cements - Resin-modified cements) for luting and base/lining materials, namely the radiopacity ‘shall be equal to or greater than of the same thickness of aluminum’. Previous studies used ISO 6876 to test the radiopacity of ProRoot MTA (Danesh et al. 2006). The radiopacity results of ProRoot MTA and Dycal were similar to that reported in previous studies (Danesh et al. 2006, Devito et al. 2006, Pekkan et al. 2011). No radiopacity values are stated by the manufacturer in the data sheet of the products.

Another serious disadvantage of $Ca(OH)_2$-based and CaO-based materials for pulp capping is setting failure to set in the presence of blood and other biological fluids with related clinical/operative problems. So, the possibility to light-cured pulp capping material is a potential major advantage for clinicians. TheraCal is set after a light curing of 20 s with a DOC of approximately 2 mm, to give rapid attainment of its physical properties.

The ability to release biologically active ions (biointeractivity) is a prerequisite for a material to be bioactive and trigger the formation of apatite. Previous studies demonstrated the formation of apatite on the surface of calcium silicate MTA cements when immersed in phosphate-containing solutions (Gandolfi et al. 2010a,b,c, 2011a,d). Apatite formation offers many advantages such as the exposure of a suitable surface for cells (Gandolfi et al. 2010d, 2011a,d), and may induce odontoblast-like cells to produce new dentine tissue and remineralize the adjacent dentine through the deposition of apatite crystals (Tay & Pashley 2008, Gandolfi et al. 2011e, Prati et al. 2011). Encouraging preliminary evidence on the formation of apatite on TheraCal as well as ProRoot MTA and Dycal has been obtained: the phosphate ions of biological fluids (blood, exudate, plasma, dentinal fluid) may react with Ca and OH ions leached from the materials and trigger the precipitation of apatite crystals.

Conclusions

TheraCal is a new light-curable pulp capping material able to release calcium ions and create an environmental pH close to physiological pH after 7 days. Its ability to polymerize to a depth of 1.7 mm may avoid the risk of untimely dissolution. The ability of TheraCal to provide free calcium ions could favour the formation of apatite and induce the differentiation of odontoblasts with the formation of new dentine.

References

Bogen G, Kim JS, Bakland LK (2008) Direct pulp capping with mineral trioxide aggregate. An Observational Study. Journal of American Dental Association 139, 305-15.

Clapham DE (1995) Calcium signaling. Cell 80, 259-68.

Danesh G, Dammaschke T, Gerth HUV, Zandbiglari T, Schafer E (2006) A comparative study of selected properties of ProRoot mineral trioxide aggregate and two Portland cements. International Endodontic Journal 39, 213-9.

Desai S, Chandler N (2009) Calcium hydroxide-based root canal sealers: a review. Journal of Endodontics 39, 415-22.

Devito LK, Ortega AI, Haiter-Neto F (2006) Effect of the storage in water on the radiopacity of calcium hydroxide cements. Brazilian Journal of Oral Sciences 5, 958-62.

Dougherty EW (1962) Dental cement material. US patent 3047408.

Estrela C, Holland R (2003) Calcium hydroxide study based on scientific evidences. Journal of Applied Oral Sciences 11, 269-82.

European Society of Endodontology (2006) Quality guidelines for endodontic treatment: consensus report of the European Society of Endodontology. International Endodontic Journal 39, 921-30.

Furey A, Hjelmhaug J, Lobner D (2010) Toxicity of Flow Line, Durafill VS, and Dycal to dental pulp cells: effects of growth factors. Journal of Endodontics 36, 1149-53.

Gandolfi MG, Pagani S, Perut F, Ciapetti G, Baldini N, Prati C (2008) Innovative silicate-based cements for endodontics: a study of osteoblast-like cell response. Journal of Biomedical Materials Research 86(A), 477-86.

Gandolfi MG, Ciapetti G, Perut F et al. (2009) Biomimetic calcium-silicate cements aged in simulated body solutions. Osteoblasts response and analyses of apatite coating. Journal of Applied Biomaterials and Biomechanics 7, 160-70.

Gandolfi MG, Taddei P, Tinti A, Prati C (2010a) Apatite-forming ability of ProRoot MTA. International Endodontic Journal 43, 917-29.

Gandolfi MG, Van Landuyt K, Taddei P, Modena E, Van Meerbeek B, Prati C (2010b) ESEM-EDX and Raman techniques to study ProRoot MTA and calcium-silicate cements in wet conditions and in real-time. Journal of Endodontics 36, 851-7.

Gandolfi MG, Taddei P, Tinti A, Dorigo De Stefano E, Rossi PL, Prati C (2010c) Kinetics of apatite formation on a calcium-silicate cement for root-end filling during ageing in physiological-like phosphate solutions. Clinical Oral Investigations 14, 659-68.

Gandolfi MG, Ciapetti G, Taddei P et al. (2010d) Effect of ageing on bioactivity and in vitro biological properties of calcium-silicate cements for dentistry. Dental Materials 26, 974-92.

Gandolfi MG, Shah SN, Feng R, Prati C, Akintoye SO (2011a) Biomimetic calcium-silicate cements support differentiation of human orofacial bone marrow stromal cells. Journal of Endodontics 37, 1102-8.

Gandolfi MG, Taddei P, Siboni F, Modena E, Ginebra MP, Prati C (2011b) Fluoride-containing nanoporous calcium-silicate MTA cements for endodontics and oral surgery: early fluorapatite formation in a phosphate-containing solution. International Endodontic Journal 44, 938-49.

Gandolfi MG, Taddei P, Tinti A, De Stefano Dorigo E, Prati C (2011c) Alpha-TCP improves the apatite-formation ability of calcium-silicate hydraulic cement soaked in phosphate solutions. Materials Science Engineering C 31, 1412-22.

Gandolfi MG, Taddei P, Siboni F, Modena E, Ciapetti G, Prati C (2011d) Development of the foremost light-curable calcium-silicate MTA cements root-end in oral surgery. Chemical-physical properties, bioactivity and biological behaviour. Dental Materials 27, e134-57.

Gandolfi MG, Taddei P, Siboni F, Modena E, Prati C (2011e) Biomimetic remineralization of human dentine using promising innovative calcium-silicates hybrid ''smart'' materials. Dental Materials 27, 1055-69.

Goldberg M, Smith AJ (2004) Cells and extracellular matrices of dentin and pulp/a biological basis for repair and tissue engineering. Critical Reviews in Oral Biology & Medicine 15, 13-27.

Hebling J, Lessa FCR, Nogueira I, Carvalho RM, de Souza Costa CA (2009) Cytotoxicity of resin-based light-cures liner cements. Journal of Dental Research 87B, 470.

Horsted-Bindslev P, Lovshall H (2002) Treatment outcome of vital pulp treatment. Endodontic Topics 2, 24-34.

Hosoya N, Takahashi G, Arai T, Nakamura J (2001) Calcium concentration and pH of the periapical environment after applying calcium hydroxide into root canals in vitro. Journal of Endodontics 27, 343-6.

Islam I, Chng HK, Yap AUJ (2006) Comparison of the physical and mechanical properties of MTA and Portland cement. Journal of Endodontics 32, 193-7.

ISO 4049 (2000) Dentistry-polymer-based filling, restorative and luting materials. Geneva: International Organization for Standardization ISO 4049.

ISO 6876 (2002) Dental root canal sealing materials. Geneva: International Organization for Standardization ISO 6876.

Jung GY, Park YJ, Han JS (2010) Effects of HA released calcium ion on osteoblast differentiation. Journal of Materials Science: Materials in Medicine 21, 1649-54.

Lazic S (1995) Microcrystalline hydroxyapatite formation from alkaline solutions. Journal Crystal Growth 147, 147-54.

Lopez-Cazaux S, Bluteau G, Magne D, Lieubeau B, Guicheux J, Alliot-Licht B (2006) Culture medium modulates the behaviour of human dental pulp-derived cells: technical note. European Cells & Materials Journal 11, 35-42.

Maeno S, Niki Y, Matsumoto H et al. (2005) The effect of calcium ion concentration on osteoblast viability, proliferation and differentiation in monolayer and 3D culture. Biomaterials, 26, 4847-55.

Meyer JL, Eanes ED (1978) A thermodynamic analysis of the amorphous to crystalline calcium phosphate transformation. Calcified Tissue Research 25, 59-68.

Min KS, Lee SI, Lee Y, Kim EC (2009) Effect of radiopaque Portland cement on mineralization in human dental pulp cells. Oral Surgery Oral Medicine Oral Pathology Oral Radiology and Endodontology 108, e82-6.

Modena KC, Casas-Apayco LC, Atta MT et al. (2009) Cytotoxicity and biocompatibility of direct and indirect pulp capping materials. Journal of Applied Oral Science 17, 544-54.

Moghaddame-Jafari S, Mantellini MG, Botero TM, McDonald NJ, Nor JE (2005) Effect of ProRoot MTA on pulp cell apoptosis and proliferation in vitro. Journal of Endodontics 31, 387-91.

Mohammadi Z, Dummer PMH (2011) Properties and applications of calcium hydroxide in endodontics and dental traumatology. International Endodontic Journal 40, 697-730.

Nekoofar MH, Adusei G, Sheykhrezae MS, Hayes SJ, Bryant ST, Dummer PMH (2007) The effect of condensation pressure on selected physical properties of mineral trioxide aggregate. International Endodontic Journal 40, 453-61.

Okiji T, Yoshiba K (2009) Reparative dentinogenesis induced by mineral trioxide aggregate: a review from the biological and physicochemical points of view. International Journal of Dentistry 2009, 1-12.

Parirokh M, Torabinejad M (2010a) Mineral trioxide aggregate: a comprehensive literature review-Part I: chemical, physical, and antibacterial properties. Journal of Endodontics 36, 16-27.

Parirokh M, Torabinejad M (2010b) Mineral trioxide aggregate: a comprehensive literature review-Part III: clinical applications, drawbacks, and mechanism of action. Journal of Endodontics 36, 400-13.

Pekkan G, Saridag S, Beriat NC (2011) Evaluation of the radiopacity of some luting, lining and filling dental cements. Clinical Dentistry and Research 35, 2-9.

Prati C, Parrilli AP, Fini M, Dummer PMH, Gandolfi MG (2011) Interface porosity of human root canals sealed with a new flowable MTA-based sealer: a high-resolution microcomputed tomography study. International Endodontic Journal 44, 28.

Rashid F, Shiba H, Mizuno N et al. (2003) The effect of extracellular calcium ion on gene expression of bone-related proteins in human pulp cells. Journal of Endodontics 29, 104-7.

Sawicki L, Pameijer CH, Emerich K, Adamowicz-Klepalska B (2008) Histological evaluation of mineral trioxide aggregate and calcium hydroxide in direct pulp capping of human immature permanent teeth. American Journal of Dentistry 21, 262-6.

Schroder U (1985) Effects of calcium hydroxide-containing pulp-capping agents on pulp cell migration, proliferation, and differentiation. Journal of Dental Research 64, 541-8.

Shen Q, Sun J, Wu J, Liu C, Chen F (2010) An in vitro investigation of the mechanical-chemical and biological properties of calcium phosphate/calcium silicate/bismutite cement for dental pulp capping. Journal of Biomedical Materials Research Part B: Applied Biomaterials 94, 141-8.

Shubich I, Miklos FL, Rapp R, Draus FJ (1978) Release of calcium ions from pulp-capping materials. Journal of Endodontics 4, 242-4.

Suh B, Cannon M, Yin R, Martin D (2008) Polymerizable dental pulp healing, capping, and lining material and method for use. International Patent A61K33/42; A61K33/42 Application number WO2008US54387 20080220; Publication number WO2008103712 (A2); Publication date 2008-08-28.

Taddei P, Tinti A, Gandolfi MG, Rossi PL, Prati C (2009) Ageing of calcium silicate cements for endodontic use in simulated body fluids: a micro-Raman study. Journal of Raman Spectroscopy 40, 1858-66.

Takita T, Hayashi M, Takeichi O et al. (2006) Effect of mineral trioxide aggregate on proliferation of cultured human dental pulp cells. International Endodontic Journal 39, 415-22.

Tamburic SD, Vuleta GM, Ognjanovic JM (1993) In vitro release of calcium and hydroxyl ions from two types of calcium hydroxide preparation. International Endodontic Journal 26, 125-30.

Tay FR, Pashley DH (2008) Guided tissue remineralisation of partially demineralised human dentine. Biomaterials 29, 1127-37.

Torabinejad M, Parirokh M (2010) Mineral trioxide aggregate: a comprehensive literature review 2013 part ii: leakage and biocompatibility investigations. Journal of Endodontics 36, 190-202.

Torabinejad M, White DJ (1995) US Patent Number 5,769,638.

Torneck CD, Moe H, Howley TP (1983) The effect of calcium hydroxide on porcine pulp fibroblasts in vitro. Journal of Endodontics 9, 131-6.

Tronstad L, Andreason JO, Hasselgren G, Kristerson L, Riis I (1981) pH changes in dental tissues after root canal filling with calcium hydroxide. Journal of Endodontics 7, 17-21.

Tuna D, Olmez A (2008) Clinical long-term evaluation of MTA as a direct pulp capping material in primary teeth. International Endodontic Journal 41, 273-8.

Wilson AD (1976) Specification test for the solubility and disintegration of dental cements: a critical evaluation of its meaning. Journal of Dental Research 55, 721-9.